IRF5 directs colonic inflammation and control of mononuclear phagocyte adaptation to the tissue environment

Alastair Lawrence Corbin

Lady Margaret Hall

A Thesis submitted for the degree of Doctor of Philosophy

Kennedy Institute of Rheumatology,

Nuffied Department of Orthopaedics, Rheumatology and Musculoskeletal Sciences,

University of Oxford

Supervisor: Prof. Irina Udalova

Co-Supervisor: Prof. Fiona Powrie

October 2017

Abstract

Macrophages are leukocytes of the innate immune system that display great phenotypic plasticity to mediate diverse functions. The ontogeny of tissue resident macrophages has been debated in recent decades. It is now recognised that tissue macrophages can be replenished from embryonically-derived precursors, and/or monocyte intermediates in a tissue specific manner.

Interferon Regulatory Factor 5 (IRF5) is a transcription factor that promotes a pro-inflammatory phenotype in macrophages *in vitro* and *in vivo*. Indeed, IRF5 contributes to the pathogenesis of experimental inflammatory arthritis, lupus, and obesity via recruitment and activation of effector cells.

Research described here as part of this thesis, involves the profiling of the intestinal Mononuclear Phagocyte system to investigate the role of IRF5 in the development of monocyte-derived macrophages in the Colonic Lamina Propria (cLP) which are exclusively replenished by adult Ly6C^{hi} monocytes. Using Mixed Bone Marrow Chimaeras (MBMCs) we showed that in shared environment Wild-Type (WT) cLP macrophages dominated IRF5-deficient (*Irf5*$^{-/-}$) cLP macrophages in both steady state and inflammation. The development of *in vitro* bone marrow derived macrophages, and the reconstitution of the haematopoietic compartment in bone marrow of MBMCs were not significantly affected by IRF5 deficiency. IRF5 promoted the accumulation of WT monocytes in the cLP of MBMCs in a process possibly dependent on the CCL2/CCR2 axis. Furthermore, IRF5 expression committed Ly6C^{hi} monocytes to a pro-inflammatory macrophage fate in the inflamed cLP, characterised by protein expression of the cytokines IL1β, and TNFα, and the expression of *Ccl4* and *Ccl8* transcripts, whilst loss of IRF5 favoured accumulation of CD11b^{+} IRF4-dependent Dendritic Cells. Of significance, IRF5 expression might have prevented further differentiation of inflammatory macrophages into tissue-resident macrophages, thus supporting an inflammatory state.

Irf5$^{-/-}$ mice were protected from *Helicobacter hepaticus* + αIL10R colitis. Intriguingly, protection from colitis may also be conferred by the presence of *Irf5*$^{-/-}$ haematopoietic cells, evidenced by WT:*Irf5*$^{-/-}$ MBMCs . Modulation of IRF5 activity may therefore be a viable therapeutic strategy. RNA sequencing identified that *C1q*, *Cd81*, and *Ccl8* were upregulated in WT macrophages from MBMC, which may prove therapeutic targets.

Acknowledgements

First, I would like to thank my supervisor, Prof. Irina Udalova, for her support, and guidance, and especially for her time spent reading and critiquing this thesis. I would also like to thank my co-supervisor Prof. Fiona Powrie for her support and guidance of my project. To Dr. Steve Sansom, I would like to extend my thanks for his shaping of the genomics branch of my project which would not have been possible without his expertise.

I would like to acknowledge the financial support granted by The Kennedy Trust for Rheumatology Research for providing my scholarship, and the Computational Genomics and Training centre for funding the SmartSeq2-mixed chimaera project.

Thanks to Dr Sarah Teichmann, and Dr Ricardo Miragaia, for collaborating on the SmartSeq2 single cell RNA seq project.

Thank you to the Powrie and Udalova members whose scientific discussion, advice and humour have kept me going in the lab. Thank you to Dr Isabelle Arnold for getting me started with the model, and helping to shape the early stages of the project. Special thanks go to Claire and Hayley, whose organisation and management have allowed the Powrie and Udalova labs run smoothly. Thanks to Sam for the beautiful graphics he has shared with the lab and for getting me into cycling.

I would like to thank my family and friends for their encouragement during my DPhil.

Finally, thank you to Tanya for your patience and support, I couldn't have done it without you!

Declaration

I declare that the thesis presented is the result of my own work. All experimental data presented in this thesis are original and were performed by myself unless indicated otherwise in the text.

The experiments described below were performed with assistance from others:

Dr Isabelle Arnold assisted with the set up and harvesting of WT and *Irf5*$^{-/-}$ Hh + αIL10R experiments, and the intra venous injections on one mixed bone marrow chimaera. Dr Claire Pearson also assisted with the intravenous injections to generate one mixed bone marrow chimaera, and one whole bone marrow chimaera experiment.

Dr. David Saliba conducted the IRF5-ChIPseq experiment.

Fluorescence-Activated Cell Sorting of macrophages was conducted by Mr. Jonathan Webber of the Kennedy Institute of Rheumatology Flow Cytometry Facility.

SmartSeq2 single cell library preparation was conducted in collaboration with the Teichmann Group (Wellcome Trust Sanger Institute, University of Cambridge).

10X mononuclear phagocyte capture, library prep of small bulk RNAseq, and 10X and small bulk RNA sequencing was conducted by the Bowden Group (Wellcome Trust Centre for Human Genetics).

Dr Stephen Sansom performed computational analysis of genomic datasets (ChIPseq, mini bulk-RNAseq, scRNAseq, 10X RNAseq).

Hh + αIL10R timecourse cDNA microarray data was generated by the Dr Chris Schiering, and Dr Matthew Shale and is available as a resource for the Powrie Lab.

Histology was sectioned and stained by the Kennedy Institute of Rheumatology Histology team (Dr. Bryony Stott, Dr. Ida Parisi, and Ms. Marcia Curtinha).

Approximate Word Count: 40,000

List of Abbreviations

ANOVA	Analysis of Variance
APC	Antigen Presenting Cell
ATACseq	Assay for Transposase Accessible Chromatin Sequencing
BCR	B cell Receptor
BSA	Bovine Serum Albumin
CD	Crohn's disease
CDP	Common Dendritic Cell Progenitor
cDC	Classical Dendritic Cell
cdtB	Cytolethal Distending Toxin B
cfu	Colony Forming Unit
ChIP	Chromatin Immunoprecipitation
ChIPseq	Chromatin Immunoprecipitation Sequencing
cLP	Colonic Lamina Propria
CLP	Common Lymphoid Progenitor
cMoP	Common Monocyte Progenitor
CMP	Common Myeloid Progenitor
Cre	Cre-recombinase
Crypt	Crypt of Lieberkühn
CSF1R	Colony-Stimulating Factor-1 Receptor
CyTOF	Time of Flight Mass Cytometry
d	Day
DC	Dendritic cell
ELISA	Enzyme-Linked Immunosorbant Assay
EMP	Erythro-Myeloid Progenitor
FACS	Fluorescence-Activated Cell Sorting
FCS	Foetal Calf Serum
FL	Foetal Liver
GM-BMDM	GM-CSF- differentiated Bone Marrow Derived macrophage
GM-CSF	Granulocyte-Macrophage Colony Stimulating Factor
GM-CSFR	Granulocyte-Macrophage Colony Stimulating Factor Receptor
G	Gauge
GMP	Granulocyte Macrophage Progenitor
GO	Gene ontology
αIL10R	Anti-Interleukin 10 Receptor monoclonal antibody

H3K4me	Histone 3 Lysine 4 methylated
H3K27ac	Histone 3 Lysine 27 acetylated
HBSS	Hank's Buffered Saline Solution
Hh	*Helicobacter hepaticus*
H&E	Haematoxylin and Eosin
HSC	Haematopoietic Stem Cell
HSPC	Haematopoietic Stem and Progenitor Cell
IBD	Inflammatory Bowel disease
IFN	Interferon
Ig	Immunoglobulin
IL	Interleukin
ILC	Innate lymphoid cell
IRF	Interferon Regulatory Factor
IRF5	Interferon Regulatory Factor 5
$Irf5^{-/-}$	IRF5-knockout
i.v.	Intravenous
KLF	Kruppel-Like Factor
L/D	Live/Dead viability dye
LP	Lamina Propria
LPL	Lamina Propria Leukocyte
LPS	Lipopolysaccharide
MBMC	Mixed Bone Marrow Chimaera
M-CSF	Macrophage Colony Stimulating Factor
MDP	Macrophage-Dendritic Cell Progenitor
MEP	Megakaryocyte-Erythroid Progenitor
MHC	Major Histocompatibility Complex
MNP	Mononuclear Phagocyte
NLR	NOD-Like Receptor
PAMP	Pathogen Associated Molecular Pattern
PBS	Phosphate Buffered Saline
PCR	Polymerase Chain Reaction
pDC	Plasmacytoid Dendritic Cell
PRR	Pattern Recognition Receptor
qPCR	Quantitative Polymerase Chain Reaction
RA	Retinoic Acid
RNAseq	RNA Sequencing
SCFA	Short Chain Fatty Acid

scRNAseq	Single Cell RNA Sequencing
SLE	Systemic Lupus Erythematosus
TCR	T cell Receptor
T_{eff}	T effector cell
TF	Transcription Factor
T_H	T helper cell
TipDC	TNFα - iNOS-producing Dendritic Cell
T_{reg}	T regulatory cell
TSB	Tryptone Soya Broth
UC	Ulcerative colitis
WT	Wild-type
WBMC	Whole Bone Marrow Chimaera
YS	Yolk Sac

Table of Contents

Table of Figures

1 Introduction

1.1 The immune system

The immune system evolved to protect the host from harmful pathogenic invasion and tissue damage. To achieve this function, the immune system must detect and eliminate invasive non-self-antigens belonging to parasites, fungi, viruses, and bacteria. As pathogens evolved more complex mechanisms to evade the host defences, the vertebrate immune system has evolved highly complex mechanisms to provide both short and long term immunity, termed innate and adaptive immunity respectively. In conjunction with anti-pathogen immunity, the host must restore damaged tissues through the clearance of cellular debris and somatic proliferation to maintain homeostasis [1]. The failure to clear damaged tissue can lead to the exposure of self-antigens, the continuation of inflammation, and autoimmunity [2]. In order to successfully bring about immune responses, the host must recognise foreign antigens, bring effector mechanisms to bear to clear the insult, and then dampen the immune response. Immunological memory is then generated to prevent future infections by the same pathogen [3].

1.1.1 The innate immune system

The body is constantly exposed to trillions of micro-organisms, but relatively rarely suffers from disease [4]. Therefore, most barrier breaches are detected and eliminated rapidly. The initial contact with pathogens normally occurs at barrier sites such as the skin and mucosal surfaces. Barrier sites display physical (mucous) and chemical (e.g. AMPs and anti-microbial enzymes) methods to prevent pathogen translocation [5]. If these defences are breached, cellular immunity is initiated, leading to the release of effector molecules such as complement, perforins, major basic protein, granzymes and cytokines that expel pathogens [5, 6].

The immune system must first recognise non-self in order to initiate immunity. All innate recognition and response molecules are directly encoded by the germline. These are

termed Pattern Recognition Receptors, and recognise conserved traits, also known as Pathogen Associated Molecular Patterns (PAMPs) in micro-organisms. Nucleotide Oligomerisation Domain-Like Receptors (NLRs) and Toll-Like Receptors (TLRs) are canonical Pattern Recognition Receptors (PRRs). Activation of PRRs leads to downstream signalling events that shape the immune response.

1.1.1.1 Granulocytes

The term Granulocyte encompasses mast cells, basophils, eosinophils, and neutrophils. They are so called because of the highly vacuolar cytoplasm which appears granular under a light microscope [7].

1.1.1.2 Mast Cells

Mast cells are most abundant in connective and mucosal tissues, are associated with allergic immunity, are able to produce large quantities of IL4, and release granules that contain histamine and heparin upon IgE stimulation [8].

1.1.1.3 Basophils

Basophils play a role in the defence against parasites, and are also associated with allergic immunity. Similar to Mast cells, Basophil granules contain histamine and heparin. Their name derives from the fact that they stain positive for basic dyes such as Haematoxylin. Basophils arise from separate haematopoietic progenitors to mast cells, and circulate in the blood [7].

1.1.1.4 Eosinophils

Eosinophils stain positive for acidic dyes such as eosin, and display a multi-lobed nucleus. Eosinophil granules contain many cytotoxic molecules, such as eosinophil peroxidase, proteases, and DNA- and RNA-nucleases, along with Major Basic Protein [9].

1.1.1.5 Neutrophils

Neutrophils are particularly abundant granulocytes in blood, and are rapidly mobilised to sites of inflammation. Neutrophils are highly motile and avidly phagocytic, making them

specialised to eliminate invading pathogens [10]. Like other granulocytes, neutrophil granules contain cytotoxic molecules, including myeloperoxidase, neutrophil elastase, and AMPs [10]. In addition to these functions, neutrophils are also able to release Neutrophil Extracellular Traps (NETs) upon neutrophil death by NETosis, which releases DNA that binds and ensnares pathogens [11].

1.1.1.6 NK cells and ILCs

Natural Killer (NK) cells, Innate Lymphoid Cells (ILCs), derive from the Common Lymphoid progenitor, but lack the T- or B- cell antigen-specific receptors. NK cells are specialised at eliminating virus-infected cells once activated due to their high expression of cytokines, granzyme, and perforins [12]. ILCs are specialised to produce cytokines, and fall into three classes based on the expression of transcription factors analogous to the T cell subsets of adaptive immunity [13]. ILC1s express T-bet (T_H1), ILC2s express GATA-3 (T_H2), and ILC3s express RORγt (T_H17) [14]. The cytokines expressed by the respective ILC subsets mirror those of their respective T cell subsets (See Chapter.1.1.2) [15].

1.1.1.7 Phagocytes

Phagocytes are the largest subset of the innate immune system numerically. The term Phagocyte encompasses neutrophils, monocytes, macrophages and DCs. These cells are able to engulf particles and micro-organisms that have been opsonised with antibodies, complement proteins, or pentraxins, collectins and ficolins, and digest them in intracellular vacuoles (e.g. lysosomal compartments). Monocytes, macrophages, and dendritic cells are considered professional Antigen Presenting Cells (APCs). The professional APCs bridge innate and adaptive immunity as they present antigens that have been processed in endosomal compartments after phagocytosis on Major Histocompatibility Complex (MHC) class II molecules to naïve T cells to generate specific immune responses. APCs are discussed in greater detail in Chapter.1.2, 1.4, and 1.6

1.1.2 The adaptive immune system

The adaptive immune system provides memory response to pathogens through the generation of antibodies. The effector cells of the adaptive immune sytem are T lymphocytes (T cells) and B lymphocytes (B cells). Immune memory is provided by the expansion of memory lymphocytes that proliferate more rapidly than naïve lymphocytes.

1.1.2.1 T cells

T cell precursors arise from Common Lymphoid Progenitors (CLPs) in the bone marrow which migrate to the Thymus [16]. T cell precursors undergo maturation via positive and negative selection in the Thymus [17]. The T cell Receptor (TCR) gene fragments undergo V(D)J recombination to generate TCRs with unique specificities [18]. TCRs must display weak affinity for MHC-bound self-antigen and therefore no self-reactivity upon maturation [19]. T cells may commit to either $CD4^+$ $CD8^-$ T Helper (T_H) or $CD4^-$ $CD8^+$ cytotoxic T cell lineages. After pathogen recognition, $CD4^+$ and $CD8^+$ T cells face a fate choice, and can become memory T cells that are able to rapidly proliferate upon secondary encounter a specific antigen [20]. This mechanism allows for rapid pathogen clearance upon reinfection.

$CD4^+$ T_H cells support immune responses through the production of high quantities of cytokines that direct specific immune responses to different classes of pathogen [21, 22]. To generate T_H responses, naïve T cells must receive three signals: 1) TCR stimulation by MHC II-bound antigen, 2) costimulation of CD28 by either CD80 or CD86 on DCs or Macrophages, 3) cytokine receptor signalling to drive T_H polarising transcription factor expression (e.g. T-bet, GATA-3, RORγt) [19, 23, 24].

T_H1 cells are dependent on the transcription factor T-bet, which is induced by Interleukin 12 (IL12) and Tumour Necrosis Factor alpha (TNFα) [25]. T_H1 cells participate in the response to intracellular pathogens, such as *Mycobacterium* sp., by producing Interferon γ (IFNγ) [26]. T_H2 cell development is dependent on GATA-3. T_H2 cells produce the cytokines IL4, IL5, and IL13 and are important mediators of anti-parasite immunity [27]. Dysregulation of T_H2 immunity leads to allergic responses. The cytokines IL1β, IL6, and IL23 promote

T_H17 development by activating RORγt [28, 29]. T_H17 cells are specialised to clear extracellular pathogens such as Fungi, but are also associated with autoimmunity. In order to resolve inflammatory responses, naïve T cells can also become inducible T regulatory cells (T_{regs}) under the control of FoxP3 [30].

$CD8^+$ T cells are specialised cytotoxic T cells that eliminate viruses, and tumours [31]. $CD8^+$ T cells recognise MHC I-bound antigens, allowing the recognition of 'altered self', and therefore directed cytotoxicity [32].

1.1.2.2 B cells

B cells are specialised antibody producing cells of the adaptive immune system, but can also act as professional APCs to present antigen to T_H cells. B cells also arise from CLPs in the bone marrow. Before migration to B cell follicles present in Secondary Lymphoid Organs, B cells undergo two developmental checkpoints similar to T cell maturation in the Thymus [33]. Self-reactive B cells either undergo receptor editing, die, or become anergic [34].

To facilitate antigen recognition, the B cells expresses B Cell Receptors (BCRs). In common with TCRs, BCRs also arise through VDJ recombination. B cells can be activated in two manners: 1) thymus-dependent, and 2) thymus-independent. In thymus-dependent activation, B cells first act as APCs. Once antigen is encountered by the BCR and phagocytosed, it is processed, loaded onto MHC II, and presented to T_H cells [35]. Upon T_H:MHC II interaction, T_H cells produce cytokines that stimulate the activation and proliferation of B cells [36]. Similar to T cells, activation of B cells also requires co-stimulation with can derive from Thymus-dependent antigens, CD40L on T_H cells binding to CD40, or TLR ligation alongside the BCR. B cells can also be activated independently of the Thymus, where antigen ligation must be coupled with strong PRR signalling to elicit a response. Activated B cells either differentiate into antibody-secreting plasma cells, or memory B cells in the germinal centres of SLOs. Plasma cells are specialised antibody

producing cells that are short lived [37]. B cells activated independently of the Thymus typically give rise to antibodies with lower affinity for their cognate antigen than Thymus-dependent B cell activation [38]. Before antibody production begins, B cells, undergo antibody class-switching [39]. Meanwhile, somatic hypermutation in memory B cells results in high affinity antibodies. The antibodies produced by B cells are the secreted form of the BCR. Secreted antibodies bind to their cognate ligands, neutralising and opsonising pathogens.

1.2 The mononuclear phagocyte system

1.2.1 Nomenclature and function

Ilya Metchnikoff first described phagocytes, a term that encompasses neutrophils, macrophages and DCs, in Starfish larvae over one century ago, as mobile cells with the capacity to engulf and dispose of pathogens, debris, and dead cells [40]. The term mononuclear phagocyte (MNP) is now used to describe monocytes, macrophages, and dendritic cells [41]. MNPs are highly phagocytic, professional antigen presenting cells that are critical for bridging innate and adaptive immunity [42, 43].

Monocytes are ~15 μm diameter MNPs with a bean shaped nucleus. In mice, monocytes exist in two major subtypes in the blood, Ly6C^{hi} and Ly6C^{lo}, which are analogous to CD14^{+} CD16^{lo} (classical), and CD14^{-} CD16^{+} (non-classical) monocytes respectively in man [44]. Although similar, human and mouse monocytes display species-specific gene expression profiles [45]. At steady state, upon leaving the bone marrow, Ly6C^{hi} monocytes enter the blood and circulate with a $t_{1/2}$ of approximately 2 days before entering tissues, such as the spleen or intestine, or differentiating into Ly6C^{lo} monocytes [46-49]. Ly6C^{lo} monocytes patrol blood vessel walls and facilitate their repair, but their presence in peripheral tissues at steady state has been questioned [50-53]. During inflammation, Ly6C^{hi} monocytes are mobilised to inflamed tissues from the spleen and bone marrow via the blood [54]. Newly recruited Ly6C^{hi} monocytes then differentiate into inflammatory macrophages, and possibly dendritic cells upon encountering polarising stimuli [54, 55].

Macrophages are large, avidly phagocytic MNPs with a highly granular cytoplasm that can be found in peripheral tissues and in abundance at mucosal tissues such as the lung and gut [56, 57]. Their functions include clearance of apoptotic debris, modulation of tissue repair, engulfment and neutralisation of microbes, directing the recruitment of leukocytes in response to infection, and potentiating primed-T cell responses [43]. Because of these diverse functions, macrophages display great plasticity in their response and thus are exceptionally responsive to microenvironmental cues [58]. To achieve these varied responses, macrophages express a wide repertoire of cell surface receptors, such as integrins, lectins, PRRs, Fc receptors, and cytokine and chemokine receptors [59-61]. Tissue macrophages do not migrate to lymph nodes to stimulate naïve T cells, in contrast to classical Dendritic Cells (cDCs) [62].

DCs are the final constituent of the MNP system, divided into two major classes, Plasmacytoid DCs (pDCs), and cDCs. cDCs display stellate morphology, reside in both lymphoid and non-lymphoid tissue and are also highly phagocytic professional APCs [63, 64]. cDCs are specialised in priming naïve T cells and can migrate from non-lymphoid to lymphoid tissue to carry out this function in a CCR7-dependent process [62]. cDCs are present in non-lymphoid tissues in an immature state, and mature into T cell-stimulating, migratory DCs upon PRR engagement [65]. pDCs are specialised in the production of Type I interferons in response to viral infection, may prime naïve T cells during infection [66].

1.2.2 Development of mononuclear phagocytes

In the adult mouse, the classical model of haematopoiesis posits that MNPs arise through the step-wise differentiation of haematopoietic precursors (Fig.1.1) [67]. In steady state adults, haematopoiesis occurs in the bone marrow, but in exceptional circumstances, such inflammation or myelofibrosis, extramedullary myelopoiesis can occur in the spleen or liver [68, 69]. Self-renewing Haematopoietic Stem Cells (HSCs) undergo multiple differentiation stages, during which HSCs lose self-renewal capacity in a process dependent on the reduced expression of the transcription factor, p64 [70]. HSCs differentiate into progenitor cells which can expand in situ to greatly amplify the pool of lineage-restricted progenitors [71, 72].

1.2.3 Lineage-determining transcription factors

Regulation of gene expression is a non-linear process: interplay between chromatin modifications, Trascription Factors (TFs), and signalling molecules as cells develop results in the formation of cell identity, and functional plasticity [73]. TFs are recognised to bind specific DNA motifs, the availability of which is regulated by epigenetic modifications such as DNA methylation and histone acetylation [46]. TF motifs are organised into promoters and enhancers in sequences approximately 200 bp long, which co-ordinate the recruited TFs, and therefore the genes transcribed [74]. Pioneer TFs, of which PU.1 is an example, can bind partially obscured motifs and displace nucleosomes to facilitate further TF binding and transcription, and are therefore key in lineage commitment [75].

It was previously believed that TFs regulate small sets of genes at fate decision points during differentiation, e.g. CSF1R, to determine lineage commitment [76]. It is now recognised that lineage-determining TFs construct a framework of active or poised gene regulatory elements which regulate the housekeeping genes critical for cell identity [73]. Stimulus-activated TFs operate within these confines to regulate contextual responses [73]. The process of myelopoiesis, outlined below, highlights these processes.

1.3 Myelopoiesis

In the classical model of haematopoiesis, Common Myeloerythroid Progenitors (CMPs) arise at the first branch of lineage restricted progenitors, distinct from CLPs [67]. The ETS family TF, PU.1, is a critical determinant of myeloid fate, as loss of PU.1 function resulted in ablation of the macrophage compartment [77, 78]. Not only did PU.1 directly regulate genes, but it regulated the chromatin landscape, acting as a pioneer TF to facilitate the recruitment of lineage-determining TFs [79-81]. Granulocyte-Macrophage Progenitors (GMPs) are the next stage of myelopoiesis. GMPs generate the granulocytes, neutrophils and eosinophils via separate progenitors not discussed further. Expression of the TFs PU.1, IRF8, EGR1 and EGR2 restrict GMP fate to the Monocyte-macrophage and DC lineage via Monocyte-Dendritic cell Progenitors (MDPs) [82]. IRF8 was shown to control DC fate at the GMP stage, as loss of IRF8 led to increased numbers of granulocytes, particularly neutrophils, and an almost complete loss of DC subsets, including pDCs. [83, 84]. Meanwhile, regulation of EGR1 and EGR2 by PU.1 prevented granulocyte fate of GMPs [85]. Single-cell RNA sequencing (scRNAseq) of MDPs, Common Dendritic cell Progenitors (CDPs), and pre-DCs showed that lineage commitment of cDCs became evident at CDP stage, with Siglec H^- $Ly6C^-$ CDPs giving rise to BATF3-dependent $CD11b^-$ cDC1s, and Siglec H^- $Ly6C^+$ CDPs generating IRF4-dependent $CD11b^+$ cDC2s [86]. MDPs develop into either CDPs, or common Monocyte Progenitors (cMoPs), identified by an MDP-monocyte intermediate phenotype which exclusively gave rise to monocytes [49].

The classical haematopoietic model was challenged in a study by Sathe *et al.,* (2014), who found that MDPs isolated using a strategy described by Fogg *et al.,* (2006) predominantly gave rise to cells of monocyte-macrophage lineage, and very few resident cDCs in clonal culture systems or when adoptively transferred [87].

The current view, is that tissue cDC1s arise through a migratory pre-DC intermediate, derived from the CDP, whereas cDC2s are seeded by both pre-DCs and moDCs. Meanwhile, pDCs are generated from the CDP and migrate to peripheral tissues via the

blood [86]. cMoPs generate the monocyte lineage and can differentiate into Ly6C^{hi} monocytes, or Ly6C^{lo} monocytes [46, 49]. Ly6C^{hi} monocytes then migrate into the blood where they can be recruited to peripheral tissues, or convert into Ly6C^{lo} monocytes after a period of approximately 2 days [48, 50].

The classical model of haematopoiesis has been challenged by recent studies that identified heterogeneity and non-canonical lineage commitment in HSPCs [88-92]. Therefore, a new model incorporating recent advances postulates that the developmental stages defined in the classical haematopoietic model are bridged by transient progenitor states that are susceptible to major environmental perturbations, allowing re-commitment to other lineages within the confines of the enhancer landscape generated by pioneer TFs [92].

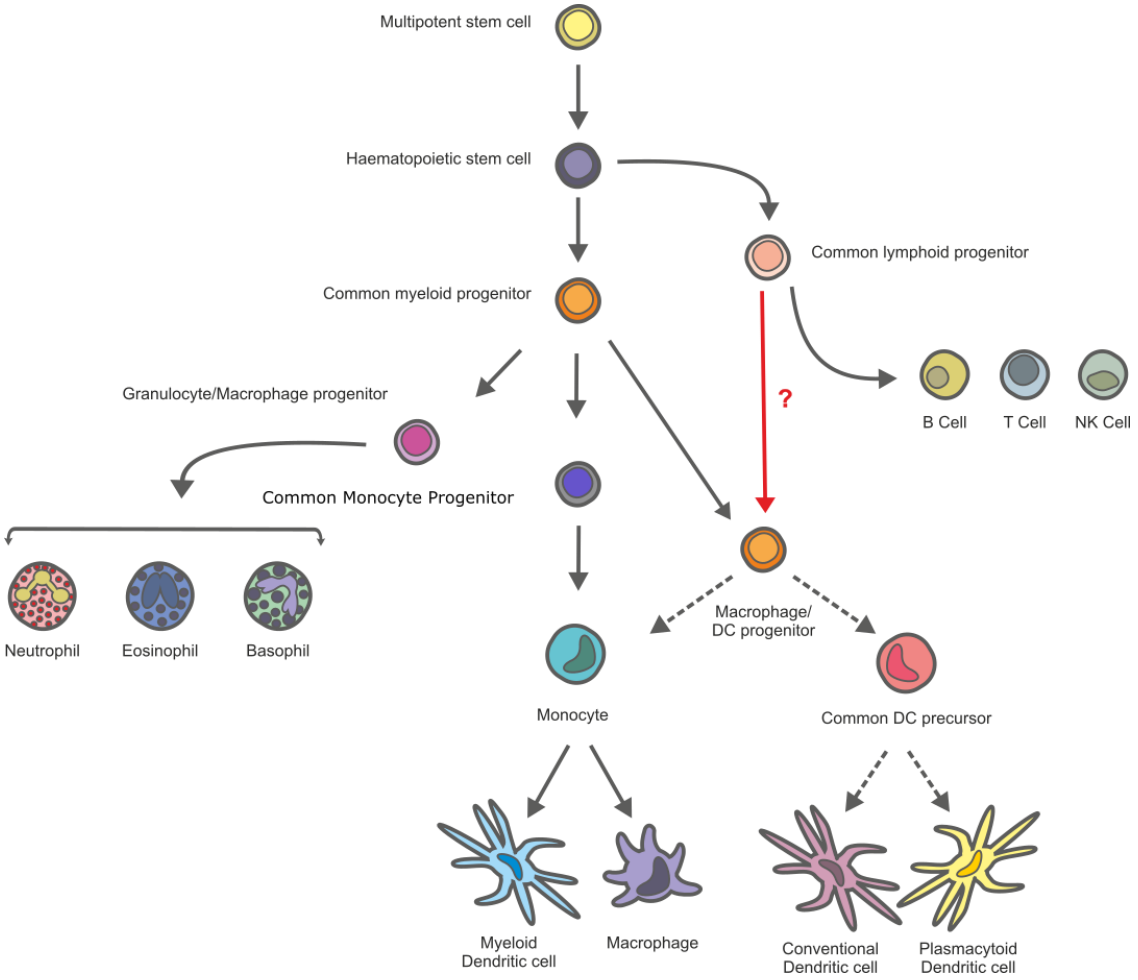

Fig.1.1: The classical model of myelopoiesis

Post-natal haematopoiesis predominantly occurs in the bone marrow at steady state. Self-renewing Haematopoietic Stem Cells (HSCs) give rise to Common Lymphoid Progenitors (CLPs) or Common Myeloerythroid Progenitors (CMPs). CMPs in turn generate Granulocyte-Macrophage Progenitors (GMPs). GMPs generate neutrophil and eosinophil granulocytes via progenitors not displayed in this figure. Monocyte-Dendritic cell Progenitors (MDPs) may also generate granulocytes, but predominantly develop into either Common Dendritic cell Progenitors (CDPs) or common Monocyte Progenitors (cMoPs). CDPs may also arise from CLPs, but the factors that define this process are unknown. CDPs develop into the Dendritic Cell (DC) lineage, giving rise to plasmacytoid DCs (pDCs), and classical DCs (cDCs) via a pre-DC intermediate. cMoPs generate the monocyte lineage and can differentiate into $Ly6C^{hi}$ monocytes. $Ly6C^{hi}$ monocytes then migrate into the blood where they can be recruited to peripheral tissues and differentiate into macrophages of myeloid-derived DCs, or convert into $Ly6C^{lo}$ monocytes.

1.4 The ontogeny of tissue-resident macrophages

The topic of the origin of MNPs has seen much debate over the century since their discovery by Metchnikoff. In 1968, van Furth and Cohn proposed that tissue macrophages were derived from circulating monocytes [93]. This hypothesis was adapted based on the results of chimaeric, parabiotic, and adoptive transfer studies to include self-renewal as a source of tissue macrophages [94-97]. Newer studies then identified that tissue resident macrophages are present in the mammalian embryo at Embryonic day 7.5 (E7.5), before monocytes [98], and HSCs, highlighting their developmental importance, and opening the avenue of embryonic development as a source of macrophages [99].

Mammalian embryonic haematopoiesis occurs in three waves [100]. The first wave occurs in the primitive Yolk Sac, beginning at E7.25, and is termed “Primitive Haematopoiesis”. Primitive haematopoiesis gives rise to erythroblasts, megakaryocytes, and macrophages [100, 101]. These cells derive from poorly defined progenitors that are $CSF1R^{+}$ $cMyb^{-}$, designated “Erythro-Meyeloid Progenitors” (EMPs), and colonise most tissues. However, EMP-derived macrophages do not persist in great numbers in adults, except as microglial cells of the brain [102, 103]. From E8.5, a second wave of EMPs emerges [104]. This EMP wave is designated the “Transient Definitive Wave”, which itself comprises two stages. The first transient definitive wave generates macrophages, and the second has monocyte, macrophage, and granulocyte potential [105]. The third embryonic haematopoietic wave occurs almost simultaneously with the Transient Definitive Wave, and generates HSCs that colonise the foetal liver and foetal bone marrow [106]. EMPs migrate through the primitive circulation to the foetal liver where they expand to produce monocytes, granulocytes, and megakaryocytes. The foetal liver and foetal bone marrow HSCs generate adult HSCs, which then generate the immune system. In the foetal liver, $CSF1R^{lo}$ $cMyb^{+}$ EMP produce the foetal liver monocytes which are considered to contribute the most to the adult tissue-resident macrophage pool [102, 103, 105]. Foetal liver monocytes were first described by Naito *et al.,* (1990) [98], and arise at E12.5. Foetal liver monocytes are released into blood

at E13.5, and at E14.5 were described to colonise all organs except the brain [105, 107, 108]. In contrast to adult monocytes, foetal liver monocytes are highly proliferative, and do not express many genes related to pathogen responsiveness [105, 109]. The contribution of various embryonic sources to adult tissue-resident macrophage populations is debated (Fig.1.2), due to the limited resolution of fate mapping studies at the early embryonic stages [110].

Embryonic macrophages persist in adult brain (microglia), skin (Langerhans cells), lung (alveolar macrophages), and liver (Kupffer cells) as parabiotic studies confirmed that renewal was largely independent of $CCR2^{+}$ $Ly6C^{hi}$ blood monocytes at steady state [111]. However, dermal, cardiac, and colonic macrophages in adult mice were demonstrated to also be replenished from the blood by $Ly6C^{hi}$ monocytes [57, 61, 112-115].

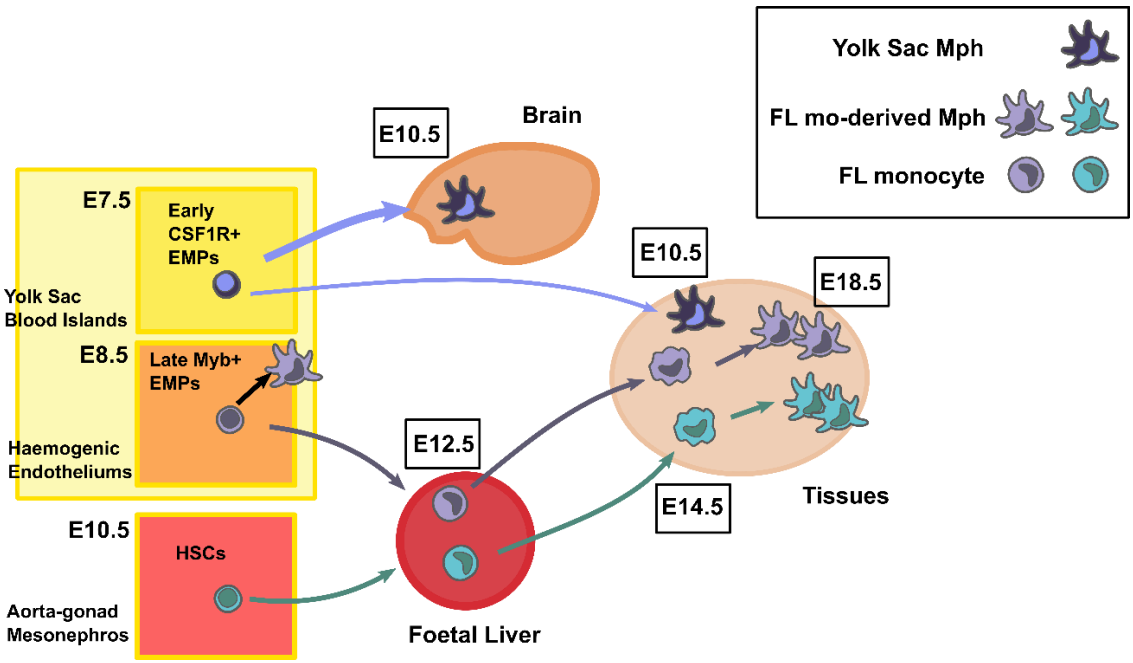

Fig.1.2: Foetal macrophage ontogeny

Figure depicting modes of macrophage ontogeny in the foetus. Arrows depict major route of origin. Cell ontogeny is coded by colour. Early CSF1R^{+} EMPs can give rise to adult microglia, and possibly contribute to adult tissue macrophages. Late Myb^{+} EMPs seed the embryo, and may also give rise to some tissue macrophage directly. Late EMPs also give rise to FL monocytes, which then seed tissues later in development. HSCs arising at E10.5 give rise to FL monocytes that can then seed tissue macrophages.

EMP: Erythro-Myeloid Progenitor, FL: Foetal Liver, HSC: Haematopoietic Stem Cell, Mo: Monocyte, Mph: Macrophage

1.5 The architecture of the colonic lamina propria

The intestine is a highly specialised mucosal organ that facilitates the absorption of nutrients and water from the diet. To achieve this function, the intestinal LP has the largest surface area of any organ in the body. Because of the nutrient rich environment, the intestine is host to antigens and immunomodulatory factors, such as Short Chain Fatty Acids (SCFAs), generated by trillions of bacteria, both commensal, and pathogenic [116, 117]. To maintain homeostasis, the intestine is therefore hosts a complex immune network. As this thesis focusses on the adaptation of colonic monocytes and macrophages, this section will address the anatomy of the colon.

The large intestine begins at the caecum and is followed by the proximal, mid, and distal colon, ending at the rectum. The intestinal lumen is lined by columnar epithelial cells that are renewed by multipotent stem cells located at the base of the Crypts of Lieberkühn (Crypts) which push newly differentiated epithelial cells towards the lumen as epithelial cells are sloughed off. Crypt multipotent stem cells also generate Paneth cells, mucus-producing goblet cells, and neuroendocrine cells. The goblet cells secrete mucins that form a thick layer of mucus when combined with water that is difficult for bacteria to penetrate, which helps to maintain the sterility of the LP. The mucosa, comprising the epithelium, LP, and muscularis mucosa, contains most of the intestinal immune cells (Fig.1.3) [118]. The submucosa lies beneath the muscularis mucosa, is highly innervated with parasympathetic neurones, and perfused with blood vessels. The submucosa is also densely packed with connective tissue to support the structure of the intestine, and lies on top of a layer of smooth muscle which aids the passage of faeces by peristaltic contraction. Finally, the serosa is a fibrous band surrounding the intestine, and separates the intestines from the peritoneal cavity.

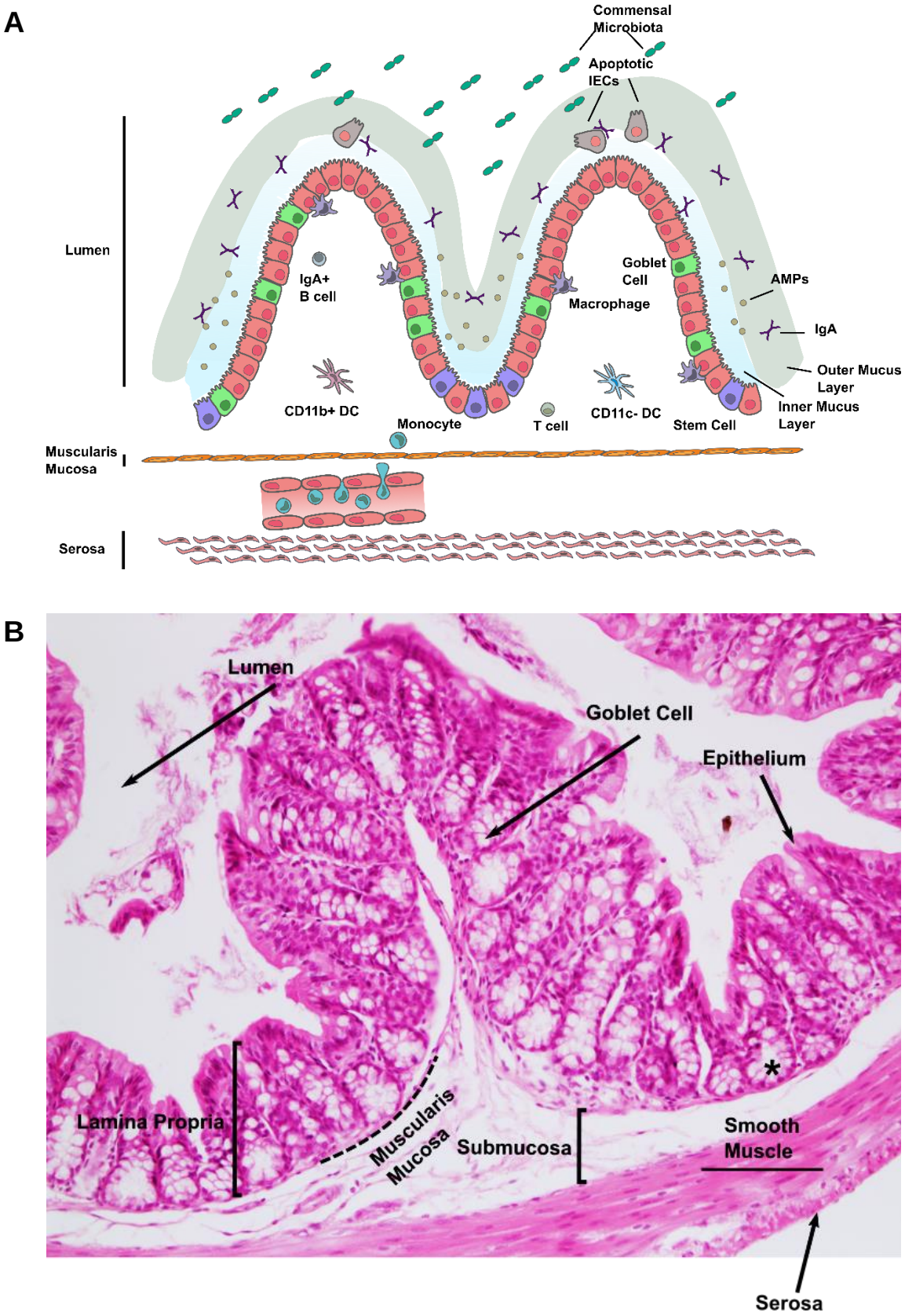

Fig.1.3: Structure of the colonic lamina propria

The colon is specialised for the reabsorption of water from faeces. Intestinal epithelial cells (IECs) are constantly sloughed off by the passage of faeces. To replace the lost IECs, stem cells located at the base of the Crypts of Lieberkühn (Crypts) proliferate. IECs are pushed up the Lamina

Propria (LP) as the space below them is occupied by newly differentiated IECs. Crypt stem cells also give rise to mucus producing goblet cells, and anti-microbial peptide producing Paneth cells, which are rare in the colon. Unlike the small intestine, the colon lacks villi, with a broad epithelial surface between the Crypts. Underneath the LP lies the muscularis mucosae, a layer of smooth muscle that aids the expulsion of Crypt secretions, which separates the LP from the submucosa. The submucosa contains connective tissue which supports the lamina propria, and is perfused by blood vessels and nerves. The submucosa is separated from the serosa by a layer of smooth muscle that aids the passage of faeces by peristalsis. **A)** Cartoon of the colonic LP (cLP). **B)** Representative micrograph of the mouse cLP (40 X magnification)

***** = Crypt of Lieberkühn

1.6 The murine intestinal mononuclear phagocyte system

MNPs, including monocytes, macrophages, and cDCs, are present in large numbers in the cLP, and carry out diverse, overlapping functions summarised below and in Table.1.1. MNPs are critical to the maintenance of intestinal homeostasis, as dysregulation of the intestinal MNP system leads to infection and inflammation [62, 119-125]. Inconsistent nomenclature has proved a barrier to understanding the precise roles of intestinal MNPs. Previously, markers such as CD11b, CD11c, and MHC II were used to discriminate macrophages from DCs [126, 127]. It is now appreciated that intestinal macrophages and DCs can co-express these markers and CX_3CR1 [61]. Similarly, CD103 was unable to clearly distinguish macrophages from DCs, as some $CD11b^+$ DCs were negative for CD103 [128]. Therefore, F4/80, and CD64 are used as discrete macrophage markers in the steady state murine cLP [57, 61]. F4/80 is also expressed on intestinal eosinophils, and so Siglec F^+ SSC^{hi} cells must be excluded from analysis [69, 129]. The structure and functions of the intestinal MNP compartment are outlined below.

Three major subpopulations comprise intestinal cDCs: $CD11b^+$ $CD103^+$, $CD11b^+$ $CD103^-$, and $CD11b^-$ $CD103^+$. These cDCs can be derived from FLT3L-dependent common dendritic cell progenitors in the bone marrow, and possibly from $CCR2^+$ monocytes from the circulation [86, 130]. cLP $CD11b^-$ $CD103^+$ DCs were derived from CDPs, demonstrated by genetic mapping of $DNGR1^+$ progenitors using fluorescent proteins under the control of *Clec9a*^{Cre} (encoding DNGR1) [131]. The ontogeny of $CD11b^+$ DCs in the cLP is less clear: *In vitro* cultured monocytes were not labelled using the DNGR1 system, and likewise, $CD11b^+$ $Gr1^+$ cells, phenotypically resembling DCs were not labelled using the DNGR1 system during intestinal inflammation, possibly indicating that DCs could be derived from monocytes [131]. However, the $CD11b^+$ $GR1^+$ gating strategy used to define these cells could in fact represent inflammatory monocyte-derived macrophages [57, 113]. More recently however, a subset of blood monocytes identified by the expression of *Cd209a* was described to preferentially give rise to DCs, and these may represent the precursors to

intestinal CD11b^{+} DCs, but their contribution to the intestinal DC pool is yet to be formally proved [46, 132]. Interestingly, a recent study using single cell clonal assays indicated that multipotent lymphoid progenitors had the capacity to generate both CD11b^{-} and CD11b^{+} DCs, challenging the step-wise classical model of haematopoiesis [133].

cDCs display heterogeneous distribution along the length of the intestine with high numbers of CD11b^{+} CD103^{+} DCs in the small intestine that diminish towards the colon [43]. CD11b^{-} CD103^{+} DCs are the dominant population in the colonic Lamina Propria (cLP), express CCR7, and migrate to the Mesenteric Lymph Nodes (MLN) to prime naïve T cells and induce pathogenic and T regulatory cell (T_{reg}) development [62, 122]. Despite their ability to induce T_{reg} development, CD11b^{-} CD103^{+} DCs can be pro-inflammatory during inflammation [134].

Plasmacytoid DCs (pDCs) are very rare in the cLP, but can be recruited in larger numbers during inflammation [135]. This thesis will primarily focus on the contribution of cDCs, monocytes and macrophages to intestinal homeostasis and inflammation, therefore pDCs will not be discussed further.

Table.1.1: Mononuclear phagocyte subsets in the colonic lamina propria

Phenotype			Ontogeny			Function
Common	**Subset-Specific**		**Progenitor**	**TF**	**Shared**	**Unique**
$CD11c^+$ $MHC\ II^+$ $F4/80^-$ $Ly6C^-$ $CD64^-$ $MerTK^-$	$XCR1^+$	$CD11b^-$ $CD103^+$ CX_3CR1^-	FLT3L-dependent CDP	IRF8 BATF3 ID2 ZBTB46	Migration to MLN (CCR7-dependent)	Cross-presentation T_H1 induction $CD8^+$ T cell induction
	$SIRP\alpha^+$	$CD11b^+$ $CD103^+$ CX_3CR1^+		IRF4 KLF4 Notch2 ZBTB46		ILC3 T_H2 T_H17
		$CD11b^+$ $CD103^-$ CX_3CR1^+		Zeb2 IRF4 ZBTB46		ILC3 T_H1 T_H2 T_H17
$CD11b^+$ $MerTK^+$ $Ly6G^-$ $Siglec\ F^-$	CX_3CR1^{int}	**(P1)** $Ly6C^{hi}$ $MHC\ II^-$ $CD11c^{lo}$	M-CSF-dependent	Runx3 PU.1	TGFβR-signalling IL10R-signalling	Respond to microenvironmental cues Phenotypic plasticity Pro-inflammatory potential
		(P2) $Ly6C^+$ $MHC\ II^+$ $CD11c^{+/-}$				
		$Ly6C^-$ $MHC\ II^+$ $CD11c^{-/+}$ $F4/80^+$				
	CX_3CR1^{hi}	$Ly6C^-$ $MHC\ II^+$ $CD11c^{-/+}$ $F4/80^+$				Anergic Clearance of apoptotic cells/debris Tissue remodelling Pass antigen to cDCs & T_{eff}

The origin of tissue macrophages has been a source of contention in recent years. Macrophages were originally thought to derive from monocytes [41]. However, recent studies indicated that most tissue macrophages were derived and maintained by self-renewal from embryonic precursors [136]. In contrast to this view, Bain and colleagues demonstrated that macrophages in the adult mouse cLP were exclusively derived from monocytes using fate mapping of embryonic macrophages, and haematopoietic progenitors [57]. Monocytes have not been shown to proliferate in tissues or blood, but macrophages replenished by monocytes may self-renew [50, 137]. To date, only TGFβ and IL10 have been described as specifically required for the development of cLP tissue-resident macrophages (Fig.1.4) [138, 139]. CX_3CR1^{IL10R-} mice exhibited heightened inflammation which held macrophages in a pro-inflammatory state, preventing their full differentiation and initiating spontaneous colitis [139]. Loss of TGFβ-Receptor on macrophages resulted in only a minor impairment of macrophage differentiation, defined by transcriptional profiling of monocyte to macrophage transition in the cLP [138]. Therefore the molecules that promote monocyte to macrophage transition in the colon remain poorly characterised.

The highest frequencies of intestinal macrophages are in the colon in both human and mouse [140, 141]. Macrophages appear to be equally distributed along colon, localised close to epithelium [113, 142-144], and deep within the lamina propria [145].

Macrophages in the cLP express the markers CD11b, Ly6C, MHC II, F4/80, CD64, and CX_3CR1 (Table.1.1) [61, 113]. Intestinal macrophages, in contrast to cDCs, do not migrate to the MLN [122]. cLP macrophages are spread throughout the lamina propria, and can sample luminal antigens, engulf apoptotic debris, and mediate tissue repair [43, 141, 146, 147]. At steady state, macrophages are considered to be anti-inflammatory, express high levels of CX_3CR1 and are anergic when stimulated with PRR agonists [57, 59]. IL10R signalling on macrophages appears critical for this phenotype, as selective loss of IL10R, but not IL10, on CX_3CR1^{Cre} mice resulted in spontaneous colitis [139].

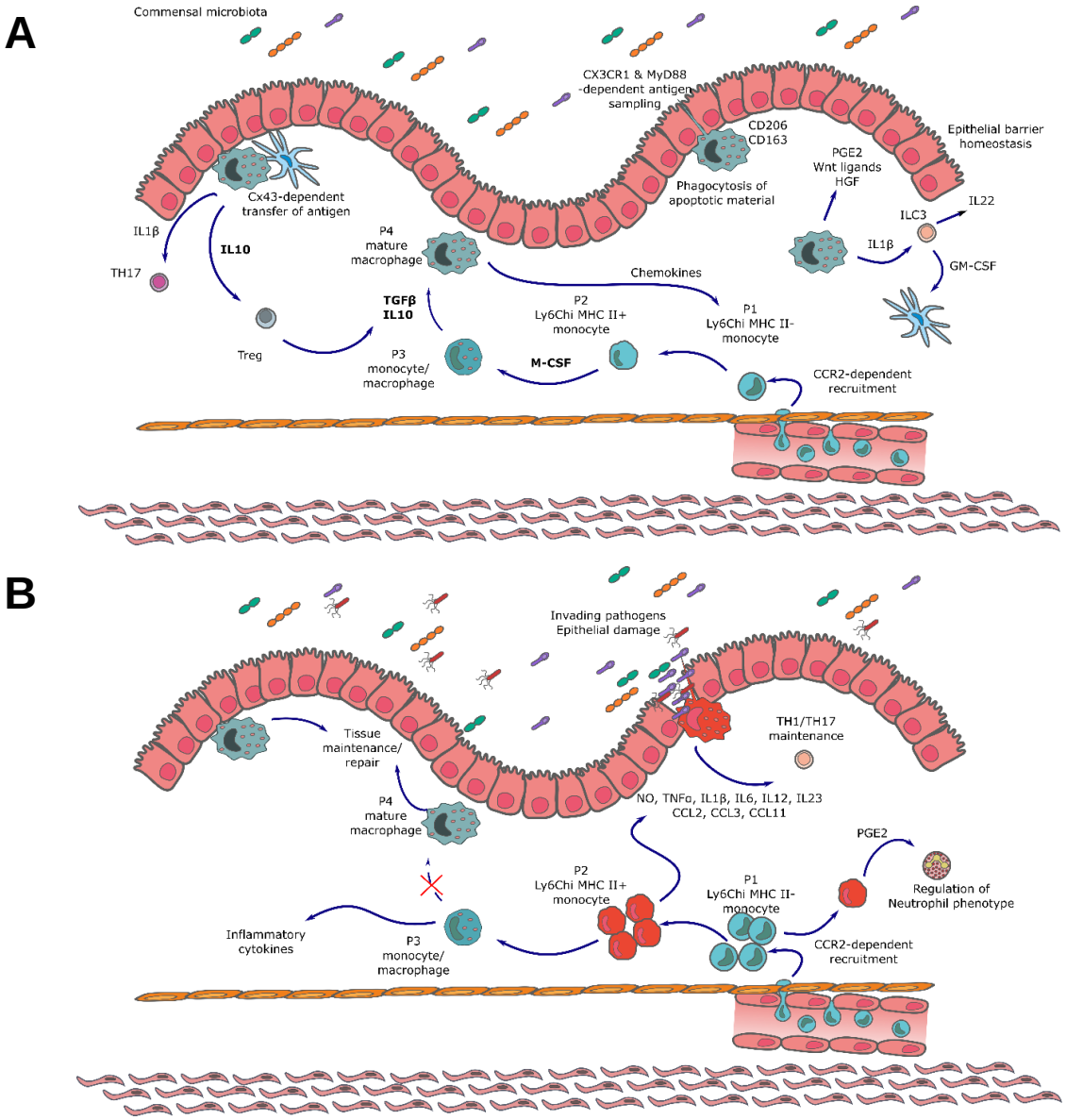

Fig.1.4: Intestinal macrophages at steady state and during inflammation

In the adult mouse at homeostasis, blood Ly6C^{hi} monocytes are recruited in a CCR2-dependent manner to the colonic Lamina Propria (cLP). **A)** Upon arrival, Ly6C^{hi} (P1) monocytes respond to microenvironmental cues and begin the process of differentiation into macrophages. They pass through what is known as the "monocyte waterfall", gradually losing expression of Ly6C, and upregulating mature macrophage markers such as MHC II, F4/80, CD64, and CX_3CR1 progressing through Ly6C^{+} MHC II^{+} F4/80^{lo} CX_3CR1^{int} (P2 monocyte), and Ly6C^{lo} MHC II^{+} F4/80^{+} CX_3CR1^{int} (P3 macrophage), before finally adopting a Ly6C^{-} MHC II^{+} F4/80^{+} CX_3CR1^{hi} (P4 macrophage) resident macrophage phenotype. In this thesis, $CX_3CR1^{GFP/+}$ mice were not used, therefore discrimination between P3 and P4 macrophages was not possible. Resident macrophages carry out diverse functions, such as the transfer of luminal antigens to dendritic cells, production of IL10, clearance of apoptotic material, and promotion of intestinal barrier function via IL1β and PGE_2-mediated control of ILC3 function which occur without an inflammatory response being initiated. **B)** Inflammatory response of cLP macrophages. Inflammatory stimuli leads to the recruitment of P1 monocytes which differentiate into inflammatory effector monocyte/macrophages. These monocyte/macrophages express inflammatory cytokines such as Nitric Oxide, TNFα, IL1β, IL6, IL12, and IL23, and the chemokines CCL2, CCL3, and CCL11 that recruit other inflammatory effector cells, and modulate the immune response. The mediators that prevent differentiation into P4 resident macrophages are unknown at present.

The *Helicobacter hepaticus* model of colitis

Helicobacter hepaticus (Hh) is a helical, bipolar-flagellated, Gram negative bacterium of the Helicobacteraceae family, first isolated from the livers of mice with active hepatitis [148]. Hh is a commensal bacterium that colonises the crypts of the colon and caecum in mice [148, 149]. Hh is considered a pathobiont, in that it may cause inflammation of the large bowel under certain circumstances, such as in the intestines of IL10-deficient mice, but normally forms a symbiotic relationship with the host [150, 151]. Infection with Hh in WT mice results in tolerogenic T_{reg} responses that prevent intestinal inflammation in an IL10-dependent process [152]. Intestinal inflammation in response to Hh can be induced in Wild-Type (WT) mice by the concomitant administration of the anti-Interleukin 10 Receptor (αIL10R) blocking antibody [153]. Multiple studies have demonstrated the importance of the IL10-IL10R pathway in mediating intestinal inflammation, and defects in the IL10R pathway in intestinal macrophages are sufficient to induce spontaneous colitis in mice [139, 154-156]. However, some studies reported that Hh infection of IL10-deficient mice did not induce disease in Specified Pathogen Free (SPF) or germ-free mice, indicating that the host microbiota plays a key role in the progression of intestinal inflammation in response to Hh [157].

The Hh + αIL10R model of colitis is also dependent on intestinal $CD11c^+$ MNP-derived IL23, also shown to be critical in the induction of pathogenic T_H1/T_H17 and ILC3 responses in IBD patients [124, 153, 158]. Infection with Hh alone induces IL23 expression, but does not result in colitis, highlighting the importance of the IL10 axis in this model [153]. A recent study by Danne *et al.,* (2017) demonstrated that Hh infection in the absence of αIL10R resulted in CREB activation and adoption of a tolerogenic phenotype in macrophages in a process dependent on the secretion of an unidentified polysaccharide TLR2 ligand by the Hh bacterium [159].

Administration of αIL10R blocking antibody alone does not induce pathology in the Kennedy Institute of Rheumatology or John Radcliffe Hospital animal facilities, which are

free of Helicobacter species (unpublished data). Therefore, the native microbiota in these facilities is insufficient to induce colitis.

Pathology in the Hh + αIL10R model is driven by innate and T_H1/T_H17 processes that result in the production of high quantities of IFNγ, IL17A, IL17F, and IL22, that help to shape the inflammatory evironment [160, 161].

The Hh + αIL10R model mimics the aberrant host response against commensal microbiota, and reflects aspects of human IBD, such as the accumulation of pathogenic MNPs and altered cytokine milieu, T_H1/T_H17-driven pathology, improper T_{reg} induction.

The intestinal immune system, and the Hh + αIL10R model are therefore useful to study the effects of IRF5 on monocyte-macrophage transition and polarisation in the intestine because cLP macrophages are constantly replenished by blood monocytes, and IRF5 requires a stimulus to exert significant phenotypic effects *in vitro* and *in vivo* [57, 162, 163].

1.8 Inflammatory bowel disease

IBD is a group of debilitating inflammatory conditions of the intestinal tract that affect ~0.5-1% of western populations [21]. Patients with IBD present with a wasting disease, abdominal pain and diarrhoea. The aetiology of IBD is unknown, but interplay between host genetics, and environmental factors, including the diet and microbiota, contribute to disease pathogenesis [21].

Crohn's Disease (CD), and Ulcerative Colitis (UC) are the two principal forms of IBD, but have differing pathologies. CD can affect the entire gastrointestinal (GI) tract, and patients present with skip lesions that can penetrate the entire depth of the intestinal wall, leading to the formation of fistulae [164]. Inflammation is restricted to the colon and rectum in UC patients, and inflamed sites are contiguous and ulcerations are restricted to the mucosa, in contrast to CD [165-167].

CD and UC pathology is accompanied by marked changes in the leukocyte milieu in the colon [21]. A network of cytokines and chemokines (including, but not limited to IFNγ, TNFα, IL1β, IL6, IL12p70, IL17A, IL17F, IL18, IL22, IL23, CCL2-6, CCL20, CXCL8, CXCL10, CXCL11) are released to recruit and activate cells [22, 168]. Neutrophil numbers, and levels of faecal calprotectin (S100A8 and S100A9), are positively correlated with disease severity [169]. Lesions display increased numbers of monocytes and macrophages, and many pathways associated with IBD are shared with macrophage function [143, 170, 171].

Traditional therapeutic strategies use small molecule inhibitors to block inflammation via anti-inflammatory medications such as glucocorticosteroids, and aminosalicylates, or suppress the immune system using azathioprine, cyclosporine or methotrexate [172]. Current gold-standard therapy utilises anti-TNF (αTNF) biologics which have seen great efficacy in the clinic [172]. However, 40% of patients treated are not responsive to αTNF, and 40% of those treated become refractory therapy [173]. Recently, strategies to block other cytokines were tested, however, many of these such as αIL6, and αIL17A failed clinical trials due to adverse effects [165, 172, 174]. Targeting IL23, a T_H1/T_H17 polarising cytokine that is highly produced by intestinal macrophages has shown promise in clinical trials [175]. Nevertheless, there is unmet clinical need for novel IBD therapies, and targeting macrophage pathways may prove a viable strategy to achieve remission.

1.9 Novel genomic techniques offer insights into tissue mononuclear phagocyte identity and function

In order to generate next generation therapies for disease, better understanding of immune regulation is required. Regulation of gene expression in immune cells is controlled by a network of TFs, co-regulatory proteins, and chromatin modifications, which regulate cell differentiation and functional adaptations [73]. The section below outlines how technological advances in functional genomics, specifically in single-cell genome-wide

sequencing, have aided the deconvolution of the molecular basis of myeloid cell differentiation and functional specification.

RNA sequencing

Traditional molecular biology techniques such as qPCR, and microarrays, have proved reliable techniques for the study of gene regulation and cell function. qPCR allows fluorescent quantification of single cell mRNA levels without library preparation or deep sequencing, and is therefore rapid and quantitative [176-178]. Throughput of qPCR can be increased through multiplex setups utilising up to 96 probes, however, because the probes are preselected, little room is left for the discovery of novel genes of interest [179, 180]. Microarrays were the first attempt at quantifying the expression of large numbers of genes, but suffered due to bias introduced by probe selection, photobleeding, and cross-hybridisation [181-184]. To overcome these issues, RNA sequencing technologies were developed but required millions of cells (> 1 μg mRNA input), limiting analysis to common, homogenous populations [184, 185]. In order to study rare populations of biological interest, lower limits of detection were required to facilitate lower input RNA quantities. The Illumina body map expression atlas, Differentiation Map Project, and ImmGen projects utilised these advances to improve the understanding of differential gene expression across tissues and immune cells [186-188].

Next Generation Sequencing technologies

Current analysis of cell types using flow cytometry grouped cells into clusters based on the expression of up to 17 markers (for the most advanced analysers, typically 8-14 markers), followed by sorting and transcriptional/epigenetic profiling. Subsequently, this approach requires *a priori* knowledge or inference to determine relevant parameters to study. Coexpression of markers, and heterogeneity within cell populations defined by traditional gating strategies result in difficulty interpreting the diversity of cell states identified in this manner. Furthermore, the unambiguous detection and functional attribution of distinct lineages is impaired by indirect associations of function with cell surface marker expression

that may not capture the true nature of immune responses. Unsupervised sampling, followed by modelling of transcriptional states in single cells, avoids these pitfalls as they can be used to distinguish stochastic transcriptional variation in resting cells from *bona fide* stimulus responses [92, 130, 189]. Despite this, single cell RNA sequencing (scRNAseq) analyses are limited by amplification bias and labelling error which must be corrected using statistical methods. Recent advances in single cell RNAseq technologies have constantly increased the throughput and sensitivity, and reduced the cost of operation [190]. RNAseq approaches require reverse transcription of cells followed by library preparation and sequencing leading to lengthy protocols.

Single cell RNA sequencing techniques

The advent of scRNAseq technologies began with plate based approaches, where isolated single cells were placed in wells of a qPCR plate containing lysis buffer. Examples of this pioneering technology include STRT, and SmartSeq. Cells could be isolated by microdissection or by Fluorescence-Activated Cell Sorting (FACS) directly into lysis buffer. Plate based technologies suffered from the length of time required to complete the protocol, but this was mitigated by the ability to store the cells before processing and at discrete stages of processing. The SmartSeq2 protocol improved the efficiency of reverse transcription, template switching and pre-amplification over SmartSeq resulting in high sensitivity using this method, with up to 5000-10000 genes detected per cell [191].

The next advance in scRNAseq technologies arose from pooled approaches which barcoded cells at the point of reverse transcription. Barcoding of samples facilitated the pooling of sample to reduce costs and increase throughput. A notable example of this approach is MARSseq described by Jaitin *et al.,* (2014), which combined FACS 384 well cell capture with barcoding to increase throughput and lower costs. [92]

Massively parallel approaches allowed the profiling of tens of thousands of single cells, but reduced the sensitivity of the assay: only 3-10% of transcripts were detected, compared to 10-20% for plate based methods [189]. Massively parallel RNAseq facilitated unbiased cell

capture of single cells into droplets containing lysis buffer and unique barcodes using microfluidics and reverse emulsion technologies, described in DropSeq, inDrop, and 10X [192-194].

The main drawback of RNAseq is that it fails to capture non-poly-A RNAs, including microRNAs (miRNA), long non-coding RNA, circular RNA, and bacterial RNAs which are discarded by poly-T priming of reverse transcription. High-throughput multiplexed samples are also limited in that they only sequence the 3 prime end of transcripts and thus cannot recover splicing patterns or sequence variants. All RNAseq technologies also struggle to detect low abundance transcripts [189].

TFs as key regulators of both myeloid lineage fate and function

Tissue macrophages have diverse functions: microglia prune synapses, red pulp macrophages recycle haem, and peritoneal macrophages regulate Ig production [195-198]. Most tissue macrophages are embryonically-derived, and self-renew *in situ*, however, it is recognised that environmental factors and TFs shape the function of tissue-resident macrophages. For example, the TF Spi-C is critical for haem metabolism in splenic red pulp macrophages [197, 199, 200]. Retinoic Acid induces GATA6 in peritoneal cavity macrophages, and TGFβ regulates microglia phenotype through SMADs, and is partially required for terminal intestinal mph differentiation [138, 198, 201, 202]. Furthermore, epigenetic modification can influence macrophage identity by regulating availability of TF motifs [73]. The pioneer TF, PU.1, is necessary for maintaining Histone 3 Lysine 4 monomethylation (H3K4me1) to open TF motifs to facilitate the binding of other TFs [80, 81, 203]. Cobinding of lineage-specific TFs leads to cell specification by establishing the chromatin landscape [81, 85]. Cell-specific responses to stimuli are co-ordinated by stimulus-specific TFs that bind poised enhancers marked by H3K4me1, and active enhancers marked by Histone 3 Lysine 27 acetylation (H3K27ac) [204-206].

Heterogeneity within defined cell populations can be uncovered by unsupervised clustering of cell surface molecules (flow cytometry and CyTOF), and RNA transcripts [191, 207].

Combining RNA-Seq with other genomic approaches detecting (1) areas of open chromatin (Assay for Transposase Accessible Chromatin (ATAC)-seq [208]) and (2) the regulatory proteins bound to specific regions of the genome (Chromatin Immuno-Precipitation (ChIP)-Seq [39]), Lavin *et al.,* (2014) profiled the expression patterns and chromatin landscape of seven tissue macrophage populations to determine tissue-macrophage specific signatures (Fig.1.5) [58].

Integration of ATACseq with H3K4me1 marks revealed that open regions of chromatin correlated with poised enhancers and gene expression profiles, allowing the identification of putative enhancer signatures to identify candidate regulators for each tissue macrophage cluster [58]. RUNX3 was specifically highly enriched for small and large intestinal macrophages whilst GATA6 was specifically enriched in peritoneal macrophages. This lead Lavin *et al.,* to hypothesise that GATA6 was a likely regulator of peritoneal-specific macrophage enhancers [209, 210].

Lavin *et al.,* then demonstrated that macrophages derived from transplanted adult bone marrow after lethal irradiation of host mice acquired enhancers specific to the reconstituted niche [58]. Fully differentiated macrophages from the peritoneal cavity could be adoptively transferred intratracheally into the alveoli of host mice, and subsequently adopted a resident alveolar macrophage phenotype. The data suggest that some macrophage can retain phenotypic plasticity even after transfer, and that tissue specific signals are the key determinant of macrophage function.

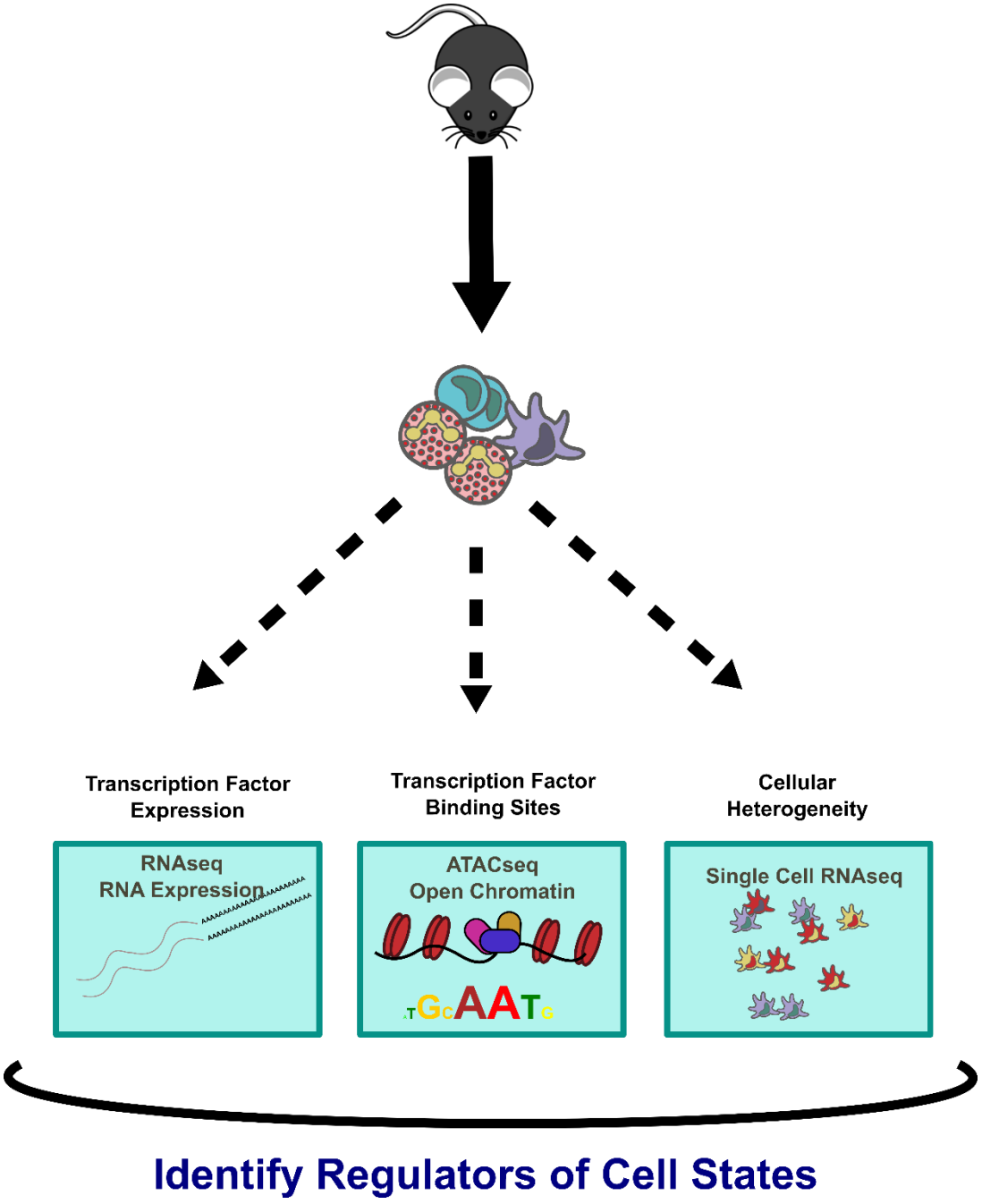

Fig.1.5: Novel genomic techniques for analysis of cell function and ontogeny

Workflow of how next-generation techniques can be utilised to understand molecular biology. Isolated cells can be streamlined into discrete analytical techniques. Bulk RNA sequencing can be used to profile differences in gene expression between conditions. Single cell RNA sequencing can define the heterogeneity of a defined pool of cells. ATACseq profiles regions of open chromatin to identify candidate transcription factors. Integration of these techniques can be used to probe cell-subset specific regulators.

Dissecting cell fate branching points

Developmental processes can be represented as a continuum of transitional cell states. Capturing cells in an unbiased manner across multiple developmental stages and reconstructing the progression allows a method to study cell decision making and differentiation. Bendall *et al.,* created the program, Wanderlust, to reconstruct B cell development from CyTOF data at one timepoint [211]. Meanwhile, Trapnell *et al.,* developed the "monocle" package for the trajectory reconstruction of scRNAseq data, and demonstrated the process on muscle development [212]. Schlitzer *et al.,* analysed the control of DC progenitor fate decisions that committed to either cDC1 or cDC2 phenotype. Using a pool of only 250 cells, including MDP, CDP, and pre-DC, Schlitzer *et al.,* were able to identify the bifurcation point of progenitors marked by differential expression of Siglec H and Ly6C [86]. Siglec H^- and $Ly6C^-$ CDPs gave rise to for cDC1 committed pre-DCs, whereas Siglec H^- $Ly6C^+$ generated cDC2 primed pre-DCs, which were validated *in vitro* [86]. scRNAseq is also useful for the deconvolution of haematopoietic cell states. Paul *et al.,* applied scRNAseq to 2730 haematopoietic progenitor cells. In contrast to the classical model of haematopoiesis, Paul *et al.,* identified 19 cell clusters representing distinct or transitional cell states. In this study, the data suggested that CMPs defaulted to myeloid fate, whilst C/EBPα and C/EBPε were required to specify Granulocyte-monocyte and Neutrophil fate of CMPs.[213]. The findings of the above studies therefore suggest a model whereby a continuum of cell states bridges discrete progenitor stages to generate mature myeloid populations.

Unbiased genomic profiling and deep epigenetic profiling approaches therefore represent powerful tools to appreciate the variety of states present in a pool of defined cells, to delineate haematopoietic hierarchies, and to discover novel gene regulatory elements.

1.10 IRF5 as a regulator of inflammatory macrophage state

The transcription factor, IRF5, is a member of the Interferon Regulatory Factor (IRF) family, first described as a regulator of IFN I response resulting in the activation of distinct IFNα genes [214, 215]. The human IRF5 gene is located on chromosome 7q32, and comprises nine exons [216]. IRF5 transcription is known to be induced by GM-CSFR, IFNγR, and LPS:TLR4 signalling (Fig.1.6) [162, 217] via yet to be explored transcriptional mechanisms, which may include the transcription factors, SP.1, and IRF4 [218]. IRF5 protein has two Nuclear Localisation Signals (NLS), a weakly active C-terminal NLS in the DNA-binding domain, and a phosphorylation-inducible N-terminal NLS. IRF5 also contains a dominant, constitutively active Nuclear Export Signal (NES) [219]. Post-translationally, IRF5 is activated by interaction with MyD88, TRAF6, and IRAK1. IRF5 is also a substrate of IKKε and TBK1, which results in the phosphorylation of the NES and the nuclear retention of IRF5 [220, 221]. However, this phosphorylation event does not result in gene transcription, indicating that other co-factors or post-translational modifications are required for full activation of IRF5.

IRF5 is activated by multiple PRRs, including NOD1, NOD2, TLR2, TLR4, TLR5, and TLR7/9, leading to phosphorylation, ubiquitination, dimerisation, translocation to the nucleus, binding to gene promoters and activation of inflammatory gene transcription [221]. Thus, highlighting the importance of IRF5 in the response to pathogens. One of the cofactors identified is RelA (NFκBp65), of critical importance in inflammatory gene transcription [163].

Another member of the IRF family, IRF4, polarises macrophages *in vitro* to M2 phenotype, whilst IRF5 polarises towards M1 [162]. Contrary to the scientific consensus, a paper from the Hamilton lab (2012) proposed that M-CSF induced IRF5 and GM-CSF induced IRF4, and that IRF4 promoted inflammatory cytokine production [222]. However, differences in GM-CSF concentration used in Hamilton's studies may account for the differences, as in the context of intestinal inflammation differential GM-CSF abundance mediates both pro-

and anti-inflammatory effects [129, 158, 222-225]. IRF5 and IRF4 appear to have an antagonistic relationship, as IRF4 occupies the IRF5 promoter to prevent transcription of the IRF5 gene [226], and is also activated via direct interaction with MyD88, therefore competing for MyD88 binding with IRF5. In this manner, IRF4 is proposed to negatively regulate IRF5 signalling and promote M2 phenotype in macrophages.

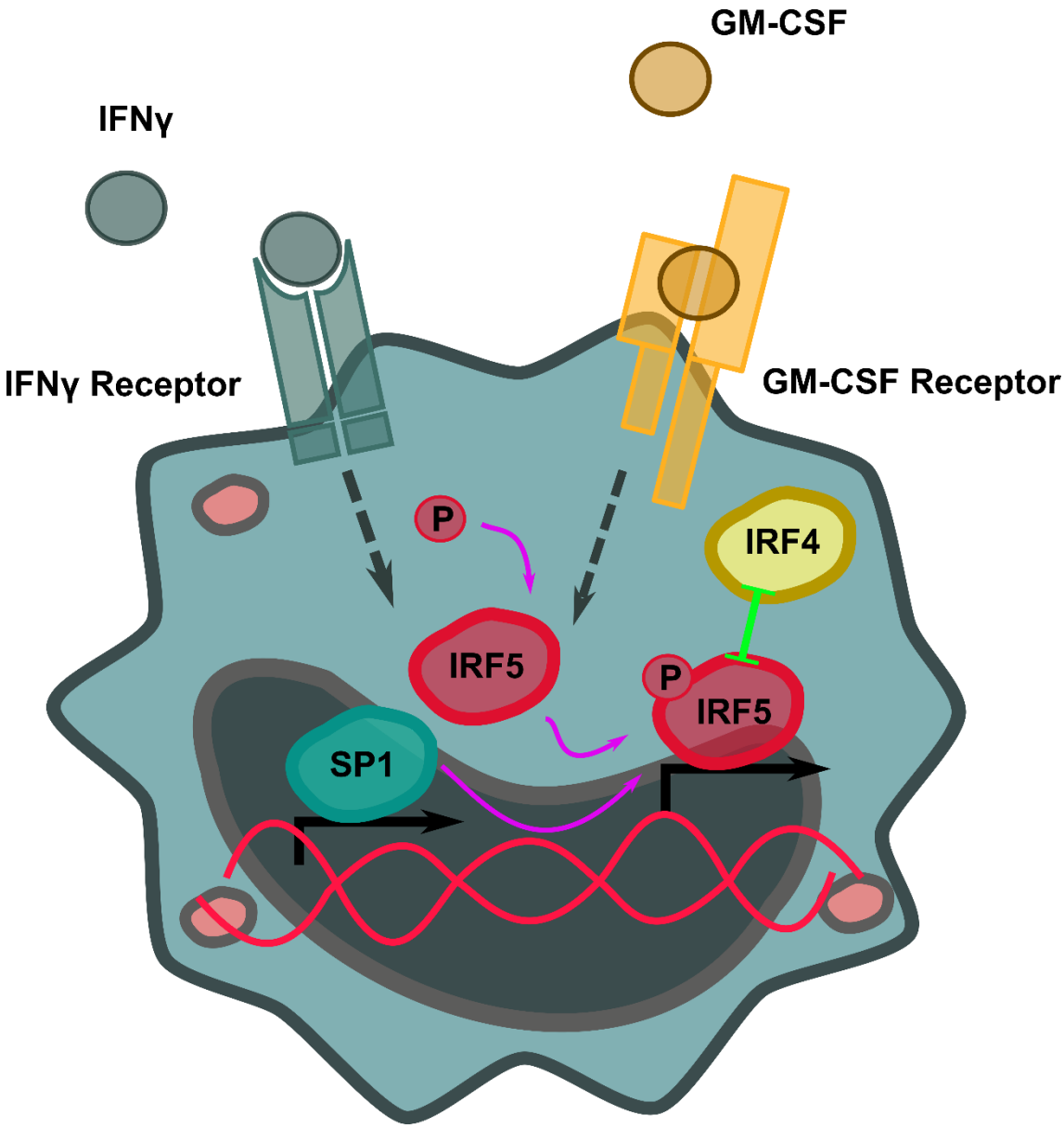

Fig.1.6: Regulation of IRF5 activation

Signalling via the GM-CSF-Receptor (GM-CSFR) promotes IRF5 transcription via the transcription factor, SP.1. Ligation of the Interferon gamma Receptor (IFNγR), or pattern recognition receptors, such as Toll Like Receptor (TLR) 4 by their cognate ligands results in Post-Translational Modification (PTM) of IRF5. PTMs such as ubiquitination or phosphorylation of specific residues allow the dimerisation and nuclear translocation of IRF5. Nuclear IRF5 is then able to promote pro-inflammatory cytokine production (*Tnf*, *Il12b*, *Il23a*), and directly repress the transcription of the anti-inflammatory cytokine, *Il10*. IRF4 is able to compete with IRF5 for promoter binding.
P: Phosphorylation, IRF: Interferon Regulatory Factor

IRF5 was demonstrated to regulate macrophage activation status in murine bone marrow cultures, whilst ectopic expression in human monocyte-derived macrophages also promoted this status [162]. IRF5 expressing macrophages were able to elicit T_H1 and T_H17 responses *in vitro* and expressed inflammatory cytokines (*Il1b*, *Tnf*, *Il12b*, *Il23a*) to a greater degree than IRF5-deficient (*Irf5*$^{-/-}$) macrophages [162]. IRF5 was shown to directly regulate these inflammatory cytokines using ChIPseq [163]. More recently, IRF5 was shown to promote a glycolytic state in macrophages, which supports M1 polarisation [227].

In addition to these T_H1/T_H17 polarising effects, IRF5 is also reported to act as a tumour suppressor. *Irf5*$^{-/-}$ fibroblasts were protected from apoptosis [228], and IRF5 was described as a target of the prototypical tumour suppressor, p53 [229]. IRF5 induced the expression of p21 and Bax in response to DNA damage independently of p53 [230]. Furthermore, TRAIL induced nuclear localisation of IRF5 resulting in the apoptosis of tumour cells [231]. Meanwhile, Fas signalling activated IRF5 upstream of Caspase-8 to promote apoptosis [232]. Consistent with these effects, loss of IRF5 function is associated with many cancers, including Chronic Myeloid Leukaemia, gastric, and breast cancer [233-236].

Gain of function mutations in the IRF5 gene and promoter region increased the risk for a host of inflammatory conditions, including Rheumatoid Arthritis, Systemic Lupus Erythematosus (SLE), atherosclerosis, and Inflammatory Bowel Disease (IBD) [237, 238]. Conversely, loss of IRF5 function resulted in increased predisposition to the Type 2 immune disorder, asthma [56].

IRF5 transcript expression has been described at high levels in pDCs, monocyte-derived DCs, NK cells, and B cells, but not in T cells [162, 239-241]. Taken together, the actions of IRF5 to promote T_H1 and T_H17 responses, produce inflammatory cytokines and chemokines, and the cells that express IRF5 help to partially explain why gain of function mutations in IRF5 predispose to these diseases. Nevertheless, the role of IRF5 in IBD has not been characterised, and the cell intrinsic functions of IRF5 are poorly defined.

1.11 Hypothesis and Aims

Previous work in the IRF5 field has focussed on the macrophage-polarising effect of IRF5 [162, 217, 242]. The contribution of IRF5 to the pathogenesis of various inflammatory disorders, including models of inflammatory arthritis, lupus, asthma and obesity, via recruitment and activation of other effector cells has been characterised [56, 217, 239, 243, 244]. However the intrinsic function of IRF5 within MNP system development has not yet been addressed. The intestine provides a model system to investigate the intrinsic role of IRF5 within a macrophage system that is continually replenished by adult Ly6C^{hi} monocytes [57, 112]. In addition, gain of function mutations in the IRF5 promoter were associated with increased incidence of IBD across multiple populations [237, 238, 245]. But the mechanisms responsible for this association have not been characterised. We hypothesised that IRF5 plays a key role in defining macrophage signature in intestinal inflammation. Therefore, the purpose of this thesis was to:

1. Characterise the role of IRF5 in the mononuclear phagocytes development during haematopoiesis

2. Examine the contribution of IRF5 in the mononuclear phagocytes development in the colonic lamina propria during the steady state and inflammation

3. Identify IRF5-controlled molecular mediators of the intestinal inflammation

2 Materials and Methods

2.1 Mice

Table.2.1 Mouse strains used across DPhil project

Mouse identifier	Strain name	Source	Notes
WT	C57Bl/6 *Ptprc*^{b}	In house	
C57Bl/6 SJL CD45.1	C57Bl/6 SJL *Ptprc*^{a}	In house or University of Oxford Biomedical Services	
Irf5$^{-/-}$	C57Bl/6 *Irf5*^{tm1Ppr}	Takaoka et al., (2005), bred in house	DOCK2 mutant null
$CX_3CR1^{gfp/+}$	C57Bl/6.*Cx3cr1*$^{tmLitt/J}$	Jackson Laboratories, maintained in house	$CX_3CR1^{GFP/+}$ mice used in experimetns
$CX_3CR1^{gfp/+}$ *Irf5*$^{-/-}$	C57Bl/6.*Cx3cr1*$^{tmLitt/J}$ x *Irf5*^{tm1Ppr}	In house	C57Bl/6 *Irf5*^{tm1Ppr} crossed to C57Bl/6.*Cx3cr1*$^{tmLitt/J}$

Mice were bred and maintained under SPF conditions in accredited animal facilities at the University of Oxford. All procedures were conducted according to the Operations of Animals in Scientific Procedures Act (ASPA) of 1986 and approved by the Kennedy Institute of Rheumatology Ethics Committee. Animals were housed in individually ventilated cages at a constant temperature with food and water *ad libitum*. Mice were free of known intestinal pathogens and negative for *Helicobacter* species. Mice used in this thesis are detailed in Table.2.1.

Equal numbers of male and female mice were used in WT vs *Irf5*$^{-/-}$ experimental groups. Male mice were exclusively used as donors and recipients in mixed and whole bone marrow chimaeras.

2.2 Generation of chimaeric mice

≥ 20 g male C57Bl/6SJL (CD45.1^{+}) mice were selected as bone marrow recipients. 2 days before irradiation, mice were fed antibiotic-treated water (Co-trimoxazole, Aspen Pharma) which was maintained until 2 weeks post-irratiation (PI). Recipients were lethally irradiated

by exposure to 10 Gy split into 2 equal doses 6 hours apart in an X-ray irradiator (Gulmay). 6 hours PI on the second day, 4 x10^6 freshly isolated wild-type or *Irf5*$^{-/-}$ (CD45.2$^+$) bone marrow cells in 200 µL sterile PBS (Lonza) were injected intravenously (i.v.) into the tail vein of CD45.1$^+$ wild-type hosts for chimaeras. For mixed chimaeras, 4 x10^6 freshly isolated bone marrow cells at a 1:1 ratio (CD45.1$^+$ wild-type:CD45.2$^+$ *Irf5*$^{-/-}$) were injected i.v. into the tail vein of CD45.1$^+$ wild-type hosts.

6 weeks PI, reconstitution was assessed by collecting blood leukocytes by tail vein bleed, and labelling cells with αCD45.1 or αCD45.2 antibodies to identify recipient and donor cells respectively.

2.3 Culture of Helicobacter hepaticus

Helicobacter hepaticus (*Hh*) NCI-Frederick isolate 1A (Hh1a; strain 51449; American Type Culture Collection) was grown at 37°C on blood agar plates containing Campylobacter-Selective Supplement (skirrow) (CSS, Oxoid) under microaerophilic conditions (10% CO_2, 10% H_2, balance N_2) in a vented CampyPak jar (Oxoid).

After 2 days of incubation on blood agar plates, cultures were harvested using cotton swabs and transferred to liquid culture media (tryptan soya broth (Sigma Aldrich) dissolved in 1000 mL MilliQ H_2O, and autoclaved) + 10% FCS + CSS (Oxoid). *Hh* culture was inoculated at 0.05 OD_{600} in a 500 mL vented Erlenmeyer flasks (Corning). Liquid culture was maintained at 37°C shaking at 140 rpm under microaerophilic conditions (outlined above), and split every 24 hours to 0.05 OD_{600} to maintain stable growth.

Hh viability was assessed by labelling with a fluorescent live/dead assay kit (Molecular probes/Life Technologies) according to the manufacturer's protocol using an Olympus CKX41 microscope (Olympus).

2.4 Assessment of *Helicobacter hepaticus* colonisation

Presence of H. hepaticus in faeces were quantified using the following primers: Fwd; ATG GGT AAG AAA ATA GCA AAA AGA TTG CAA, Rev; CTA TTT CAT ATC CAT AAG CTC

TTG AGA ATC. The thermal cycling was performed on a C1000 Touch (BioRad). Thermal cycling parameters are described in Table.2.2.

Table.2.2: *Helicobacter hepaticus* PCR protocol

# cycles	Time (s)	Temperature (°C)
1	30	94
30	30	94
	45	58
	60	72
1	600	72
1	∞	4

PCR product was run for 45 min - 1 hr at 120 V on a 2% agarose gel stained with RedSafe (Chembio). Gels were visualised using a GelDoc XR System (BioRad).

Caecal contents were collected after mice were sacrificed. DNA was isolated from faeces using Stool DNA extraction kit (Qiagen) as per manufacturer's instructions. qPCR was performed with primers against the *Hh cdtB* gene (Table.2.3) using a Viia7 Real-Time PCR system (Applied Biosystems) as described by Maloy *et al.,* (2003) [160]. In order to construct standard curves, DNA was extracted from Hh cultures using a DNeasy Kit (Qiagen). 10 ng Caecal DNA extract was added to PrecisionFAST qPCR Master Mix (Primerdesign).

Table.2.3: Helicobacter hepaticus Taqman probes

Primer	Sequence
*cdt*B Reverse	TCG TCC AAA ATG CAC AGG TG
*cdt*B Forward	CCG CAA ATT GCA GCA ATA CTT
*cdt*B Probe	AAT ATA CGC GCA CAC CTC TCA TCT GAC CAT

2.5 Helicobacter hepaticus + αIL10R colitis

Mice were infected with $1x10^8$ colony forming units (cfu) *Helicobacter hepaticus* in 200 µL sterile PBS on days 0 and 1 by oral gavage with a 22G curved, blunted needle (Popper & Sons). Mice were injected intraperitoneally once weekly starting on day 0 with 1 mg anti-IL10R blocking antibody (clone 1B1.2) in a volume of 200 µL. Infected mice were monitored weekly for colitis symptoms. Mice were culled by a schedule 1 method on day 20 and organs were harvested for analysis.

2.6 Histological assessment of disease

Post-sacrifice, 0.5 cm pieces of caecum, and proximal, mid and distal colon were fixed in 4% formalin (Sigma Aldrich) diluted in PBS. Fixed tissue was embedded in paraffin blocks, sectioned using a microtome, and subsequently stained with Haematoxylin and Eosin (H&E) by the Kennedy Institute of Rheumatology Histology Facility (Kennedy Institute of Rheumatology, University of Oxford).

Sections were scored in a blinded manner by two researchers according to Izcue *et al*., (2008) set out in Table.2.4 [246].

Table.2.4: Scoring system for *Helicobacter hepaticus* + αIL10R colitis			
Epithelium	**Hyperplasia**	**and/or**	**Goblet Cell Depletion**
0	None		None
1	Mild (1.5x)		Mild (25%)
2	Moderate (2-3x)		Marked (25-50%)
3	Severe (>3x)		Substantial (>50%)

Inflammation in the Lamina Propria	
0	None - few leukocytes
1	Mild - some increase in leukocytes at tips of crypts of many lymphoid follicles
2	Moderate - marked infiltrate (notable broadening of crypts)
3	Severe - dense infiltrate throughout

Area affected	(% of section)
0	None
1	<25
2	25-50
3	>50

Markers of severe inflammation	
0	None
1	Submucosal inflammation OR Few crypt abscesses (<5)
2	Submucosal inflammation AND Few crypt abscesses (<5)
2	Many crypt abscesses (>5) OR Extensive submucosal inflammation OR Crypt branching
3	Many crypt abscesses (>5) AND Extensive submucosal inflammation / Crypt branching
3	Ulceration OR Extensive fibrosis

2.7 Cell isolation protocols

2.7.1 Isolation of intestinal lamina propria leukocytes

Colons and/or caeca were harvested from mice, washed in PBS/BSA and contents were flushed with forceps. Intestines were then opened longitudinally and washed once more before blotting to remove mucus. Gut tissue was then cut into 1 cm long pieces and placed in 50 mL centrifuge tube (Greiner) in ice cold PBS + 0.1% BSA. Sections were allowed to sediment before the supernatant was aspirated. Colons were incubated sideways with

shaking at 200 rpm in 40 mL HBSS + 0.1% BSA + 1% Penicillin-Streptomycin (PS, Lonza) + 5mM EDTA (Sigma-Aldrich) at 37 °C for 10 min before the supernatant was aspirated. This was repeated twice. Tissue was placed in 40 mL PBS + 0.1% BSA + 1% PS for 5 min to dilute EDTA. Intestines were then incubated with 20 mL RPMI + 10% FCS +1% PS + 2.5 U/mL Collagenase VIII (Sigma-Aldrich) + 2 U/mL DNAse I (Roche) sideways with shaking at 200 rpm for 45 mins - 1 hour at 37 °C. Supernatant was filtered through a 70 µm cell strainer to which 30 mL of ice cold PBS + 0.1% BSA + 1% PS + 5 mM EDTA was added to chelate divalent cations and ablate collagenase/DNase activity. Cells were washed in 30 mL PBS/BSA before filtering once more through a 40 µm cell strainer. The cells were then pelleted by centrifugation at 400 g for 10 minutes at 4 °C.

LPLs were isolated by resuspending cells in 4 mL P80 percoll in a 15 mL centrifuge tube (Greiner) before overlaying 4 mL P40 layer. Cells were spun at 3000 rpm for 20 min at room temperature, slow acceleration with no brake applied. Mucus and cellular debris were aspirated from the surface of the P40 layer with a Pasteur pipette and ~7 mL of percoll/LPL mixture was recovered and washed in 40 mL of cold PBS + 0.1% BSA. Cells were pelleted by centrifugation at 400 g for 10 min and resuspended in 1 mL RPMI + 10% FCS + 1% PS before counting.

2.7.2 Isolation of blood leukocytes

Blood was harvested by either tail vein bleed or cardiac puncture. Mice were culled by Schedule 1 method in accordance with the project licence. Prior to cardiac puncture a 1 mL syringe was coated with PBS + 2 mM EDTA. Cardiac puncture was performed with a 29G needle attached to the aforementioned 1 mL syringe.

Tail vein bleeds were performed using a #24 blade scalpel (Swann-Morton Ltd.)

Collected blood was placed in 1 mL of sterile 2 mM EDTA/PBS solution to prevent coagulation in a 15 mL centrifuge tube (Greiner). Tubes were topped up with ice-cold PBS + 0.1% BSA. Cells were pelleted by centrifugation at 400 g for 10 mins at 4 °C and the supernatant discarded. Erythrocytes were then lysed using 10x the blood sample volume

of ACK lysis buffer (Gibco) for 3 mins. Tubes were then topped up to 15 mL with ice cold PBS + 0.1% BSA to quench the lysis buffer. Cells were washed in PBS/BSA, resuspended in PBS/BSA to the desired cell concentration, and stored at 4 °C until required.

2.7.3 Bone marrow isolation

Whole hind legs of mice were harvested and stored at 4 °C until processing. Processing was carried out in a class II lamina flow hood. Femurs and tibia muscle tissue was removed using scissors, followed by dessication in 70% ethanol solution for 3 mins to sterilise bones and for ease of cleaining. Remaining muscle was cleaned using a lint-free tissue.

Scissors were used to cut the ends of bones. A 26G needle was inserted into the opening, and marrow was flushed into a 50 mL centrifuge tube using 10 mL of sterile, ice cold PBS. Cells were then filtered through a 70 µm cell strainer (Greiner). Red blood cells were lysed as described above, using ACK. Cells were resuspended in PBS/BSA at 4 °C until required.

2.7.4 Splenocyte isolation

Spleens were harvested from mice and stored in RPMI + 2% FCS at 4 °C until required. Spleens were then mashed through a 70 µm strainer, and washed through with 10 mL ice cold PBS + 1 mM EDTA. Cells were pelleted by centrifugation for 10 mins at 400 xg at 4 °C and the supernatant was discarded. Erythrocytes were lysed as described above. Cells were resuspended in ice cold PBS/BSA until required.

2.7.5 Monocyte enrichment

Splenocytes or bone marrow leukocytes were prepared as described above. Monocytes were enriched by negative selection using an EasySep™ Mouse Monocyte Isolation Kit (StemCell) according to the manufacturer's instructions. Cells were then resuspended in ice cold PBS + 0.1% BSA for counting and downstream processing.

Cell purity was assessed after each isolation by flow cytometry.

2.7.6 *In vitro* differentiation of bone marrow cells

Bone marrow cells were isolated as described above, counted and $5x10^6$ cells in 10mL BM media (RPMI + 10% FCS + 1% Pen/Strep + 0.001 M β-mercaptoethanol) were seeded in 10 cm bacterial dishes (Falcon, UK). Macrophages were generated either by addition of 20 ng/mL murine GM-CSF (Peprotech). On day 3, 10ml of BM media supplemented with 20 ng/mL GM-CSF was added to the cultures. On day 6, 10 mL of media was collected and floating cells were pelleted by centrifugation at 400 g for 5 min. Pellets were resuspended in 10 ml of BM media supplemented with 20 ng/mL GM-CSF and transferred back to the original culture dishes. Cells were harvested on day 8, resuspended in fresh BM media (without GM-CSF) to a density of 10^6 cells/ml and seeded appropriately.

2.8 Analysis of cytokines in supernatant

2.8.1 Sample preparation

5 mm length segments of colon were excised and placed in 500 µL Bone marrow medium in flat-bottomed 48 well plates (Corning) for 24 hours at 37 °C. After incubation, supernatant was aspirated and placed in 1.5 mL Eppendorf tubes (Eppendorf), spun at 750 g for 5 min at room temperature, and stored at -20 °C.

2.8.2 CCL8 ELISA

Levels of CCL8 in explant culture supernatants was quantified using the Mouse CCL8/MCP-2 DuoSet ELISA (#DY790, R&D systems). Clear 96 well plates (ThermoFisher) were coated with Capture Antibody in PBS and incubated at 4 °C overnight. The next day, plates were washed three times with PBS + 0.05% Tween 20 (Sigma) (PBS/T). Plates were blotted onto paper towel to remove residual liquid after the final wash step. Plates were blocked with 300 µL Reagent Diluent (DY995, R&D) overnight. A standard curve (2000 pg/mL - 15.6 pg/mL was generated by 1:1 serial dilution of purified CCL8 with Reagent Diluent. After blocking, plates were washed again with PBS/T three times. 50 µL of sample (diluted appropriately in Reagent Diluent) was added to each well and incubated overnight at 4 °C. Analysis was performed in duplicate. 100 µL of Detection Antibody, diluted in

Reagent Diluent was added to each well and incubated for 2 hrs at room temperature. Plates were again washed three times in PBS/T and blotted. Next, 100 µL of Streptavidin-Horse Radish Peroxidase (HRP, DY998, R&D) at the working concentration was added to each well. The plate was then covered with a plate sealer and incubated for 20 min at room temperature in the dark. The wash step was then repeated three times. 100 µL of HRP Substrate Solution (DY999, R&D) was then added to each well and incubated for a further 20 minutes at room temperature in the dark. Next, 50 µL of Stop Solution (DY994, R&D) was added to each well and mixed by gentle agitation. Immediately following the addition of Stop Solution, the optical density of each well was quantified at 450 nm wavelength on a SPECTROstar nano spectrophotometric Plate Reader (BMG Labtech), and analysed by MARS Data Analysis software (BMG Labtech)

2.9 Quantitative Polymerase Chain Reaction

Tissue Collection

1 mm sections of proximal, mid, and distal colon were cut using a scalpel, placed in a 2 mL threaded cryovial (Corning) and snap frozen on dry ice. Cryovials were stored at -80°C until required.

Tissue Dissociation

Tissue was placed in a Precellys 2 mL homogenisation tube containing ceramic beads (Precellys) with 300 µL buffer RLT (Qiagen) containing β-mercaptoethanol as per manufacturer's instructions.

Tissue was dissociated by vigorous oscillation (6500 rpm x 20 s followed by 30 s pause, then 6500 rpm x 20 s) in a Precellys 24 homogeniser (Precellys).

RNA extraction

RNA was extracted from tissue homogenate using a Qiagen RNeasy (Qiagen) kit according to manufacturer's instructions. RNA was quantified using a NanoDrop 1000 (ThermoFisher).

cDNA Synthesis

cDNA synthesis was performed using a High Capacity cDNA Reverse Transcription Kit (Applied Biosystems) according to manufacturer's instructions.

Taqman qPCR

For each reaction, 10 ng cDNA was added to 2.5 µL 2X qPCR FAST mastermix (Primerdesign). 0.1 µL primer + Taqman probe mix (Table.2.6) was added to each sample, and the reaction volume was topped up to 5 µL with RNase/DNase-free H_2O (Promega).

Thermal cycling was carried out using a Viia7 real time PCR system (Applied Biosystems). The following protocol was followed for thermal cycling (Table.2.5)

Table.2.5: Thermal cycling parameters for whole colon tissue qPCR

# cycles	Time (s)	Temperature (°C)
1	120	95
40	5	95
	20	60

Table.2.6: Taqman probes

Target	Assay ID	Supplier
Ccl2	Mm00441242_m1	ThermoFisher
Ccl4	Mm00443111_m1	ThermoFisher
Ccl5	Mm01302427_m1	ThermoFisher
Csf2	Mm01290062_m1	ThermoFisher
Cxcl1	Mm00433859_m1	ThermoFisher
Cxcl3	Mm01701838_m1	ThermoFisher
Cxcl5	Mm00436451_g1	ThermoFisher
Il1b	Mm00434228_m1	ThermoFisher
Il10	Mm00439614_m1	ThermoFisher
Il12b	Mm01288990_m1	ThermoFisher
Il5	Mm01290072_g1	ThermoFisher
Il6	Mm00446190_m1	ThermoFisher
Tnf	Mm00443258_m1	ThermoFisher

2.10 Restimulation of T cells for intracellular cytokine labelling

A minimum of 1 x10^6 freshly isolated LPLs were incubated in V-bottomed 96 well plates (Corning) in 250 µL Iscove's Modified Dulbecco's Medium (Gibco) supplemented with 10% FCS + 1% P/S + 0.1 µM phorbol 12-myristate 13-acetate (PMA, Sigma Aldrich) + 1µM Ionomycin (Sigma Alrich) + 10 µg/mL GolgiPlug (BD) for 4 hrs at 37 °C. Cells were washed 3 x in 150 µL FACS buffer before extracellular and intracellular staining.

Macrophage culture for intracellular cytokine labelling

A minimum of 1 x10^6 freshly isolated LPLs were incubated in U-bottomed 96 well plates (Corning) in 250 µL RMPI (Lonza) supplemented with 10% FCS + 1% P/S + 0.1 + 10 µg/mL

GolgiPlug (BD) for 4 hrs at 37 °C. Cells were washed 3 x in 150 µL FACS buffer before extracellular and intracellular staining.

2.11 Flow cytometry

2.11.1 Extracellular labelling of cells

$5x10^5$ - $2x10^6$ cells were plated on either V-bottomed or U-bottomed 96 well plates. The cells were washed twice with 150 µL FACS buffer (PBS + 0.1 % BSA + 1 mM EDTA + 0.01% Sodium Azide) at 400 g for 3 min 4°C. Cells were then Fc blocked for 10 min with αCD16/CD32 (BD) 1/100 in 20 µL FACS buffer at room temperature (RT) followed by washing once in 150 µL FACS buffer. Fixable Viability Dye eFluor®780 (ThermoFisher) and primary extracellular antibodies (Table.2.7) were added at indicated concentrations for 20 min at 4 °C in 20 µL FACS buffer in the dark. Labelled cells were then washed twice with 150 µL FACS buffer. Cells were then fixed for 30 mins in 50 µL Cytofix (BD), washed twice with 150 µL FACS buffer, and resuspended in 200 µL FACS buffer before acquisition.

2.11.2 Intracellular labelling of cytokines

Surface markers were labelled as described above. For Cytokine labelling, cells were fixed in 50 µL Cytofix/Cytoperm (BD), washed twice in 150 µL Perm/Wash buffer (BD) at 600 g, 4 °C. Intracellular antibodies were incubated in 20 µL Perm/Wash at the indicated concentrations (Table.2.7) for 20 mins at 4 °C in the dark, after which samples were washed twice in 150 µL Perm/Wash, and once in 150 µL FACS buffer before resuspension in 200 µL FACS buffer for acquisition.

2.11.3 Intracellular labelling of transcription factors

Surface markers were labelled as described above. For nuclear staining, cells were fixed in 50 µL Fix/Perm (eBioscience) according to manufacturer's instructions, washed twice in 150 µL Perm buffer (eBioscience) at 600 g, 4 °C. Intracellular antibodies were incubated in 20 µL Perm at the indicated concentrations (Table.2.7) for 20 mins at 4 °C, protected from

light. Next, samples were washed twice in 150 µL Perm, and once in 150 µL FACS buffer before resuspension in 200 µL FACS buffer for acquisition.

Table.2.7: Flow cytometry antibodies

Epitope	Colour	Clone	Manufacturer	Cat #	Dilution
Annexin V	APC	N/A	Biolegend	640919	1/20
B220	PerCP Cy5.5	RA3-6B2	eBio	45-0452-82	1/200
CD3	PerCP Cy5.5	145-2C11	Biolegend	100328	1/200
CD4	BV605	RM4-5	Biolegend	100547	1/400
CD11b	V500	M1/70	BD	562128	1/200
CD11b	BV510	M1/70	Biolegend	101245	1/200
CD11c	BV605	N418	Biolegend	117333	1/200
CD11c	BV785	N418	Biolegend	117335	1/200
CD11c	PerCP-Cy5.5	N418	ThermoFisher	45-0114-82	1/200
CD16/32	APC	93	eBioscience	17-0161-82	1/200
CD24	BV711	M1/69	BD	563450	1/200
CD45	V500	30-F11 RUO	BD	561487	1/400
CD45	BV650	30-F11 RUO	BD	563410	1/200
CD45.1	APC	A20	eBioscience	17-0453-82	1/200
CD45.1	BV650	A20	Biolegend	110735	1/200
CD45.1	PE	A20	eBio	12-0453-82	1/200
CD45.1	PE Cy7	A20	eBioscience	25-0453-82	1/200
CD45.2	AF700	104	Biolegend	109822	1/200
CD45.2	FITC	104	BD Pharmingen	553772	1/200
CD45.2	PE	104	eBio	12-0454-83	1/200
CD45.2	PE Cy7	104	Biolegend	109830	1/200
CD45.2	PerCP Cy5.5	104	eBio	45-0454-82	1/200
CD64	PE	X54-5/7.1	Biolegend	139303	1/100
CD81	APC	Eat-2	Biolegend	104909	1/200
CD81	PE	Eat-2	Biolegend	104905	1/200
CD103	PE	2.00E+07	eBioscience	12-1031-82	1/100
CD115	PE	AFS98	eBio	25-1152-82	1/200
CD115	PE/Dazzle 594	AFS98	Biolegend	135527	1/200
CD135	BV421	A2F10	Biolegend	135313	1/200
CD135	PE	A2F10.1	BD Pharmingen	553842	1/200
CD206	APC	CO68C2	Biolegend	141708	1/100
cKit	PB	2B8	Biolegend	105820	1/200
F4/80	APC	BM8	eBio	17-4801-82	1/200
F4/80	PerCP-Cy5.5	BM8	eBioscience	45-4801-82	1/100
F4/80	PE	BM8	Biolegend	123109	1/200
F4/80	PE/Dazzle 594	BM8	Biolegend	123145	1/200
IL-7Ra	PerCP Cy5.5	A7R34	Biolegend	135021	1/200
Ly6C	PE-Cy7	HK1.4	Biolegend	128017	1/200
Ly6C	BV785	HK1.4	Biolegend	128041	1/300

Ly6G	PerCP Cy5.5	1A8	Biolegend	127615	1/200
Ly6G	PE-CF594	1A8	BD	562700	1/200
MHC II	AF700	M5/114.15.2	eBioscience	56-5321-80	1/200
NK1.1	PerCP Cy5.5	PK136	eBioscience	45-5941-82	1/200
Sca1	AF700	D7	eBio	56-5981-82	1/200
Siglec F	BV421	E50-2440	BD	562681	1/200
Siglec F	PE	E50-2440	BD	552126	1/200
Streptavidin	BV605	N/A	Biolegend	405229	1/300
TCRb	PerCP-Cy5.5	H57-597	eBioscience	45-5961-82	1/200
TCRb	AF700	H57-597	Biolegend	109223	1/400
Ter119	PerCP-Cy5.5	TER-119	Biolegend	116227	1/200
Intracellular					
Anti-rabbit	AF488	Polyclonal	Life Technologies	A-11008	1/300
Foxp3	PE-eFluor 610	FJK-15S	ThermoFisher	61-5773-82	1/200
IL-17A	FITC	17B7	eBioscience	11-7177-81	1/200
IFNg	APC	XMG1.2	eBioscience	17-7311-81	1/200
IRF5	N/A	Rabbit polyclonal	abcam	21689	1/100
Live/Dead	eF780	N/A	ThermoFisher	65-0865-14	1/1000
Pro-IL-1b	PE	NJTEN3	ebioscience	12F114-80	1/100

2.11.4 Flow cytometry acquisition and analysis

CompBeads (BD) were used to prepare single stained controls as per manufacter's instructions to set up fluorophore compensation. Fluorescence minus one (FMO) controls were used to set gates for cell populations. Labelled cells were acquired using either an LSR II (BD), or Fortessa X20 (BD) flow cytometer using FACSDiva (BD). Data were analysed using Flowjo (Treestar, Inc.), or viSNE for clustering and dimensionality reduction in Cytobank [247].

2.11.5 FACS

Cells were stained with extracellular cytokines as described above, except no fixation step was performed. Cells were then sorted using a FACSAria™ II (BD) at the Kennedy Institute of Rheumatology FACS facility by Jonathan Webber (University of Oxford).

2.11.5.1 Single cell collection

Single cells were sorted through a 100 µm diameter nozzle into 2 µL of Smart-seq II lysis buffer [191].

2.11.5.2 "Mini-bulk" collection

100 cell "mini bulk" samples were collected for sequencing as described for single cell collection. Samples were processed by the Bowden group (Wellcome Trust Center for Human Genetics, University of Oxford)

2.12 RNAseq Analysis

2.12.1.1 Sequencing of single cells

RNA libraries were prepared using Nextera XT kits (Illumina) followed by Illumina sequencing was carried out according to the protocol described by Picelli *et al.,* (2014) on a Hiseq2000v4 sequencer (Illumina) [191]. This work was carried out in collaboration with the Teichmann group (Wellcome Trust Sanger Institute). Library concentration was assessed by 2100 BioAnalyzer (Agilent).

2.12.1.2 Sequencing of "mini bulks"

RNA libraries were prepared using Nextera XT kits (Illumina) followed by Illumina sequencing was carried out according to the protocol described by Picelli *et al.,* (2014) on a Hiseq2000v4 sequencer (Illumina) [191]. This work was carried out by the Bowden High-Throughput Genomics group at the Wellcome Trust Centre for Human Genetics (University of Oxford).

2.12.1.3 Sequencing data analysis

Data analysis was performed in collaboration with Dr Stephen Sansom (Kennedy Institute of Rheumatology, University of Oxford).

Before in depth analysis of sequencing data was conducted, stringent quality control (QC) parameters were applied using FastQC (*Andrews S. (2010)*

FastQC: a quality control tool for high throughput sequence data. Available online at: http://www.bioinformatics.babraham.ac.uk/projects/fastqc). FastQC was able to generate per-base read quality (Phred score), per-sequence quality score, per base sequence content (GC, N), and analyse sequence length distribution, sequence duplication, over-representation of sequences, adapter content and Kmer content.

Data were mapped to the mm10 genome by hisat2 using a two-pass strategy [248]. featureCounts was used to generate read counts used for downstream statistical analysis [249]. Cufflinks generated per-gene length-normalised frequency per kilobase million mapped reads (FPKMs) for direct comparison of gene expression levels between samples [250].

Post-mapping QC was performed using the Picard Tools developed at the Broad Institute (Broad Institute, http://broadinstitute.github.io/picard), or bespoke functions developed by Dr Stephen Sansom (University of Oxford).

Data normalisation, transformation, and differential expression analysis were carried out with the DEseq2 package in R by Dr S. Sansom [251].

2.12.2 10X single cell RNA sequencing

Analysis of 10X data was performed by Dr. S Sansom (University of Oxford). Single cells were captured and barcoded using the 10X protocol (https://www.10xgenomics.com). Indexed cells were sequenced by Hiseq4000. Fastqc files were generated and passed through the Cellranger pipeline (10X Genomics). Read alignment was performed using STAR (10X Genomics) which allowed identification of single cells using Unique Molecular Identifiers (UMIs). Cellranger was then used to perform preprocessing and downsampling of reads. Downsampled reads was passed through the Seurat package in R [252]. Cells expressing fewer than 500 genes were discarded, as were cells with a fraction of mitochondrial reads over 0.05. Genes expressed in fewer than three cells were removed from the data before analysis. A linear model was used to regress out the latent variables: (nUMI,percent.mito), before further analysis. Regression was performed to remove highly

variable samples before Principle Component Analysis (PCA) was performed where a standard deviation threshold of 0.5 was used to identify variable genes. The top 25 principle components were analysed using the tSNE algorithm to visualise the data in two dimensions. Clustering of tSNE was performed using the “Original Louvain” algorithm with resolution set to 0.6. Differential expression testing was performed with the “negbinom.cluster.dir” function.

2.12.3 Pseudotime analysis of colonic lamina propria mononuclear phagocytes

Pseudotime analysis was performed using the R package “monocle” to order cells in terms of differentiation state [212]. Analysis was performed by Dr. Stephen Sansom (Kennedy Institute of Rheumatology, University of Oxford).

2.12.4 ChIPseq peak calling

ChIPseq was performed on *in vitro* differentiated GM-BMDMs [163]. Peaks were called by Dr. Stephen Sansom (Kennedy Institute of Rheumatology, University of Oxford). Reads (50bp paired-end) were quality trimmed with Trimmomatic (options=LEADING:5) [253]. Trimmed reads were then mapped to the mouse genome (mm10) with Bowtie2 [254]. Mapped reads were filtered to remove those with a mapping quality < 10. Peaks were called 2hrs after LPS stimulation (against IRF KO control pulldowns) using MACS2 (https://github.com/taoliu/MACS).

Reproducibility was assessed (n=2 replicates) using the Irreproducibility Discovery Rate (IDR: https://sites.google.com/site/anshulkundaje/projects/idr). 1409 peaks (with an IDR < 10%) were found to be associated to 810 genes using default GREAT promoter definitions [255]

2.13 Boyden chamber migration assay

Easysep-enriched monocytes were seeded at 20,000 cells/well in 80 uL on, Wells of a 96 well ChemoTX disposable chemotaxis system (Neuro Probe) were filled with 300 µL Boyden Media (RPMI + 0.1% BSA + 25 mM HEPES) with or without chemotaxis stimuli at

desired concentrations. A 96 well, 8 µm pore size mesh was placed on top of filled wells. 80 µL of enriched monocytes at a concentration of 250 cells/µL in Boyden Media was overlaid on each membrane well. Cells were incubated for 90 mins at 37 °C, 5% CO_2 in a humidified HeraCell 150 incubator (ThermoFisher).

After incubation, the media were discarded, and the membrane was rinsed briefly with PBS + 0.1% BSA to remove loosely, and non-adherent monocytes. The membrane was then fixed for 3 hours - overnight in 4% paraformaldehyde/PBS solution, rinsed with PBS, and again incubated for 3 hrs – overnight in 30% sucrose/PBS. The membrane was rinsed in PBS one final time, before air drying. Air-dried membranes were excised from the frame, and experimental groups were mounted on positively charged polysine slides in Glycerol Mounting Medium with DAPI + DABCO (ab188804, Abcam). Slides were coverslipped, and covers were painted around the edges with nail polish to seal. Slides were kept overnight in the dark at room temperature to air dry.

Slides were then imaged using a BX51 fluorescent microscope (Olympus). Four images/well were acquired at 10 x magnification and resolution of 1240 x 1024 pixels. Numbers of cells/field were counted using ImageJ [256]. For counting, images were converted into 16 bit format. Cells were defined as having a circularity coefficient ≥ 0.8 and between 25 and 400 pixels in diameter.

2.14 Statistical analysis

Data were analysed using Prism V.7 (GraphPad). Statistical tests were performed as indicated in figure legends. Cell numbers and percentages identified by flow cytometry, and histological scoring are represented by dot plots. Mean Fluorescence intensity (MFI), protein abundance, and relative RNA abundance are displayed as bar plots.

Pooling of experimental repeats was accepted when Bias ≤ 1 and all data points fell within 95% CI after data were plotted using the Bland-Altman method. Where experiments did not

show concordant results, alternatively shaded symbols are shown to distinguish separate experiments.

Statistical analysis of RNA sequencing data was performed by Dr. Stephen Sansom (Kennedy Institute of Rheumatology, University of Oxford).

Differences were considered statistically significant when $p \leq 0.05$.

3 IRF5 in the homeostatic colon lamina propria

3.1 Introduction

The intestinal lamina propria is a mucosal organ that facilitates the selective absorption of nutrients and water from the diet [257]. Because of this nutrient-rich environment, the intestine is host to trillions of microorganisms which engage in a symbiotic relationship with the host to facilitate nutrient digestion and absorption [117, 257]. However, some of the microflora are pathogenic and invade the host tissues resulting in inflammation as with *Clostridium difficile* infections [258]. In some patients, the host mounts aberrant immune responses against the commensal microbiota, leading to Inflammatory Bowel Disease (IBD) [21]. The balancing act of maintaining intestinal homeostasis is carried out by a network of immune and non-immune cells that reside in the intestinal mucosa [21].

Genome-Wide Association Studies (GWAS) have identified many defects in human immune pathways that increase the risk of IBD [22, 259, 260]. Many of the affected pathways are present in macrophages, highlighting a central role for macrophages in IBD pathogenesis [171]. One such factor is Interferon Regulatory Factor (IRF) 5, which is highly expressed in macrophages, but thus far has not been characterised in the intestine [162, 237, 261].

Macrophages are highly plastic cells, able to respond and adapt to environmental cues [262, 263]. Intestinal macrophages are critical effector cells in the establishment of intestinal inflammation and return to homeostasis [264]. The scientific consensus is that colonic Lamina Propria (cLP) macrophages are exclusively derived from circulating monocytes that enter the tissue, but the factors that promote macrophage fate have not been identified [43, 57]. The replenishment of intestinal macrophages by monocytes adds another layer of regulation to macrophage effector functions; the ability to rapidly modulate the number of effectors within the cLP, and facilitating their phenotypic adaptation to fluctuating environmental cues upon entry [198, 210, 265].

Monocytes arise through the stepwise differentiation of haematopoietic stem and progenitor cells (HSPCs) [49]. In the bone marrow, Haematopoietic stem cells give rise to Common Myeloerythroid Progenitors (CMPs) that can differentiate into either Megakaryocyte-Erythroid Progenitors (MEPs), or Granulocyte-Macrophage Progenitors (GMPs). GMPs may produce granulocytes, including neutrophils and eosinophils, or myeloid progenitors, which are committed to the production of monocytes, macrophages and Dendritic Cells (DCs) via Monocyte-Macrophage Dendritic cell progenitors (MDPs). MDPs bifurcate into common Monocyte Progenitors (cMoPs) or common Dendritic Cell Progenitors. cMoPs preferentially give rise to $Ly6C^{hi}$ monocytes, but are also able to differentiate directly into patrolling $Ly6C^{lo}$ monocytes [46]. cMoPs are defined: Lin^- $cKit^+$ $CD135^-$ $CD115^+$ $Ly6C^{-/+}$ $CD11b^-$ $CD11c^-$ MHC II^-, but also express CX_3CR1 [49].

PU.1 (Spi1) is a lineage defining transcription factor for macrophages in mice and humans [266, 267]. Expression of PU.1 in HSPCs is induced by M-CSF receptor signalling, which is able to ensure commitment of CMP to the monocyte lineage via upregulation of Kruppel-Like Factor 4 (KLF4) [268, 269]. PU.1 also promotes EGR1 and EGR2 expression, and interacts with C/EBPα to repress neutrophil fate of GMPs via activation of macrophage-specific genes [85, 270, 271]. IRF8, another lineage defining transcription factor, is expressed from GMP stage onwards, and also represses neutrophil development [83, 84, 272].

Griseri *et al.,* (2012) demonstrated a skewing of haematopoiesis towards increased numbers of CMPs and GMPs in mouse models of colitis, driven by GM-CSF, a growth factor that also promotes a colitis-driving pathogenic eosinophil phenotype in the cLP [69, 129]. Resetting the immune system by radiation depletion of leukocytes followed by transplantation of haematopoietic progenitors may be a therapeutic option for IBD [273, 274]

GM-CSF is a well characterised growth factor that supports the differentiation of GMPs into macrophage/DCs, and the survival of neutrophils, monocytes, macrophages and DCs via

binding to the heterodimeric GM-CSF Receptor (GM-CSFR). Interferon gamma (IFNγ) signalling is able to modulate haematopoiesis, reducing the CFU activity of Haematopoietic Stem Cells (HSCs), and promoting the production of monocytes from GMPs via reduction of STAT3 signalling [275].

IRF5 was described to be important in the development of AIA in mice, and has been characterised in the response of GM-CSF-differentiated Bone Marrow Derived Macrophages (GM-BMDMs) to Lipopolysaccharide (LPS) [162, 217, 261]. The paradigm of macrophage ontogeny has been subject to multiple shifts since their discovery; macrophages were originally believed to be derived purely from monocytes, then macrophages were derived only from the yolk sac or foetal liver [57, 136, 199]. It was then accepted than in inflammation macrophages could derive from monocytes. Only recently, have monocyte-derived macrophages been described in steady state colon [57]. The colon represents a shift in the paradigm, in that it is the only organ described where macrophages in the adult mouse are currently believe to be derived exclusively from monocytes [264].

The role of IRF5 in the polarisation of tissue macrophages has been characterised, and tissue macrophage development did not appear to be affected [162, 239, 261]. The colon represents a revisited paradigm in macrophage development because cLP macrophages were shown to be exclusively derived from blood Ly6C^{hi} monocytes, in a process that is partially dependent on the microbiota [57]. *Irf5*$^{-/-}$ monocytes experienced defective accumulation in a pristane-lupus model indicating that activation of IRF5 by extrinsic signals may be required for phenotypes to manifest [239]. The colon presents an excellent system to test the hypothesis that monocyte to macrophage replenishment and development may be defective in IRF5 deficiency due to the continued stimulation of PRRs by the microbiota [276]. This chapter therefore examines the impact of IRF5 deficiency on the homeostatic cLP and haematopoietic system Using global IRF5 knockout mice (*Irf5*$^{-/-}$), mixed bone marrow chimaeras, and *in vitro* culture approaches, IRF5 expression and myelopoiesis are investigated in steady state (uninfected) mice.

3.2 Results

3.2.1 Phenotypic characterisation of Irf5$^{-/-}$ mice at steady state

Here, we use the mouse cLP as a model system of macrophage development and function. IRF5 expression in the colonic Lamina Propria (cLP) has not been described, nor the effects of IRF5 deficiency. To better understand the role of IRF5 in the colon, *Irf5*$^{-/-}$ mice were profiled at steady state.

The cLP of *Irf5*$^{-/-}$ mice were largely similar to WT in their phenotype. Colons (Fig.3.1), and caeca (Fig.3.2) of WT and *Irf5*$^{-/-}$ were comparable in morphology, and did not display obvious signs of inflammation (colitis score < 3).

The immune compartment of the cLP was then profiled by flow cytometry. The numbers of leukocytes in the colon (Live CD45^{+}) were comparable between WT and *Irf5*$^{-/-}$ (Fig.3.3).

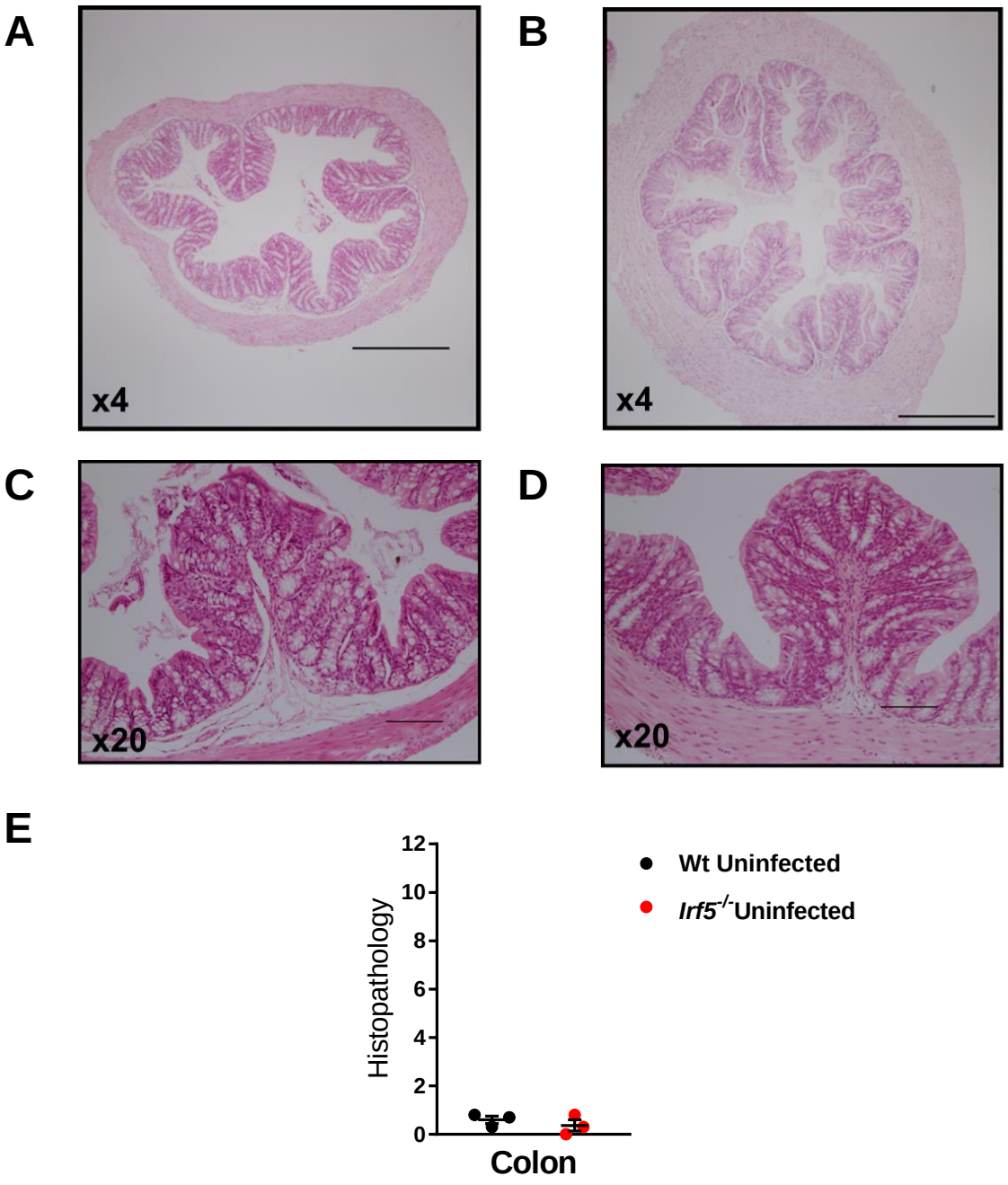

Fig.3.1: Colon morphology is unchanged by IRF5 deficiency at steady state

Segments of mouse colon were excised upon sacrifice and fixed in neutral buffered formalin for 24 hrs. Specimens were dehydrated in Xylene and mounted in paraffin blocks for sectioning. Sections were stained with haematoxylin and eosin and imaged. Photomicrographs depict: steady state **A)** Wild Type (WT), and **B)** *Irf5*$^{-/-}$ colon at x4 magnification. Steady state **C)** WT, and **D)** *Irf5*$^{-/-}$ colon at x20 magnification. No gross morphological changes were observed in the absence of inflammation. **E)** Sections were scored for signs of inflammation according to the defined strategy (Table.2.4). Briefly, epithelial dysplasia, nucleated cell infiltrate, area affected, and submucosal oedema were subjectively measured. WT and *Irf5*$^{-/-}$ colons did not display signs of inflammation (score < 3). No Histological differences were detected between WT and *Irf5*$^{-/-}$.

Statistics:
Data presented are representative of two independent experiments WT n = 3, *Irf5*$^{-/-}$ n = 3
Mean + SEM. Unpaired t test.

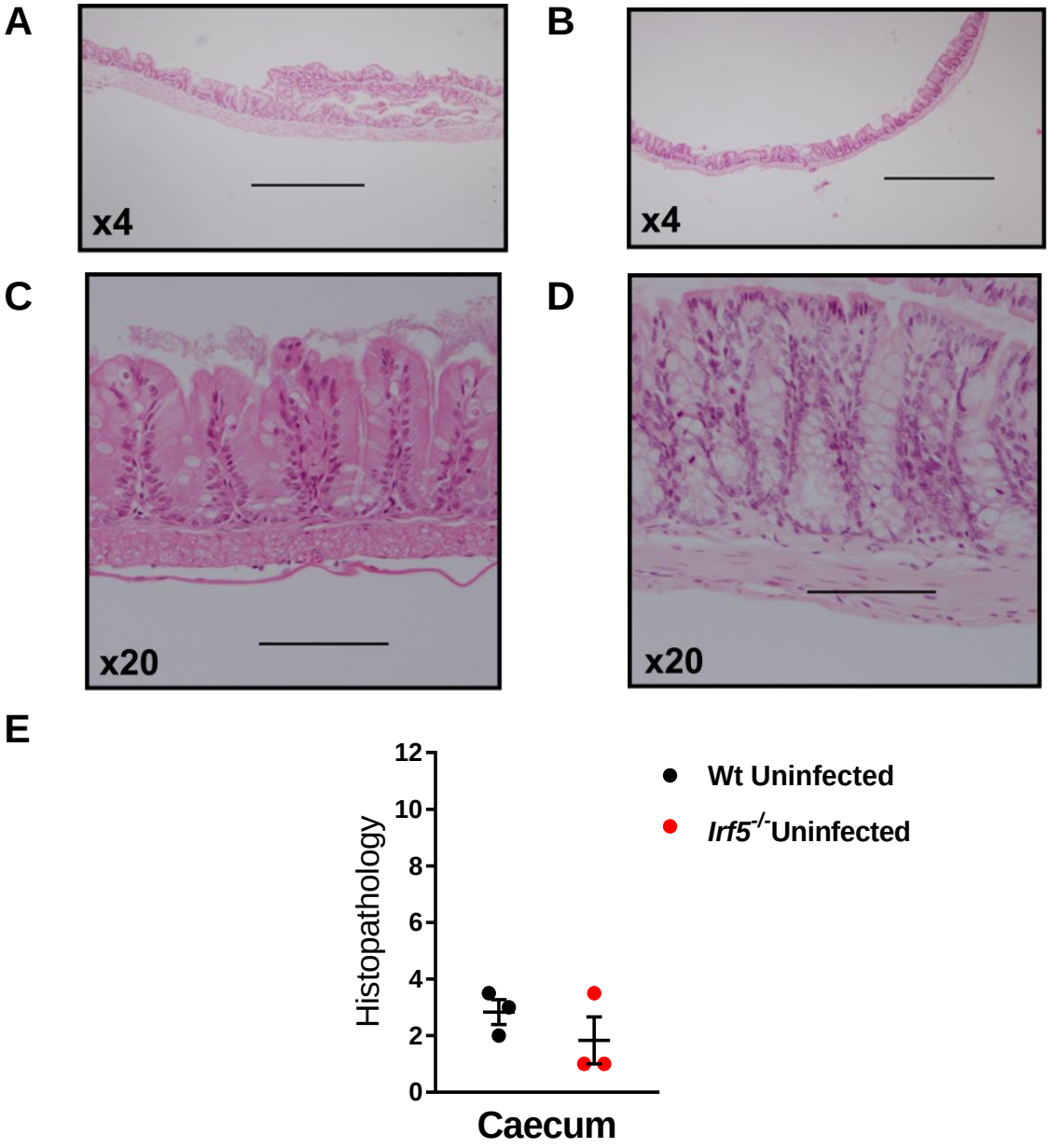

Fig.3.2: Caecum morphology is unchanged by IRF5 deficiency at steady state

Segments of mouse caecum were excised upon sacrifice and fixed in neutral buffered formalin for 24 hrs. Specimens were dehydrated in Xylene and mounted in paraffin blocks for sectioning. Sections were stained with haematoxylin and eosin and imaged. Photomicrographs depict: steady state **A)** Wild Type (WT), and **B)** *Irf5*$^{-/-}$ caeca at x4 magnification. Steady state **C)** WT, and **D)** *Irf5*$^{-/-}$ caeca at x20 magnification. No gross morphological changes were observed in the absence of inflammation. **E)** Sections of steady state WT and *Irf5*$^{-/-}$ caeca were scored for signs of inflammation according to the defined strategy (Table.2.4). Epithelial dysplasia, nucleated cell infiltrate, area affected, and submucosal oedema were subjectively measured. WT and *Irf5*$^{-/-}$ caeca displayed mild signs of inflammation, but no significant difference was detected between genotypes.

Statistics:
Data presented are representative of two independent experiment. WT n = 3 *Irf5*$^{-/-}$ n = 3.
Mean + SEM. Unpaired t test.

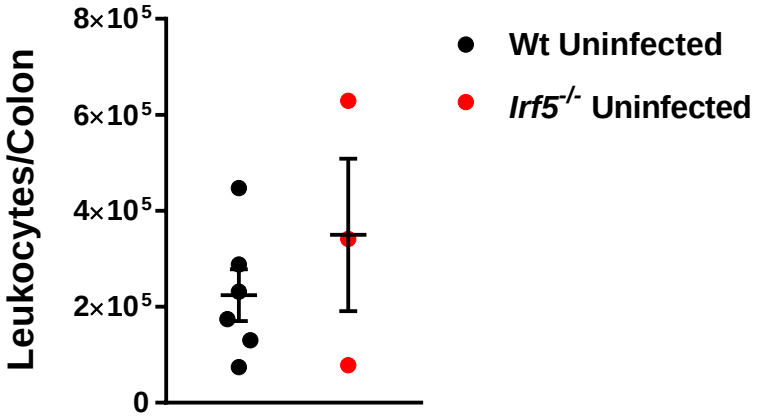

Fig.3.3: The number of leukocytes isolated from mouse colons is unaffected by IRF5-deficiency.

cLP cells were isolated from WT or *Irf5*$^{-/-}$ mice and counted. The percentage of cLP leukocytes was determined by flow cytometry. The number of leukocytes per colon was determined by multiplying the number of isolated cells by the percentage of leukocytes in each colon. No difference was detected between WT and *Irf5*$^{-/-}$ in the number of cLP leukocytes.

Statistics:
Data are representative of two independent experiments, WT n = 6, *Irf5*$^{-/-}$ n = 3 Mean + SEM
Unpaired t test; ns = not significant

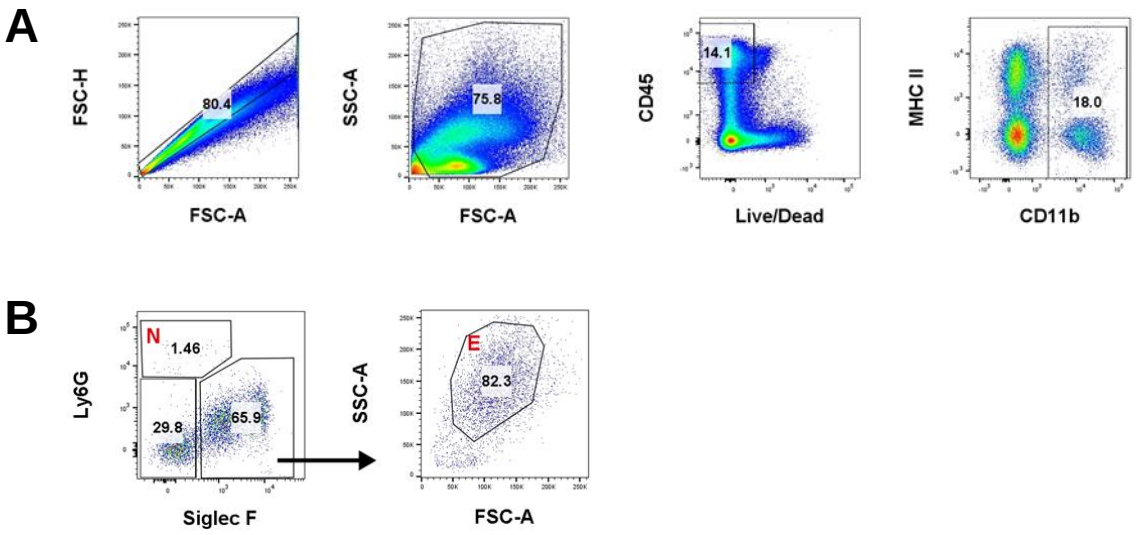

Fig.3.4: Granulocyte gating strategy

cLP leukocytes were isolated from the colons of WT and *Irf5*$^{-/-}$ mice and profiled by flow cytometry. Gating strategies for delineating: **A)** myeloid cells **B)** granulocytes; (N) neutrophils, (E) eosinophils Flow cytometry tiles are representative of steady state WT mice.

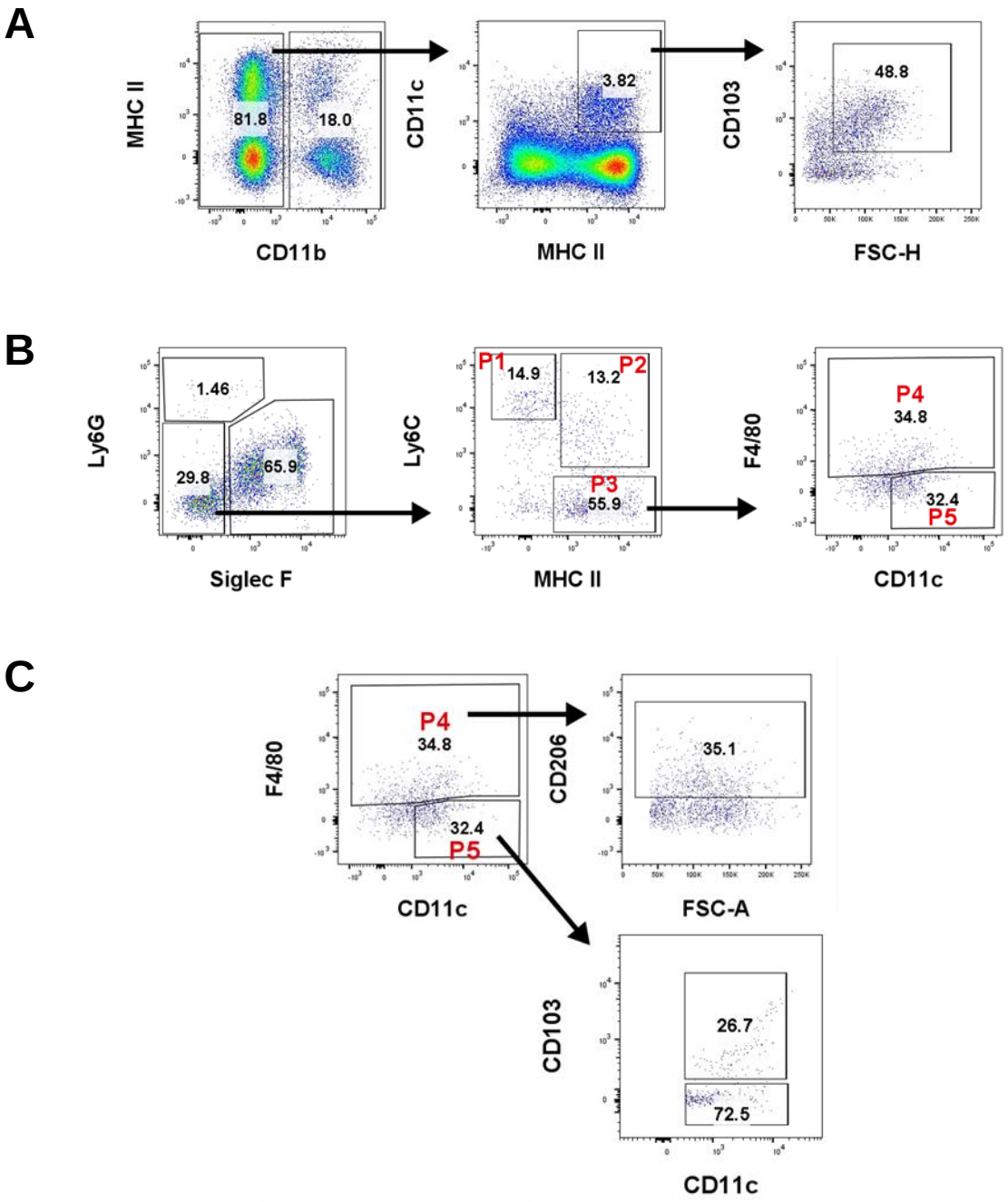

Fig.3.5: Mononuclear phagocyte gating strategy

cLP leukocytes were isolated from the colons of WT and *Irf5*$^{-/-}$ mice and profiled by flow cytometry. Gating strategies for: **A)** Gated Live CD45^{+}, CD11b^{-} CD103^{+} DCs, **B)** Gated Live CD45^{+} CD11b^{+}, (P1) Ly6C^{hi} MHC II^{-} monocytes, (P2) Ly6C^{hi} MHC II^{+} monocytes, (P4) macrophages, **C)** CD206^{+} macrophages, CD11b^{+} CD103^{-} DCs, CD11b^{+} CD103^{+} DCs
Flow cytometry tiles are representative of steady state WT mice.

3.2.2 Characterisation of IRF5 expression in the steady state colonic lamina propria

Macrophages are known to express IRF5 in many tissues, but the profile of IRF5 expression in the cLP was not described at the time of writing. Expression of IRF5 in the cLP was therefore measured by flow cytometry. Granulocytes (Fig.3.4), and mononuclear phagocytes (MNPs, Fig.3.5) were identified using the defined gating strategies. Neutrophils did not express IRF5 at steady state, and a low percentage of eosinophils expressed IRF5 to a low level (Fig.3.6A, Fig.3.6B). High percentages of monocytes, macrophages and DCs expressed IRF5, and these populations expressed IRF5 to a high level, but IRF5 expression was not significantly different amongst MNPs at steady state (Fig.3AB, Fig.3B). Very few $CD45^-$ (Stroma and epithelia), and $CD11b^-$ cells expressed IRF5, and the level of IRF5 expression was very low in these cells (Fig.3.7)

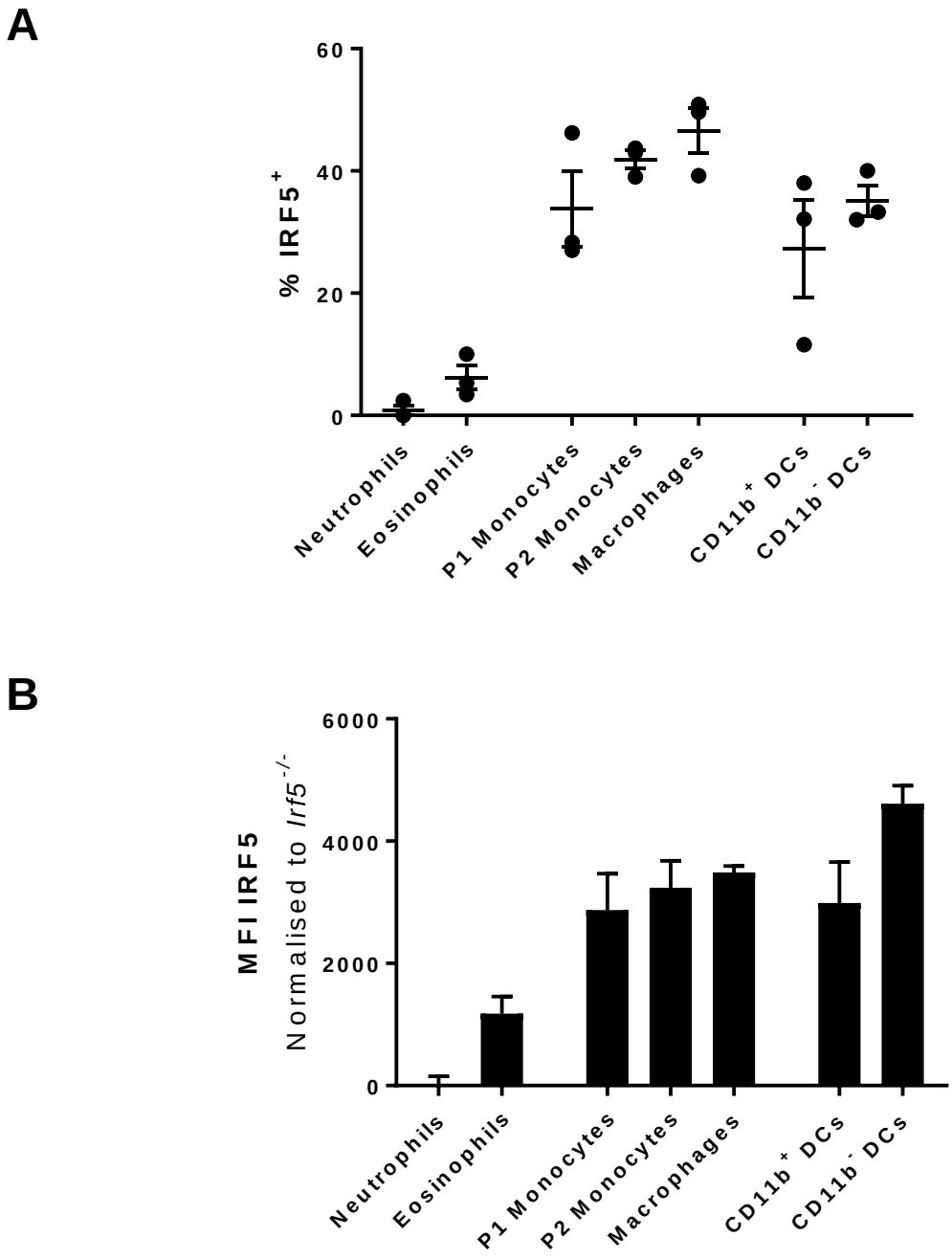

Fig.3.6: IRF5 expression in the steady state colonic lamina propria

cLP leukocytes were isolated from the colons of steady state WT and *Irf5*$^{-/-}$ mice and profiled by flow cytometry. The expression of IRF5 was assessed and normalised to the autofluorescent signal from *Irf5*$^{-/-}$. Neutrophils and eosinophils expressed low levels of IRF5. P1 monocytes, P2 monocytes, macrophages, CD11b^{+} DCs, and CD11b^{-} DCs expressed high levels of IRF5.
Data shown are n = 3 of WT normalised to n = 3 *Irf5*$^{-/-}$ are representative of two independent experiments

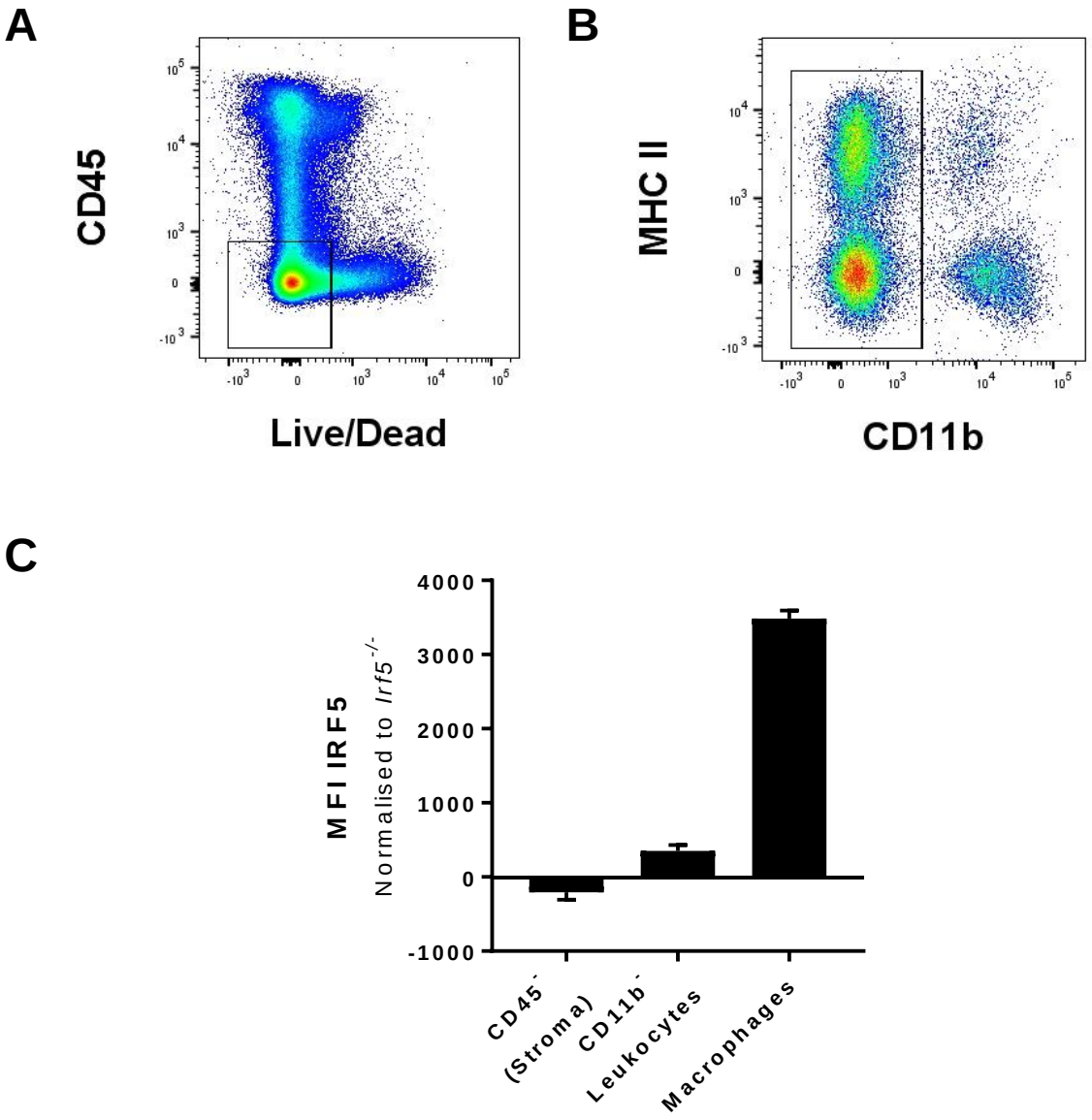

Fig.3.7: Expression of IRF5 in stroma and lymphoid compartments.

Expression of IRF5 in non-myeloid cells was quantified by flow cytometry. **A)** Stroma (defined Live $CD45^-$), and **B)** $CD11b^-$ leukocytes (Live $CD45^+$ $CD11b^-$) expressed low levels of IRF5 **C)** compared with macrophages at steady state.

Data presented are representative of two independent experiments. WT n = 3, *Irf5*$^{-/-}$ n = 3 (for MFI normalisation)

3.2.3 T_H1 and T_H17 cells in the steady state colonic lamina propria of *Irf5*$^{-/-}$ mice

IRF5 expressing macrophages are known to drive T_H1 and T_H17 responses *in vitro*, and in a model of Rheumatoid Arthritis (RA), and to repress transcription of the anti-inflammatory cytokine, IL10, which may impact the development of T-regulatory cells (T_{regs}) [162, 261, 277]. T cells in the cLP were therefore profiled by flow cytometry (Fig.3.8); T_H1, T_H17, and T_H1/T_H17 cells were not affected by IRF5 deficiency at steady state (Fig.3.8A, Fig.3.8B, Fig.3.8C). T_{regs} were also present in equal proportions at steady state (Fig.3.8D).

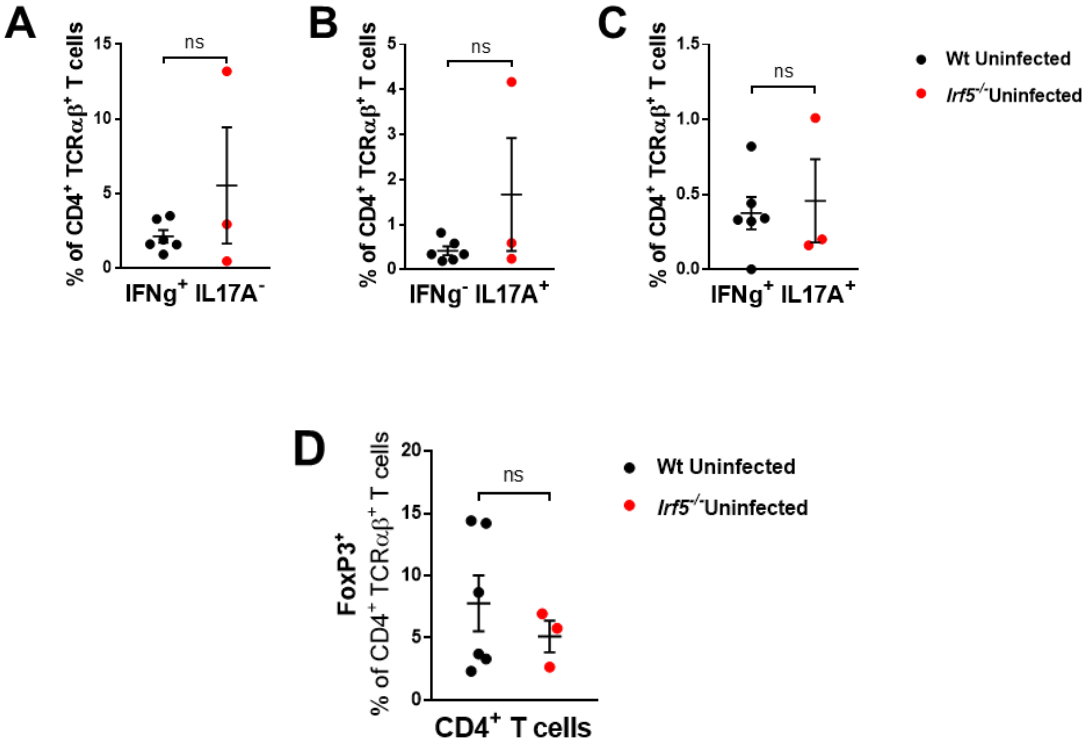

Fig.3.8: WT and *Irf5*$^{-/-}$ mice have similar percentages of T_H1, T_H17, and T-regulatory cells at steady state

cLP leukocytes were isolated from steady state WT or *Irf5*$^{-/-}$ mice and cultured in the presence of PMA:Ionomycin + protein transport inhibitor for 4 hrs. Proportions of T_H cells expressing IL17A, IFNγ, or FoxP3 were analysed by flow cytometry. No difference in the percentages of **A)** T_H1, **B)** T_H17, or **C)** T_H1/T_H17 cells were detected between WT and *Irf5*$^{-/-}$. **D)** FoxP3$^+$ T cells (T_{regs}) in the cLP were not significantly affected between steady state WT and *Irf5*$^{-/-}$ mice.

Statistics:
Results are representative of two independent experiments. WT: n = 6, *Irf5*$^{-/-}$: n = 3
Mean + SEM. **A-C)** Unpaired t test; ns = not significant **D)** Mann-Whitney U-test: ns = not significant

3.2.4 *Irf5*$^{-/-}$ mice display reduced frequencies of macrophages within the mononuclear phagocyte compartment at steady state

The myeloid compartment of the cLP was then profiled to assess whether there were any defects in *Irf5*$^{-/-}$. Granulocytes were defined according to the gating strategy (Fig.3.4). Neutrophils are CD45^{+} CD11b^{+} Ly6G^{+}/Gr1^{hi}. Eosinophils were defined CD45^{+} CD11b^{+} Siglec F^{+} SSC^{hi}. Neither the proportion of neutrophils (Fig.3.9A), nor eosinophils (Fig.3.9B) was significantly affected by IRF5 deficiency at steady state in the cLP.

Next, the percentage of DCs in the cLP were assessed. In the cLP, there are three major populations of DCs: CD11b^{-} CD103^{+}, CD11b^{+} CD103^{+}, and CD11b^{+} CD103^{-}. CD11b^{-} CD103^{+} DCs were defined in Fig.3.5A and were not found to be affected by *Irf5*$^{-/-}$ (Fig.3.10A). CD11b^{+} DCs were defined in accordance with the gating strategy (Fig.3.5B), and could be split into two populations based on the expression of the integrin CD103 (integrin α_E). No difference was detected in CD11b^{+} CD103^{+} (Fig.3.10B), or CD103^{-} (Fig.3.10C) DCs.

Macrophages of the cLP are exclusively derived from blood Ly6C^{hi} monocytes, progressively losing monocyte markers, such as Ly6C, and upregulating macrophage markers, including MHC II, CD64, and F4/80 [217, 261]. In this thesis, newly entered monocytes are designated CD45^{+} CD11b^{+} Ly6G^{-} Siglec F^{-} Ly6C^{hi}, MHC II^{-}, referred to hereafter as P1 monocytes (Fig.3.5B). P2 monocytes are directly derived from P1 monocytes and express Ly6C and MHC II (Fig.3.5B). Macrophages (P4) have lost Ly6C expression and express F4/80 (Fig.3.5C).

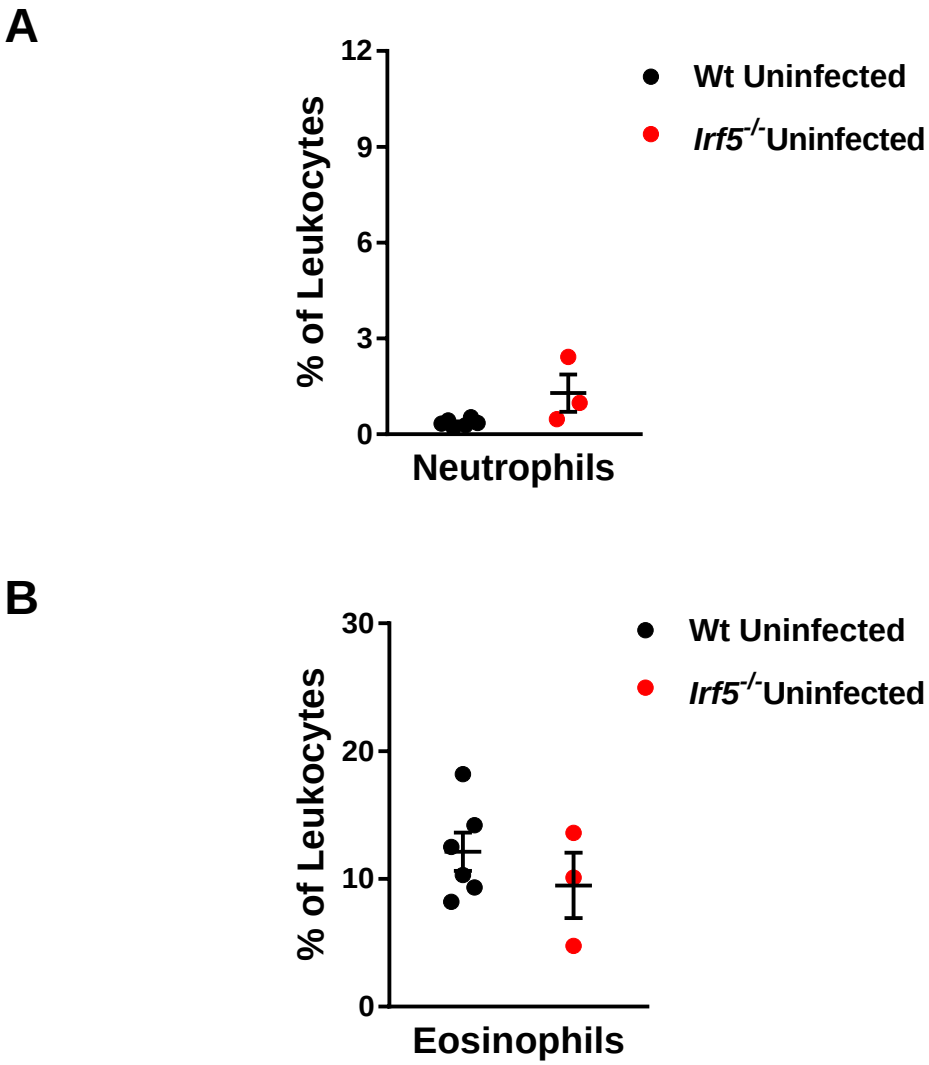

Fig.3.9: The composition of the granulocyte compartment in the colonic lamina propria is not affected by IRF5 deficiency

cLP leukocytes were isolated from the colons of WT and *Irf5*$^{-/-}$ mice and profiled by flow cytometry. The proportion of **A)** neutrophils, and **B)** eosinophils was unchanged between WT and *Irf5*$^{-/-}$ mice.

Statistics:
Results are representative of two independent experiments. WT: n = 6, *Irf5*$^{-/-}$: n = 3
Mean + SEM. Unpaired t test.

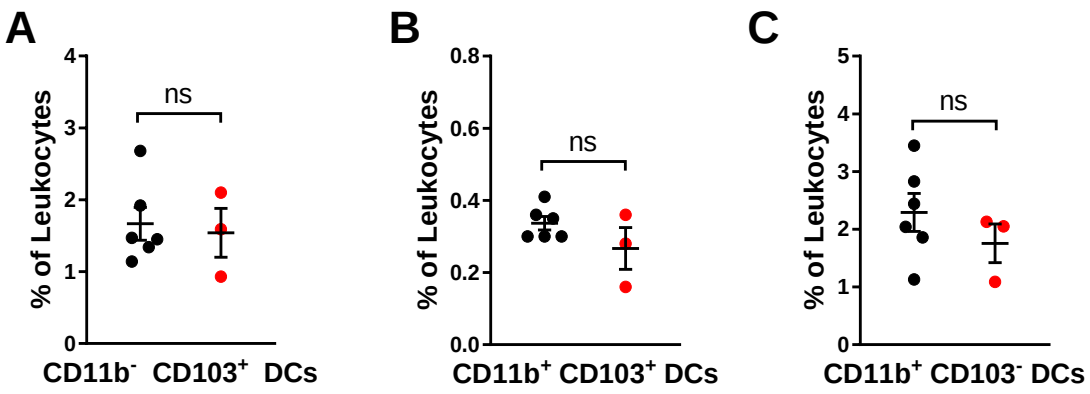

Fig.3.10: Dendritic cells are present at equal proportions in WT and *Irf5*$^{-/-}$ steady state mice

cLP leukocytes were isolated from the colons of steady state WT and *Irf5*$^{-/-}$ mice and profiled by flow cytometry. The proportions of **A)** CD11b^{-} CD103^{+}, **B)** CD11b^{+} CD103^{+}, and **C)** CD11b^{+} CD103^{-} was unaffected by IRF5-deficiency.

Statistics:
Data are representative of two independent experiments. WT n = 6, *Irf5*$^{-/-}$ n = 3
Mean + SEM. Unpaired t-test; ns = not significant

As a percentage of total leukocytes, P1 and P2 monocyte frequencies appeared to be unchanged at steady state (Fig.311A, Fig.3.11B), but a trend towards more WT macrophage was observed ($p = 0.0952$, Fig.3.11C).

This trend towards more WT macrophage warranted closer inspection of the MNP compartment. The composition of the cLP MNP compartment (CD45^{+} CD11b^{+} Ly6G^{-} Siglec F^{-}) were profiled. Within MNPs, Macrophages represented a greater frequency of MNPs in WT mice than in *Irf5*$^{-/-}$ mice ($p \leq 0.001$), which was compensated by an increase in the frequency of P1 monocoytes in *Irf5*$^{-/-}$ relative to WT mice (Fig.3.12, $p \leq 0.001$.)

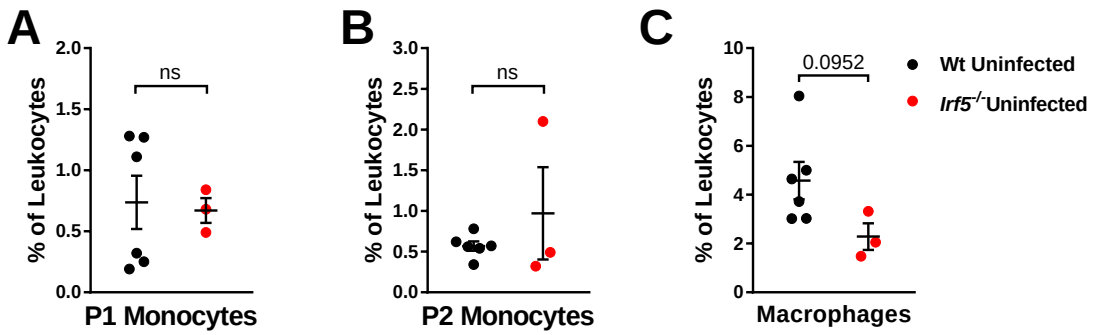

Fig.3.11: At steady state, mononuclear phagocytes as a proportion of total leukocytes are not significantly affected by IRF5 deficiency

cLP leukocytes were isolated from the colons of steady state WT and *Irf5*$^{-/-}$ mice and profiled by flow cytometry. The proportion of **A)** P1 monocytes, and **B)** P2 monocytes, was unchanged between WT and *Irf5*$^{-/-}$ mice. **C)** Macrophages displayed a trend towards an increased proportion of WT, but this was not statistically significant (p = 0.0952).

Statistics:
Data are representative of two independent experiments. WT n = 6, *Irf5*$^{-/-}$ n = 3
Mean + SEM, **A-C)** Mann-Whitney U test: ns = not significant

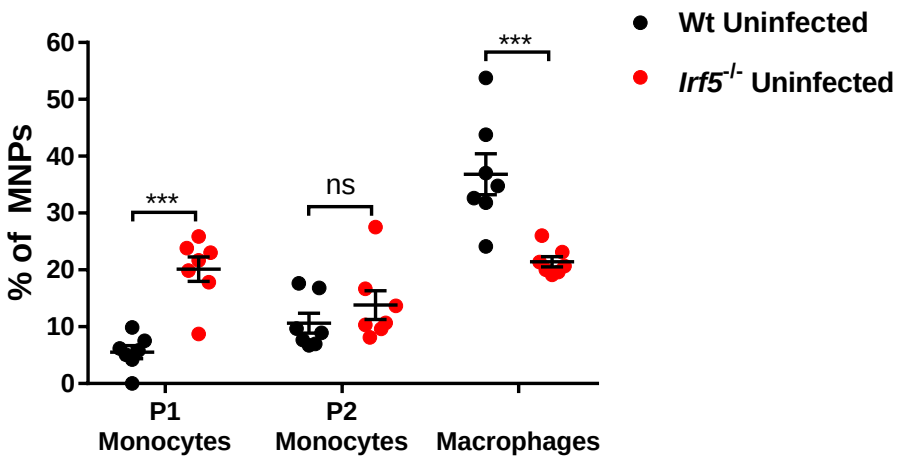

Fig.3.12: Macrophages represent a higher proportion of MNPs in WT than in *Irf5*$^{-/-}$

cLP leukocytes were isolated from the colons of steady state WT and *Irf5*$^{-/-}$ mice and profiled by flow cytometry. The frequencies of P1 monocytes, P2 monocytes, and macrophages were assessed relative to the MNP pool. *Irf5*$^{-/-}$ P1 monocytes were more abundant in *Irf5*$^{-/-}$ mice than in WT mice (mean difference = 16.6 ±3.12, p = 0.0005). The frequency of P2 monocytes was not affected by IRF5-deficiency. In WT mice, macrophages represented a greater fraction of MNPs than macrophages in *Irf5*$^{-/-}$ mice (median difference = 15.43, p = 0.0002).

Statistics:
Data are representative of three independent experiments, WT n = 7, *Irf5*$^{-/-}$ n = 7. Mean ± SEM. 2-Way ANOVA with Tukey correction: ns = not significant, *** p ≤ 0.001

3.2.5 CD11c^{+} macrophages express high levels of IRF5

Because IRF5 expression is associated with an inflammatory macrophage state, the expression of the macrophage markers, CD11c and CD206 were assessed. CD11c was reported to be expressed on inflammatory macrophages in atherosclerosis, and is directly regulated by IRF5 [278]. CD11c was expressed on high percentages of P2 monocytes and macrophages, but not on P1 monocytes (Fig.3.13A). Expression of CD11c increased as MNPs differentiated into macrophages (Fig.3.13B). The MFI of CD11c was highest in *Irf5*$^{-/-}$ macrophages at steady state (p ≤ 0.05), in contrast to the literature [278]. P2 monocytes also express CD11c. A greater frequency of CD11c^{+} P2 monocytes expressed IRF5, and exhibited a trend towards increased IRF5 expression in CD11c^{+} P2 monocytes (Fig.3.14A p ≤ 0.01, Fig.3.14B p = 0.0614). More CD11c^{+} macrophages expressed IRF5 than CD11c^{-} (p ≤ 0.01, Fig.3.14C), and the level of IRF5 expression was higher in CD11c^{+} macrophages (p ≤ 0.01, Fig.3.14D). CD206 is considered a marker of anti-inflammatory macrophages in

the cLP [264]. An equal percentage of WT and *Irf5*$^{-/-}$ macrophages expressed CD206 (Fig.3.15A), and per-cell expression of CD206 was unchanged in *Irf5*$^{-/-}$ macrophages (Fig.3.15B).

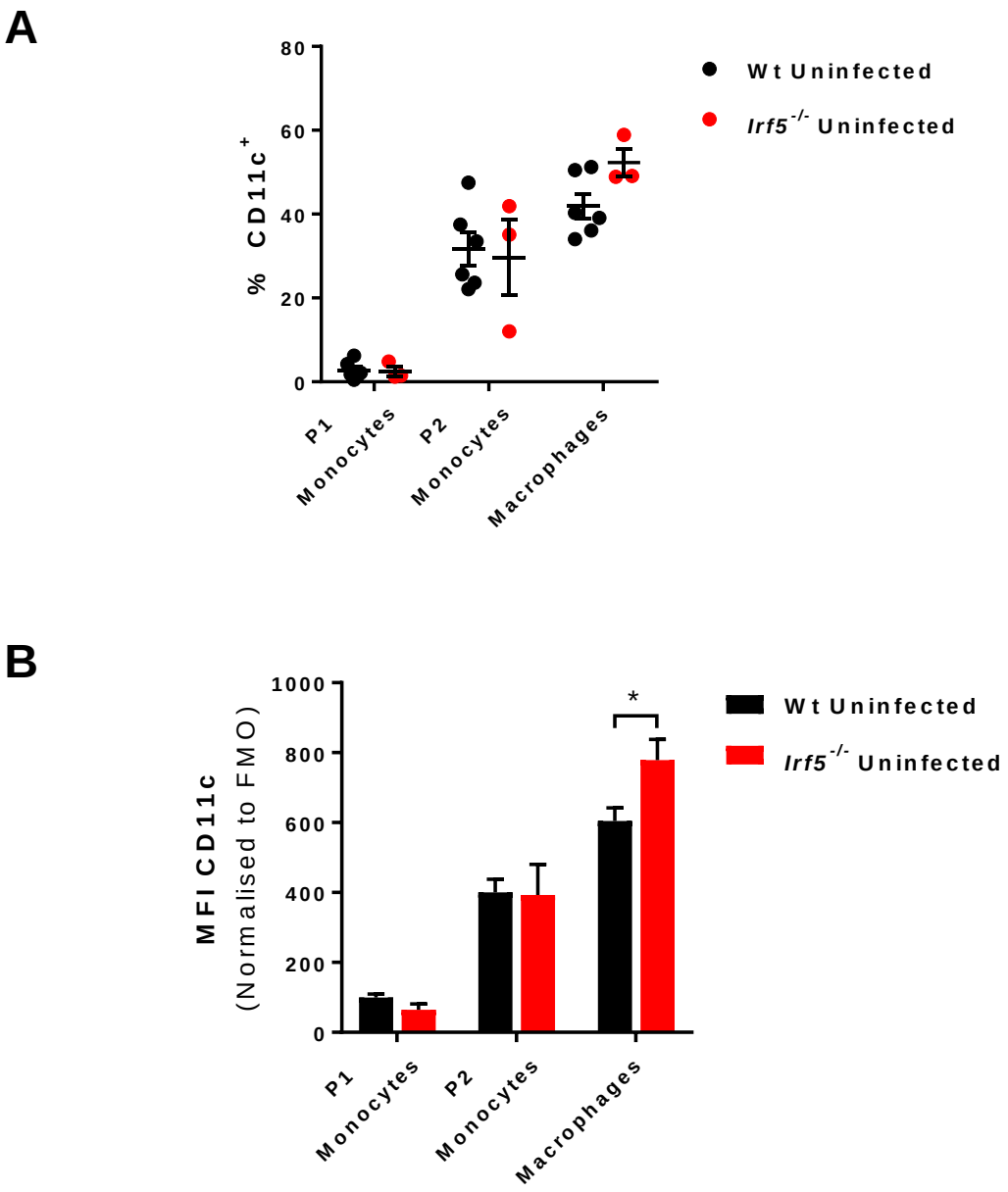

Fig.3.13: CD11c expression on steady state MNPs

Expression of CD11c on monocyte-derived MNPs was analysed by flow cytometry. **A)** The percentage of respective MNPs expressing CD11c was not altered by IRF5 status. **B)** The MFI of CD11c was higher in *Irf5*$^{-/-}$ relative to WT macrophages at steady state (p = 0.0279).

Statistics:
Data are representative of two independent experiments. Steady state WT n = 6, *Irf5*$^{-/-}$ n = 3
Mean + SEM
2-Way ANOVA with Sidak correction; * $p \leq 0.05$

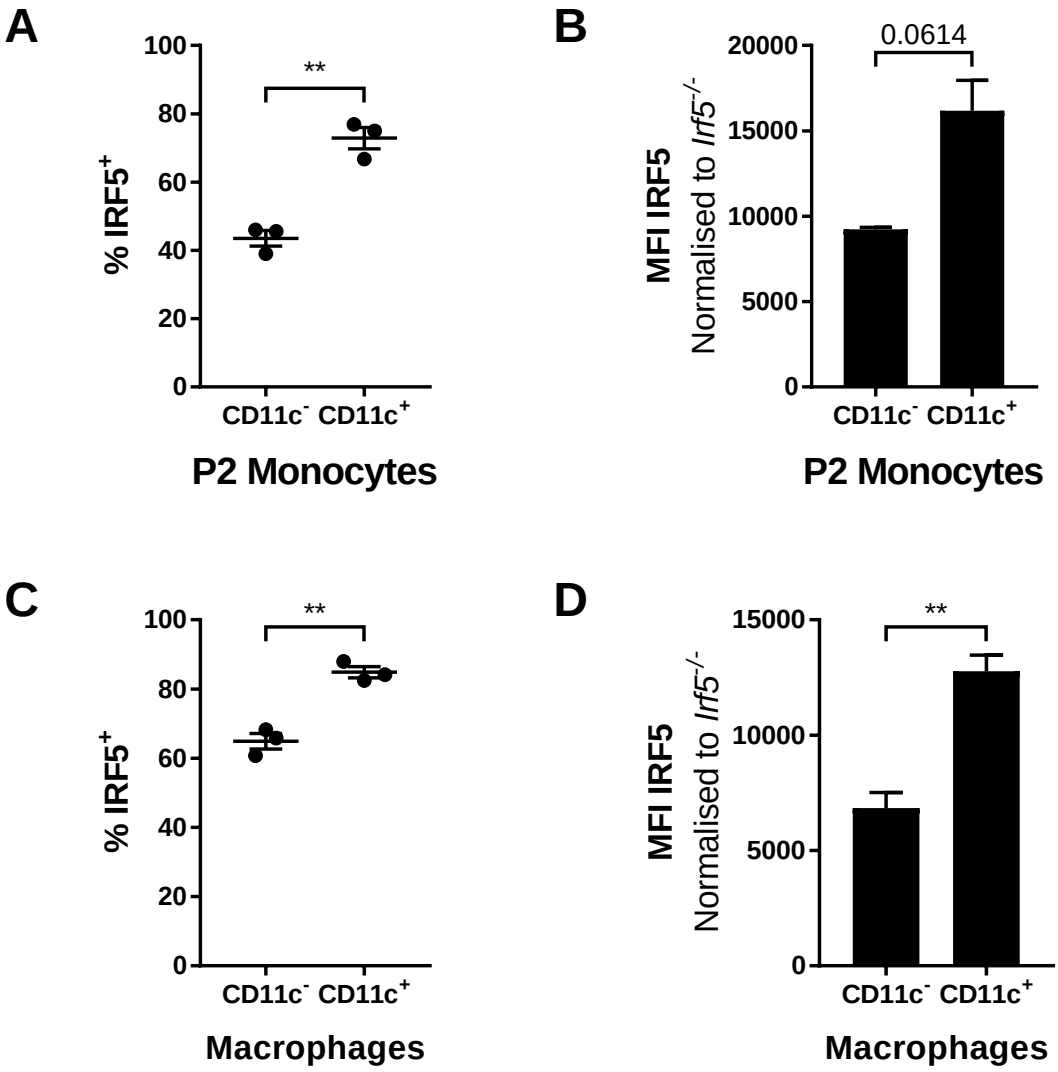

Fig.3.14: CD11c$^+$ P2 monocytes and macrophages express higher levels of IRF5 than CD11c$^-$ P2 monocytes and macrophages

The expression of IRF5 in CD11c$^+$ vs CD11c$^-$ P2 monocytes and macrophages was quantified by flow cytometry. **A)** A higher percentage of CD11c$^+$ P2 monocytes expressed IRF5 than CD11c$^-$, ($p = 0.0013$), **B)** CD11c$^+$ P2 monocytes did not express higher levels of IRF5 than CD11c$^-$ P2 monocytes. **C)** Significantly more CD11c$^+$ macrophages expressed IRF5 ($p = 0.0093$), and **D)** expression of IRF5 was higher in CD11c$^+$ macrophages than CD11c$^-$ macrophages ($p = 0.0054$).

Statistics:
Data are representative of two independent experiments. WT n = 3, *Irf5*$^{-/-}$ n = 3 (for MFI normalisation). Paired t test: ** $p \leq 0.01$

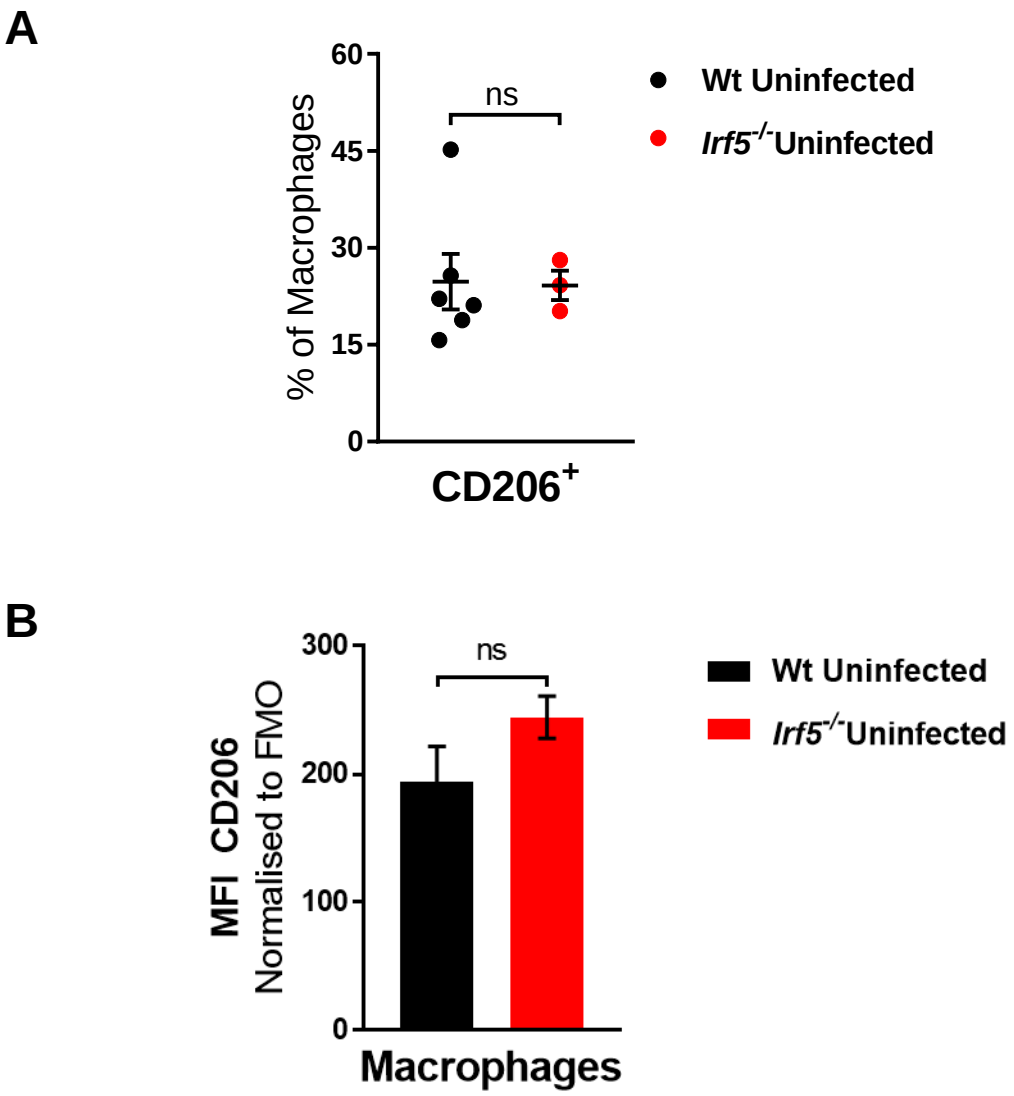

Fig.3.15: Macrophage CD206 expression is unaffected by IRF5 deficiency at steady state

cLP leukocytes were isolated from the colons of steady state WT and *Irf5*$^{-/-}$ mice and profiled by flow cytometry. The expression of CD206 on macrophages was assessed. **A)** Equal frequencies of macrophages expressed CD206 in WT and *Irf5*$^{-/-}$. **B)** The level of CD206 expression was unchanged by *Irf5*$^{-/-}$ deficiency.

Statistics:
Data are representative of two independent experiments. **A)** Mann-Whitney U-test: WT n =6, *Irf5*$^{-/-}$ n = 3, ns = not significant, **B)** Unpaired t-test: WT n = 6, *Irf5*$^{-/-}$ n = 3., ns = not significant

3.2.6 IRF5 Does Not Control Bone Marrow-Derived Macrophage Differentiation in Response to GM-CSF

WT macrophages in the cLP were found to be present at higher frequencies in the MNP compartment compared to *Irf5*$^{-/-}$ (Fig.3.12). In order to investigate whether IRF5 affected the ability of haematopoietic progenitor cells to generate monocytes and macrophages, macrophages were differentiated from mouse bone marrow using GM-CSF referred to henceforth as GM-BMDMs. The differentiation process was tracked using flow cytometry to assess the cellular composition of the culture using the gating strategies outlined below (Fig.3.16A, Fig. 3.16B). Haematopoietic Stem and Progenitor Cells (HSPCs), including Long Term Haematopoietic Stem Cells (LT-HSCs), Short Term Haematopoietic Stem Cells (ST-HSCs), Megakaryocyte-Erythroid Progenitors (MEPs), Common Myeloerythroid Progenitors (CMPs) and Granulocyte-Monocyte Progenitors (GMPs) were defined according to the gating strategy described (Fig. 3.16A). The percentage of CMPs, GMPs, and MEPs in culture remained steady until day four (between 1-5% of cells for each population), after which they were undetectable (Fig.13.7A-C). cMoPs, however, increased to 15% of total cells after day 3, implying lineage commitment to support monocyte and macrophage generation (Fig.3.17D). No differences were detected between WT and *Irf5*$^{-/-}$ cells in the composition of progenitors during GM-CSF culture (Fig.3.17, Fig.3.19).

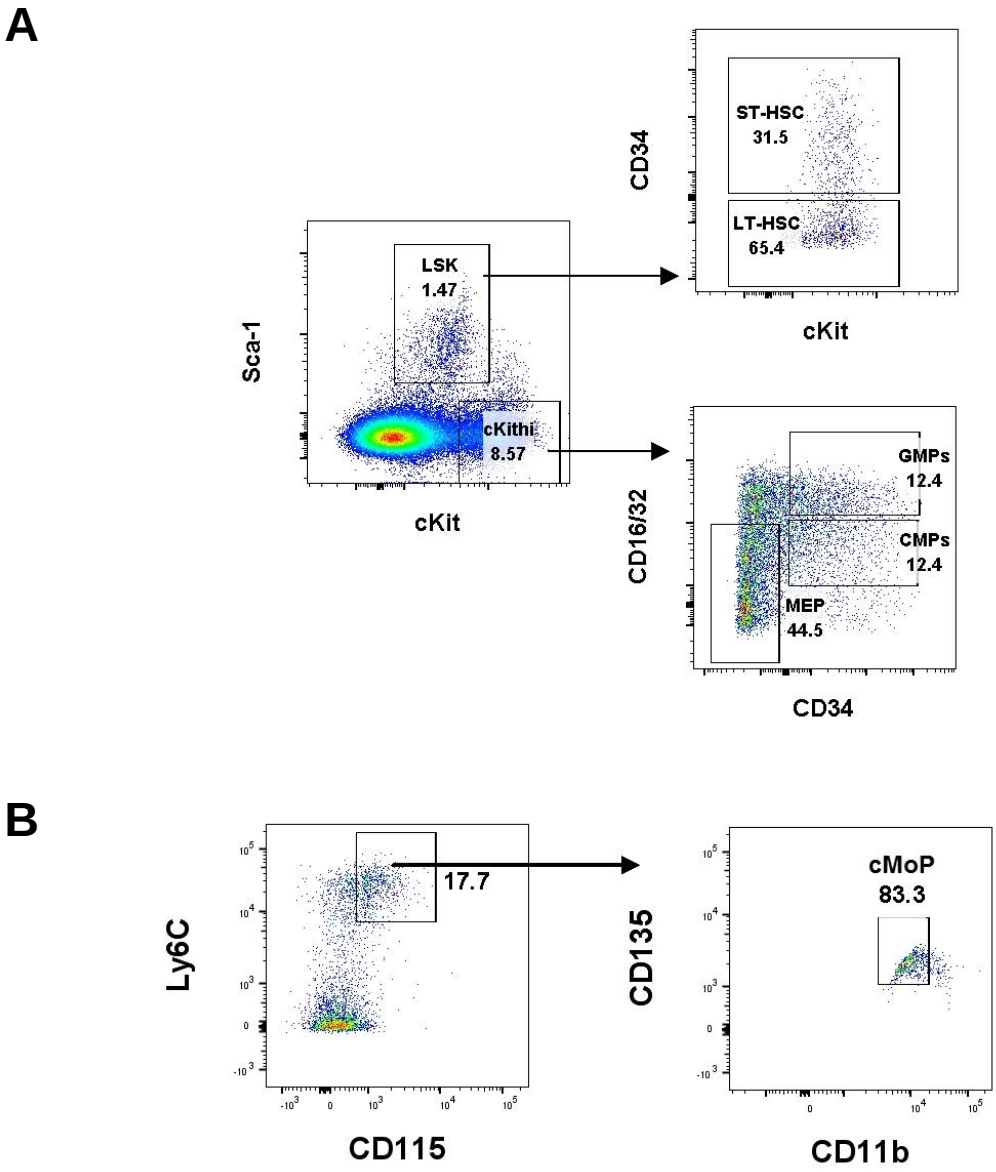

Fig.3.16: Gating strategy for haematopoietic stem and progenitor cells

Bone marrow was isolated from tibias and femurs of mixed bone marrow chimaeras and analysed by flow cytometry. All samples were gated to exclude doublets and dead cells. **A)** Identification of LT-HSCs, ST-HSCs, CMPs, GMPs, and MEPs**. B)** Identification of cMoPs pre-gated on lin^{-} cKit^{hi}

LSK: Lin^{-} Sca-1^{+} cKit^{lo}, ST-HSC: Short term haematopoietic stem cells, LT-HSC: long term haematopoietic stem cells, MEP: megakaryocyte-erythroid progenitors, GMP: granulocyte-macrophage progenitor, CMP: common myeloid progenitor, cMoP: common monocyte progenitor

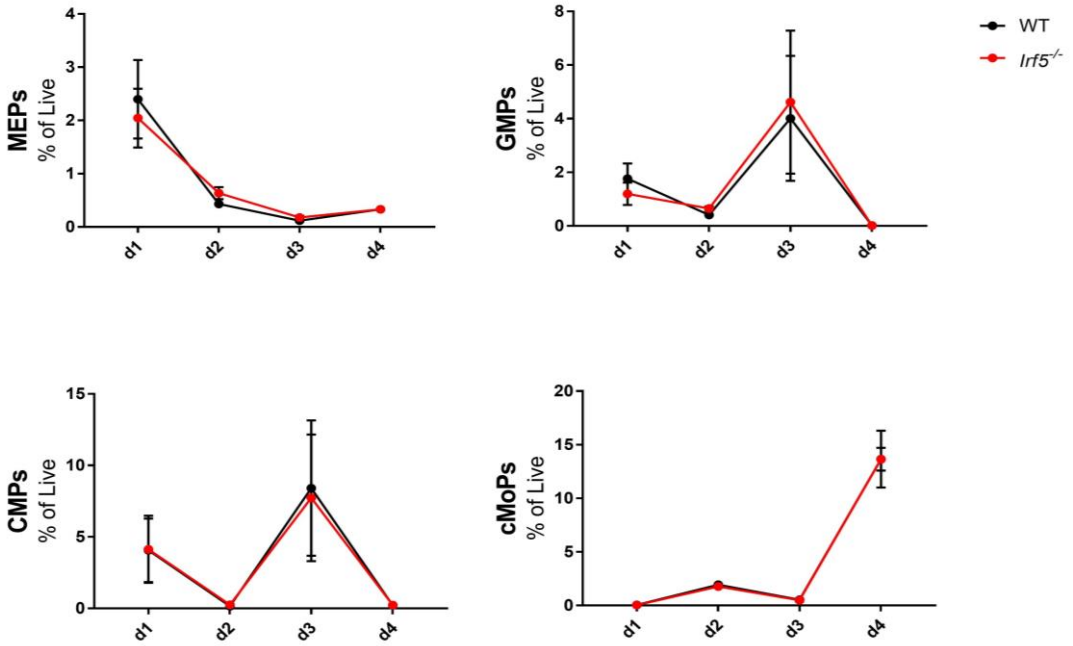

Fig.3.17: IRF5 does not affect the frequency of progenitor cells in culture

Bone marrow cells were cultured in the presence of GM-CSF for four days. At each day of culture, cells were harvested and profiled by flow cytometry for changes in progenitor cell composition. No differences in progenitor composition were noted across four days of GM-CSF culture. The percentage of MEPs decreased to less than 1% of live cells after d1. GMPs and CMPs increased marginally as a percentage of live cells between d2-d3, but decreased to undetectable levels by d4. cMoPs remained a low percentage of cells from d1-d3, before peaking at d4.

Mean + SEM data are compiled from four independent experiments with n = 2 per group for each experiment. WT n = 8, *Irf5*$^{-/-}$ n =8.

MEP: Megakaryocyte-erythroid progenitor, GMP: Granulocyte-macrophage progenitor, CMP: Common myeloid progenitor, cMoP: common monocyte progenitor.

3.2.7 IRF5 expression in Haematopoietic Stem and Progenitor Cells

Until now, the expression of IRF5 in HSPCs was undefined. Bone marrow cells from steady state mixed bone marrow chimaeras were isolated, and labelled for flow cytometry as previously described (Chapter.2.7.3, and Chapter.2.11). Intracellular staining for IRF5 was performed, and the geometric mean fluorescence intensity of IRF5 in WT HSPCs was normalised to the corresponding *Irf5*$^{-/-}$ in each chimaera (Fig.3.18). LT-HSCs, ST-HSCs, and CMPs express low levels of IRF5 (mean MFI ~200), GMPs (MFI ~500) and MEPs (MFI ~700) express moderate levels, whilst bone marrow Ly6C^{hi} monocytes (MFI ~1600) express the highest levels of IRF5 in the tested populations (Fig.3.18).

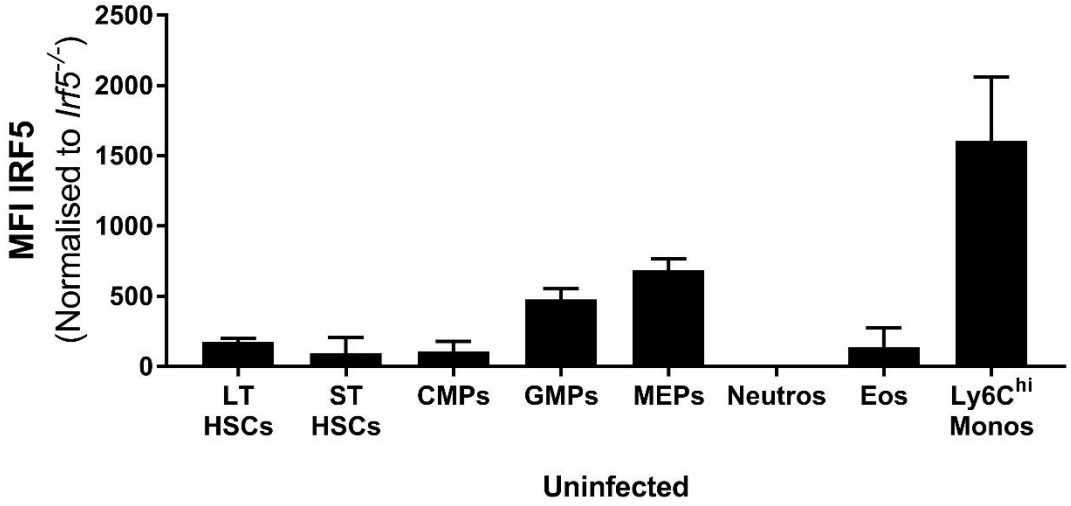

Fig.3.18: IRF5 expression in haematopoietic stem and progenitor cells

Bone marrow cells were isolated from tibias and femurs of WT:*Irf5*$^{-/-}$ mixed bone marrow chimaeras. Haematopoietic stem and progenitor cells, and mature leukocytes were identified by flow cytometry, and geometric mean fluorescence intensities of IRF5 were normalised to the autofluoresence of corresponding *Irf5*$^{-/-}$ populations. No IRF5 was detected in mature bone marrow neutrophils. LT-HSCs, ST-HSCs, CMPs, GMPs, and Eosinophils expressed low amounts of IRF5. Ly6C^{hi} monocytes expressed the highest levels of IRF5 of the cells tested.

Data are representative of two independent experiments Where n = 3.

LT-HSC: Long term haematopoietic stem cell, ST-HSC: Short term haematopoietic stem cell, CMP: Common myeloid progenitor, GMP: Granulocyte-macrophage progenitor, MEP: Megakaryocyte-erythroid progenitor, Neutros: Neutrophils, Eos: Eosinophils, Ly6C^{hi} Monos: Ly6C^{hi} Monocytes.

The total number of cells in culture decreased between d1-d2, but increased steadily in a linear fashion thereafter, with no differences in the number of cells between WT and *Irf5*$^{-/-}$ cultures (Fig.3.19A).

At the beginning of the culture period, neutrophils were the dominant cell population, totalling ~40% of cells in culture from d1-d4 (Fig.19B). However, the percentage of neutrophils declined after d4 to ~15% of total cells by day nine in both WT and *Irf5*$^{-/-}$ (Fig.3.19B). Concordant with the cMoP peak, the percentage of Ly6C^{hi} monocytes peaked around 25% on d4 (Fig.3.19C). Again, no differences were detected between WT and *Irf5*$^{-/-}$ cultures. Macrophages represented a tiny fraction of naïve GM-CSF bone marrow cultures from d1-d3. On d4, the percentage of macrophages increased to ~20% of cultured cells, and increased rapidly to 80% of the culture by d9 in both WT and *Irf5*$^{-/-}$ cells (Fig.3.19D). On d9 of culture, the expression of mature macrophage markers on GM-BMDMs was assessed by flow cytometry to test for phenotypic differences (Fig.3.20). No significant difference was found between WT and *Irf5*$^{-/-}$ cells on the markers assayed, although GM-BMDMs displayed a trend of lower expression of CD64, and CD81.

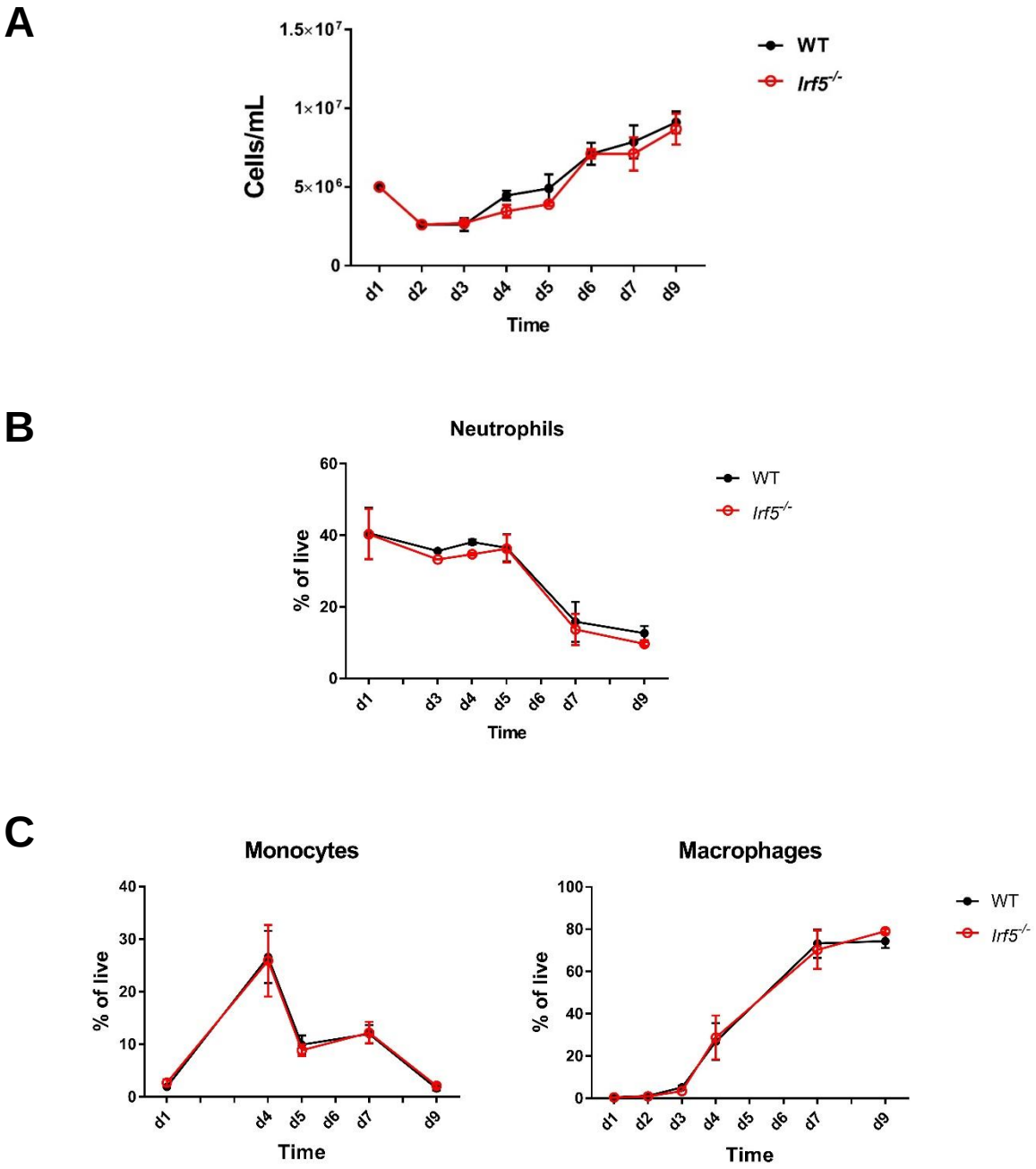

Fig.3.19: IRF5 does not affect generation of macrophages in bone marrow cultures

Bone marrow isolated from wild-type or *Irf5*$^{-/-}$ mice was cultured with GM-CSF for 9 days. Cells were harvested from the culture periodically, and cellular heterogeneity was assessed by flow cytometry. **A)** Number of cells retrieved/mL of culture medium **B)** % of Neutrophils **C)** % of Monocytes and % of Macrophages in culture.

Mean + SEM, n = 4 mice per timepoint from two independent experiments.

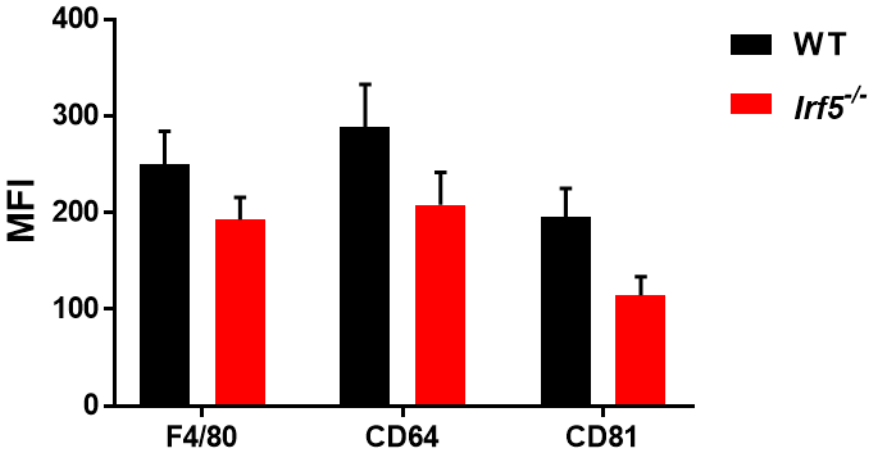

Fig.3.20: Expression of mature macrophage markers on GM-CSF bone marrow-derived macrophages

Bone marrow cells isolated from WT or *Irf5*$^{-/-}$ mice were cultured for nine days in the presence of GM-CSF. Protein expression of F4/80, CD64, and CD81 on macrophages (CD11b^{+} CD11c^{+} MHC II^{+}) was quantified by flow cytometry. No significant difference in the expression of the three markers was detected between genotypes. However, *Irf5*$^{-/-}$ displayed a trend towards lower expression of mature macrophage markers.

Statistics:
Data presented are the results pooled from four independent experiments with a two biological replicates per genotype per experiment. 2-Way ANOVA with Sidak correction. WT n = 8 *Irf5*$^{-/-}$ n = 8.

3.3 Discussion

Irf5$^{-/-}$ mice did not display any gross morphological discrepancies compared to WT mice, and did not react aberrantly to the homeostatic commensal microbiota, indicated by histopathological scoring (Fig.3.1, Fig.3.2). The expression of IRF5 within the cLP was profiled, and it was discovered that myeloid populations expressed the highest levels of IRF5, with a negligible expression of IRF5 in the stromal and lymphoid cells at steady state (Figs.3.6, Fig.3.7), which fit with the understanding of IRF5 expression thus far [162]. The distribution of myeloid populations was largely unaffected by IRF5 deficiency, except for the MNP compartment (Fig.3.12). Macrophages were less abundant in the MNP compartment of *Irf5*$^{-/-}$ mice than in WT mice, with a corresponding increase in the percentage of P1 monocytes in *Irf5*$^{-/-}$. This effect may be due to increased conversion of monocytes to macrophages within the cLP, as the accumulation of P1 monocytes did not appear to be deficient, in fact, P1 monocyte accumulation was greater in *Irf5*$^{-/-}$ than in WT. Investigation into this effect would require psuedotime analysis of WT and *Irf5*$^{-/-}$ cLP monocytes and macrophages sharing the same environment to enumerate transcriptional and cell surface marker expression differences and monocytes differentiated to macrophages.

To investigate a possible intrinsic effect of IRF5 on myelopoiesis, Bone Marrow Derived Macrophages (GM-BMDMs) were differentiated *in vitro* using GM-CSF, and profiled over the course of nine days (Fig.3.17, Fig.3.19). No effect of IRF5 deficiency on the generation of mature macrophages could be detected (Fig.3.19D), no effect was detected on the expression of the mature macrophage markers, CD64, and F4/80, and the tetraspanin, CD81 (Fig.3.20).

Irf5$^{-/-}$ macrophages have previously been described to have an “M2” phenotype after GM-CSF differentiation, demonstrating that effector function is affected [162, 217]. However, most of the differences between WT and *Irf5*$^{-/-}$ GM-BMDMs are observed when macrophages were stimulated, for example with LPS (unpublished observations), and that

subtle differences in macrophage phenotype may be missed in the absence of inflammation. If IRF5 activation is important for the differentiation of macrophages in the cLP, this may help to explain the reduced frequencies of macrophages in *Irf5*$^{-/-}$ mice at steady state. The cLP is not sterile; microbial factors have been detected in the lamina propria even during steady state [279, 280]. As Ly6C^{hi} monocytes enter the cLP, they become exposed to PRR agonists, which could then activate IRF5 and stimulate macrophage fate. In addition to the psuedotime analysis mentioned earlier, intestinal barrier function would need to be tested, possibly using *in vitro* macrophage-epithelial cell culture systems combined with *in vivo* imaging of colonic epithelial tight junctions in *Irf5*$^{-/-}$ mice.

We found that IRF5 is highly expressed in steady state bone marrow Ly6C^{hi} monocytes, but its expression is also detected in GMPs and MEPs (Fig.17). MEPs give rise to Megakaryocytes, which produce platelets. Platelets were first described to be critical for haemostasis, yet more recently platelets have been shown to interact with both monocytes and neutrophils to amplify innate immune responses [281, 282]. However, MEPs are not known to contribute to disease pathology directly, although a study has shown MEPs to be able to promote a lupus phenotype in antigen presenting cell-depleted mice [283]. Additionally, a 2015 study identified human MEPs as MHC II-expressing antigen presenting cells that were able to support T_H1/T_H17 expansion. This study also detected IRF5 mRNA in these cells, a result confirmed by intracellular labelling of IRF5 (Fig.3.18), and that MEPs produced cytokines that supported T_H1 and T_H17 expansion, including IL1, IL6, and IL23 [284]. It may be possible that MEPs contribute to host defence where extramedullary haematopoiesis is required, such as IBD. During T cell transfer colitis, however, the proportion of GMPs in the bone marrow increased at the expense of MEPs [69]. The same study also noted that cLP GMPs were proliferating more rapidly than cLP MEPs based on the expression of Ki67 [69]. As MEPs represent a tiny fraction of the cLP milieu, it is unlikely that they play a major role in host defence during experimental colitis. Nevertheless, the role of IRF5 in MEPs is unclear, and warrants further investigation. Future study could

investigate the ability of IRF5 deficient MEPs to produce megakaryocytes and therefore platelets, and their ability to support T_H1 and T_H17 cell proliferation [284]. Activated platelets complexed with neutrophils and monocytes have been detected in IBD patients, which may indicate augmented host defence, whilst depletion of platelets reduced leukocyte rolling and adhesion, therefore justifying further investigation of IRF5 in this area [285, 286].

GMPs express lower levels of IRF5 than MEPs at steady state. Despite this, a clearer role for GMPs in colitis has been defined [69]. GMPs can respond to PAMPs, via PRRs, and are also responsive to IFNγ and IL17 signalling [287-289]. GMPs are highly proliferative and may give rise to neutrophils, eosinophils, and monocytes in support of homeostasis and inflammatory responses [69]. GMPs are dependent on PU.1, and IRF8 [82]. As MDP progress to cMoP, and then to $Ly6C^{hi}$ monocytes, IRF5 expression was upregulated [49]. Because IRF5 is inducible, activation may prime monocytes for function in tissues: systemic IL12p70 was shown to induce the release of bone marrow IFNγ, which may provide a mechanism for long distance programming of monocytes for inflammatory responses as they develop [290]. The data presented in this chapter suggest that in the absence of inflammatory stimulation, IRF5 may not be important for lineage commitment of GMPs. Future studies conducted should test the dependence on *Irf5*$^{-/-}$ GMPs via extra signals, for example, IFNγ or bacterial components such as LPS to mimic inflammatory conditions.

The data presented here suggest that loss of IRF5 does not affect the ability of progenitors to produce mature macrophages in response to GM-CSF (Fig.16, Fig.19). However, the proliferative capacity of progenitors may be affected by IRF5 deficiency in inflammation: *In vivo*, the haematopoietic niche is radically different, and IRF5 transcription-inducing factors other than GM-CSF, IFNγ and LPS have not been defined. Investigation of HSPC proliferation should be investigated by Ki67 labelling or *cfu* assays using Methocult protocols of HSPCs sorted from WT:*Irf5*$^{-/-}$ uninfected and Hh + αIL10R mixed bone marrow chimaeras.

Supplementing *in vitro* BMDM cultures with other growth factors, such as M-CSF, and known haematopoietic-skewing factors, such as IFNγ, could also be tested to further probe IRF5 dependence. A 2012 study investigated the effects of combined GM-CSF and M-CSF treatment and found that M-CSF largely suppressed the inflammatory effects of GM-CSF [222]. However, concentrations of GM-CSF and M-CSF differed to those routinely used by the Udalova lab, which may explain some of the differences in GM-BMDM phenotype seen in the study [162, 261].

Next generation sequencing of progenitors from mixed bone marrow chimaeras may also provide vital clues to the role of IRF5 in haematopoiesis should upstream methods demonstrate an effect of IRF5 deficiency. In addition it is likely to shed light on the question of whether the expression of IRF5 is heterogeneously distributed throughout the populations. The expression of IRF5 in MEPs indicates that platelet level and function should be investigated in *Irf5*$^{-/-}$ mice.

These studies did not involve investigating the impact of IRF5 on extramedullary haematopoiesis, which may be impacted by loss of IRF5 due to the unique inflammatory environment in which extramedullary haematopoiesis takes place.

3.4 Conclusion

Here, we have characterised the colonic lamina propria (cLP) of IRF5-deficient mice. *Irf5*$^{-/-}$ mice did not display any morphological defects of the colonic lamina propria, and only the cLP mononuclear phagocyte system of *Irf5*$^{-/-}$ mice displayed perturbation; macrophages comprised a lower frequency of MNPs in the cLP of *Irf5*$^{-/-}$ mice. Therefore bone marrow myelopoiesis was investigated *in vitro*. The roles of PU.1, KLF4, and IRF8 as lineage defining transcription factors has been defined [84, 266, 269, 272]. The data presented here indicates that IRF5 is not a macrophage lineage-defining transcription factor in the bone marrow in spite of its polarising effects [261]. The literature suggests that IRF5 may play a role in modulating MNP phenotype to contribute to autoimmune disease, supported by the observation of decreased CD64 and F4/80 expression in *Irf5*$^{-/-}$, whereas the role of

IRF5 in HSPCs is unclear and requires investigation. Extramedullary haematopoiesis should also be investigated, as both proliferation and recruitment of leukocytes to the tissue may be affected by loss of IRF5.

From these data, IRF5 does not appear to affect haematopoiesis, however, the *in vivo* environment is complex, and thus IRF5 may yet impact myelopoiesis in a manner outlined by proposed future experimentation.

4 IRF5 controls the tissue adaptation of mononuclear phagocytes in the colonic lamina propria

4.1 Introduction

Mononuclear Phagocytes (MNPs), encompassing monocytes, macrophages and dendritic cells (DCs) are critical effector cells in the maintenance of homeostasis in the intestinal mucosa [124, 139, 264]. Intestinal MNPs sample luminal antigens, clear cellular debris, destroy invading microorganisms, and mediate tissue homeostasis and repair [59, 60, 113, 123, 291, 292]. The intestinal lumen is host to trillions of bacteria and other microorganisms [293]. At steady state, Pathogen-Associated Molecular Pattern (PAMP) ligation of Pattern Recognition Receptors (PRRs) leads to bacterial clearance, but does not result in full MNP activation, and thus maintains homeostasis [59, 113].

MNP ontogeny in the intestine has been the focus of much investigation in recent years [57, 213, 294]. Three major subsets of classical Dendritic Cells (cDCs) reside in the colonic Lamina Propria (cLP): $CD11b^{-}$ $CD103^{+}$, $CD11b^{+}$ $CD103^{+}$, and $CD11b^{+}$ $CD103^{-}$ [295]. cDCs are believed to be derived from Common Dendritic cell Progenitors (CDPs), in contrast to adult intestinal macrophages, which are thought to derive from monocytes [57, 296, 297]. However, the factors that promote macrophage fate have not been defined [43]. *Irf5*$^{-/-}$ mice displayed altered MNP compartment composition, with decreased percentages of macrophages, and a compensatory increase in the frequency of P1 monocytes, whilst myelopoiesis did not appear to be affected (Fig.3.12, Fig.3.15, Fig.3.17). Therefore it was hypothesised that IRF5 may play a role in directing MNP fate in the cLP.

Macrophage function in the cLP was shown to be essential for the development of colitis: loss of IL10R signalling on macrophages resulted in spontaneous colitis, whilst $CD11c^{Cre}$-mediated deletion of *Il23a* was sufficient to protect mice from colitis [124, 139].

Macrophages and monocytes were also demonstrated to have beneficial roles in other models of intestinal inflammation, promoting tissue repair via ILC3-derived GM-CSF or through the production of prostaglandin E2 in response to *Toxoplasma gondii* infection [147, 223]. Inflammatory cytokine and chemokine release is important for the appropriate recruitment of effector leukocytes to the site of inflammation [146, 224, 298]. Intestinal insults result in the accumulation of Ly6C^{hi} MHC II^{+} (P2) monocytes, derived from blood Ly6C^{hi} monocytes [299]. P2 monocytes are highly inflammatory, IL23-expressing CD11c^{+} MNPs [124]. *In vitro*, IRF5 boosts the transcription of many of the cytokines and chemokines that are integral components of inflammatory cascades, including *Il23a* by direct regulation of transcriptional activity, and promotes pathogenic T_H1 and T_H17 responses [162, 163, 300]. Decreased expression of inflammatory mediators and lowered T_H1/T_H17 activation may provide an explanation for the protection from Hh + αIL10R colitis observed in *Irf5*$^{-/-}$.

Mixed bone marrow chimaeric approaches allow the direct comparison of cells derived from different haematopoietic sources, as cells in this setting share the same environment. WT:*Irf5*$^{-/-}$ Mixed Bone Marrow Chimaeras (MBMCs) have previously been used to investigate IRF5 in the context of pristane-induced Lupus and identified increased accumulation of WT monocytes in the blood at steady state, and this was heightened in the blood and peritoneal exudate after pristane challenge [239]. However, the steady state peritoneum, and reconstitution in other organs were not measured.

WT mice displayed a higher percentage of macrophages in the MNP pool at steady state compared to *Irf5*$^{-/-}$ but no defect in the GM-CSF-directed development of bone marrow macrophages was detected (Fig.3.12). Due to this observation, it was hypothesised that IRF5 may play a role in directing MNP fate within the cLP. In this chapter, MBMCs were utilised to uncover intrinsic defects in *Irf5*$^{-/-}$ haematopoietic cells. Therefore, MNPs from the MBMC cLP were profiled at day (d) 21 of the *Helicobacter hepaticus* + anti-Interleukin 10

Receptor (Hh + αIL10R) model of colitis to assess reconstitution, cell fate, and activation status.

4.2 Results

4.2.1 IRF5 does not affect the reconstitution of haematopoietic stem and progenitor cells in mixed bone marrow chimaera

In Chapter.3, we demonstrated that IRF5 did not affect myelopoiesis in response to GM-CSF. However, the bone marrow nice in WT:*Irf5*$^{-/-}$ MBMC has not been characterised, and to accurately interpret finding in the colon and blood, the reconstitution efficiency in the bone marrow must be characterised. Haematopoietic stem and progenitor cells (HSPCs), and "mature" bone marrow populations were identified (Fig.4.1, Fig.4.3), and assessed for donor origin by expression of either CD45.1 (WT) or CD45.2 (*Irf5*$^{-/-}$) (Fig.4.1B). Reconstitution of LT- and ST-HSCs were not affected (data not shown). Progenitor reconstitution was not significantly affected in uninfected animals (Fig.4.2A). However, MEPs displayed greater reconstitution by WT in Hh + αIL10R treated mice ($p \leq 0.05$, Fig.4.2B).

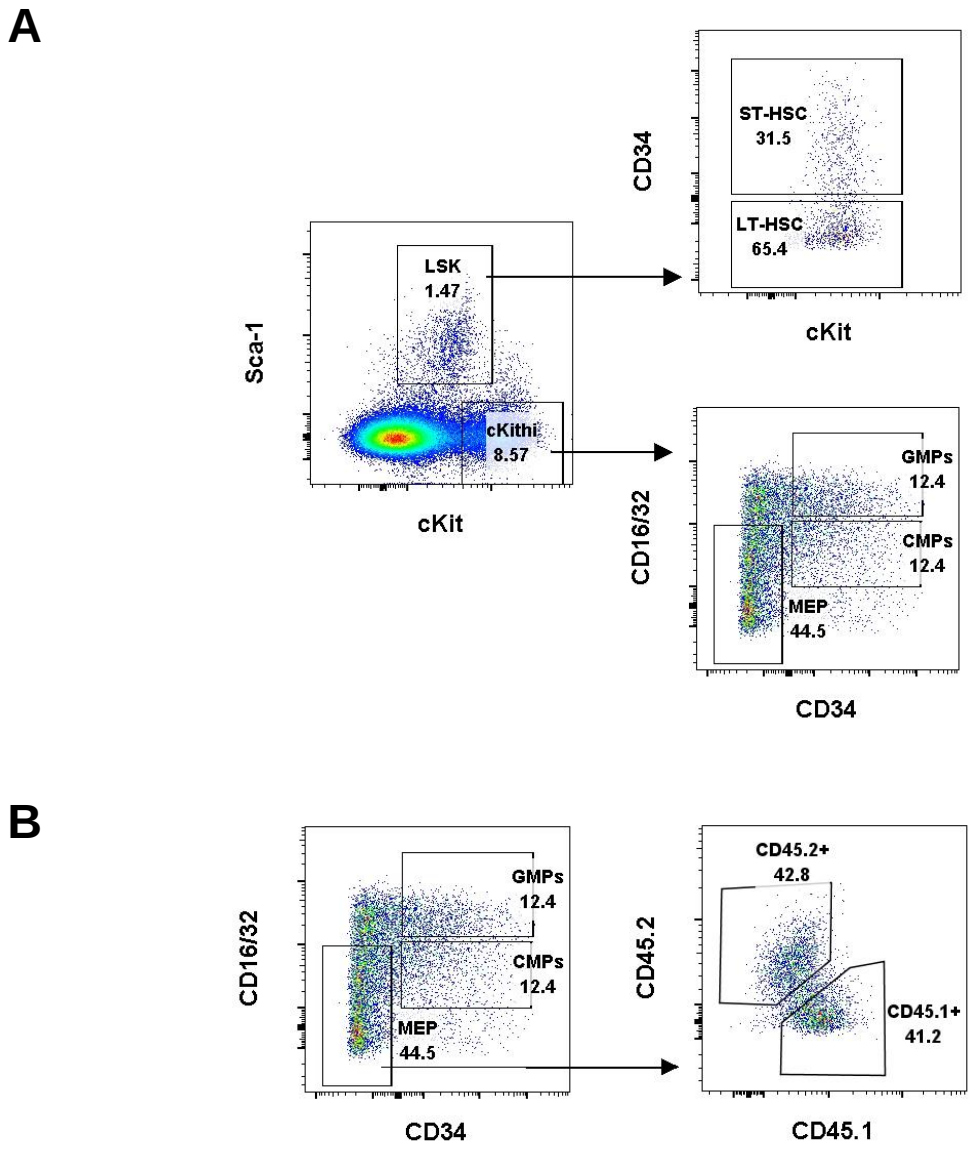

Fig.4.1: Gating strategy for haematopoietic stem and progenitor cells

Bone marrow was isolated from tibias and femurs of mixed bone marrow chimaeras and analysed by flow cytometry. All samples were gated to exclude doublets and dead cells. **A)** identification of LT-HSCs, ST-HSCs, CMPs, GMPs, and MEPs **B)** identification of, donor-derived cells were identified on the basis of CD45.1 or CD45.2 expression.

LSK: Lin^{-} $Sca\text{-}1^{+}$ $cKit^{lo}$, ST-HSC: Short term haematopoietic stem cells, LT-HSC: long term haematopoietic stem cells, MEP: megakaryocyte-erythroid progenitors, GMP: granulocyte-macrophage progenitor, CMP: common myeloid progenitor

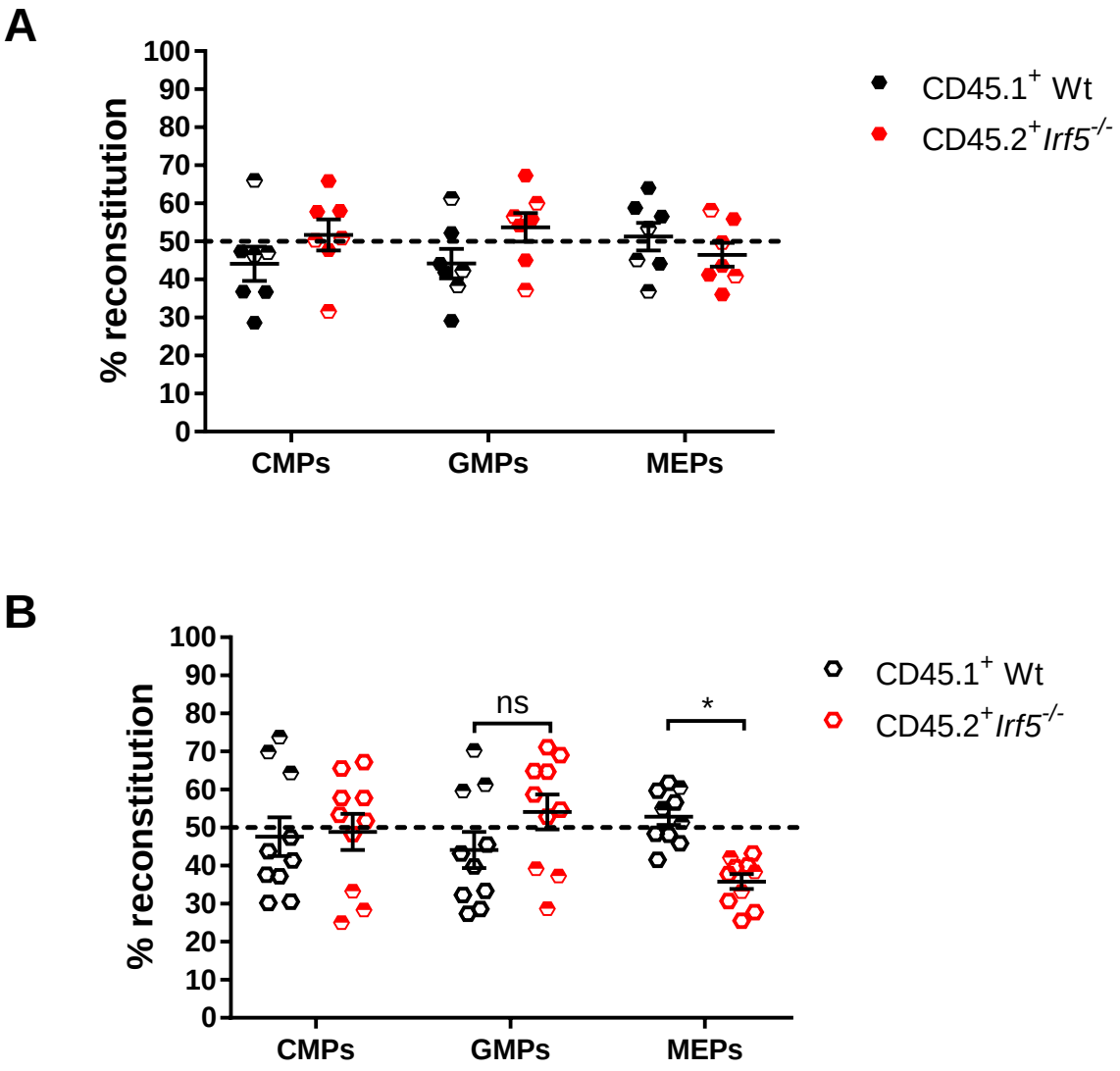

Fig.4.2: Reconstitution of haematopoietic progenitors in mixed bone marrow chimaera

WT CD45.1$^+$ mice were reconstituted with an equal mix of CD45.1$^+$ WT and CD45.2$^+$ *Irf5*$^{-/-}$ bone marrow and allowed to reconstitute for 8 weeks. Bone marrow was extracted from mice upon sacrifice and profiled by flow cytometry **A)** Analysis of haematopoietic progenitor reconstitution in uninfected mice, no differences in reconstitution were detected, **B)** Analysis of haematopoietic progenitors after 3 weeks of *Helicobacter hepaticus* + αIL10R colitis. WT reconstitution of MEPs was favoured p = 0.0141.

Data presented are Mean ± SEM from two collated independent experiments. Steady state n = 7, Hh + αIL10R n = 11 experimental replicates are distinguished by shading of symbols
2 way ANOVA with Sidak correction, multiple comparisons between genotypes
* $p \leq 0.05$

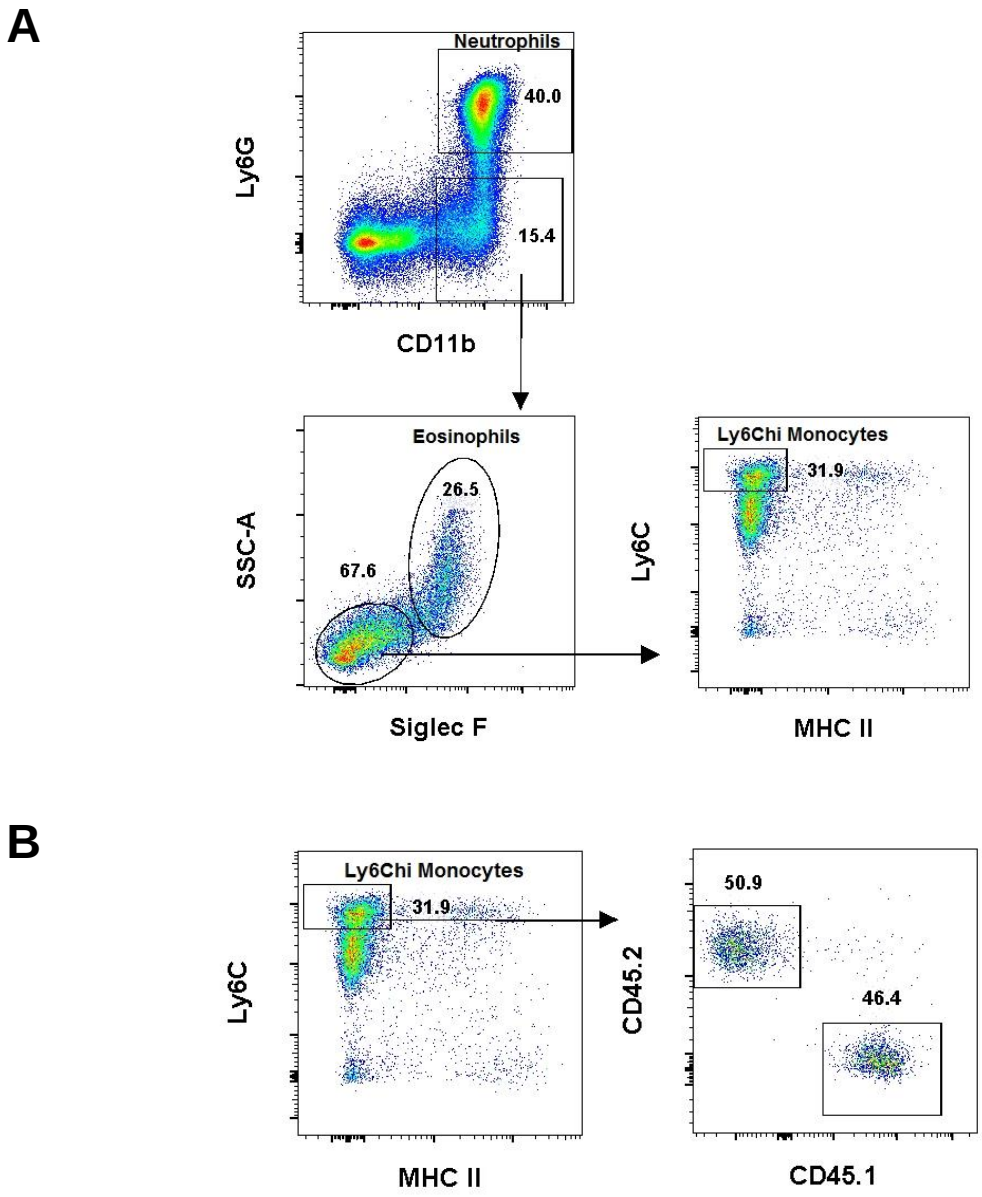

Fig.4.3: Gating strategy for mature bone marrow populations

Bone marrow leukocytes were isolated from mixed bone marrow chimaeras and analysed by flow cytometry. Plots were pre-gated: Live CD45^{+} Single Events. **A)** Identification of neutrophils (CD11b^{+} Ly6G^{+}), eosinophils (CD11b^{+} Siglec F^{+}), Ly6C^{hi} monocytes (CD11b^{+} Ly6G^{-} Siglec F^{-} Ly6C^{hi}). **B)** WT and *Irf5*$^{-/-}$ donor-derived leukocytes were identified by expression of either CD45.1 or CD45.2

4.2.2 *Irf5*$^{-/-}$ myeloid cells are overrepresented in *Helicobacter hepaticus* + αIL10R-treated mice

In addition to the reconstitution of HSPCs, it was unknown whether IRF5 deficiency would affect the reconstitution of myeloid cells in mixed bone marrow chimaeras. Myeloid cells were identified according to the gating strategy outlined (Fig.4.3A, Fig.4.3B). In uninfected mixed bone marrow chimaeras, no difference in reconstitution was observed (Fig.4.4A). However, *Irf5*$^{-/-}$ total leukocytes, neutrophils (Mean diff = 20.43, $p < 0.0001$), eosinophils (mean diff = 20.54, $p < 0.0001$), and Ly6C^{hi} monocytes (mean diff = 23.76, $p \leq 0.001$) were overrepresented vs WT in the bone marrow of Hh + αIL10R colitic chimaeras (Fig.4.4B).

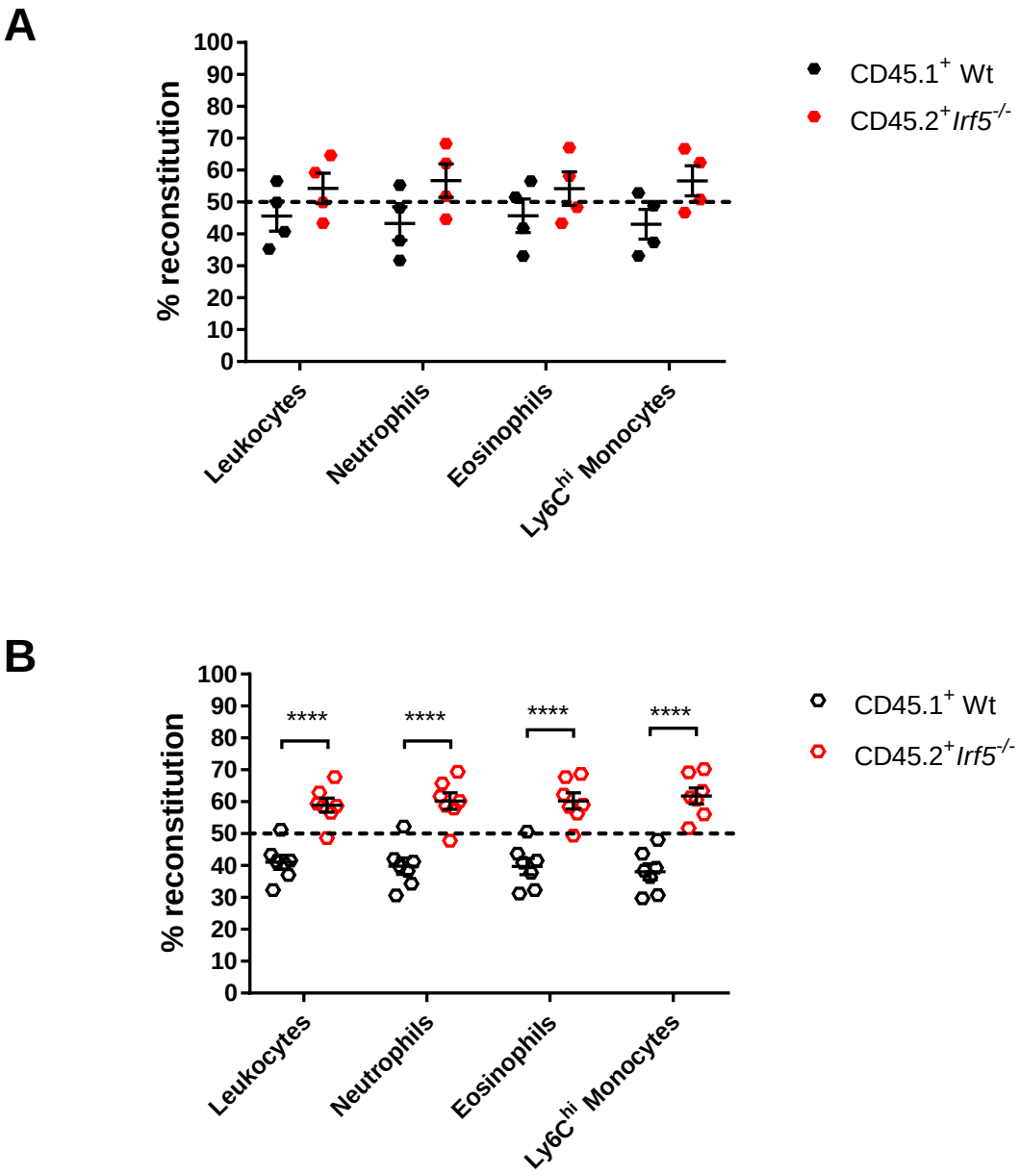

Fig.4.4: Reconstitution of bone marrow leukocytes in mixed bone marrow chimaera

Bone marrow cells were isolated from tibias and femurs of WT:*Irf5*$^{-/-}$ mixed bone marrow chimaeras at **A)** steady state, **B)** d21 of *Helicobacter hepaticus* + αIL10R colitis and reconstitution of leukocytes was analysed by flow cytometry. Leukocytes, including neutrophils, eosinophils, and Ly6C^{hi} monocytes displayed increased reconstitution following *Helicobacter hepaticus* + αIL10R colitis

Donor derived leukocytes were identified by expression of CD45.1 or CD45.2.
Leukocytes: Live CD45^{+}, Neutrophils: Live CD45^{+} CD11b^{+} Ly6G^{+}, Eosinophils: Live CD45^{+} CD11b^{+} Siglec F^{+}, Ly6C^{hi} monocytes: Live CD45^{+} CD11b^{+} Ly6G^{-} Siglec F^{-} Ly6C^{+} MHC II^{-} F4/80^{-}

Statistics
Data presented are Mean ± SEM representative of two independent experiments. Steady state n = 4, Hh + αIL10R n = 7. 2 way ANOVA with Sidak correction for multiple comparisons between genotype, **** p<0.0001,

4.2.3 Equal reconstitution of wild type and irf5 deficient leukocytes in the blood of mixed bone marrow chimaeras at steady state

Generation of WT and *Irf5*$^{-/-}$ myeloid cells was unaffected by IRF5-deficiency (Chapter.3), and reconstitution of progenitors and mature myeloid populations in the bone marrow was found to be equal, except during Hh + αIL10R colits (Fig.4.4). However, the effect of IRF5 on cellular migration was not addressed. Recruitment of CCR2^{+} monocytes to the cLP is a key step in the initiation of inflammation in response to DSS, but has not been demonstrated for the Hh + αIL10R model [301, 302]. In order to characterise the role of IRF5 in mediating recruitment, the reconstitution of haematopoietic cells in blood was assessed by flow cytometry at steady state (Fig.4.3) and during Hh + αIL10R colitis (Fig.4.4).

The reconstitution of the blood at steady state was largely unaffected by IRF5 deficiency, with total leukocytes, neutrophils, and Ly6C^{hi} moncoytes equally derived from each donor, but eosinophils were preferentially derived from *Irf5*$^{-/-}$ ($p < 0.05$, Fig.4.5). During Hh + αIL10R inflammation, reconstitution was also not affected in neutrophils and eosinophils, but Ly6C^{hi} monocytes were preferentially derived from *Irf5*$^{-/-}$ ($p = 0.0140$), albeit this was a modest increase (Fig.4.6) Neutrophils and eosinophils also trended in this manner (Fig.4.6).

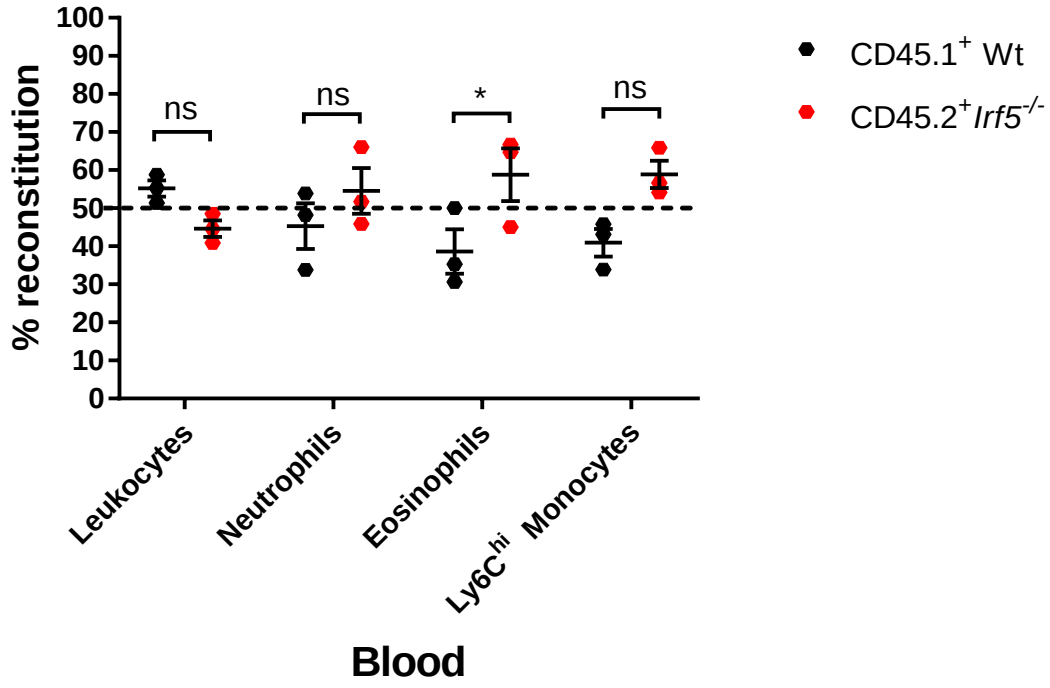

Fig.4.5: Reconstitution of blood leukocytes in mixed bone marrow chimaeras at steady state

Mixed bone marrow chimaeras were generated by reconstitution of lethally irradiated CD45.1$^+$ WT mice with an equal mix of CD45.1$^+$ WT and CD45.2$^+$ *Irf5*$^{-/-}$ bone marrow. Mice were culled by schedule 1 method, followed by cardiac puncture to harvest blood. Erythrocytes were lysed with ACK buffer, and cells were labelled with fluorescently conjugated antibodies to cell surface antigens and analysed by flow cytometry. Donor origin was assessed by expression of either CD45.1 or CD45.2.
Reconstitution of total leukocytes was not affected by IRF5 deficiency, but eosinophils were preferentially reconstituted by *Irf5*$^{-/-}$ donors ($p = 0.0388$).

Statistics:
Data are representative of two independent experiments, n = 3
Mean + SEM. 2 Way ANOVA with Sidak correction. * $p \leq 0.05$

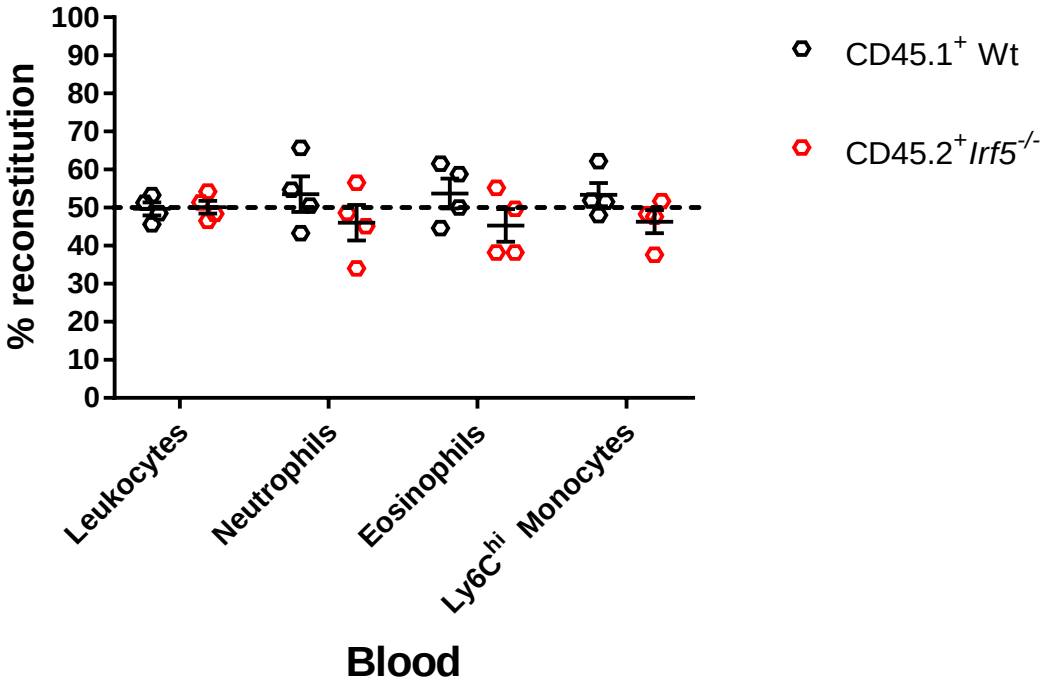

Fig.4.6: Reconstitution of blood leukocytes in mixed bone marrow chimaeras during Hh + αIL10R colitis

Mixed bone marrow chimaeras were generated by reconstitution of lethally irradiated CD45.1$^+$ WT mice with an equal mix of CD45.1$^+$ WT and CD45.2$^+$ *Irf5*$^{-/-}$ bone marrow. Mice were culled by schedule 1 method, followed by cardiac puncture to harvest blood. Erythrocytes were lysed with ACK buffer, and cells were labelled with fluorescently conjugated antibodies to cell surface antigens and analysed by flow cytometry. Donor origin was assessed by expression of either CD45.1 or CD45.2.
Total leukocytes reconstituted equally, no significant differences in reconstitution efficiency was detected in, neutrophils, eosinophils or Ly6C^{hi} monocytes.

Statistics:
Data are representative of two independent experiments, n = 4. Mean + SEM. 2 Way ANOVA with Sidak correction for multiple comparisons.

4.2.4 WT leukocytes predominantly reconstitute the colonic lamina propria at steady state and during Hh + αIL10R colitis

Recruitment of myeloid cells to the cLP is required for the development of DSS colitis, but has not been demonstrated in the Hh + αIL10R model [302]. Although the presence of progenitors at extramedullary sites facilitates the *in situ* derivation of effector leukocytes at sites of inflammation, the major contribution of inflammatory effectors is from the blood [54, 69, 303]. Progenitor cells are depleted by lethal irradiation of mice, therefore, myeloid populations are exclusively derived from donor haematopoietic stem and progenitor cells in MBMC. Flow cytometric analysis of cLP leukocytes was performed to assess the effect of IRF5 on the reconstitution of myeloid cells in steady state (Fig.4.7) and Hh + αIL10R treated (Fig.4.8) MBMCs. At steady state, total leukocytes were found to be preferentially derived from WT progenitors in MBMCs (Fig.4.7A, $p < 0.0001$). Characterisation of the granulocyte compartment revealed that WT neutrophils were overrepresented vs *Irf5*$^{-/-}$ ($p \leq 0.01$), but not eosinophils (Fig.4.7A). The proportion of WT and *Irf5*$^{-/-}$ P1 (Ly6C^{hi}/classical) monocytes was also assessed. WT P1 were significantly enriched over *Irf5*$^{-/-}$ (Fig.4.7A, $p < 0.0001$), Strikingly, in contrast to the overarching phenotype, CD11b^{+} and CD11b^{-} DCs reconstituted in equal proportions in the cLP of mixed bone marrow chimaeras, except for CD11b^{+} CD103^{-} DCs which were marginally, but significantly, reconstituted from WT, (Fig.4.7B, $p = 0.0004$).

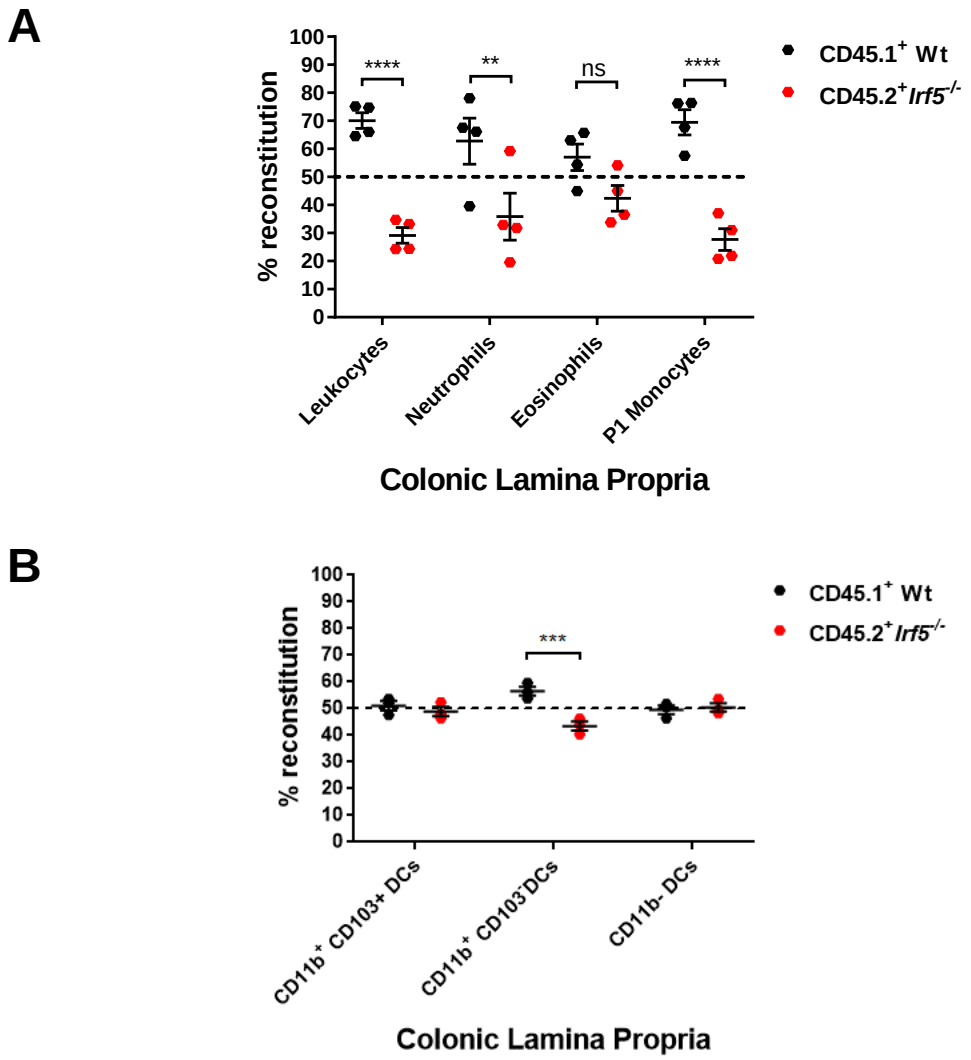

Fig.4.7: Reconstitution of colonic lamina propria leukocytes in mixed bone marrow chimaeras at steady state

Mixed bone marrow chimaeras were generated by reconstitution of lethally irradiated CD45.1$^+$ WT mice with an equal mix of CD45.1$^+$ WT and CD45.2$^+$ *Irf5*$^{-/-}$ bone marrow. Mice were culled by Schedule 1 method, and LPLs were isolated. LPLs were labelled with fluorescently conjugated antibodies to cell surface antigens and analysed by flow cytometry. Donor origin was assessed by expression of either CD45.1 or CD45.2. **A)** Total leukocytes were preferentially reconstituted from WT (mean diff = 40.93% ±7.59, $p < 0.0001$). Neutrophils (mean diff = 26.93% ±7.59, $p = 0.0066$), were preferentially reconstituted from WT. Reconstitution of P1 monocytes were significantly affected by IRF5 deficiency: P1 monocytes (mean diff = 41.78% ±7.59, $p < 0.0001$) displayed greater reconstitution from WT. **B)** CD11b$^+$ CD103$^-$, reconstitution was preferentially from WT (mean diff = 56.53% ±2.398, $p = 0.0004$). However, reconstitution of CD11b$^+$ CD103$^+$, and CD11b$^-$ CD103$^+$ DCs was not affected by IRF5 deficiency.

Statistics:
A: Data are representative of two independent experiments, n = 4 Mean + SEM
B: Data are from one experiment, n = 3 Mean + SEM

2 Way ANOVA with Sidak correction for multiple comparisons; ns = not significant, ** $p \leq 0.01$, *** $p \leq 0.001$, **** $p \leq 0.0001$

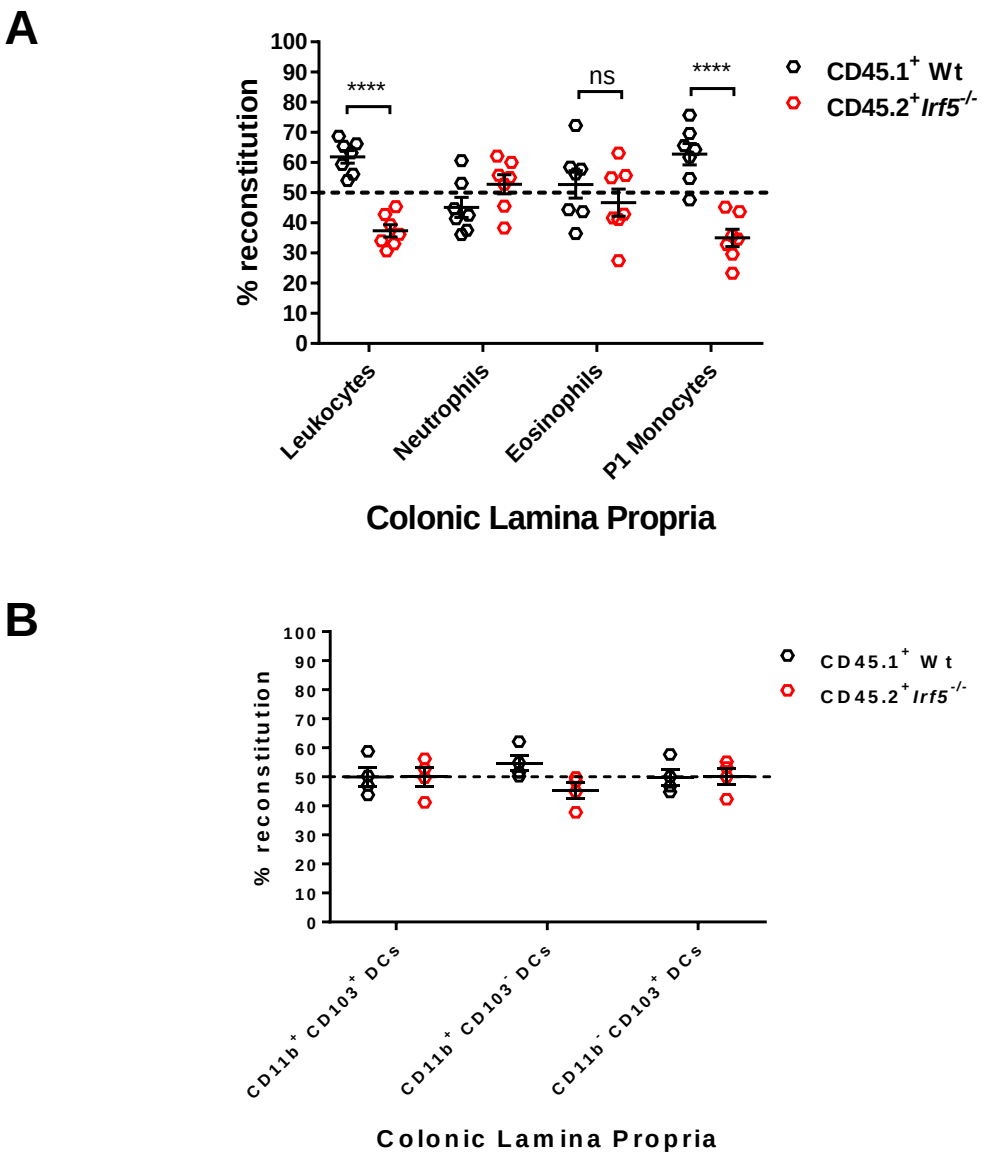

Fig.4.8: Reconstitution of colonic lamina propria leukocytes in mixed bone marrow chimaeras during Hh + αIL10R colitis

Mixed bone marrow chimaeras were generated by reconstitution of lethally irradiated CD45.1$^+$ WT mice with an equal mix of CD45.1$^+$ WT and CD45.2$^+$ *Irf5*$^{-/-}$ bone marrow. Mice were culled by Schedule 1 method, and LPLs were isolated. LPLs were labelled with fluorescently conjugated antibodies to cell surface antigens and analysed by flow cytometry. Donor origin was assessed by expression of either CD45.1 or CD45.2.
Total leukocytes were preferentially reconstituted from WT (mean diff = 24.5% ±4.78, $p < 0.0001$). Neutrophil and Eosinophil reconstitution were not affected during inflammation. Reconstitution of monocyte-derived MNPs were significantly affected by IRF5 deficiency: P1 monocytes (mean diff = 27.76% ± 4.78, $p < 0.0001$). However, reconstitution of CD11b$^+$ CD103$^+$, CD11b$^+$ CD103$^-$, and CD11b$^-$ CD103$^+$ DCs was not affected by IRF5 deficiency.

Statistics:
A: Data are representative of two independent experiments. n = 7. Mean + SEM
B: Data are from one experiment n = 4

2 Way ANOVA with Sidak correction for multiple comparisons; ns = not significant, **** $p \leq 0.0001$

The observed reconstitution phenotype was largely replicated in MBMC treated with Hh + αIL10R with the exception of neutrophils, which reconstituted in equal proportions (Fig.4.8). P1 monocytes ($p < 0.0001$), were reconstituted preferentially by WT (Fig.4.8A). In keeping with the steady state phenotype, reconstitution of DC populations was not affected by IRF5 deficiency. Reconstitution of WT DCs during Hh + αIL10R was not significantly altered by inflammation (Fig.4.8B), although, $CD11b^{+}$ $CD103^{-}$ DCs were reconstituted equally, (Fig.4.8B).

P1 monocyte reconstitution was preferentially by WT donor-derived monocytes during steady state and during Hh + αIL10R inflammation (Fig.4.7A, Fig.4.8A). P1 monocytes represent direct descendants of blood $Ly6C^{hi}$ monocytes. A significant increase in the reconstitution of P1 monocytes relative to blood could indicate that IRF5 mediates processes in monocytes related to their accumulation. cLP P1 monocyte reconstitution was compared with blood $Ly6C^{hi}$ monocyte reconstitution during steady state and during Hh + αIL10R inflammation: WT $Ly6C^{hi}$ monocytes reconstituted in blood at approximately 48% during steady state vs ~70% for P1 monocytes (Fig.4.9A, $p = 0.0163$). At d21 Hh + αIL10R, WT blood monocytes represented ~45% of reconstitution vs ~65% of P1 monocytes in the cLP (Fig.4.9B, $p < 0.0001$).

Irf5$^{-/-}$ monocytes were shown to express less CCR2, the chemokine receptor for CCL2, known to be critical for accumulation of monocytes in the cLP at steady state [113]. However, monocyte responsiveness to CCL2 was not shown to be affected in this study. Therefore, Boyden chambers were performed to quantify WT and *Irf5*$^{-/-}$ monocyte chemotaxis in response to CCL2. CCL2 did not induce *Irf5*$^{-/-}$ monocyte chemotaxis to the extent seen in WT monocytes (Fig.4.10, fold change WT = 1.75 ±0.16 vs fold change *Irf5*$^{-/-}$ 1.21 ±0.15, $p = 0.0283$).

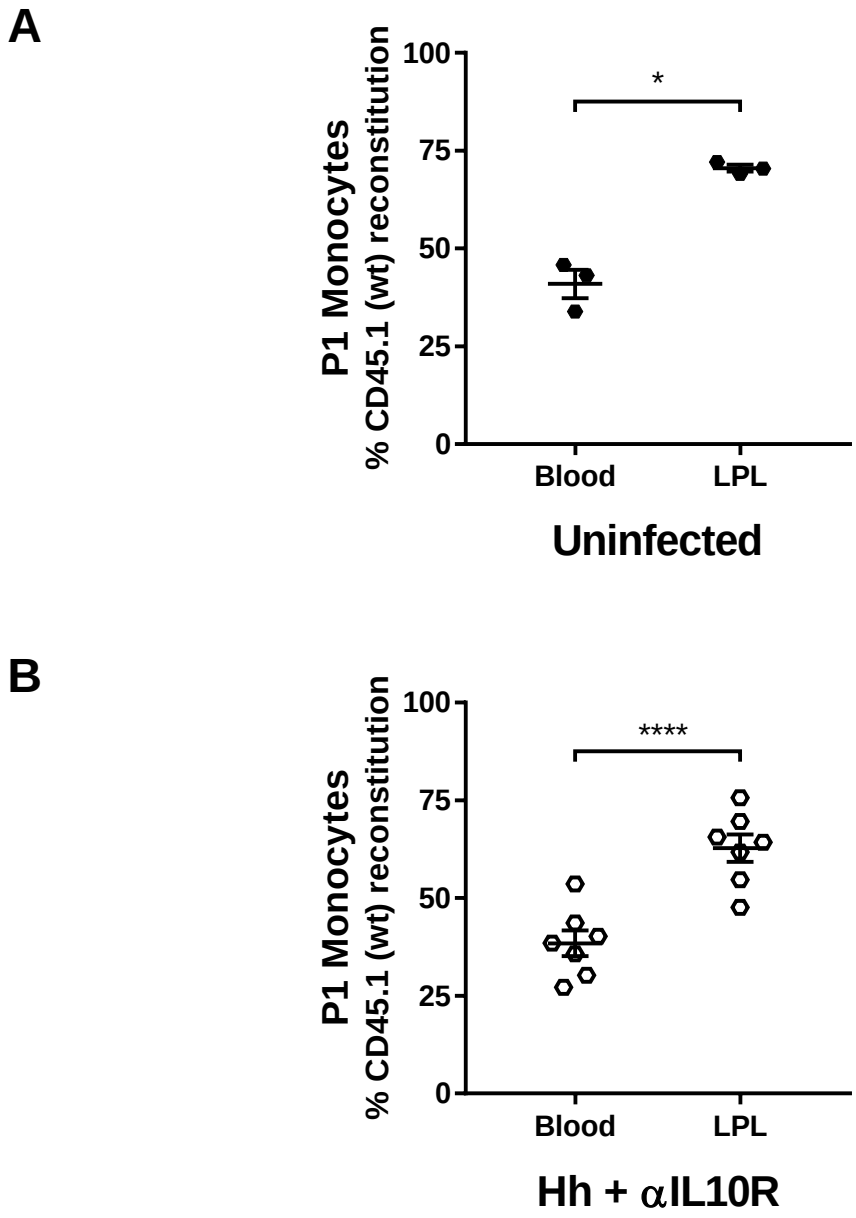

Fig.4.9: WT P1 monocytes preferentially accumulate in the cLP in mixed bone marrow chimaeras

The reconstitution of P1 monocytes (Ly6C^{hi} monocytes in blood) was compared. **A)** in steady state blood, WT and *Irf5*$^{-/-}$ P1 monocytes reconstituted equally, however, in the cLP, the proportion of WT P1 monocytes was significantly elevated (mean difference = 29.6, p = 0.0163). This effect was consistent during Hh + αIL10R colitis **(B)** (mean difference = 24.33, p < 0.0001).

Statistics:
Data are representative of two independent experiments. Steady state: n = 3, Hh + αIL10R: n = 7
Mean + SEM
Paired t test; * p ≤ 0.05, **** p < 0.0001

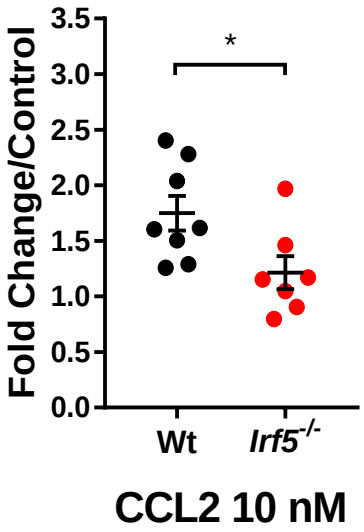

Fig.4.10: WT Ly6Chi monocytes are more migratory towards CCL2 than *Irf5*$^{-/-}$

Ly6C^{hi} monocytes were isolated from the spleens of WT or *Irf5*$^{-/-}$ mice. Boyden chamber migration assays were performed to test the chemotactic potential of Ly6C^{hi} monocytes to 10 nM CCL2. The fold change response to 10 nM CCL2 of WT Ly6C^{hi} monocytes was greater than that of *Irf5*$^{-/-}$ (mean WT = 1.75 ±0.16, mean *Irf5*$^{-/-}$ = 1.21 ±0.15 p = 0.0283).

Statistics:
Data presented are average fold change/control of sextuplicate values from three pooled independent experiments. Experimental replicates were plotted using the Bland-Altman Ratio vs Average method to assess whether experimental results could be pooled. Pooling was considered appropriate when all values fell within the 95% Confidence Interval and bias was ≤ 1. Minimum 2 biological replicates per genotype per experiment. Mean + SEM. Unpaired t test; * p ≤ 0.05.

4.2.5 IRF5 deficiency leads to perturbation of the mononuclear phagocyte compartment in mixed bone marrow chimaeras

IRF5-deficient mice displayed altered composition of the MNP compartment at steady state. In the global knockout environment, the entire architecture of the mouse in altered. MBMC allows WT and *Irf5*$^{-/-}$ haematopoietically-derived cells to share the same environment, thus any defects in myeloid cells may be attributed directly to IRF5. The composition of respective MNP pools (WT or *Irf5*$^{-/-}$) in MBMCs was analysed by flow cytometry. In contrast to the global *Irf5*$^{-/-}$ setting where P1 monocytes were elevated in *Irf5*$^{-/-}$ (Fig.3.12), P1 monocytes comprised the same percentage of MNPs irrespective of donor origin (Fig.4.11A). P2 monocytes as a percentage of MNPs in WT vs *Irf5*$^{-/-}$ mice were unchanged, (Fig.3.12), and, in MBMC, P2 monocytes were unaffected at steady state (Fig.4.11A). P2 monocytes were not significantly affected, in *Irf5*$^{-/-}$ MNPs during Hh + αIL10R in contrast to non-irradiated WT mice (Fig.4.11B). Consistent with the global *Irf5*$^{-/-}$ phenotype, macrophages represented a greater proportion of MNPs both at steady state ($p = 0.0001$) and inflammation (Fig.4.11A, Fig.4.11B, $p = 0.0148$). These increased frequencies of WT macrophages in the MNP pool were compensated by expansion of the CD11b^{+} DC pool at steady state (Fig.4.11A, $p = 0.003$), and inflammation ($p < 0.0001$, Fig.4.11B).

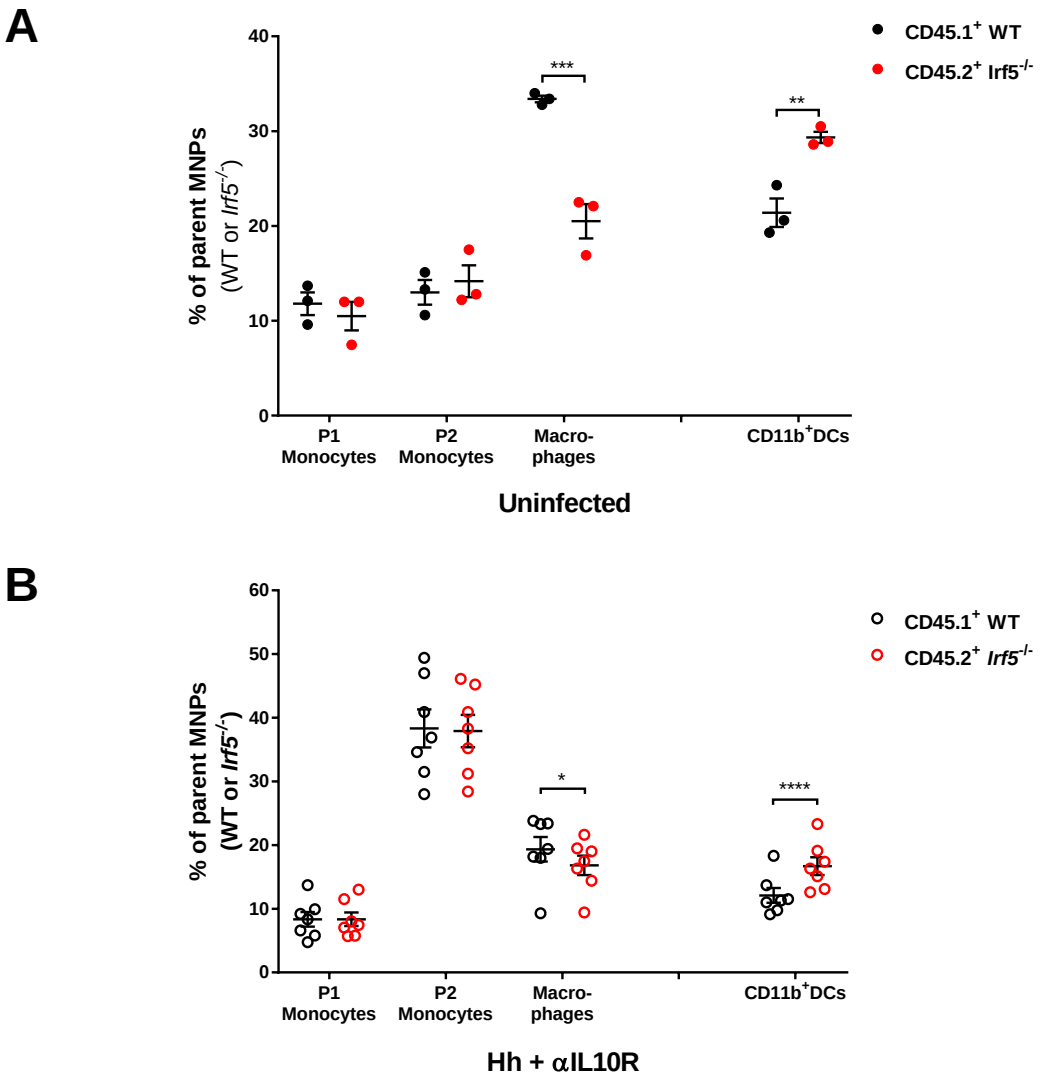

Fig.4.11: WT macrophages represent a higher frequency of MNPs than *Irf5*$^{-/-}$ macrophages

The structure of the MNP compartment in mixed bone marrow chimaeras was assessed by gating on either WT or *Irf5*$^{-/-}$ MNPs and assessing the composition of the respective MNP pool. **A)** Composition of the MNP compartment during steady state: P1 and P2 monocytes were equally represented among WT and *Irf5*$^{-/-}$ MNPs at steady state. WT macrophages were overrepresented (mean diff = 12.9, p = 0.0001). CD11b^{+} DCs represented a greater part of *Irf5*$^{-/-}$. MNPs than in WT (mean diff = 7.93, p = 0.003). **B)** Composition of the MNP compartment at d21 Hh + aIL10R colitis: P1 and P2 monocytes represented equal proportions of the respective MNP compartments in mixed bone marrow chimaeras during inflammation. WT macrophages were present at higher frequencies of MNPs relative to *Irf5*$^{-/-}$ (mean diff = 2.52, p = 0.0148). CD11b^{+} DCs were a higher frequency of *Irf5*$^{-/-}$ MNPs (mean diff = 4.6, p < 0.0001).

Statistics:
Data are representative of two independent experiments. Uninfected: n = 3, Hh + αIL10R n = 7
Mean + SEM
2-way ANOVA with Sidak correction: * p ≤ 0.05, ** p ≤ 0.01, *** p ≤ 0.001, **** p < 0.0001

4.2.6 IRF5 expression drives a macrophage fate in Ly6C^{hi} monocytes in mixed bone marrow chimaeras

Here we have demonstrated that IRF5 promotes the accumulation of WT MNPs which may be via affected CCL2 responsiveness. Within the MNP compartment, WT macrophages are overrepresented to a greater extent than WT P1 monocytes at steady state and during inflammation (Fig.4.12A, Fig.4.12B), indicating a pathway other than recruitment is affecting macrophage accumulation. The increase in macrophages is offset by a corresponding increase in CD11b^{+} DCs in the *Irf5*$^{-/-}$ MNP compartment (Fig.4.11A, Fig.4.11B). To explore the phenotype of IRF5-deficient MNPs in greater depth, massively-parallel Single Cell RNA Sequencing (scRNAseq), using the 10X-seq protocol (10X scRNAseq, Chapter.2.12.2) was performed on CX_3CR1^{+} mononuclear phagocytes isolated from MBMCs infected with Hh + αIL10R. QC identified 1454 cells expressing more than 500 genes and less than 5% fraction of mitochondrial reads.

Analysis of 10X sequencing of WT and *Irf5*$^{-/-}$ CX_3CR1^{+} MNPs isolated from MBMCs using the Seurat package in R (http://satijalab.org/seurat/) revealed that CX_3CR1^{+} MNPs separated into eight distinct clusters based on unsupervised clustering (Fig.4.13) [192, 252]. MNP subtypes could be identified based on the differential expression of markers between clusters (Fig.4.14), summarised in Table.4.1. Macrophages could be separated into two similar clusters: Cluster 5 (resident macrophages), defined by high expression levels of prototypical macrophage markers (*Adgre*, *Cd14*) and cLP macrophage markers (*Cd81*, *Dnase1l3*, *Zmynd15* as well as *Ccl2, Ccl3*, *Ccl4*, *Ccl7,* and *Ccl9* chemokines) Cluster 2 (inflammatory macrophages), expressing high levels of cLP macrophage markers (*Cd81*, *C1qa*,*b*,*c*, *Cd63*, *Cd72*), the chemokine *Ccl8* and anti-microbial molecules (*Lyz2*, *Acp5*, Fig.4.14, Table.4.1).

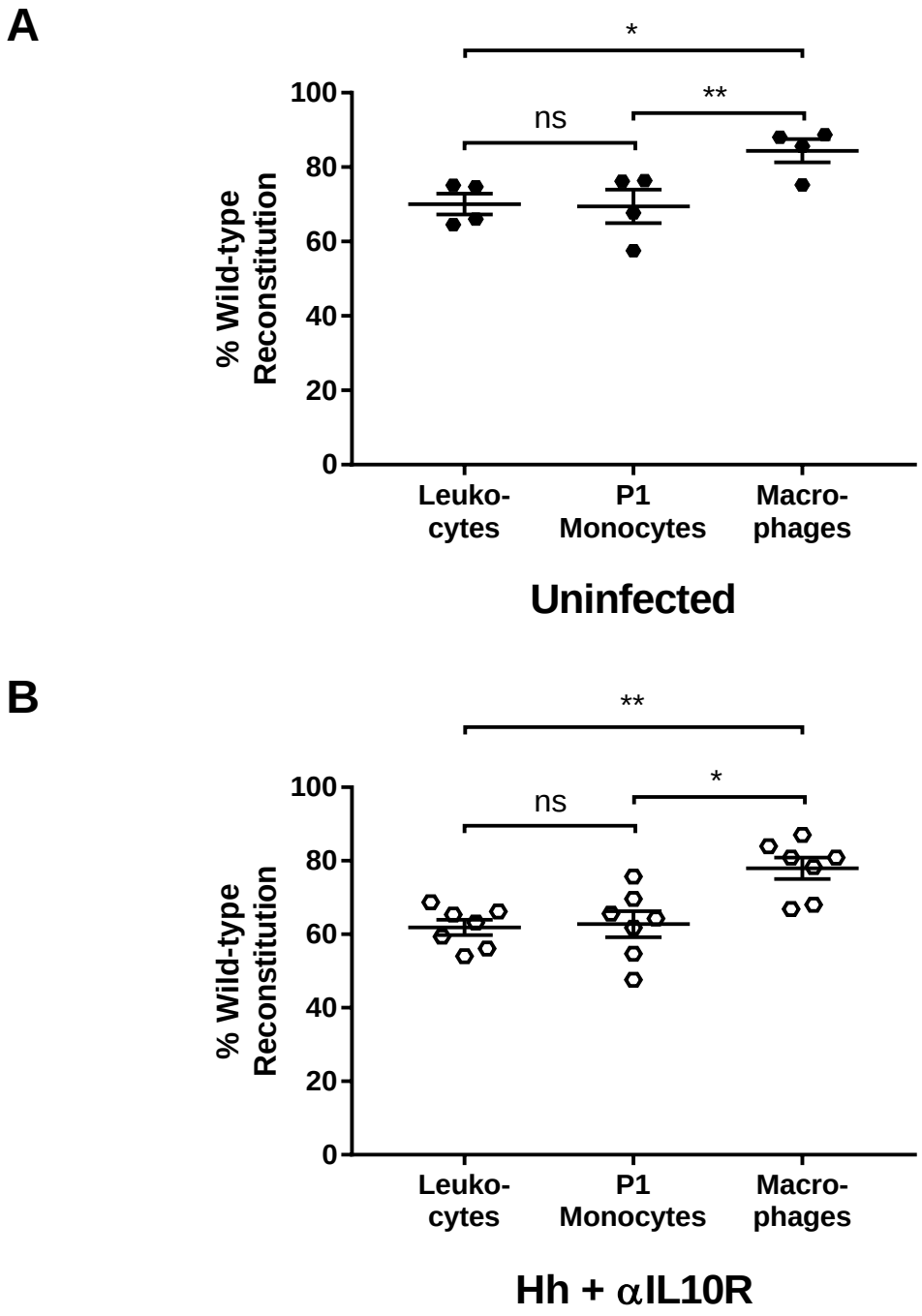

Fig.4.12: WT macrophages exhibit enhanced reconstitution relative to P1 monocytes

WT reconstitution of total leukocytes was compared with that of P1 monocytes and macrophages in the cLP of mixed bone marrow chimaeras. **A)** In steady state the proportion of macrophages reconstituted by WT was significantly elevated vs total leukocytes (mean diff = 14.31 ±2.49, p = 0.0212) and P1 monocytes (mean diff = 14.94 ±1.67, p < 0.0061). **B)** This effect was consistent during Hh + αIL10R colitis between leukocytes and macrophages (mean diff = 16.11 ±2.46, p < 0.0015) and P1 monocytes and macrophages (mean diff = 15.21 ±3.69, p = 0.0146).

Statistics:
Data are representative of two independent experiments. Steady state: n = 4. Hh + αIL10R: n = 7. Mean + SEM. One-way repeated measures ANOVA with Tukey correction; * p ≤ 0.05, ** p ≤ 0.01

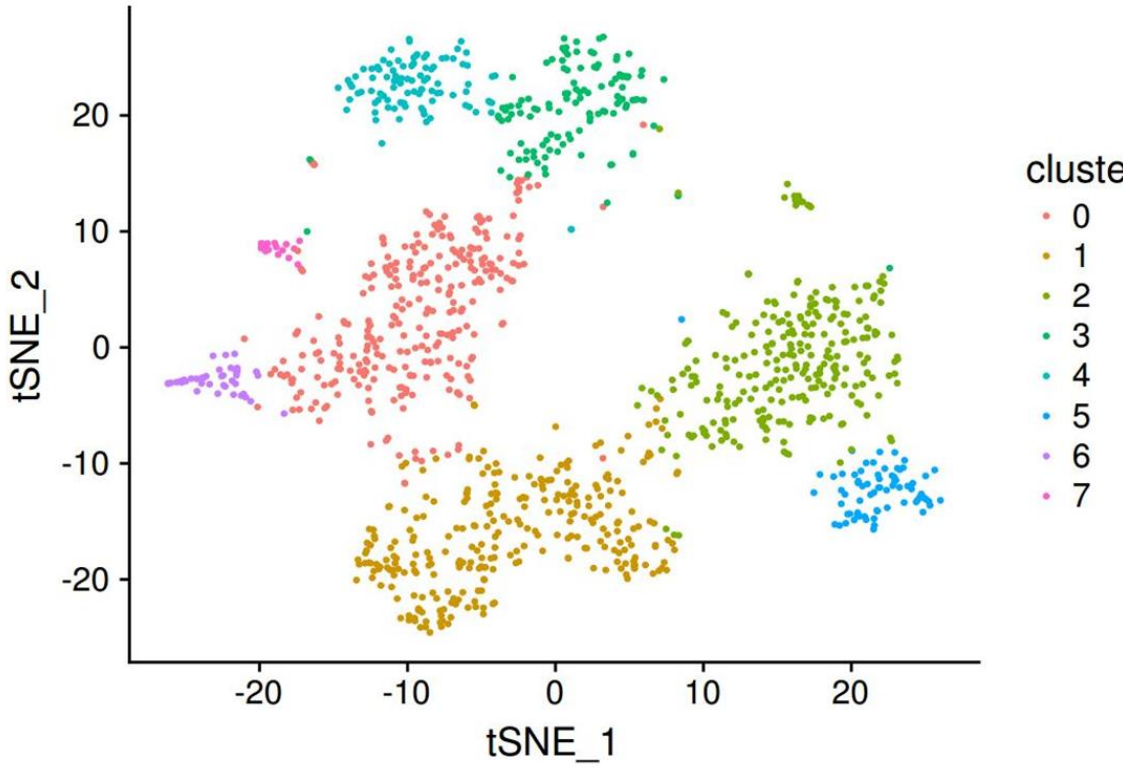

Fig.4.13: CX_3CR1^+ wild-type and *Irf5*$^{-/-}$ colonic lamina propria mononuclear phagocytes are separated into eight clusters by analysis of 10X sequencing

WT or *Irf5*$^{-/-}$ cLP CX_3CR1^+ MNPs were isolated from WT:*Irf5*$^{-/-}$ mixed bone marrow chimaeras into culture medium. MNPs were then immediately transferred to 10X Chromium for cell capture, followed by Illumina sequencing. Data were mapped to the mm10 genome and analysed using the Seurat package in R. 593 WT cells, and 861 *Irf5*$^{-/-}$ cells passed QC and were analysed. Data were controlled for the enrichment of *Irf5*$^{-/-}$ MNPs in the analysis. Dimensionality reduction was performed using tSNE which resulted in the identification of eight distinct clusters of similar MNPs. Data analysis was performed by Dr. Stephen Sansom (University of Oxford)

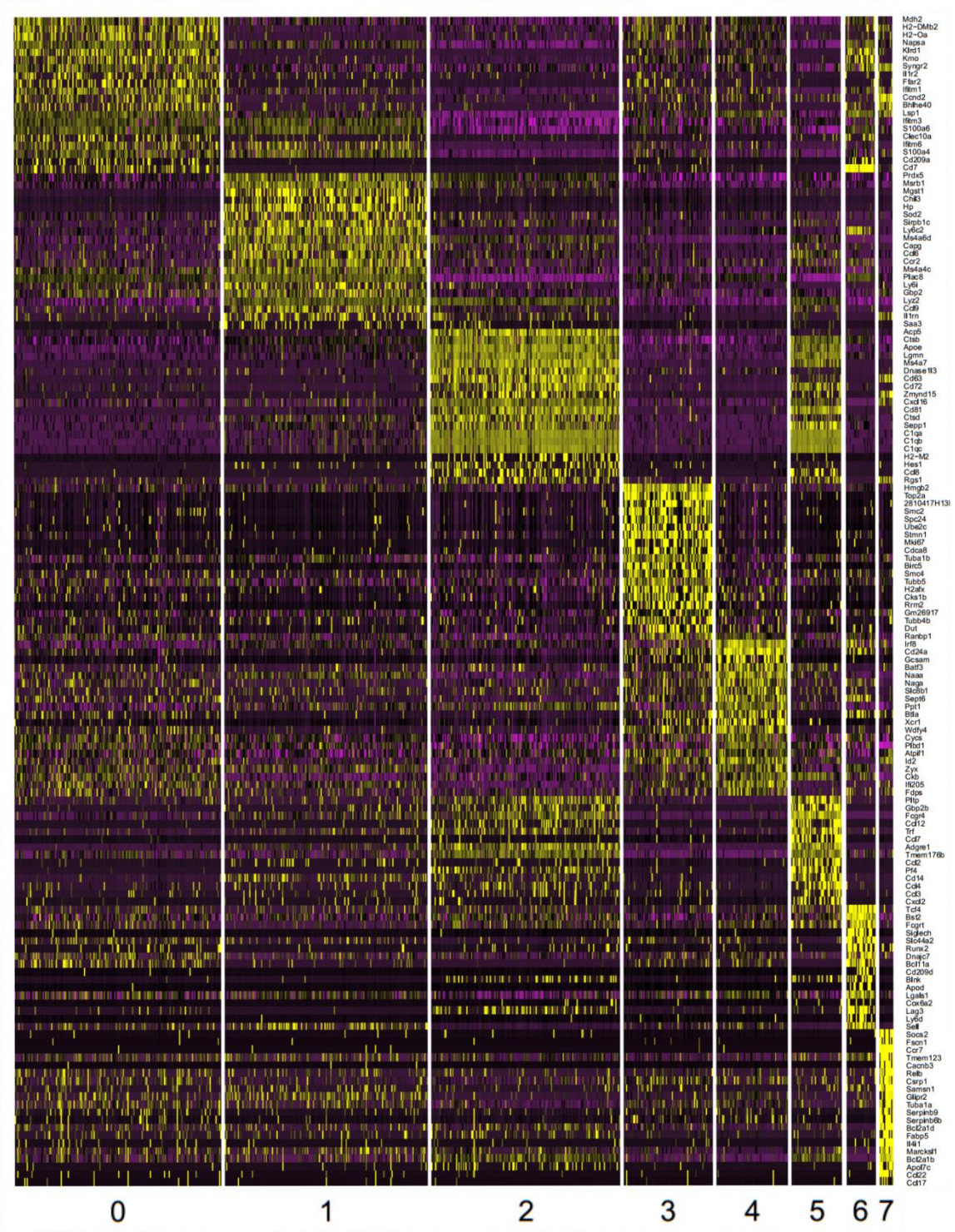

Fig.4.14: Clusters identified by Seurat display distinct transcriptional signatures

WT or *Irf5*$^{-/-}$ MNPs were sorted from mixed bone marrow chimaeras on the basis of $CX_3CR1^{gfp/+}$ and CD45.1 or CD45.2 expression. 10X sequencing followed by data analysis using the Seurat package in R was performed. Heatmap displays normalised differentially expressed genes between identified clusters.
Data analysis was performed by Dr. Stephen Sansom (University of Oxford)

Table.4.1: Identification of mononuclear phagocyte clusters

Cluster	Phenotype	Cell type
0	H2-DMb2, H2-Oa, Cd209a, Cd7	DC
1	Ly6c2, Lyz2, Ccr2, Cd14, Sell	Monocytes
2	Cd63, Cd72, C1qa, C1qb, C1qc, Cd81, Ccl8, Lyz2, Zmynd15	Inflammatory macrophages
3	Irf8, Cd24a, Batf3, Xcr1, Id2,	BATF3-dependent DC $CD103^{+}CD11b^{+}$
4	Irf8, Cd24a, Batf3, Xcr1, Id2,	BATF3-dependent DC $CD103^{+}CD11b^{-}$
5	Ccl7, Adgre1, Ccl2, Ccl3, Ccl4, Gbp2b, Cxcl2, Fcgr4, Cd14	Resident macrophages
6	Siglech, Bst2, Cd209d, Sell, Tcf4, Cd7,	Plasmacytoid DC
7	Irf8, Cd24a, Batf3, Xcr1, Id2, Ccr7, Relb, Ccl22, Ccl17, Socs2	BATF3-dependent DC Activated, migratory

Single cells were downsampled to analyse equal numbers of WT and *Irf5*$^{-/-}$ MNPs in each cluster. More macrophages were derived from WT in cluster 2 (193 WT vs 70 *Irf5*$^{-/-}$, 2.76-fold), and to somewhat lesser extent in cluster 5 (47 WT vs 24 *Irf5*$^{-/-}$, 2-fold) (Fig.4.15A, Fig.4.15B). These two clusters also displayed the highest number of differentially expressed genes between genotypes (Fig.4.16A, Cluster 2: 60, and Cluster 5: 58). The top genes differentially expressed between genotypes within clusters are presented in Fig.4.16B, and Table.4.2-4.6. Cluster2 and Cluster 5 shared genes that were associated with a cLP macrophage signature, such as *C1qa*, *b*, and *c*, *Cd81*, *Ccl8*, *Dnase1l3*, and *Zmyd15* [138]. However, these clusters could be distinguished by differential expression of several markers: Cluster 5 expressed a more terminally differentiated phenotype, demonstrated by higher levels of *Adgre1* (F4/80), *Mrc1* (CD206), analogous to Mowat's P4 CX_3CR1^{hi} whereas, Cluster 2 expressed higher levels of *Itgax* (CD11c), which may indicate that Cluster 2 represents a more inflammatory monocyte/macrophage cluster (Mowat P3) [57, 138].

Among the top differentially expressed genes in Cluster 2 was *Ccl4*, which was previously shown to be directly regulated by IRF5 (Fig.4.16) [162, 163, 261]. *Il1rn*, an anti-inflammatory decoy receptor for IL1α and IL1β, was highly expressed in Cluster 2 *Irf5*$^{-/-}$ relative to WT.

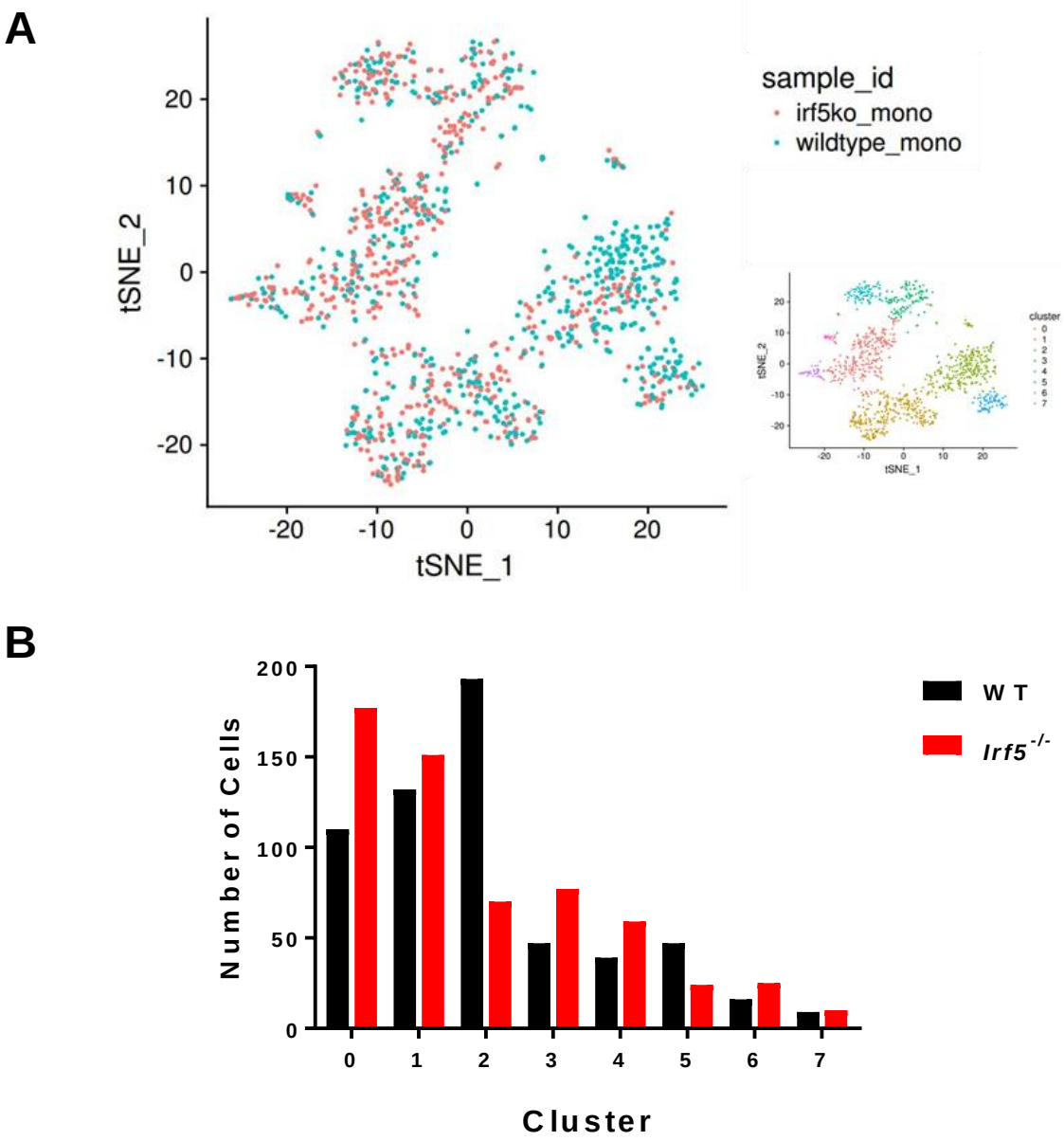

Fig.4.15: Dimensionality reduction of WT and *Irf5*$^{-/-}$ MNPs isolated from mixed bone marrow chimaeras reveals a population structure effect of IRF5-deficiency

WT or *Irf5*$^{-/-}$ MNPs were sorted from mixed bone marrow chimaeras on the basis of CX_3CR1-gfp and CD45.1 or CD45.2 expression. 10X sequencing followed by data analysis using the Seurat package in R was performed to identify clusters. **A)** tSNE plot coloured by genotype. **B)** Clusters 0, 1, 3, 4, and 6 are predominantly occupied by *Irf5*$^{-/-}$ cells. Clusters 2 and 5 are predominantly occupied by WT.
Data analysis was performed by Dr. Stephen Sansom (University of Oxford)

A

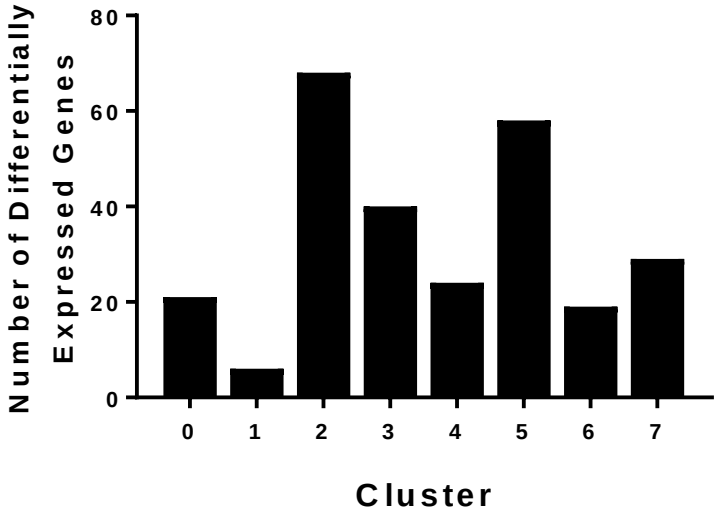
Number of Differentially Expressed Genes
80
60
40
20
0
0
1
2
3
4
5
6
7
Cluster

B

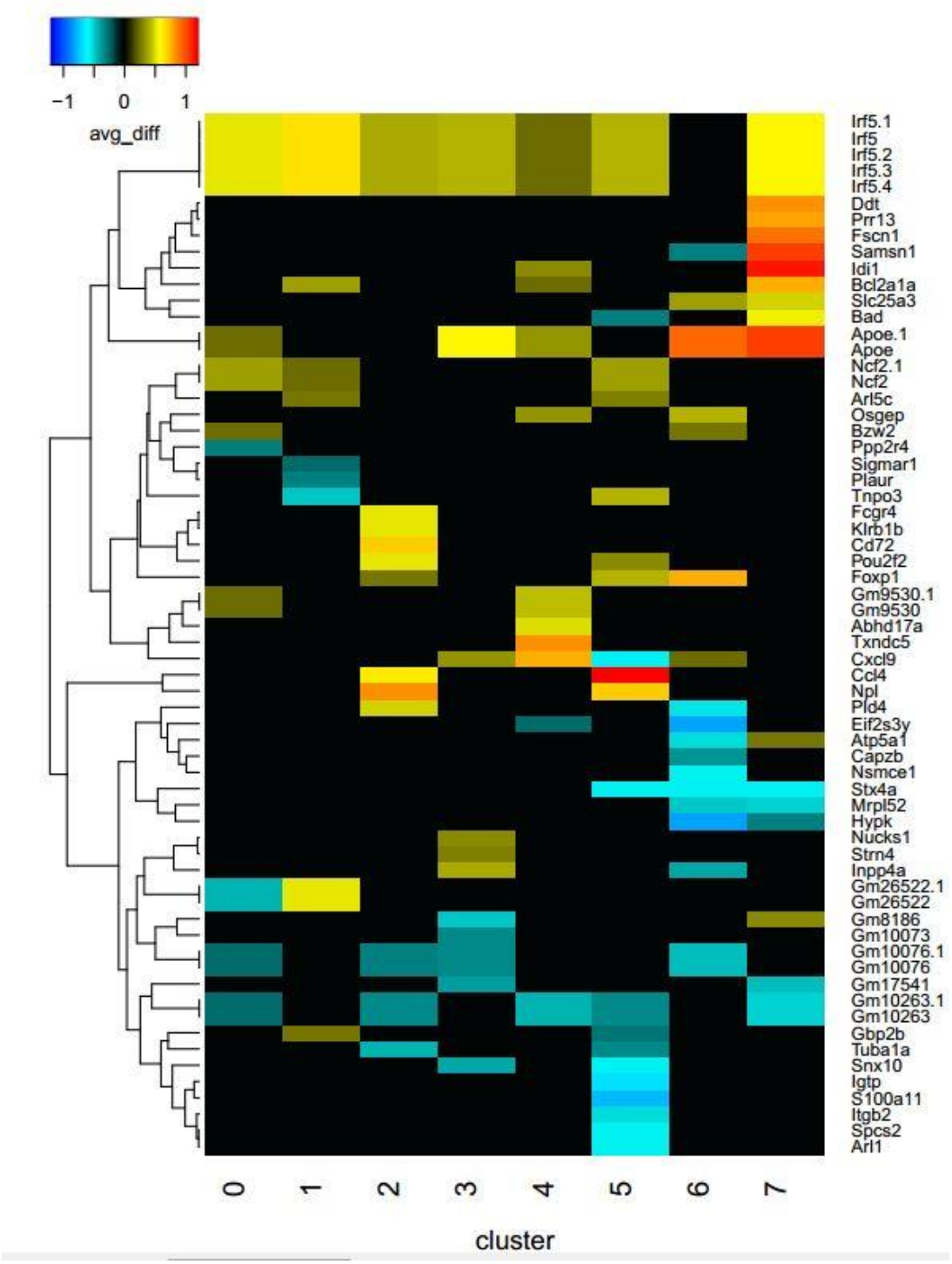

Fig.4.16: Differentially expressed genes between genotypes within clusters

WT or *Irf5*$^{-/-}$ MNPs were sorted from mixed bone marrow chimaeras on the basis of CX_3CR1-gfp and CD45.1 or CD45.2 expression. 10X sequencing followed by data analysis using the Seurat package in R was performed to identify clusters. **A)** Numbers of differentially expressed genes between genotypes in each cluster. **B)** Top differentially expressed genes within clusters identified by the function “negbinom.cluster.dir” using the Seurat package in R.
Data analysis was performed by Dr. Stephen Sansom (University of Oxford)

Table.4.2: Top differentially expressed genes in Cluster 1

Gene ID	Gene	p value	p.adj	Average Difference
ENSMUSG00000012535	Tnpo3	2.52E-07	5.57E-05	-0.46607
ENSMUSG00000036078	Sigmar1	9.78E-05	0.006364	-0.25144
ENSMUSG00000026480	Ncf2	0.001474	0.037047	0.254932
ENSMUSG00000046223	Plaur	0.003424	0.059632	-0.29153

The data presented in this chapter indicate that IRF5 may affect the development of monocytes to macrophages, and transition from inflammatory to resident macrophage states in the cLP. During monocyte to macrophage transition, modules of genes are switched on and off until a resident macrophage state is achieved [138]. Single cell analysis allows the visualisation of transient cell states that would be masked by profiling gene expressing in bulk samples. The Monocle algorithm traces the trajectory of gene expression and places single cells within that trajectory (pseudotime). Pseudotime analysis of the single cells collected using 10X was performed using the "monocle" package in R (http://cole-trapnell-lab.github.io/monocle-release/) [212].

Pseudotime analysis revealed three states adopted by the MNPs (Fig.4.17A). Transposition of the clusters identified in Seurat revealed that Cluster 1 (monocytes) was the most similar population to the other seven clusters, but was more phenotypically similar to Clusters 2 and 5 (macrophages), indicated by branching of Cluster 1 (Fig.4.17B). Clusters 0, 4, 6, and 7 (DCs) marked the right branch of the analysis which was distinct from Clusters 2 and 5 on the left. Cluster 3 mainly comprised the terminus of the right hand branch, but some cells from Cluster 3 were present in the left branch (Fig.4.17B).

A

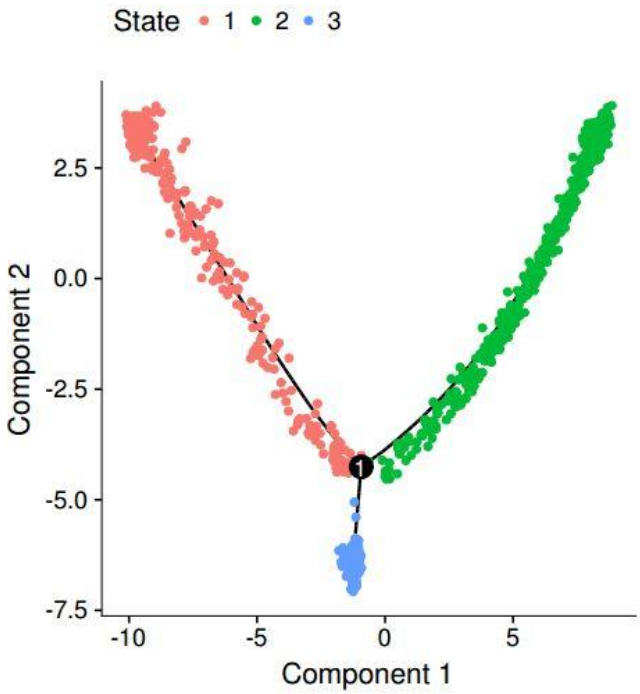

B

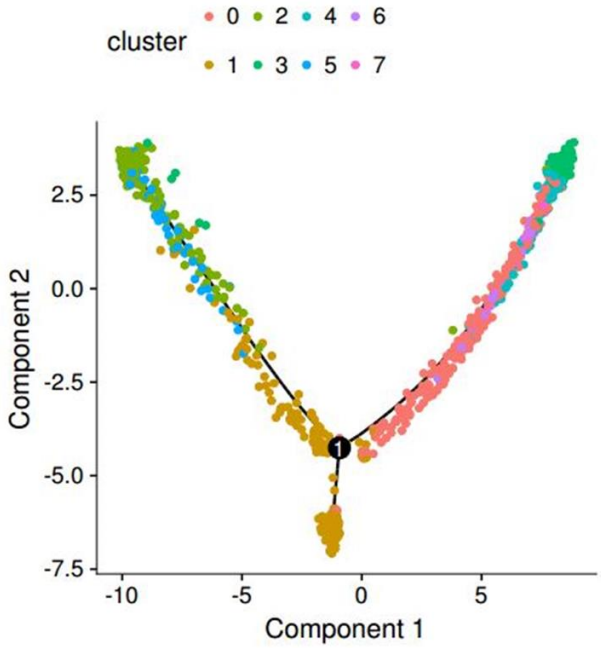

Fig.4.17: Pseudotime analysis of CX_3CR1^+ mononuclear phagocytes

WT or $Irf5^{-/-}$ MNPs were sorted from mixed bone marrow chimaeras on the basis of CX_3CR1-gfp and CD45.1 or CD45.2 expression. 10X sequencing followed by data analysis using the Seurat package in R was performed to identify clusters. Pseudotime analysis was performed by passing MNP clusters through the Monocle package. Cluster 1 was identified as the most similar cluster to each arm. Clusters 2 and 3 are the most transcriptionally distinct based on monocle analysis Data analysis was performed by Dr. Stephen Sansom (University of Oxford)

.

10X Cluster 1 represents newly entered Ly6C^{hi} P1 monocytes (Table.4.1) that give rise to macrophages in the intestine [57]. Differentially expressed genes in 10X Cluster 1, and 10X Cluster 2 may represent critical genes in the regulation of macrophage fate. Five genes were found to be significantly differentially expressed in 10X Cluster 1, summarised in Table.4.2. The top 20 up and down differentially expressed genes between WT and *Irf5*$^{-/-}$ in 10X Cluster 2 are summarised in Table.4.3 and Table.4.4. The differentially expressed genes will be discussed later in this chapter.

Table.4.3: Top upregulated genes in WT 10X Cluster 2

Gene ID	Gene	p value	p.adj	Average Difference
ENSMUSG00000042684	Npl	3.11E-12	2.82E-15	0.841994
ENSMUSG00000028459	Cd72	2.16E-08	4.88E-11	0.713218
ENSMUSG00000052160	Pld4	7.02E-07	1.90E-09	0.501079
ENSMUSG00000059089	Fcgr4	2.91E-05	1.05E-07	0.543993
ENSMUSG00000029771	Irf5	5.93E-05	2.95E-07	0.397115
ENSMUSG00000008496	Pou2f2	3.76E-04	2.40E-06	0.538759
ENSMUSG00000079298	Klrb1b	5.43E-04	3.93E-06	0.529512
ENSMUSG00000025059	Gk	1.92E-03	1.73E-05	0.46466
ENSMUSG00000040552	C3ar1	2.13E-03	2.12E-05	0.351017
ENSMUSG00000037706	Cd81	2.62E-03	2.72E-05	0.371806
ENSMUSG00000028869	Gnl2	7.29E-03	0.000115	0.431589
ENSMUSG00000028108	Ecm1	7.54E-03	0.000129	0.47454
ENSMUSG00000026548	Slamf9	9.47E-03	0.000171	0.350616
ENSMUSG00000047250	Ptgs1	2.38E-02	0.000635	0.370671
ENSMUSG00000056888	Glipr1	4.86E-02	0.00257	0.352931

Table.4.4: Top upregulated genes in *Irf5*$^{-/-}$ 10X Cluster 2

Gene ID	Gene	p value	p.adj	Average Difference
ENSMUSG00000072235	Tuba1a	0.00	1.86E-07	-0.40943
ENSMUSG00000069515	Lyz1	0.00	7.68E-06	-0.73507
ENSMUSG00000030588	Yif1b	0.01	7.49E-05	-0.33025
ENSMUSG00000029922	Mkrn1	0.01	0.000123	-0.32171
ENSMUSG00000022586	Ly6i	0.01	0.000179	-0.74128
ENSMUSG00000023913	Pla2g7	0.01	0.000202	-0.40572
ENSMUSG00000060143	Gm10076	0.01	0.0002	-0.30889
ENSMUSG00000001128	Cfp	0.03	0.001214	-0.41809
ENSMUSG00000066407	Gm10263	0.03	0.001191	-0.32323
ENSMUSG00000026981	Il1rn	0.04	0.001719	-0.33557
ENSMUSG00000075705	Msrb1	0.05	0.002304	-0.30514
ENSMUSG00000068129	Cst7	0.05	0.002908	-0.34434

A resident macrophage phenotype (*Adgre1*, *Mrc1*, *Dnase1l3*, *Zmynd15*, *Ccl7*, *Ccl2*, *Ccl3*, *Ccl4*, *Gbp2b*, *Cxcl2*, *Fcgr4*, *Cd14*) was observed in 10X Cluster 5 (Fig.4.14, Table.4.1). DEGs between WT and *Irf5*$^{-/-}$ in Cluster 5 macrophages are summarised in Table.4.5 and Table.4.6. Cluster 5 WT macrophages expressed higher levels of the monocyte chemokines *Ccl4*, and *Ccl5*, and interestingly, the atypical Inhibitor of NFκB gene, *Nfkbiz*, which is essential for production of proinflammatory cytokines and chemokines, such as IL6, IL12, and CCL2, but was also demonstrated to control macrophage IL10 production [304].

Table.4.5: Top upregulated genes in WT Cluster 5

Gene ID	Gene	p value	p.adj	Average Difference
ENSMUSG00000018930	Ccl4	0.02	5.04E-04	1.269414
ENSMUSG00000035042	Ccl5	0.05	2.55E-03	1.093933
ENSMUSG00000042684	Npl	0.05	2.76E-03	0.711522
ENSMUSG00000028465	Tln1	0.07	3.94E-03	0.499397
ENSMUSG00000005656	Snx6	0.07	4.07E-03	0.6602
ENSMUSG00000035356	Nfkbiz	0.07	4.31E-03	0.628052
ENSMUSG00000025279	Dnase1l3	0.08	6.22E-03	0.531006
ENSMUSG00000098112	Bin2	0.08	6.83E-03	0.46811

Table.4.6: Top upregulated genes in *Irf5*$^{-/-}$ Cluster 5

Gene ID	Gene	p value	p.adj	Average Difference
ENSMUSG00000027907	S100a11	0.003	3.60E-05	-0.7493
ENSMUSG00000030805	Stx4a	0.006	9.68E-05	-0.57292
ENSMUSG00000038301	Snx10	0.008	1.32E-04	-0.56125
ENSMUSG00000000290	Itgb2	0.015	3.31E-04	-0.52142
ENSMUSG00000035227	Spcs2	0.019	4.73E-04	-0.55324
ENSMUSG00000078853	Igtp	0.021	5.48E-04	-0.66527
ENSMUSG00000060904	Arl1	0.026	7.10E-04	-0.56387
ENSMUSG00000027514	Zbp1	0.029	8.66E-04	-0.49693
ENSMUSG00000040212	Emp3	0.030	9.49E-04	-0.53108
ENSMUSG00000052298	Cdc42se2	0.043	1.93E-03	-0.49502
ENSMUSG00000022488	Nckap1l	0.047	2.34E-03	-0.51686

4.2.7 RNAseq analysis of small bulk samples of WT and *Irf5*$^{-/-}$ macrophages in mixed bone marrow chimaera reveals intrinsic transcriptional differences between populations

10X is a powerful platform to analyse the transcriptome of thousands of single cells in parallel. However, 10X RNAseq suffers from relatively limited coverage of the transcriptome. To address this issue, small bulk populations of 100 cLP WT and *Irf5*$^{-/-}$ macrophages were collected from Hh + αIL10R inflamed colon. Macrophages were isolated using FACS-sorting for Live CD45^{+} CD11b^{+} Ly6C^{-} MHC II^{+} F4/80^{+} cells and cDNA libraries were prepared according to the Smart-Seq2 protocol. Expression of ~15, 000 genes were detected, of which 296 genes were found to be differentially expressed between WT and *Irf5*$^{-/-}$ macrophages (Fig.4.18A). Highly differentially expressed genes were plotted (Fig.4.18B) and summarised in Table.4.7 (Upregulated in *Irf5*$^{-/-}$), and Table.4.8 (Upregulated in WT).

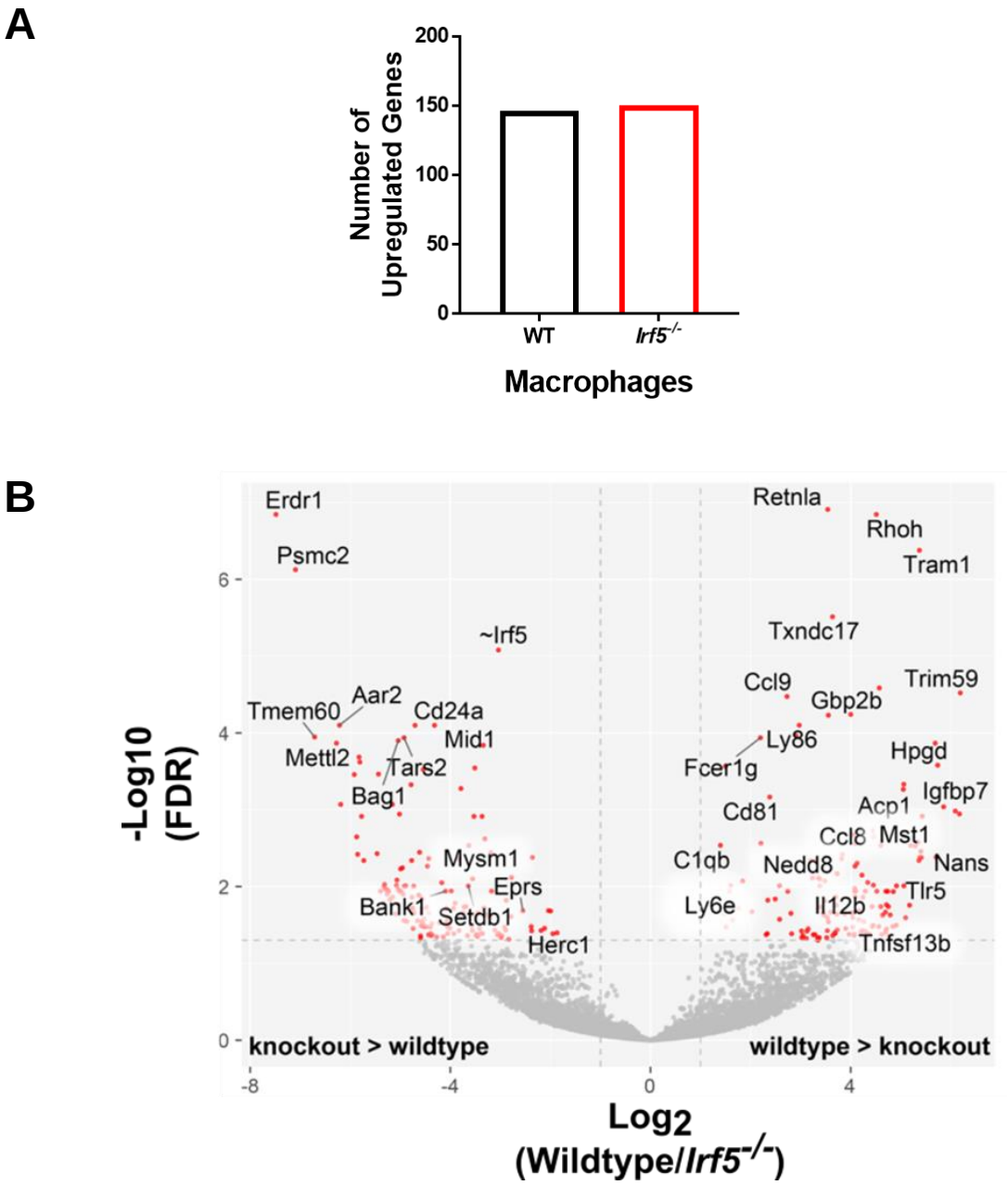

Fig.4.18: Volcano plot of differentially expressed genes between wild-type and *Irf5*$^{-/-}$ macrophages from mixed bone marrow chimaera at d21 Hh + αIL10R

LPLs were isolated from mixed bone marrow chimaeras at d21 Hh + αIL10R colitis. 100 macrophages (CD45^{+} CD11b^{+} Ly6G^{-} Siglec F^{-} Ly6C^{-} MHC II^{+} F4/80^{+}) of each genotype (WT or *Irf5*$^{-/-}$ identified by expression of either CD45.1 or CD45.2) per mouse were sorted into Smart-Seq2 lysis buffer. Nextera library preparation was performed on the bulks, followed by Illumina Hiseq2000v4 sequencing. Reads were filtered and mapped to the mm10 genome, and DESeq2 was used to identify differentially expressed genes. **A)** Numbers of genes upregulated in each genotype. **B)** Volcano plot of differentially expressed genes.

Statistics:
N = 3 biological replicates
Data analysis was performed by Dr. Stephen Sansom (University of Oxford)

Table.4.7: Top 20 genes upregulated in *Irf5*$^{-/-}$ macrophages from mixed bone marrow chimaera d21 Hh + αIL10R

Gene ID	Symbol	Base Mean	Log_2 Fold Change	lfcSE	p adj
ENSMUSG00000096768	Erdr1	87.78845	7.484952	1.135675	1.43E-07
ENSMUSG00000028932	Psmc2	92.90367	7.094149	1.133008	7.49E-07
ENSMUSG00000045435	Tmem60	55.61884	6.71201	1.292539	0.000113
ENSMUSG00000020691	Mettl2	56.82934	6.275169	1.2259	0.000136
ENSMUSG00000027628	Aar2	62.72574	6.214999	1.171759	7.94E-05
ENSMUSG00000074749	Kiz	39.67361	6.19077	1.332519	0.000851
ENSMUSG00000006736	Tspan31	44.68297	5.918877	1.216224	0.000348
ENSMUSG00000061769	Klra6	63.2024	5.871137	1.33968	0.002256
ENSMUSG00000104752	Gm5565	20.27579	5.851017	1.390004	0.003805
ENSMUSG00000022474	Pmm1	49.64771	5.823839	1.160856	0.000206
ENSMUSG00000032279	Idh3a	59.89756	5.80813	1.166218	0.000239
ENSMUSG00000040415	Dtx3	30.37504	5.774027	1.271551	0.00122
ENSMUSG00000070683	Lactbl1	19.72503	5.728614	1.387393	0.00458
ENSMUSG00000031959	Wdr59	22.33472	5.463237	1.294276	0.003726
ENSMUSG00000054942	Fam73a	60.0139	5.435956	1.114991	0.000344
ENSMUSG00000021363	Mak	14.89674	5.394879	1.414158	0.011527
ENSMUSG00000012483	Rpa3	49.16001	5.337686	1.455304	0.016437
ENSMUSG00000026784	Pdss1	29.85138	5.321845	1.376849	0.010078
ENSMUSG00000050846	Zfp623	51.65535	5.313833	1.358877	0.009411
ENSMUSG00000040112	Mrps35	34.16846	5.295907	1.378826	0.01093

Table.4.8: Top 20 genes upregulated in WT macrophages from mixed bone marrow chimaera d21 Hh + αIL10R

Gene ID	Symbol	Base Mean	Log_2 Fold Change	lfcSE	p adj
ENSMUSG00000034317	Trim59	65.45416	-6.19017	1.114154	3.01E-05
ENSMUSG00000048307	Ankrd46	35.52351	-6.17347	1.350625	0.001134
ENSMUSG00000036256	Igfbp7	40.5588	-6.09063	1.325748	0.00104
ENSMUSG00000036916	Zfp280c	40.45569	-5.85756	1.266357	0.000916
ENSMUSG00000031613	Hpgd	45.20982	-5.73803	1.158071	0.000263
ENSMUSG00000028334	Nans	29.372	-5.70802	1.363352	0.004142
ENSMUSG00000046324	Ermp1	52.10683	-5.68899	1.112852	0.000136
ENSMUSG00000044573	Acp1	54.8453	-5.42996	1.197422	0.00122
ENSMUSG00000023707	Ogfod2	29.46976	-5.41449	1.296819	0.004174
ENSMUSG00000032591	Mst1	39.5879	-5.40095	1.271529	0.003474
ENSMUSG00000073002	Vamp5	27.28197	-5.38322	1.289375	0.004174
ENSMUSG00000025935	Tram1	131.6154	-5.37329	0.841469	4.19E-07
ENSMUSG00000068551	Zfp467	23.73757	-5.36364	1.295052	0.00457
ENSMUSG00000050777	Tmem37	72.68193	-5.34483	1.231922	0.002653
ENSMUSG00000003199	Mpnd	35.09519	-5.29255	1.234789	0.002971
ENSMUSG00000035847	Ids	26.99179	-5.19749	1.209597	0.00292
ENSMUSG00000079164	Tlr5	13.67076	-5.1757	1.420053	0.017501
ENSMUSG00000003423	Pih1d1	42.54768	-5.09848	1.467239	0.025572
ENSMUSG00000020910	Adprm	56.40512	-5.06315	1.303327	0.009785
ENSMUSG00000044221	Grsf1	63.93478	-5.06193	1.054022	0.000466

Gene Ontology enrichment (GO) analysis was performed to identify pathways regulated by IRF5 that may influence disease progression (Table.4.9). Interesting and relevant GO terms included “Cellular Response to Interferon-Gamma” (Fold Enrichment (FE) = 3.6), “T cell Differentiation involved in immune response” (FE = 2.9), “Monocyte Chemotaxis” (FE = 2.1), and “Membrane Budding” (FE = 2.3).

Table.4.9: Gene Ontology enrichment associated with differentially expressed genes in macrophages

GO.ID	Term	Expected	p Value	Genes	Fold Enrichment
GO:0001955	blood vessel maturation	0.18	0.0090	Mmp2, S1pr1	11.1
GO:0002862	negative regulation of inflammatory response to antigenic stimulus	0.3	0.0046	Il12b, Psmb4	6.7
GO:0007193	adenylate cyclase-inhibiting G-protein coupled receptor signaling pathway	0.63	0.0086	Gnai3, Gpr37l1, S1pr1	4.8
GO:0071346	cellular response to interferon-gamma	1.37	0.0053	Il12b, Ccl8, Ccl9, Eprs, Gbp2b	3.6
GO:0070098	chemokine-mediated signaling pathway	0.9	0.0015	Ccl8, Ccl9, Cib1	3.3
GO:0030032	lamellipodium assembly	1.34	0.0266	Arpc2, Nup85, S1pr1, Whamm	3.0
GO:0090280	positive regulation of calcium ion import	0.69	0.0082	Clec4b1, Npsr1	2.9
GO:0002292	T cell differentiation involved in immune response	1.05	0.0321	Il12b, Ly9, Fcer1g	2.9
GO:0098869	cellular oxidant detoxification	1.1	0.0099	Txndc17, Fam213a, Prdx6	2.7
GO:0006900	membrane budding	1.31	0.0070	Tsg101, Dab2, Arf1	2.3
GO:0002548	monocyte chemotaxis	0.96	0.0026	Ccl8, Ccl9	2.1
GO:0016064	immunoglobulin mediated immune response	1.64	0.0254	C1qa, C1qb, Fcer1g	1.8
GO:2000107	negative regulation of leukocyte apoptotic process	1.13	0.0254	Fadd, Fcer1g	1.8
GO:0030593	neutrophil chemotaxis	1.7	0.0076	Ccl8, Ccl9, Fcer1g	1.8
GO:0009749	response to glucose	2.45	0.0065	Pih1d1, Pfkfb2, Mpc2, Sidt2	1.6
GO:0006612	protein targeting to membrane	1.94	0.0325	Srp19, Ssr3, Cib1	1.5
GO:0048041	focal adhesion assembly	1.31	0.0293	Sorbs1, Whamm	1.5
GO:0007389	pattern specification process	6.06	0.0164	Rgs19, Kat2a, Wls, Grsf1	0.7
GO:0006302	double-strand break repair	3.22	0.0306	Rpa3, Sfr1	0.6

To further refine the list of genes of interest, genes that were associated with GM-BMDM IRF5-ChIP peaks (reported by Saliba *et al.,* 2014) were integrated with DEGs in MBMC (Fig.4.19) [163]. *Il12b* was upregulated in WT macrophages vs *Irf5*$^{-/-}$ in mixed chimaera, and was associated with five ChIP peaks (Fig.4.19). *Cd81*, was highly expressed in Cluster 2 (inflammatory macrophages) and Cluster 5 (resident macrophages) in 10x RNAseq, and was enriched in WT in MBMC (Fig.4.18). Furthermore, *Cd81* was associated with an IRF5-ChIP peak (Fig.4.19), making *Cd81* an interesting target to validate. Table.4.10 summarises the top 20 most significantly DEGs in MBMC with IRF5-ChIP peaks.

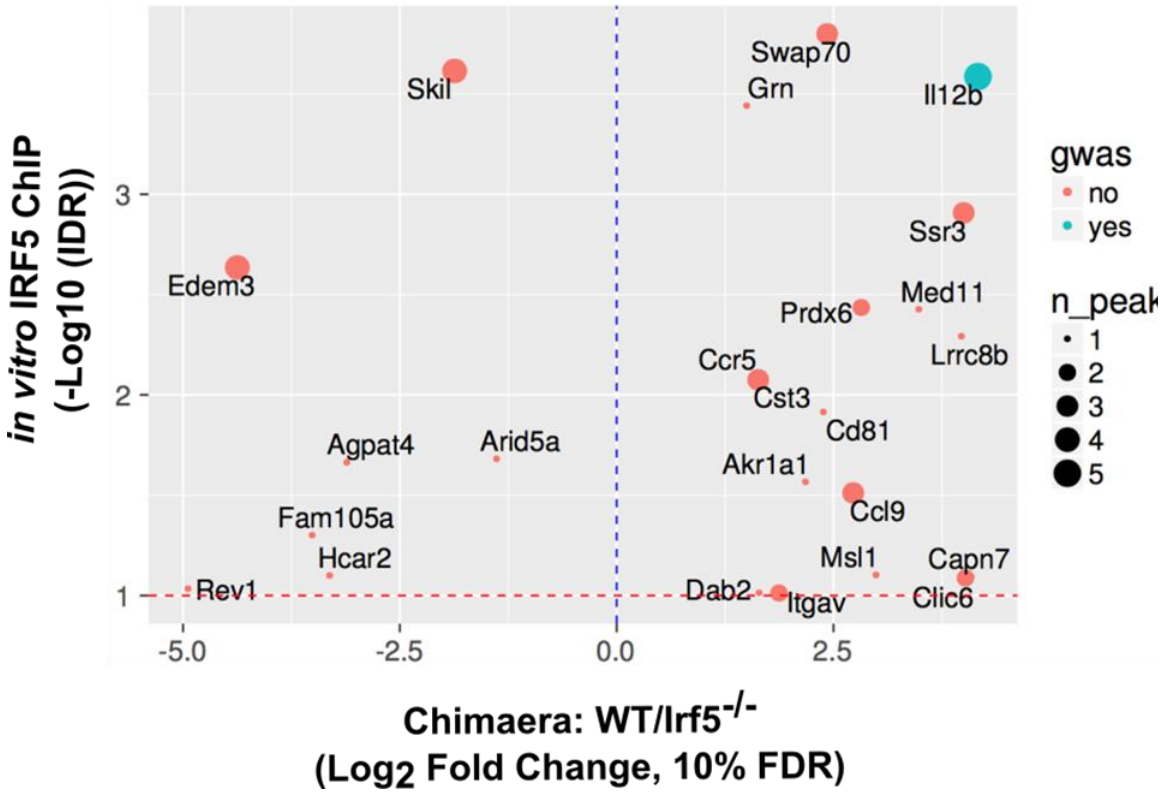

Fig.4.19: Integration of d21 Hh + αIL10R mixed bone marrow chimaera RNAseq with *in vitro*-defined IRF5 ChIP peaks to identify targets of interest

LPLs were isolated from mixed bone marrow chimaeras at d21 Hh + αIL10R colitis. 100 macrophages (CD45$^+$ CD11b$^+$ Ly6G$^-$ Siglec F$^-$ Ly6C$^-$ MHC II$^+$ F4/80$^+$) of each genotype (WT or *Irf5*$^{-/-}$ identified by expression of either CD45.1 or CD45.2) per mouse were sorted into Smart-Seq2 lysis buffer. Nextera library preparation was performed on the bulks, followed by Illumina Hiseq2000v4 sequencing. Reads were filtered and mapped to the mm10 genome, and DESeq2 was used to identify differentially expressed genes. Data are expressed as *Irf5*$^{-/-}$/WT.
Peak calling was performed on GM-BMDMs at 0 hrs and 2 hrs post LPS stimulation. 1409 IRF5 ChIP peaks with an IDR < 10% were found associated with 810 genes using GREAT promoter definitions.

Statistics:
Mixed chimaera: N = 3 biological replicates
Data analysis was performed by Dr. Stephen Sansom (University of Oxford)

Table.4.10: Top differentially expressed genes between wild-type and *Irf5*$^{-/-}$ in mixed bone marrow chimaera with *in vitro* ChIP peaks

		Mixed Bone Marrow Chimaera		*in vitro ChIPseq*	
vGene ID	**Gene Symbol**	**$Log_{(2)}$ Fold Change**	**Adjusted p-Value**	**Peak Min IDR**	**N Peaks**
ENSMUSG00000029204	Rhoh	-4.51	1.43E-07	0.38	1
ENSMUSG00000019122	Ccl9	-2.73	3.35E-05	0.0308	3
ENSMUSG00000027828	Ssr3	-4	5.73E-05	0.00124	3
ENSMUSG00000056069	Fam105a	3.51	0.000286	0.05	1
ENSMUSG00000037706	Cd81	-2.38	0.000682	0.0122	1
ENSMUSG00000028798	Eif3i	3.53	0.00122	0.369	1
ENSMUSG00000025066	Sfr1	-4.06	0.0021	0.257	1
ENSMUSG00000045502	Hcar2	3.31	0.0024	0.0794	1
ENSMUSG00000036905	C1qb	-1.4	0.0029	0.247	1
ENSMUSG00000021893	Capn7	-4.09	0.00542	0.0805	1
ENSMUSG00000040697	Dnajc16	4.96	0.0057	0.412	1
ENSMUSG00000018923	Med11	-3.48	0.00848	0.00375	1
ENSMUSG00000008384	Sertad1	3.98	0.0115	0.339	1
ENSMUSG00000026082	Rev1	4.94	0.0126	0.0924	1
ENSMUSG00000029449	Rhof	4.62	0.0131	0.3	2
ENSMUSG00000020892	Aloxe3	4.77	0.0138	0.229	1
ENSMUSG00000033470	Cysltr2	5.21	0.0147	0.128	1
ENSMUSG00000079547	H2-DMb1	-1.48	0.0225	0.435	1
ENSMUSG00000004296	Il12b	-4.17	0.0271	0.000259	5
ENSMUSG00000022150	Dab2	-1.64	0.0272	0.0969	1

*$Log_{(2)}$ Fold Change expressed as *Irf5*$^{-/-}$/WT

4.2.8 Validation of gene targets identified by integration of genomic data

Cd81 was identified as a highly differentially expressed target of IRF5 in cLP macrophages during Hh + αIL10R colitis (Fig.4.18, Fig.4.19). CD81 is a tetraspanin known to be involved in antigen presentation by MNPs to naïve T cells, but mutations in CD81 have not been associated with IBD at the time of writing [305, 306]. Expression of CD81 in WT MNPs was analysed by flow cytometry. CD81 was found to be expressed in low numbers of P1 monocytes at steady state, and was not increased during Hh + αIL10R colitis (Fig.4.20A). The expression level of CD81 was not affected by inflammatory status (Fig.4.20B). Low frequencies of P2 monocytes expressed CD81 at steady state, and expression of CD81 was low (Fig.4.20). A greater percentage of P2 monocytes expressed CD81 during Hh + αIL10R colitis than at steady state (Fig.4.20A, $p = 0.022$). However, expression of CD81 was not upregulated during colitis (Fig.4.20B). In contrast to P1 and P2 monocytes, the majority of macrophages expressed CD81 at steady state (Fig.4.20A). The percentage of $CD81^+$ macrophages was also increased during colitis (Fig.4.20A, $p = 0.031$). CD81 expression was significantly upregulated in Hh + αIL10R colitis (Fig.4.20B, $p = 0.0008$).

CCL8 was another molecule that was significantly differentially expressed in scRNAseq and in MBMC RNAseq (Fig.4.18), but was not associated with a ChIP peak (Fig.4.19). Analysis of CCL8 levels in WT vs global *Irf5*$^{-/-}$ explant culture supernatants showed that *Irf5*$^{-/-}$ expressed less CCL8 during colitis ($p = 0.0097$, Fig.4.21).

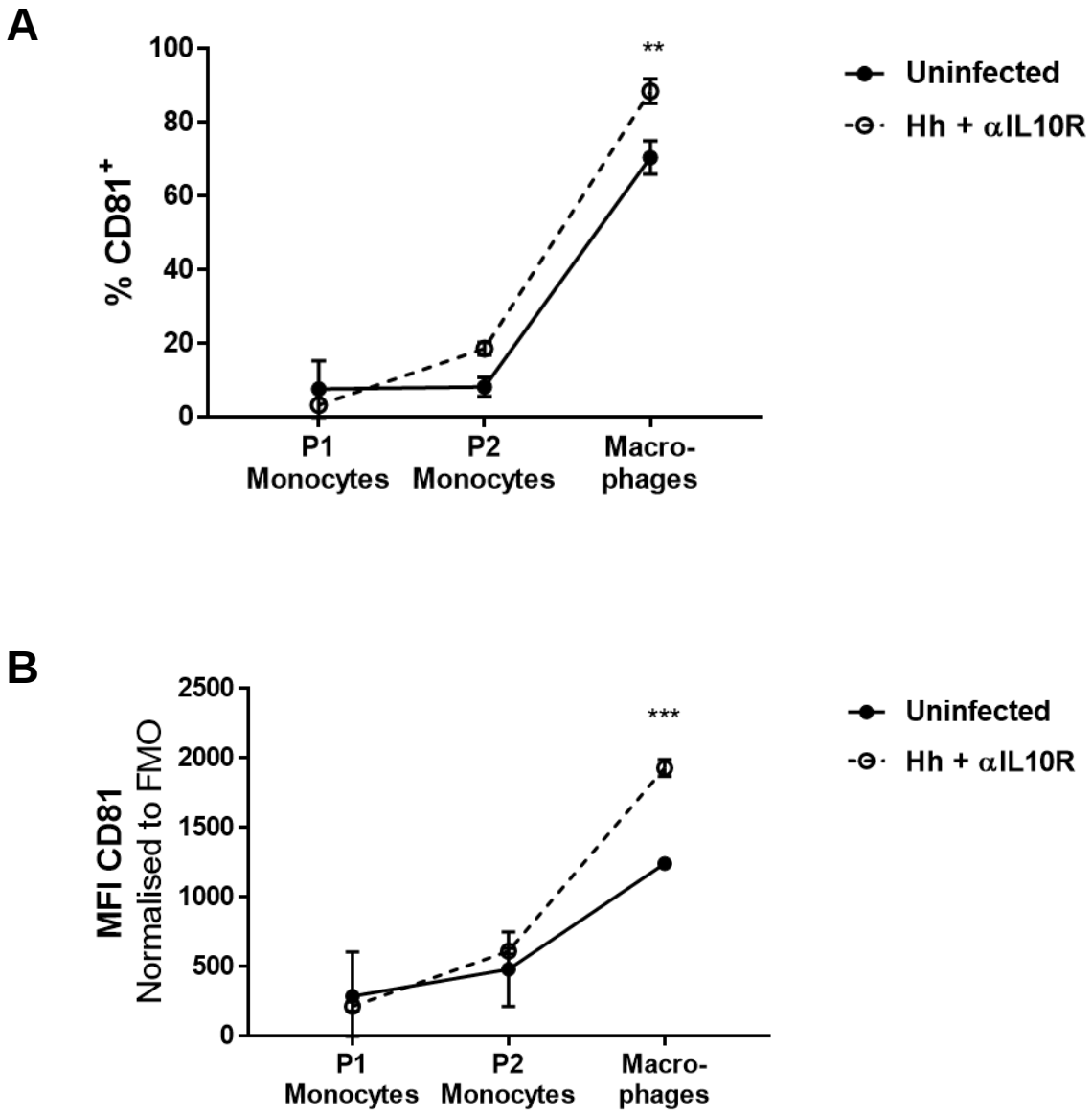

Fig.4.20: CD81 is upregulated on macrophages during Hh + αIL10 R colitis

CD81 expression in MNPs was measured by flow cytometry. **A)** the percentage of MNPs expressing CD81 increased as monocytes differentiated into macrophages and the number of $CD81^+$ macrophages was increased at d14 Hh + αIL10R colitis (mean diff = 4.33% ±4.73, p = 0.0038). **B)** The MFI of CD81 increased as monocytes differentiated into macrophages. CD81 expression on macrophages was increased with inflammation (mean diff = 71.67 ±136.1, p = 0.0002).

Statistics:
Data are from one experiment. Steady state n = 2, Hh + αIL10R n = 6
2-Way ANOVA with Sidak correction: ** $p \leq 0.01$, *** $p \leq 0.001$

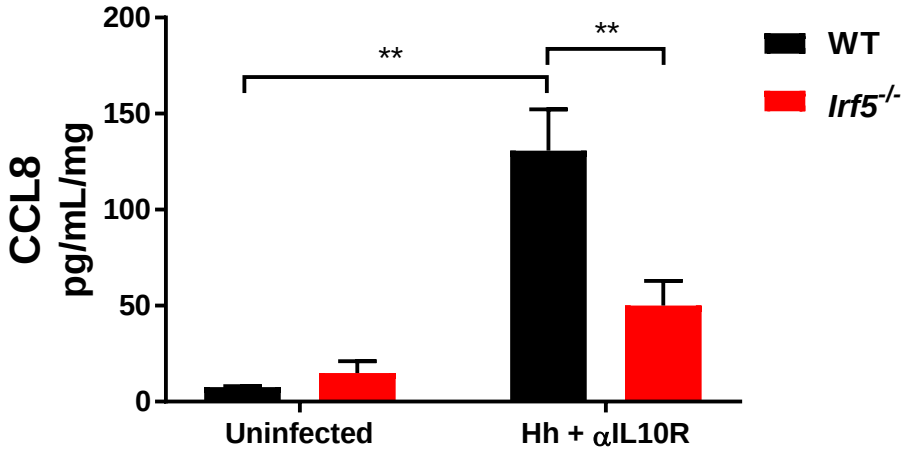

Fig.4.21: CCL8 is upregulated in WT mice at d21 Hh + αIL10R colitis

Explants were harvested from mouse colon, weighed, and then cultured for 24 hrs. Culture supernatants were then aspirated, and the level of CCL8 was assayed by ELISA and normalised to explant weights. At d21 Hh + αIL10R, the level of CCL8 was significantly elevated compared to control (mean difference = 123.2 pg/mL/mg ± 28.2, p = 0.0024), and to *Irf5*$^{-/-}$ Hh + αIL10R (mean difference = 80.56 pg/mL/mg ± 21.84, p = 0.0097).

Statistics:
Data are representative of two independent experiments. Steady state: WT n = 3, *Irf5*$^{-/-}$ n = 3. Hh + αIL10R: WT n = 7, *Irf5*$^{-/-}$ n = 7
2-Way ANOVA with Tukey correction, ** p ≤ 0.01

4.2.9 WT mononuclear phagocytes express higher levels of functional intestinal macrophage markers than *Irf5*$^{-/-}$ at steady state and during inflammation in mixed bone marrow chimaeras

To further expand the number of IRF5 controlled genes in cPL we also analysed two previously reported targets of IRF5 (TNFα, and pro-IL1β), whose mRNA expression might not have been captured during our model of colitis at day 21 analysis. TNFα is a master inflammatory cytokine, demonstrated by amelioration of multiple inflammatory diseases after blocking either TNFα itself, or the TNF receptor [173]. IL1β levels are high in IBD patients, and IL1β was demonstrated to promote Hh + αIL10R colitis through support of ILC3 and T_H17 responses [307]. An RNA microarray of the timecourse of Hh + αIL10R colitis was performed by the Powrie lab, allowing the visualisation of TNFα and IL1β expression on the whole tissue level over the course of disease (Unpublished data). The design of the Hh + αIL10R experiment was slightly different to that presented in this thesis; only two doses of αIL10R antibody were administered (d0 and d6), resulting in peak of colitis at d13, and resolution thereafter. In the experiments described here, colitis was maintained until d21 by administration of three doses of αIL10R (d0, d6, and d13). Unpublished data from the lab suggest that the Hh + αIL10R colitis phenotype is stable from d14-d28 so long as αIL10R is administered weekly. Therefore comparison of the two datasets are between d14 (microarray) and d21 (flow cytometry MFI).

In the Hh + αIL10R microarray kinetic, both *Il1b* and *Tnf* expression were significantly elevated over steady state (d0) from d6. Expression peaked at d14 and declined thereafter (once αIL10R antibody was withdrawn and disease resolved, Fig.4.22). Expression of these pro-inflammatory cytokines coincided with the peak of *Ly6c* expression in the cLP, which marks newly entered monocytes (Fig.4.22).

MBMC allowed direct comparison of the expression of TNFα and pro-IL1β in WT and *Irf5*$^{-/-}$ MNPs in the cLP. A high percentage of P1 monocytes and P2 monocytes (which express Ly6C), and macrophages, expressed TNFα and pro-IL1β (the precursor protein to IL1β) at

steady state (Fig.4.23A-C, Fig.4.24A-C). The percentage of WT Macrophages expressing TNFα increased significantly over controls during Hh + αIL10R colitis ($p = 0.0434$, Fig.4.23C), but not over *Irf5*$^{-/-}$ Hh + αIL10R MBMC. The per-cell expression (expressed as MFI by flow cytometry) increased in WT macrophages over uninfected controls (Fig.4.23A, $p = 0.0008$). TNFα expression in WT P1 monocytes and P2 monocytes from MBMCs was not significantly increased over controls, however (Fig.4.23D-F). Expression of TNFα was significantly elevated in WT macrophages over *Irf5*$^{-/-}$ (Fig.4.23F, $p < 0.0008$ respectively), but not in P1 or P2 monocytes (Fig.4.23D).

Pro-IL1β expression in MNPs from MBMCs was profiled by flow cytometry. Significantly more WT P1 monocytes ($p = 0.0215$) and P2 monocytes ($p = 0.0072$) expressed pro-IL1β at d21 Hh + αIL10R colitis vs *Irf5*$^{-/-}$, but the percentage of pro-IL1β^{+} macrophages was not significantly altered between WT and *Irf5*$^{-/-}$ (Fig.4.24A-C). The level of pro-IL1β expression in P2 monocytes was increased in WT over *Irf5*$^{-/-}$ ($p = 0.0024$, Fig.4.24E). Pro-inflammatory monocytes are present in increased numbers during colitis, therefore, even if the percentage or MFI of inflammatory cytokine positive MNPs is not increased, their number are likely to influence the level of cytokine in the tissue. Pro-IL1β was also expressed at a higher level in WT macrophages than *Irf5*$^{-/-}$ from MBMC Hh + αIL10R d21 ($p = 0.0335$, Fig.5.24F). Taken together, these results place IRF5 as a regulator of monocyte to macrophage conversion in the cLP, and support the hypothesis that one mode in which IRF5 promotes colitis is via promoting a macrophage inflammatory state, therefore modulating inflammatory cytokine production.

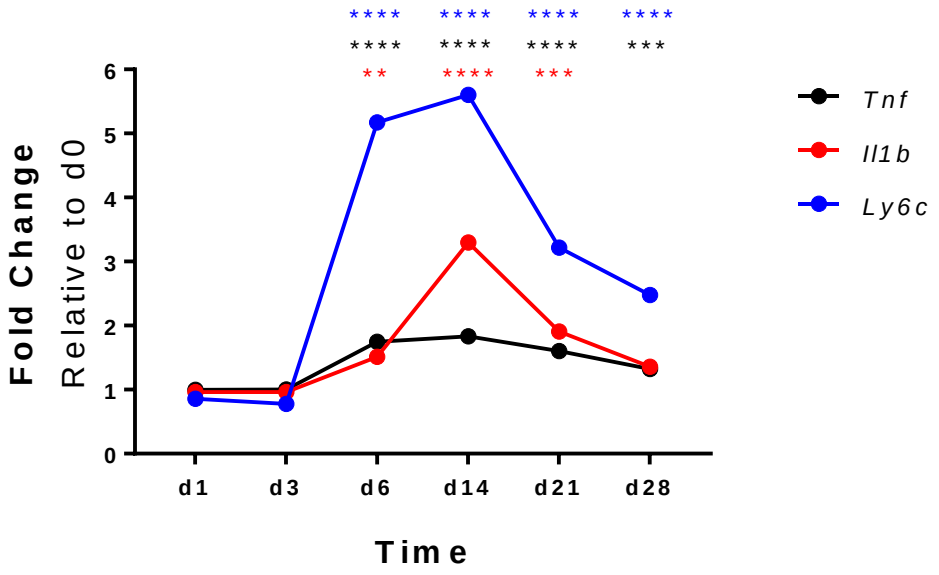

Fig.4.22: Microarray analysis of whole tissue expression of *Tnf*, *Il1b*, and *Ly6c* over the Hh + αIL10R colitis kinetic

Expression of *Tnf*, *Il1b*, and *Ly6c* increased significantly over steady state (d0) mice at d6. Expression peaked at d14 for all cytokines presented, before declining after αIL10R antibody was withdrawn.

Data were corrected for multiple comparisons by controlling the false discovery rate using the Benjamin-Hochberg method, with the false discovery rate set to 0.05. Data are presented as fold change over d0, with comparisons tested against d0 expression.
** q < 0.01, *** q < 0.01, **** q < 0.0001
Data were generated by Dr. Chris Schiering and Dr Matthew Shale (Powrie Lab, University of Oxford)

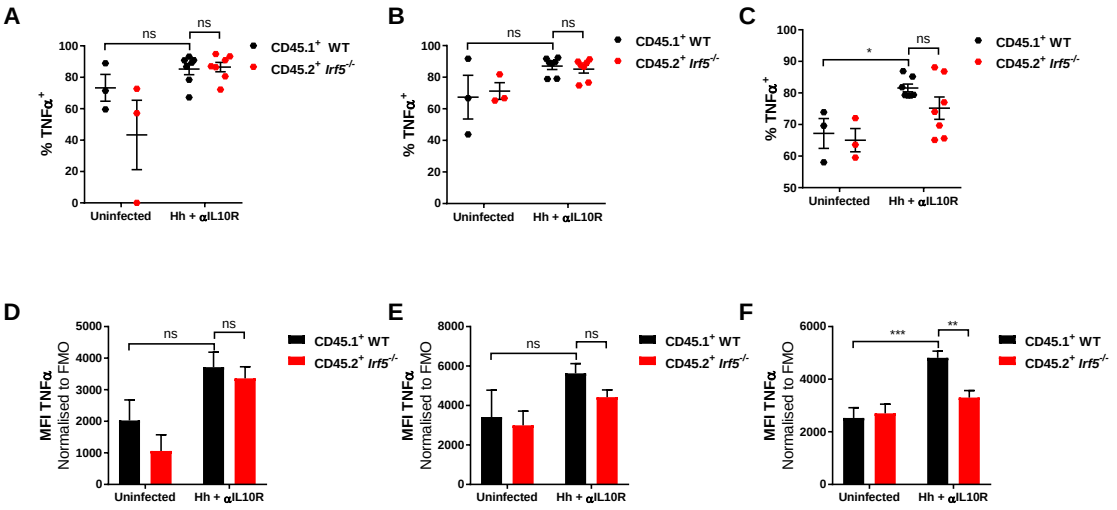

Fig.4.23: TNFα expression is upregulated in WT vs *Irf5*$^{-/-}$ macrophages and P2 monocytes during Hh + αIL10R inflammation

P1 monocytes, P2 monocytes, and Macrophages were isolated from mixed bone marrow chimaeras. Donor origin was determined by the expression of either CD45.1 (WT) or CD45.2 (*Irf5*$^{-/-}$). The percentage of respective donor **A)** P1 monocytes, **B)** P2 monocytes, and **C)** macrophages expressing TNFα was quantified. No significant difference was observed between the mean percentage of WT or *Irf5*$^{-/-}$ P1 and P2 MNPs expressing TNFα at steady state or inflammation, although there were more TNFα^{+} WT macrophges observed during Hh + αIL10R inflammation than at steady state (mean difference = 14.4 ±4.9, p = 0.0434). The per-cell expression of TNFα, expressed as MFI, was quantified in **D)** P1 monocytes, **E)** P2 monocytes, and **F)** macrophages WT macrophages upregulated TNFα, at d21 Hh + αIL10R vs controls (Mean diff = 2287 ±464.4, p = 0.0008), but TNFα was not significantly upregulated by inflammation in WT P1 monocytes or P2 monocytes. The expression of TNFα was not affected by IRF5 deficiency at steady state across the MNPs analysed. At d21 Hh + αIL10R, WT macrophages expressed higher levels of TNFα than *Irf5*$^{-/-}$ macrophages (p = 0.0034).

Statistics:
Data are from one experiment. Mean ± SEM Steady state: n = 3, Hh + αIL10R n = 7
2-Way ANOVA with Tukey correction: ns = not significant, * p ≤ 0.05, ** p ≤ 0.01, *** p ≤ 0.001.

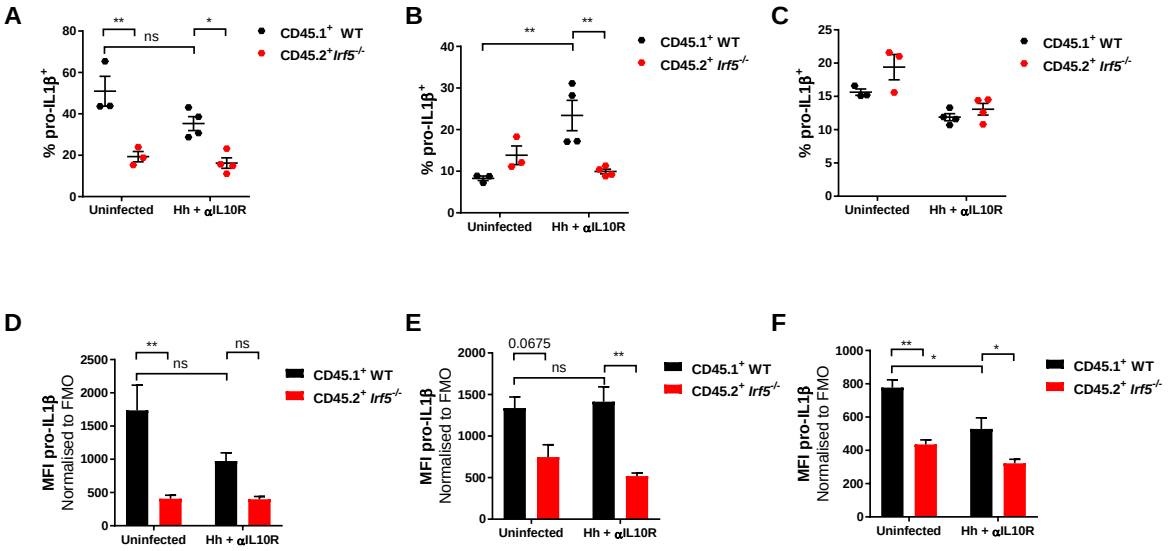

Fig.4.24: pro-IL1β expression is higher in WT MNPs in mixed bone marrow chimaera

P1 monocytes, P2 monocytes, and Macrophages were isolated from mixed bone marrow chimaeras. Donor origin was determined by the expression of either CD45.1 (WT) or CD45.2 (*Irf5*$^{-/-}$). The percentage of respective donor **A)** P1 monocytes, **B)** P2 monocytes, and **C)** macrophages expressing pro-IL1β was quantified. Greater frequencies of P1 monocytes of WT origin were found to express pro-IL1β at steady state (mean difference = 31.6 ±6.2, p = 0.002), but no significant difference was observed between the mean percentage of WT or *Irf5*$^{-/-}$ P2 monocytes and macrophages expressing pro-IL1β at steady state. At d21 Hh + αIL10R colitis, the frequency of WT P2 monocytes expressing pro-IL1β was increased over steady state (mean difference = 15.11 ±3.4, p = 0.0056). Fewer *Irf5*$^{-/-}$ P1 monocytes and P2 monocytes expressed pro-IL1β than WT at d21 Hh + αIL10R (p = 0.0215, and p = 0.0072). No difference in the frequency of macrophages expressing pro-IL1β was detected across all conditions.
The per-cell expression of pro-IL1β, expressed as MFI, was quantified in **D)** P1 monocytes, **E)** P2 monocytes, and **F)** macrophages. Pro-IL1β expression was not upregulated with inflammation in the MNPs tested. WT P1 monocytes expressed higher levels of pro-IL1β than *Irf5*$^{-/-}$ at steady state (mean difference = 1329 ±268.5, p = 0.0027), but not d21 Hh + αIL10R. At d21 Hh + αIL10R, WT P2 monocytes, expressed higher levels of pro-IL1β than *Irf5*$^{-/-}$ (mean difference = 895.5 ±178.1, p = 0.0024). WT Macrophages expressed higher levels of pro-IL1β at steady state (mean difference = 342.3 ±72.1, p = 0.0036), and at d21 Hh + αIL10R (mean difference = 206.6 ±62.4, p = 0.0335) than *Irf5*$^{-/-}$ macrophages.

Statistics:
Data are from one experiment. Steady state: n = 3, Hh + αIL10R n = 4. 2-Way ANOVA with Tukey correction. ns = not significant, * p ≤ 0.05, ** p ≤ 0.01.

IRF5 promotes an inflammatory macrophage phenotype both in GM-BMDMs and *in vivo* [162, 217]. IRF5-expressing macrophages express more MHC II, and CD11c, and less CD206 [217, 278]. The cell surface expression of these markers on MNPs in MBMCs was measured by flow cytometry. WT macrophages, but not WT P2 monocytes expressed higher levels of MHC II than *Irf5*$^{-/-}$ at steady state (Fig.4.25A, p = 0.0007), and in Hh + αIL10R colitis in MBMC (Fig.4. 25A, p = 0.0026). CD11c levels were found to largely be unchanged between WT and *Irf5*$^{-/-}$ in MBMCs, however, WT macrophages expressed marginally more CD11c at steady state than *Irf5*$^{-/-}$ (Fig.4. 25B, p = 0.032). Despite this, expression was not significantly upregulated during Hh + αIL10R inflammation, and no difference was detected between WT and *Irf5*$^{-/-}$ in the inflamed setting. F4/80 is a prototypical marker of mature macrophages, although some expression can be detected in eosinophils. 10X Cluster 5 was defined by the expression of the *Adgre* gene encoding F4/80, but it was also expressed in Cluster 2 (Fig.4.14) indicating that both Cluster 2 and Cluster 5 are macrophages. To assess whether the level of F4/80 on total macrophage population mirrored the altered differentiation status identified by pseudotime analysis (Fig.4.17), F4/80 expression was analysed by flow cytometry (Fig.4. 25C). P1 monocytes and P2 monocytes expressed F4/80 at low levels. Macrophages, however, expressed high levels of F4/80, but the level of F4/80 expression was the same between WT and *Irf5*$^{-/-}$ MNPs in MBMC (Fig.4. 25C).

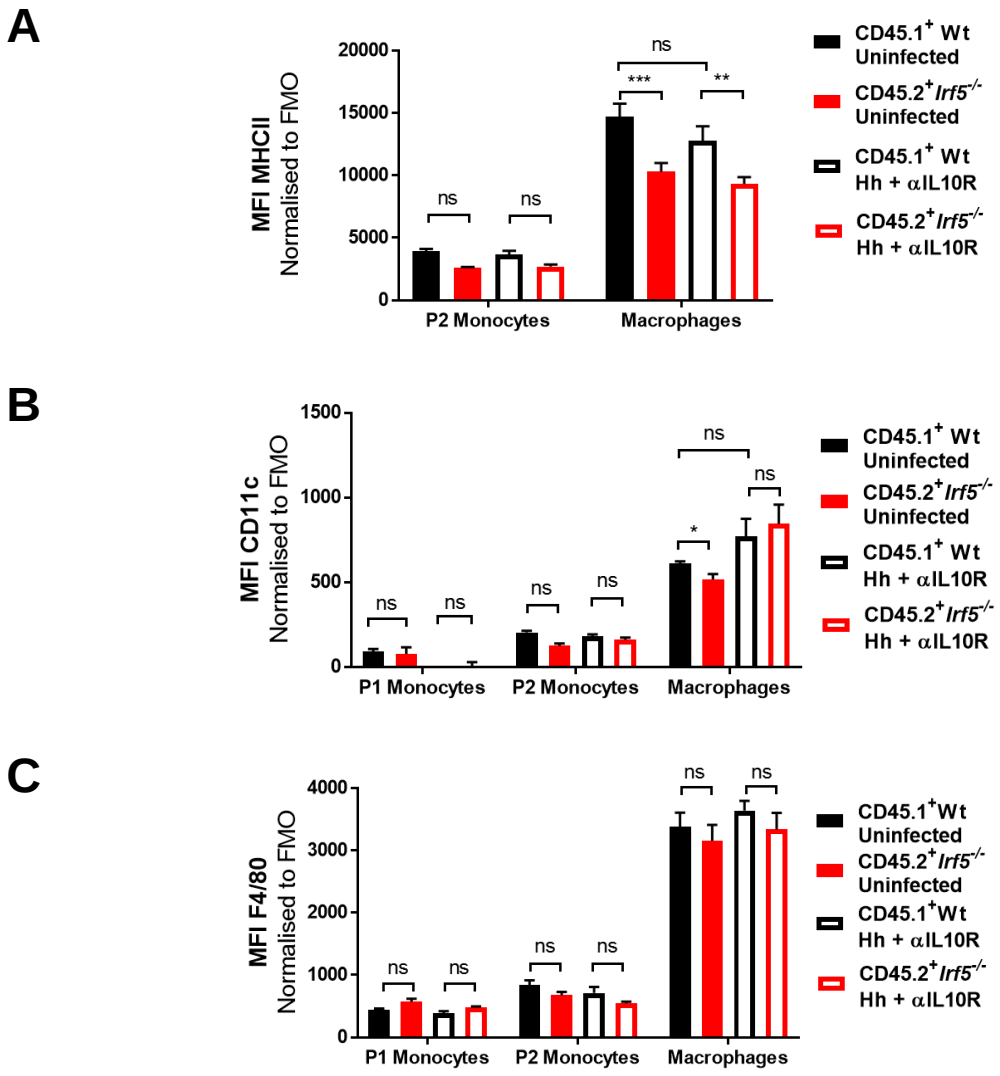

Fig.4.25: Expression of MHC II is diminished on IRF5-deficient macrophages in a shared environment

Mixed bone marrow chimaeras were generated by reconstitution of lethally irradiated CD45.1$^+$ WT mice with an equal mix of CD45.1$^+$ WT and CD45.2$^+$ *Irf5*$^{-/-}$ bone marrow. Mice were culled, and LPLs were isolated. LPLs were labelled with fluorescently conjugated antibodies to cell surface antigens and analysed by flow cytometry. Donor origin was assessed by expression of either CD45.1 or CD45.2. **A)** The MFI of MHC II on P2 monocytes and macrophages in mixed bone marrow chimaeras was profiled. There was no difference in the expression of MHC II on P2 monocytes from either WT or *Irf5*$^{-/-}$ origin at steady state or during inflammation. WT macrophages expressed more MHC II at steady state (mean diff = 4410 ±893.4, p = 0.0007) and in Hh + αIL10R colitis (mean diff = 3467 ±951.1, p = 0.0026). **B)** The MFI of CD11c on MNPs in mixed bone marrow chimaeras was profiled. There was no difference in the expression of CD11c on P1 or P2 monocytes from either WT or *Irf5*$^{-/-}$ origin at steady state or during inflammation. WT macrophages expressed more CD11c at steady state (mean diff = 92.4 ±32.46, p = 0.0318) but not during Hh + αIL10R colitis. **C)** The MFI of F4/80 on MNPs in mixed bone marrow chimaeras was profiled. There was no difference in the expression of F4/80 on MNPs from either WT or *Irf5*$^{-/-}$ origin at steady state or during inflammation.
Statistics:
Data are representative of two independent experiments. Uninfected: n = 3, Hh + αIL10R n = 7
Mean + SEM
2 Way ANOVA with Sidak correction for multiple comparisons; ns = not significant, ** p ≤ 0.01, *** p ≤ 0.001

4.3 Discussion

The intrinsic effects that IRF5 mediates could not be defined using WT vs global *Irf5*$^{-/-}$ immunological profiling. Therefore, MBMCs were generated and profiled. MBMCs allow the comparison of haematopoietically-derived cells in the same environment, meaning that discrepancies between WT and *Irf5*$^{-/-}$ leukocytes in MBMCs could be directly attributed to IRF5 deficiency.

MBMCs were reconstituted with an equal mix of WT and *Irf5*$^{-/-}$ bone marrow cells, which were shown not to be deficient in HSPCs (Fig.4.2). At a minimum of eight weeks post reconstitution, uninfected and Hh + αIL10R-treated MBMCs were assessed for reconstitution efficiency in the bone marrow (Fig.4.2, Fig.4.4), blood (Fig.4.5, Fig.4.6), and cLP (Fig.4.7, Fig.4.8). Reconstitution of the bone marrow was found to be equal in uninfected chimaeras, but more *Irf5*$^{-/-}$ leukocytes were observed in the bone marrow or Hh + αIL10R treated MBMCs (Fig.4.4A, Fig.4.4B).

Myelopoiesis is directed towards granulo- and monocytopoiesis in inflammatory conditions, including IBD [69, 287]. Changes in systemic concentrations of cytokines e.g. IFNγ, and GM-CSF, or bacterial components e.g. LPS may be able to influence haematopoiesis to counteract inflammatory insults [308]. The same signals also trigger IRF5 expression in macrophages [60, 162, 217]. It was observed that diet-induced obesity was accompanied by dysbiosis and intestinal barrier breakdown, which increased systemic inflammation [309]. IBD patients also display increased intestinal permeability and increased serum concentrations of TLR agonists such as Lipopolysaccharide (LPS), and 1,3-β-D-Glucan [310-312]. Therefore, elevated systemic levels of TLR agonists may contribute to increased myelopoiesis and thus sustain IBD pathology. It was hypothesised that differential myelopoiesis between WT and *Irf5*$^{-/-}$ may have contributed to reduced accumulation of MNPs in the mixed bone marrow chimaera, and potentially contribute to reduced disease in global *Irf5*$^{-/-}$ mice.

To investigate this avenue, the reconstitution efficiency of WT and *Irf5*$^{-/-}$ haematopoietic cells in the bone marrow was assessed by flow cytometry. The reconstitution of the bone marrow was found to be unaffected, except in the case of *Irf5*$^{-/-}$ myeloid populations at day 21 Hh + αIL10R colitis (Fig.4.2A, Fig.4.2B). Combined with this, the blood of uninfected MBMCs reconstituted equally, but *Irf5*$^{-/-}$ Ly6C^{hi} monocytes were overrepresented during Hh + αIL10R colitis (Fig.4.5, Fig.4.6) [57]. In the cLP, reconstitution was greatly affected by IRF5 deficiency: total leukocytes were preferentially derived from WT, as were WT P1 monocytes, whilst WT macrophages were further elevated vs P1 monocytes (Fig.4.7, Fig.4.8, Fig.4.9, Fig.4.11, Fig.4.12, and Fig.4.15B). This observation may be explained via four options: 1) increased apoptosis of *Irf5*$^{-/-}$ macrophages, 2) increased *in situ* proliferation of WT macrophages, 3) IRF5-driven recruitment of monocytes, 4) increased conversion of WT monocytes to macrophages. It is unlikely that *Irf5*$^{-/-}$ macrophages exhibit increased rates of apoptosis, as it was demonstrated that IRF5 is a tumour suppressor [313, 314]. It is known that macrophages proliferate *in situ* in many organs, however, proliferation of gut macrophages has not been observed, and cLP macrophages are thought to be exclusively derived from blood monocytes [137, 138]. Considering that no HSPC compartment appeared to be affected by the lack of IRF5, this observation could be explained by increased mobilisation of WT myeloid cells from the bone marrow to the blood and/or affected tissue under Hh + αIL10R inflammation, or increased retention of *Irf5*$^{-/-}$ myeloid cells relative to WT. In fact, reduced migration of *Irf5*$^{-/-}$ monocytes in response to CCL2 was observed (Fig.4.10), which correlates with the findings of Yang *et al.,* (2012), which describe reduced expression of CCR2 and CXCR4 and reduced responsiveness to the CXCR4 ligand, CXCL12. In contrast to our findings, however, Yang *et al*., showed increased WT blood reconstitution even before pristane administration [239].

Neutrophils were also preferentially derived from WT at steady state (Fig.4.7). Neutrophils were found not to express IRF5 both in the steady state bone marrow and cLP, which would indicate that they should not be affected by IRF5 deficiency in the cLP (Fig.3.6). However, GMPs expressed low levels of IRF5 (Fig.3.18) and give rise to neutrophils, therefore it

remains possible that the reduced accumulation seen in *Irf5*$^{-/-}$ neutrophils may be due to intrinsic effects of IRF5 in GMPs. Comparison of WT and *Irf5*$^{-/-}$ neutrophils from the blood and cLP using RNAseq and proteomic techniques would help to elucidate the genes and proteins important for this process.

Similar to neutrophils, eosinophils express low levels of IRF5 relative to Ly6C^{hi} monocytes in the bone marrow, and in the cLP, but WT eosinophils reconstituted in the blood of uninfected MBMCs with greater efficiency than *Irf5*$^{-/-}$, but not during Hh + αIL10R induced inflammation (Fig.4.5, Fig.4.6). Eosinophils expressed higher levels of IRF5 than neutrophils (Fig.3.6), express many of the PRRs that activate IRF5, and are activated by GM-CSFR signalling [9, 129]. Eosinophils were demonstrated to be activated in colitis, and depletion of eosinophils resulted in amelioration of Hh + αIL10R colitis [129]. Therefore, the inflammatory functions of eosinophils may be augmented by IRF5 expression. Further research in this area to understand the effects of IRF5 in eosinophils would be intriguing, however, few patients present with eosinophilic IBD, and therefore the therapeutic potential may be limited [315].

Evidence presented in this thesis indicates that WT macrophages are elevated within the MNP pool relative to *Irf5*$^{-/-}$ (Fig.3.12), and this was also true in uninfected and Hh + αIL10R colitis MBMCs (Fig.4.11, Fig.4.12), whilst P1 monocyte levels remained equal despite the reconstitution difference, perhaps indicating that IRF5 is implicated in the conversion of monocytes to macrophages, a hitherto undescribed finding (Fig.4.15, Fig.4.17) [138]. Yang *et al.,* (2012) claimed that maturation of monocytes to macrophages was not affected by *Irf5*$^{-/-}$, yet this was only based on the expression of MHC II and CD86 and they did not assess the relative contributions of Ly6C^{hi} monocytes, inflammatory macrophages/P2 monocytes, and resident peritoneal macrophages into account [239]. Based on the expression of macrophage markers quantified by flow cytometry, as presented in this chapter (Fig.4.25), it would be difficult to propose that macrophage fate was affected by IRF5 deficiency as the MNP displayed similar levels of expression. Surprisingly, WT and

Irf5$^{-/-}$ macrophages from MBMC expressed similar levels of CD11c (*Itgax*), which was shown to be directly regulated by IRF5 and marks inflammatory macrophages, indicating that the environment is more important for the expression of this gene than IRF5 expression [278].

Only five genes were found to be significantly differentially expressed between genotypes in Cluster 1 based on the 10X (Table.4.2), although 10X detects fewer genes per cell than SmartSeq 2. These genes may represent the critical targets of IRF5 expression that solidify macrophage fate of P1 monocytes. *Sigmar1* , encoding Sigma Receptor 1 was downregulated in *Irf5*$^{-/-}$ (padj = 0.006) and was described to enhance inflammatory response of retinal microglia to LPS [316]. *Ncf2* encodes p67PHOX, a HoxA10-Pbx1a target gene and phagocyte respiratory burst oxidase. Hox10A-Pbx1a is a repressor of gene transcription in undifferentiated myeloid cells, and thus may represent a target for further investigation into the differentiation question [317]. *Ncf2* is a target of SHP1-protein tyrosine phosphatase, and is induced by IFNγ signalling, and was upregulated in *Irf5*$^{-/-}$ (padj = 0.037) identifying an IRF5 ChIP peak would solidify *Ncf2* as an IRF5-repressed gene [318, 319]. Investigation of *Ncf2*$^{-/-}$ mice may help the understanding of monocyte-macrophage differentiation. *Plaur* (Plasminogen Activator, Urokinase Receptor, uPAR) fragment inhibits monocyte chemotaxis via integrin-dependent effects [320]. In AMI patients, uPAR also regulated cell adhesion via binding vitronectin and integrins [321]. uPAR was upregulated by chemokines including CCL2 in the U937 monocyte cell line [322]. Taken together, these studies indicate that regulation the above genes by IRF5 may contribute to the accumulation of WT P1 monocytes in the cLP, and their differentiation into macrophages.

10X Clusters 2 and 5 were defined by the expression of many known markers of cPL macrophages, such as *Cd81*, *Adgre1*, *C1qa*, *b*, and *c*, *Ccl8*, and *Zmynd15* [138]. 10X Cluster 5 appears to represent a terminally differentiated macrophage phenotype, based on the higher expression of *Adgre1*, and *Mrc1* compared to 10X Cluster 2 [138]. 10X Cluster 2 expressed higher levels of *Itgax* and *Lyz2* (Lysozyme M), indicating that 10X

Cluster 2 may be involved in bacterial handling, and may represent an inflammatory macrophage phenotype described by Arnold *et al*., (2016) (possibly monocyte/macrophage intermediate phenotype, Mowat P3) [57, 124]. This assessment is supported by the enrichment of KEGG pathway terms associated with responses to bacteria, such as "Toll-like receptor signaling pathway", whilst "Staphylococcus aureus infection", and "Lysosome" were the two most significantly enriched pathways in 10X Cluster 2 (data not shown).

Only a few significantly differentially expressed genes were detected between WT and *Irf5*$^{-/-}$ in these clusters (Table.4.3-Table.4.6), possibly due to the sensitivity of the 10X platform. We broadened the characterisation of cLP macrophages by conducting small bulk RNA-Seq analysis (Fig.4.18). The results demonstrated that many of the markers that define inflammatory macrophages are dependent on IRF5, some markers, e.g. *Blnk*, *Rgs1*, *Zmynd15*, *Cxcl16*, *Il1b*, *Tnf*, and *Il12b*, are direct transcriptional targets of IRF5. This indicates that IRF5 defines inflammatory phenotype of cPL macrophages and controls some of the functions associated with tolerogenic tissue resident macrophages, e.g. C1qa, b, c (10X Cluster 5), including their production of cytokines and chemokines.

IRF5 promoted the expression of *Rgs1* in 10X Cluster 2 inflammatory macrophages (Table.4.2). *Rgs1* may be important for the retention of inflammatory macrophages via downregulating the chemokine response on monocytes that had entered atherosclerotic plaques [323]. In the same publication, *Rgs1* promoted atherosclerotic aneurysm rupture. *Rgs1* may therefore help to explain why WT MNPs accumulate in MBMC.

Genes that were upregulated in *Irf5*$^{-/-}$ relative to WT in 10X Cluster 2 included *Sgk1*, *Msrb1*, and *Clec4n* (Table.4.4). *Sgk1* (Serum Glucocorticoid Kinase 1) promotes cell survival, fibrosis, and 'M2' macrophage fate [324]. *Clec4n* (Dectin 2) is an important PRR that responds to fungal antigens, and promotes T_H2 and T_H17 responses, which are protective in colitis [325]. *Msrb1* was demonstrated to promote the expression of anti-inflammatory cytokines, such as IL10, in macrophages [326]. Together, downregulation of these

molecules by IRF5 would help promote an inflammatory macrophage state and promote colitis.

DC subsets were found to be predominantly of *Irf5*$^{-/-}$ origin in the MBMC, possibly compensating for the lowered macrophage fate (Fig.4.11). This observation was also made in global *Irf5*$^{-/-}$ (Fig.3.12). Intestinal DCs are currently believed to be derived of FLT3L-dependent progenitors, whereas monocytes give rise to intestinal macrophages [43]. Replenishment of CD11b^{+} DCs by monocytes in the inflamed tissue has not comprehensively been ruled out, however [46, 55]. Some of the confusion in the field may result from the lack of a consistent nomenclature for intestinal MNPs with inflammatory macrophages, differentiating monocytes, and TNF-iNos-producing DCs all corresponding to what are referred to in this thesis as P2 monocytes [61, 121, 294, 299]. Recently it was shown that bone marrow Ly6C^{+} monocytes, were heterogenous, and a portion of these Ly6C^{+} monocytes had dendritic cell potential, and expressed SIRPα [55]. These monocytes were not dependent on the growth factor, FLT3L, but expressed FLT3, CCR2, MHC II, and CD209a, and responded to GM-CSF by differentiating into PDL2^{+} ZBTB46^{+} DCs, potentiated by increased expression of PU.1. This monocyte-derived DC (moDC) population was distinct from Ly6C^{+} FLT3^{-} BM monocytes, which differentiated into CD209a^{-} MHC II^{lo} PDL2^{+} cells in response to GM-CSF, highlighting the ontogenic difference of moDCs and mo-macrophages [55]. Another recent study describing the transcriptional changes associated with Ly6C^{hi} to Ly6C^{lo} monocyte conversion confirmed the presence of a CD209a^{+} subset of monocytes in the blood that presented as Ly6C^{int}, and concluded that this CD209a^{+} population could adopt a Ly6C^{lo} fate representing an intermediate of Ly6C^{hi} monocytes [46].

Analysis of 10X scRNAseq supports the conclusion that IRF5-deficiency results in a developmental block: Macrophage clusters are predominantly composed of WT, whilst the monocyte cluster was equally composed of WT and *Irf5*$^{-/-}$ (Fig.4.15). Pseudotime analysis of WT and *Irf5*$^{-/-}$ MNPs supports this argument, macrophages and DCs were observed on

separate branches of the trajectory, and 10X Cluster 1 was not present on the DC branch (Fig.4.17). However, monocle analysis of *Irf5*$^{-/-}$ MNPs in isolation indicated that some monocytes adopted a DC fate (data not shown), suggesting that IRF5 expression may influence fate decision in infiltrating P1 monocytes. RNAseq and ChIPseq of distinct bulk WT and *Irf5*$^{-/-}$ cLP MNP populations may shed further light on the molecules that control this conversion.

BATF3-dependent CD11b^{-} DCs were shown to be dispensable for Hh + αIL10R colitis, whilst CD11b^{+} DCs did not produce the IL23 responsible for the development of Hh + αIL10R colitis [124]. cLP DCs are able to migrate to lymph nodes and present antigen to naïve T cells, thus initiating T_{eff} responses [297, 327]. In contrast, intestinal macrophages do not migrate to lymph nodes, but are suited to be activators of primed T cells in the cLP [122, 327]. The secondary activation of T_{eff} by macrophages may be critical for development of Hh + αIL10R colitis, but the effect of IRF5 deficiency on the migratory capacity, and T cell priming ability of cLP DCs, or the T cell activating potential of macrophages was not investigated. As these processes present a critical step in the initiation of inflammation, these functions should be investigated in *Irf5*$^{-/-}$ cLP DCs and macrophages.

4.4 Conclusion

Mixed bone marrow chimaeras present an excellent method for analysing the intrinsic effects of genetic deficiencies due to the shared environment in which leukocytes develop. Here, IRF5 was shown to promote the accumulation of monocytes and macrophages in the colonic lamina propria at steady state and during inflammation. Despite their expression of IRF5 at steady state, dendritic cell reconstitution was unaffected by the loss of IRF5 in mixed bone marrow chimaeras, possibly compensating for the loss of monocytes and macrophages.

WT monocytes and macrophages accumulated in the colons of mixed bone marrow chimaeras at the expense of *Irf5*$^{-/-}$, possibly due to reduced sensitivity to CCl2 in *Irf5*$^{-/-}$, or

increased *Rgs1* expression in WT. These WT MNPs expressed higher levels of pro-inflammatory cytokines associated with the progression of IBD than *Irf5*$^{-/-}$, which may be mediated by the anti-inflammatory transcripts identified by 10Xseq. Increased numbers of highly pro-inflammatory mononuclear phagocytes provide a mechanism by which IRF5 could promote the development of colitis.

IRF5 may play a role in the fate of P1 monocytes in the cLP: *Irf5*$^{-/-}$ DCs were overrepresented within the MNP compartment of mixed bone marrow chimaeras, and monocle analysis suggested that *Irf5*$^{-/-}$ could develop into cDCs at the expense of macrophage fate. DCs in the cLP were shown to be dispensable for the development of colitis in the Hh + αIL10R model, therefore, altered MNP fate may influence the course of disease.

In addition, our data emphasised the presence of macrophages in two related but distinguishable states, which we linked to being inflammatory and tissue resident macrophages based on the markers expressed. The WT macrophages seem to preferentially accumulate in 10X Cluster 2 (inflammatory mph) where we see the biggest difference in the number of WT and *Irf5*$^{-/-}$ cells, and a direct effect on expression of some of the major markers of this cluster. Fewer *Irf5*$^{-/-}$ cells are also observed in 10X Cluster 5 (tissue resident mph), and therefore production of the cytokines and chemokines defining this macrophage state would be diminished in a global *Irf5*$^{-/-}$ mouse. This leads to the hypothesis that *Irf5*$^{-/-}$ animals might be protected from intestinal pathologies driven by inflammatory MNP function during colitis.

5 IRF5 controls intestinal inflammation

5.1 Introduction

In previous chapters, data were presented that suggested that IRF5 promotes macrophage fate in monocytes in the intestine, and that IRF5$^+$ monocyte/macrophages adopt a pro-inflammatory state in the *Helicobacter hepaticus* + anti-Interleukin-10 Receptor (Hh + αIL10R) colitis model.

In Chapter.3 the contribution of macrophages to intestinal homeostasis was discussed. However, macrophages are also important mediators of intestinal inflammation [124, 139, 299].

Monocytes and macrophages accumulate in the inflamed lamina propria of Inflammatory Bowel Disease (IBD) patients and models of colitis in a process that appears to be heavily reliant on CCL2 and CCR2, although the CCL3 and CCR1 axis may play a role [57, 298]. *Ccl2* and *Ccl3* are chemokines highly expressed in 10X Cluster 5 (resident macrophages, Fig.4.14) during Hh + αIL10R colitis, and may help to promote colitis by sustaining monocyte recruitment. Monocytes and macrophages express high levels of pro-inflammatory cytokines in the colon during intestinal inflammation (Fig.4.23, Fig.4.24) [61, 124, 223, 224, 297, 299, 328, 329]. Intestinal MNPs, including P2 monocytes and macrophages, were shown to be critical for the development of colitis as loss of IL23 expression on CD11c$^+$ MHC II$^+$ non-DC MNPs was sufficient to protect mice from Hh + αIL10R colitis [124]. Furthermore, loss of the IL10R on CX_3CR1^+ cells in the cLP was sufficient for spontaneous colitis to develop in mice [139]. Moreover, many IBD-associated pathways are present in macrophages (e.g. NOD2, TNFα, IL10, and IL12/IL23-pathways), and mathematical modelling of IBD implicated conversion of macrophage state as critical in directing both pathogenesis and return to homeostasis, highlighting their importance in colitis [171].

During colitis, monocytes fail to appropriately differentiate into anergic resident macrophages, instead remaining in a pro-inflammatory state characterised by lack of IL10 expression, which may act to sustain colitis [113, 139, 294]. Data presented in previous chapters supported this observation, although reads mapping to *Il10* were not detected in Mixed Bone Marrow Chimaera RNAseq or 10X RNA sequencing (10X RNAseq), as at steady state macrophages are the largest constituent of the $CD11b^+$ MNP pool, but are much reduced during inflammation (Fig.4.12). This is reflected in the composition of the 10X RNAseq clusters, where 10X Cluster 5 comprises fewer cells than 10X Cluster 2 (Fig.4.15). IRF5 may also fit into this paradigm, as our data suggest that IRF5 is important for the conversion of monocytes into macrophages at the early stage of monocyte entry into the cLP (Fig.4.17), as monocytes are required to pass through the P2 “inflammatory monocyte” stage before becoming macrophages. IRF5 may also be important for the development of colitis in the P2 monocyte stage by promoting inflammatory gene transcription [162, 163].

Colonic Lamina Propria (cLP) macrophages do not present antigen to naïve T cells, and do not migrate to the Mesenteric Lymph Nodes (MLN), suggesting that macrophages do not contribute directly to the initiation of T effector cell (T_{eff}) responses in the colon [61, 294, 327, 330]. Despite this, cLP macrophages were shown to pass luminal antigens to classical Dendritic Cells (cDCs), which can migrate to the MLN to stimulate naïve T cells [331, 332]. This process may be important for both the induction of tolerance and the initiation of immune responses.

The identification of an intrinsic defect in myeloid cell development in the cLP resulting from IRF5 deficiency was discussed in Chapter.3 and Chapter.4. Further to this effect, production of many molecular mediators of intestinal homeostasis and dysbiosis were altered in the Hh + αIL10R colitis model (Table.4.2-Table.4.10, Fig.4.23, Fig.4.24). Based on these results we hypothesised that IRF5 is likely to promote intestinal inflammation and

that mice deficient in IRF5 might be protected against colitis. In this chapter, this hypothesis will be addressed by examining the phenotype of *Irf5*$^{-/-}$ mice subjected to 21 days of the Hh + αIL10R colitis model. Models of intestinal inflammation have been of great use in defining cellular and molecular pathways important for the progression of IBD. Hh + αIL10R is a model of typhlocolitis (inflammation of caecum and colon) that mimics the IFNγ- and IL23-driven T_H1/T_H17 aspect of IBD, but is also able to drive inflammation in lymphocyte-deficient mice via the effects of IL23 on Innate Lymphoid Cells (ILCs) [153, 160, 333, 334]. This model is optimal for understanding the role of IRF5 as it encompasses both innate and adaptive immunity, and pathology relies upon IL23 produced by intestinal MNPs [124].

To investigate the effects of IRF5 on colonic inflammation, the Hh + αIL10R model was conducted in irf5 deficient mice. IRF5 expression in the cLP myeloid compartment was characterised. Parameters of inflammation, including histological pathology, inflammatory leukocyte and cytokine milieu alterations, and differences in MNP phenotype were measured to assess Hh + αIL10R colitis severity.

5.2 Results

5.2.1 *Irf5*$^{-/-}$ mice are protected from *Helicobacter hepaticus* + αIL10R colitis

Helicobacter hepaticus + αIL10R (Hh + αIL10R) colitis was induced in wild type (WT) or *Irf5*$^{-/-}$ mice. At peak colitis (d21), mice were culled, and organs were harvested for analysis.

Splenomegaly is an accepted measure of ongoing inflammation in mice. Spleens from steady state or Hh + αIL10R colitic mice were harvested and weighed. Spleen weights were normalised to mouse weight at time of sacrifice and plotted (Fig.5.1A). Spleen weight was not affected in *Irf5*$^{-/-}$ at steady state. Colitic WT mice had relatively larger spleens than steady state WT ($p = 0.0191$), and relatively larger spleens than colitic *Irf5*$^{-/-}$ ($p = 0.0438$) (Fig.5.1A). However, there was no difference in the fold change between WT and *Irf5*$^{-/-}$ colitic mice relative to steady state mouse spleen weight ($p = 0.8$) (Fig.5.1B).

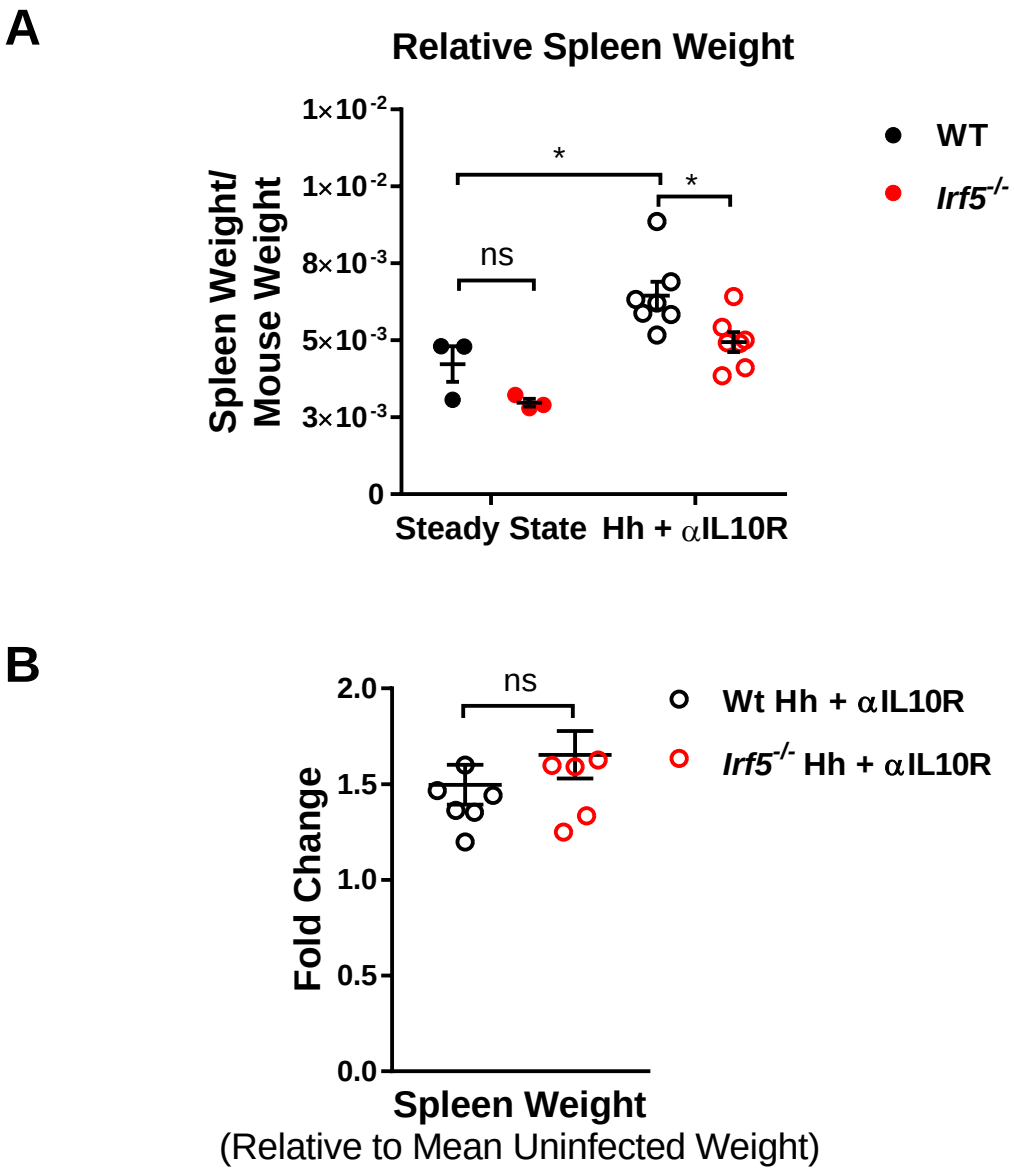

Fig.5.1: *Irf5*$^{-/-}$ mice display reduced spleen weight relative to wild type at steady state and inflammation.

Spleens were harvested from wild type and *Irf5*$^{-/-}$ mice, trimmed of adipose tissue and weighed. **A)** Spleen weights were normalised to the weight of the parent mouse. *Irf5*$^{-/-}$ mice did not affect relative spleen weights at steady state. WT spleens were enlarged relative to *Irf5*$^{-/-}$ spleens during inflammation. **B)** Fold change of normalised spleen weight in Hh + αIL10R treated mice relative to the normalised mean weight of uninfected mice. Inflamed wild type and *Irf5*$^{-/-}$ mice displayed splenomegaly after Hh + αIL10R, but inflammation did not alter the fold change of spleen weight.

Statistics:
Data are representative of two independent experiments. Steady state: WT n = 6, *Irf5*$^{-/-}$ n = 3. Hh + αIL10R: WT n = 7, *Irf5*$^{-/-}$ n = 7
A) 2-Way ANOVA with Tukey correction; * $p \leq 0.05$
B) Unpaired t test; ns = not significant

Clinical diagnosis of UC is supported by assessment of morphological changes in the cLP [167]. Similarly, colitic mice exhibit signs of inflammation when haematoxylin and eosin (H&E) stained sections are examined under a brightfield microscope for the signs of inflammation outlined in Table.2.4. Briefly, epithelial hyperplasia, goblet cell depletion, nucleated cell infiltrate, and submucosal oedema and area affected were scored according to the aforementioned scheme. Steady state mice either did not display, or exhibited very mild inflammation (score ≤ 3). WT colons showed marked nucleated cell infiltrate, and epithelial hyperplasia, concurrently with loss of goblet cells and submucosal oedema (Fig.5.2A, Fig.5.2C). Several WT sections also exhibited tertiary lymphoid structure formation (Fig.5.2C). *Irf5*$^{-/-}$ mice, however, were protected in all scoring criteria and did not show signs of tertiary lymphoid structures (Fig.5.2B, Fig.5.2D, data not shown). WT mice subjected to Hh + αIL10R exhibited high colitis scores by d21 of Hh + αIL10R treatment, these were significantly elevated compared to colitis scores of *Irf5*$^{-/-}$ mice (Fig.5.2E). Similarly, WT caeca were significantly more inflamed than *Irf5*$^{-/-}$ at d21 Hh + αIL10R (Fig.5.3E). WT mice were severely inflamed, with some specimens exhibiting complete disruption of the epithelium (Fig.5.3A, Fig.5.3C). *Irf5*$^{-/-}$ were more phenotypically similar to steady state, only showing mild goblet cell depletion and leukocyte infiltration (Fig.5.3B, Fig.5.3D).

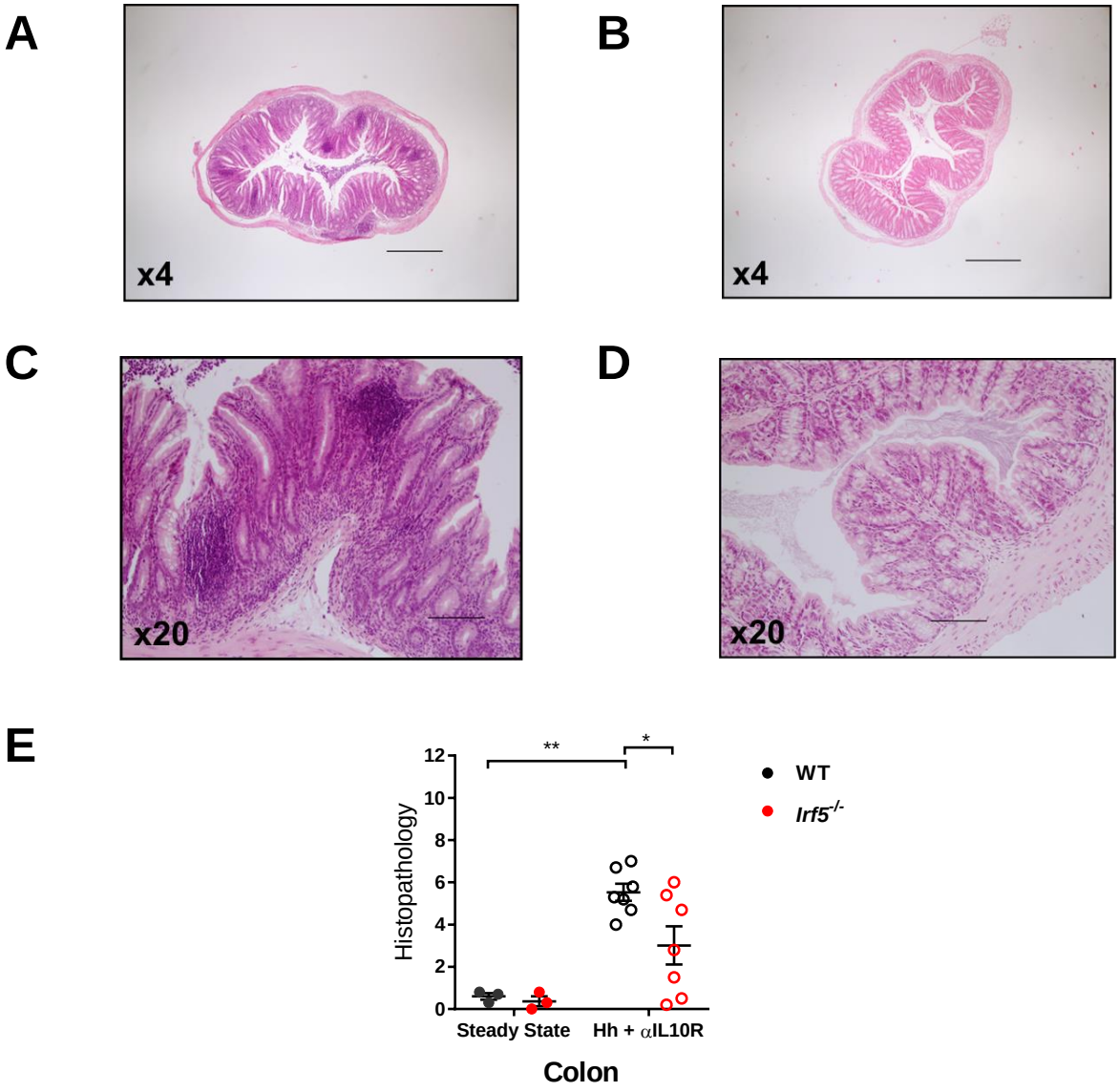

Fig.5.2: IRF5 deficient mouse colons display protection from *Helicobacter hepaticus* + αIL10R-driven inflammation relative to wild-type at d21

Segments of mouse colon were excised upon sacrifice and fixed in neutral buffered formalin for 24 hrs. Specimens were dehydrated in Xylene and mounted in paraffin blocks for sectioning. Sections were stained with haematoxylin and eosin and imaged. Photomicrographs depict: d21 Hh + αIL10R **A)** wild type (WT), and **B)** *Irf5*$^{-/-}$ colons at x4 magnification. Hh + αIL10R **C)** WT, and **D)** *Irf5*$^{-/-}$ colons at x20 magnification. WT mice displayed disrupted colon morphology, demonstrating epithelial breakdown (flattening of villi), and goblet cell depletion, submucosal oedema, and increased numbers of nucleated cells in the lamina propria. Some WT mice developed tertiary lymphoid structures (areas of dense nucleated cells). *Irf5*$^{-/-}$ colons displayed a modest increase in signs of inflammation: exhibiting a modest increase in nucleated cell infiltrate, and submucosal oedema. Epithelial integrity was largely maintained, and goblet cells lining the villi were visible. No tertiary lymphoid structures were noted in *Irf5*$^{-/-}$ mouse colon with Hh + αIL10R colitis. **E)** Steady state mice exhibited low colitis scores (≤ 3). WT colitis scores were significantly elevated vs controls (median difference = 4.929, $p \leq 0.01$), and Hh + αIL10R-treated *Irf5*$^{-/-}$ (median difference = 2.514, $p = 0.0439$).

Statistics:
Data are representative of two independent experiments. Steady state: WT n = 3, *Irf5*$^{-/-}$ n = 3. Hh + αIL10R: WT n = 7, *Irf5*$^{-/-}$ n = 7. 2-Way ANOVA with Tukey correction; * $p \leq 0.05$, ** $p \leq 0.01$

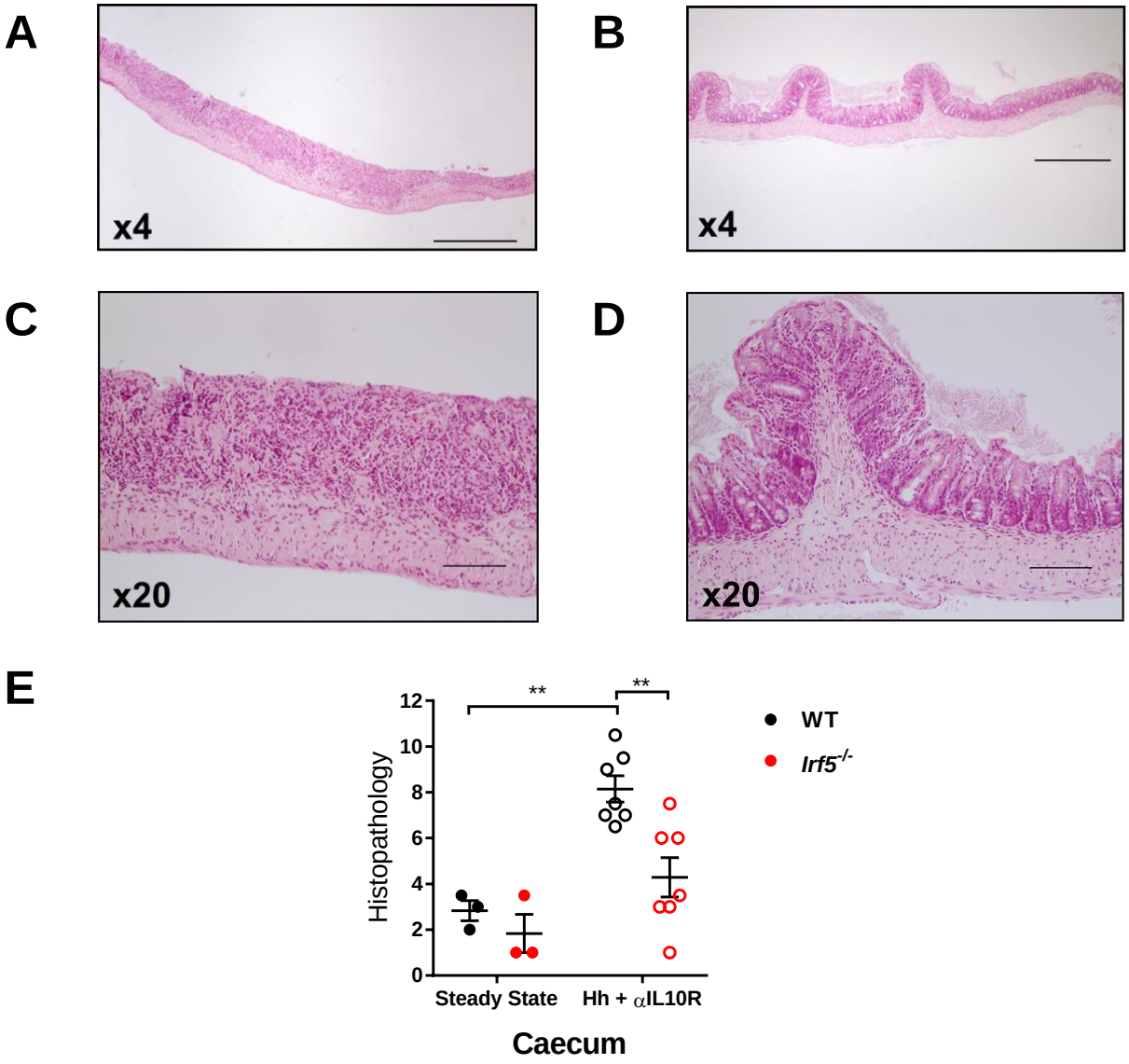

Fig.5.3: IRF5 deficient mouse caeca display reduced histological inflammation relative to wild-type at d21 *Helicobacter hepaticus* + αIL10R colitis
Segments of mouse caecum were excised upon sacrifice and fixed in neutral buffered formalin for 24 hrs. Specimens were dehydrated in Xylene and mounted in paraffin blocks for sectioning. Sections were stained with haematoxylin and eosin and imaged. Photomicrographs: d21 Hh + αIL10R **A)** wild type (WT), and **B)** *Irf5*$^{-/-}$ caeca at x4 magnification. Hh + αIL10R **C)** WT, and **D)** *Irf5*$^{-/-}$ caeca at x20 magnification. **E)** Slides were scored according to criteria describing disease severity: epithelial hyperplasia, loss of goblet cells, submucosal oedema, nucleated cell infiltrate, the area of each section afflicted, crypt branching, and crypt abscesses. WT mice displayed disrupted caecum morphology, demonstrating epithelial breakdown and goblet cell depletion, submucosal oedema, and increased numbers of nucleated cells in the lamina propria. *Irf5*$^{-/-}$ caeca displayed increased signs of inflammation, including a modest increase in nucleated cell infiltrate, and submucosal oedema. Epithelial integrity was maintained, with visible goblet cells lining the villi. Steady state mice exhibited low colitis scores (median ≤ 3) based on these parameters. WT colitis scores were significantly elevated vs controls (median difference = 5.31, p = 0.0025), and Hh + αIL10R-treated *Irf5*$^{-/-}$ (median difference = 3.857, p = 0.0044).

Statistics:
Data are representative of two independent experiments. Steady state: WT n = 3, *Irf5*$^{-/-}$ n = 3. Hh + αIL10R: WT n = 7, *Irf5*$^{-/-}$ n = 7. 2-Way ANOVA with Tukey correction; ** p ≤ 0.01

To further quantify the severity of colitis, the number of leukocytes recovered from the colonic lamina propria (cLP) of mice infected with Hh + αIL10R were quantified by multiplying the number of cells isolated from colons by the percentage of $CD45^+$ live cells per colon identified by flow cytometry. No difference between the numbers of leukocytes in the steady state cLP of WT or *Irf5*$^{-/-}$ mice was detected. Hh + αIL10R colitis resulted in an eight-fold increase in cLP leukocyte numbers ($p \leq 0.0001$, Fig.5.4). *Irf5*$^{-/-}$ mice were protected from Hh + αIL10R colitis evidenced by a 3.0 fold ($p \leq 0.0001$) increase in WT in leukocyte infiltrate vs *Irf5*$^{-/-}$ (Fig.5.4).

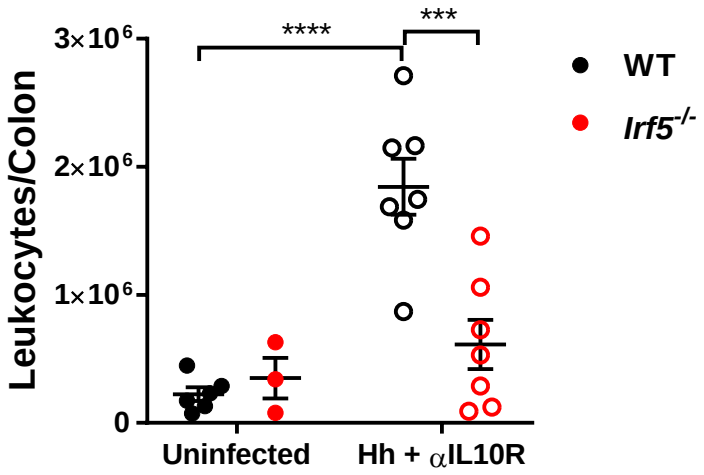

Fig.5.4: *Irf5*$^{-/-}$ mice display reduced accumulation of colonic lamina propria leukocytes relative to wild-type after Hh + αIL10R treatment

Lamina propria cells were isolated from wild type and *Irf5*$^{-/-}$ mice and counted using a CASY cell counter. The number of leukocytes was determined by multiplying the number of isolated cells by the percentage of leukocytes (Live $CD45^+$) in each sample, determined by flow cytometry. Hh + αIL10R colitis increased leukocyte accumulation in wild type cells relative to control, and *Irf5*$^{-/-}$ Hh + αIL10R.

Statistics:
Data are pooled from two independent experiments. Steady state: WT n = 6, *Irf5*$^{-/-}$ n = 3. Hh + αIL10R: WT n = 7, *Irf5*$^{-/-}$ n = 7
2-Way ANOVA with Tukey correction; *** $p \leq 0.001$, **** $p \leq 0.0001$

Bacterial presence in the lamina propria is sensed by macrophages, triggering pattern recognition receptor (PRR) signalling pathways. At steady state, this PRR signalling does not result in inflammatory responses, but under prolonged dysbiosis or the absence of IL10 signalling, pro-inflammatory mediators are released and colitis can progress [335]. For example, IL1β is released in dysbiosis and promotes a permeable gut that contributes to bacterial translocation [309]. *H. hepaticus* presence in the caecal faeces were unaffected in *Irf5*$^{-/-}$ compared to WT, quantified by detection of the *H.hepaticus* Cytolethal Distending Toxin B (cdtB) gene (Fig.5.5), indicating that differential colonisation could not explain protection from colitis. To examine the levels of cytokine production associated with colitis development and/or IBD [22], qPCR analysis was conducted on colon tissue from WT or *Irf5*$^{-/-}$ mice subjected to Hh + αIL10R colitis. Levels of inflammatory cytokines (*Il1b*, *Il6*, *Il12b*, *Ifng*, *Tnf*, and *Csf2*) appeared to be upregulated by Hh + αIL10R over steady state control in WT, and appeared lower in *Irf5*$^{-/-}$ Hh + αIL10R relative to WT, but did not attain statistical significance (possibly due to high variation in the samples tested, Fig.5.5). Levels of the anti-inflammatory cytokine, *Il10*, were not significantly altered between WT and *Irf5*$^{-/-}$, but were elevated vs steady state controls in both WT and *Irf5*$^{-/-}$. *Il5* mRNA was not affected by Hh + αIL10R or by *Irf5*$^{-/-}$.

Continued influx of leukocytes to sites of inflammation is critical for both pathogenesis and repair of tissue. Neutrophils and monocytes are key effectors in colitis [168]. The mRNA levels of potent monocyte chemokines, *Ccl4* (*Mip-1β,* $p \leq 0.01$), and *Ccl5* (*Rantes,* $p \leq 0.05$) were significantly elevated in WT colons vs control and *Irf5*$^{-/-}$ d21 Hh + αIL10R (Fig.5.6). *Ccl2* displayed a similar trend, but was not significantly upregulated in WT vs *Irf5*$^{-/-}$ Hh + αIL10R. *Cxcl1* (*Groα*), *Cxcl5* (*Ena78*), (neutrophil chemokines), and *Cxcl3* (*Gro3,* monocyte chemotaxis), and appeared to be upregulated in d21 Hh + αIL10R WT over *Irf5*$^{-/-}$, but did not obtain statistical significance (Fig.5.7).

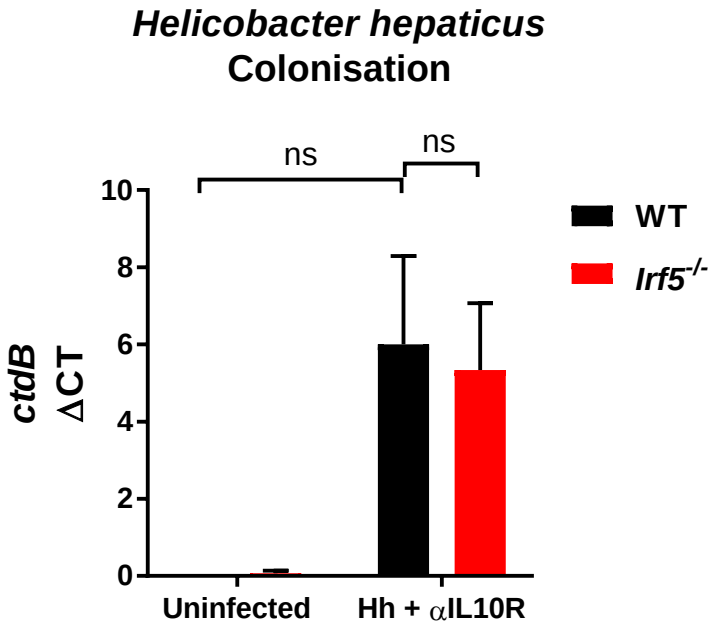

Fig.5.5: Helicobacter hepaticus colonisation is not affected by IRF5 deficiency

Caecal content from WT and *Irf5*$^{-/-}$ steady state and d21 Hh + αIL10R colitic mice was assessed for *Helicobacter hepaticus* (Hh) colonisation by qPCR of the Cytolethal Distending Toxin B (ctdB) gene. No difference was detected between WT and *Irf5*$^{-/-}$ Hh colonisation during Hh + αIL10R colitis.

Statistics:
Data are representative of 3 independent experiments. Steady state: WT n = 3, *Irf5*$^{-/-}$ n = 3. Hh + αIL10R: n = 7, *Irf5*$^{-/-}$ n = 7.
Mean + SEM
2-Way ANOVA with Tukey correction: ns = not significant

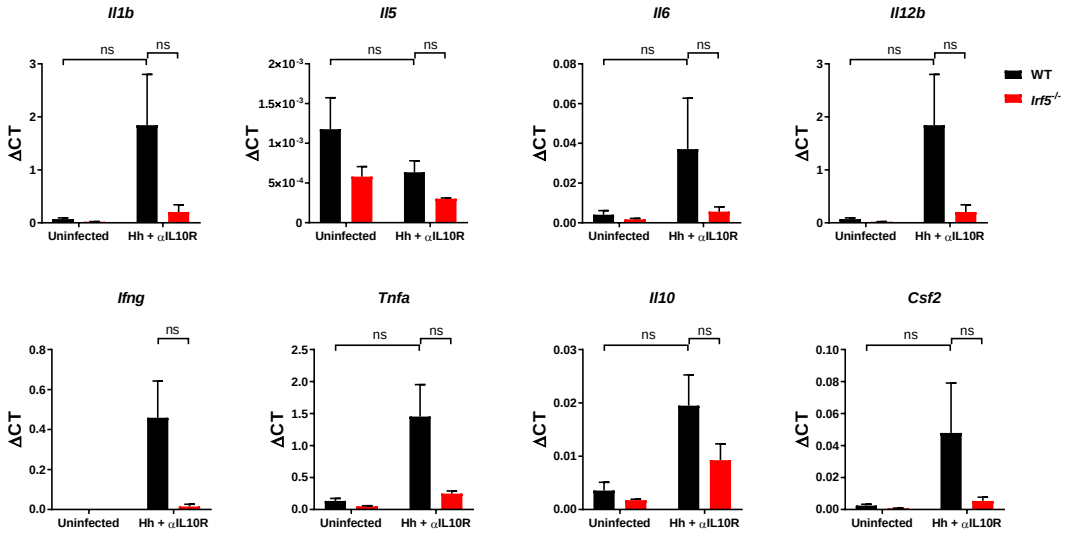

Fig.5.6: *Irf5*$^{-/-}$ mice display reduced expression of IBD-associated cytokines at d21 of Helicobacter hepaticus + αIL10R colitis

Wild type or *Irf5*$^{-/-}$ mice were subjected to Hh + αIL10R colitis. At d21, mice were culled and colon tissue was excised and snap frozen in liquid nitrogen. qPCR was performed to measure levels of IBD-associated cytokines. No significant differences were detected between conditions for the cytokines measured

Statistics:
Data are representative of two independent experiments. Steady state: WT n = 6, *Irf5*$^{-/-}$ n = 3. Hh + αIL10R: WT n = 7, *Irf5*$^{-/-}$ n = 7.
2-Way ANOVA with Tukey Correction; ns = not significant

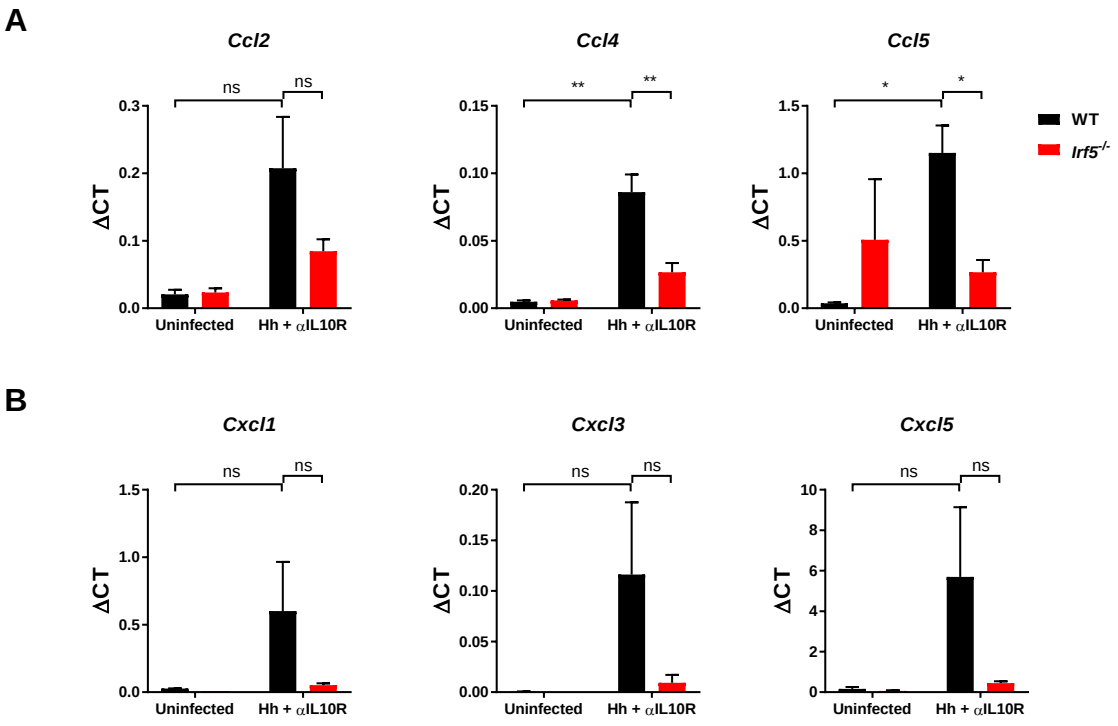

Fig.5.7: *Irf5*$^{-/-}$ mice display reduced expression of IBD-associated chemokines at d21 of *Helicobacter hepaticus* + αIL10R colitis

Wild type or *Irf5*$^{-/-}$ mice were subjected to Hh + αIL10R colitis. At d21, mice were culled and colon tissue was excised and snap frozen in liquid nitrogen. qPCR was performed to measure levels of IBD-associated chemokines. **A)** *Mip-1β* (*Ccl4*), and *Rantes* (*Ccl5*) mRNA were significantly elevated in WT colons vs control and *Irf5*$^{-/-}$ d21 Hh + αIL10R. Ccl2 displayed a similar trend, but was not significantly upregulated in WT *Irf5*$^{-/-}$ Hh + αIL10R. **B)** *Cxcl1*, *Cxcl3*, and *Cxcl5* were not significantly upregulated in d21 Hh + αIL10R WT over *Irf5*$^{-/-}$.

Statistics:
Data are representative of two independent experiments. Steady state: WT n = 6, *Irf5*$^{-/-}$ n = 3. Hh + αIL10R: WT n = 7, *Irf5*$^{-/-}$ n = 7.
2-Way ANOVA with Tukey Correction; ns = not significant, * $p \leq 0.05$, ** $p \leq 0.01$

Because IRF5 promotes T_H1 and T_H17 lymphocyte responses which are involved in the pathogenesis of colitis, T_H1 and T_H17 were profiled in WT and *Irf5*$^{-/-}$ Hh + αIL10R colitic mice [162, 259]. IFNγ and IL17A producing CD4$^+$ TCRαβ$^+$ cells were identified by flow cytometry. T_H1, T_H17, and T_H1/T_H17 cells were increased by Hh + αIL10R in WT mice ($p = 0.0001$, $p = 0.0001$, and $p \leq 0.05$ respectively, Fig.5.8A, Fig.5.8B, and Fig.5.8C). *Irf5*$^{-/-}$ colitic mice had fewer T_H1 ($p \leq 0.01$), and T_H1/T_H17 cells ($p = 0.0885$) as a proportion of CD4$^+$ TCRαβ$^+$ T cells in colitis relative to WT after restimulation (Fig.5.8A, Fig.5.8C). T_H17 cells displayed a similar trend in colitic *Irf5*$^{-/-}$ mice, but the difference was not significant (Fig.8B). T_{regs} are important in regulating the immune response in IL10-dependent and -independent pathways, and were therefore profiled [336]. T_{regs} were not affected by Hh + αIL10R colitis between WT and *Irf5*$^{-/-}$ (Fig.5.8D). Therefore, *Irf5*$^{-/-}$ mice are deficient in pathogenic T_H1/T_H17 responses but not T_{reg} in response to Hh + αIL10R colitis as hypothesised.

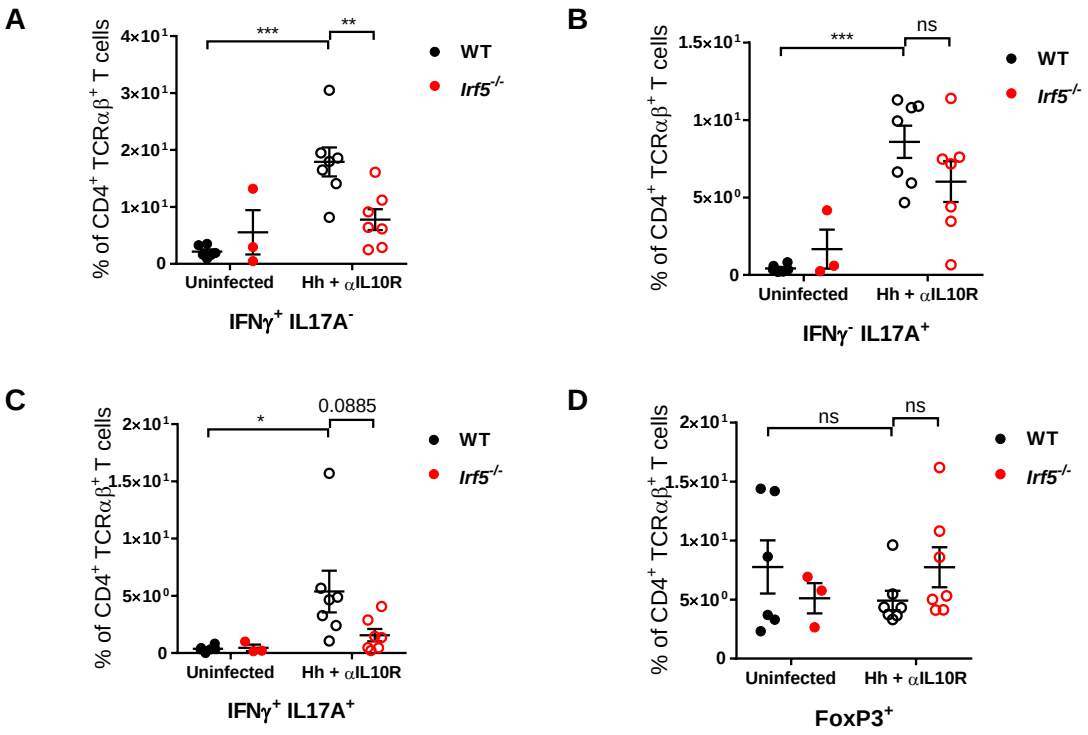

Fig.5.8: *Irf5*$^{-/-}$ mice display reduced proportions of IBD-associated T Helper cells

Lamina propria leukocytes were isolated from wild type and *Irf5*$^{-/-}$ mice and cultured for 4 hrs with PMA/Ionomycin in the presence of brefeldin A. Cells were then labelled with extracellular antibodies, fixed and permeabilised, and labelled with intracellular antibodies for cytokines. Proportions of T_H cells were quantified by flow cytometry. **A)** T_H1 cells were increased ~10 fold by Hh + αIL10R treatment in wild type relative to steady state and ~2 fold relative to *Irf5*$^{-/-}$ Hh + αIL10R, **B)** T_H17 cells were elevated in Hh + αIL10R-treated wild types vs uninfected, but were not significantly increased relative to *Irf5*$^{-/-}$ Hh + αIL10R, **C)** T_H1/T_H17 cells were increased by Hh + αIL10R, but the proportion of *Irf5*$^{-/-}$ T_H1/T_H17 cells did not increase to the same level as in wild type.

Statistics:
Data are representative of two independent experiments. Steady State: WT n = 6, *Irf5*$^{-/-}$ n = 3. Hh + αIL10R: WT n = 7, *Irf5*$^{-/-}$ n = 7.
2-Way ANOVA with Tukey correction; ns = not significant, * $p \leq 0.05$, ** $p \leq 0.01$, *** $p \leq 0.001$

5.2.2 IRF5 deficiency results in the accumulation of fewer pro-inflammatory mononuclear phagocytes in *Helicobacter hepaticus* + αIL10R colitis

IBD patients display an altered myeloid cell infiltrate in the inflamed lamina propria [337, 338]. Peak Hh + αIL10R colitis is also accompanied by similar changes to the myeloid compartment, with increases in numbers of neutrophils and pro-inflammatory Mononuclear Phagocytes (MNPs) such as monocytes and macrophages [338, 339].

The numbers of all leukocyte populations were increased in Hh + αIL10R treated WT mice consistent with the increase in the total number of leukocytes (data not shown, Fig.5.4). Therefore, the proportions of different leukocytes isolated from cLP of d21 Hh + αIL10R mice were analysed (defined in Fig.5.9A-E). No difference in the proportion of neutrophils in the cLP of colitic mice from WT or *Irf5*$^{-/-}$ mice was detected (Fig.5.10A). Interestingly, the proportion of colonic eosinophils was elevated in *Irf5*$^{-/-}$ vs WT ($p = 0.0373$, Fig.5.10B).

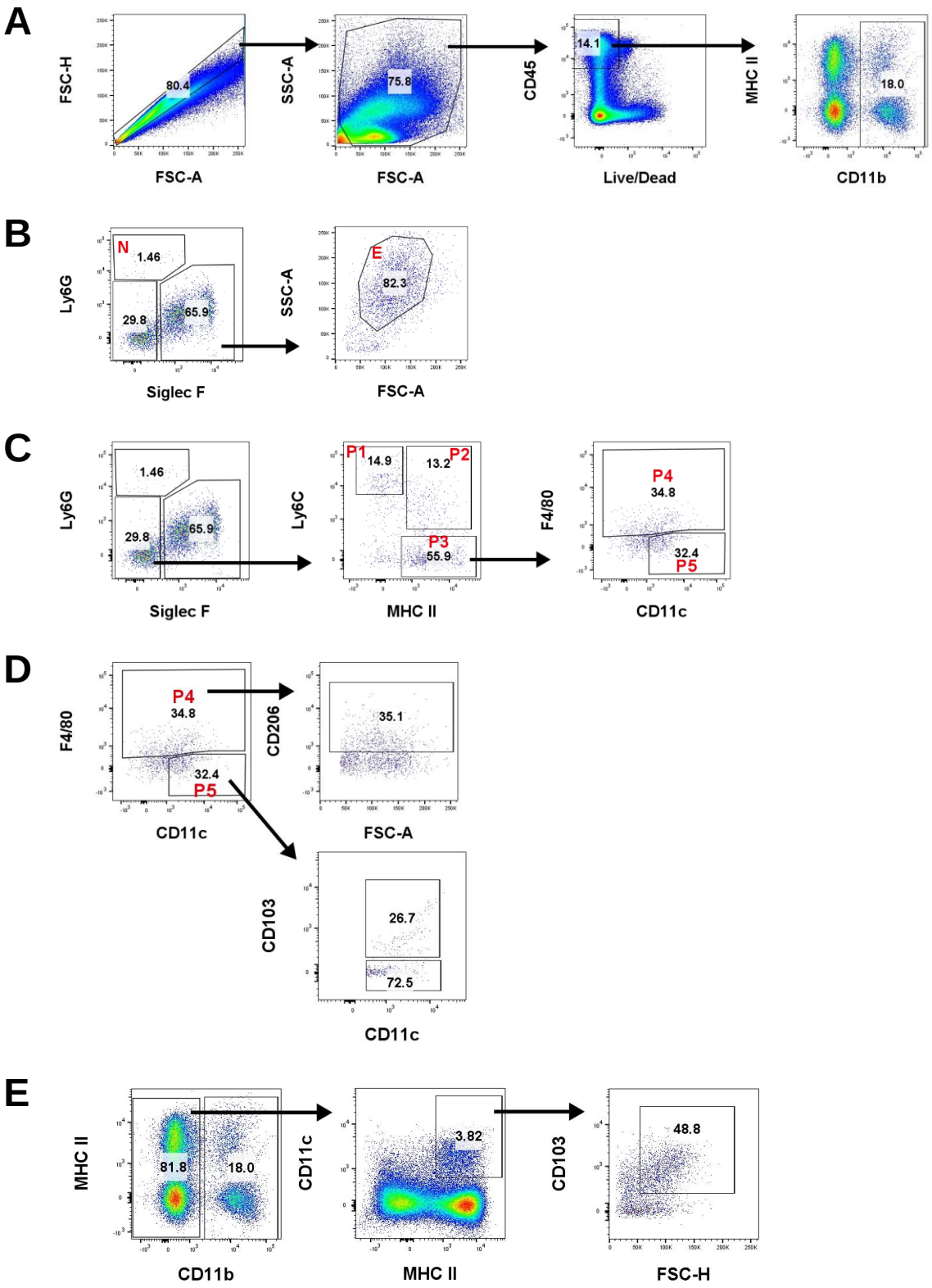

Fig.5.9: Gating strategy to define colonic lamina propria myeloid cells

A) exclusion of doublets and dead cells, identification of CD11b^{+} leukocytes. **B)** Identification of N: neutrophils (Ly6G^{+}) and E: eosinophils (Siglec F^{+} SSC^{hi}). **C)** MNPs were identified: P1 monocytes, P2 monocytes, and macrophages **D)** CD11b^{+} DCs were split into two populations based on CD103 expression. **E)** Identification of CD11b^{-} CD103^{+} DCs

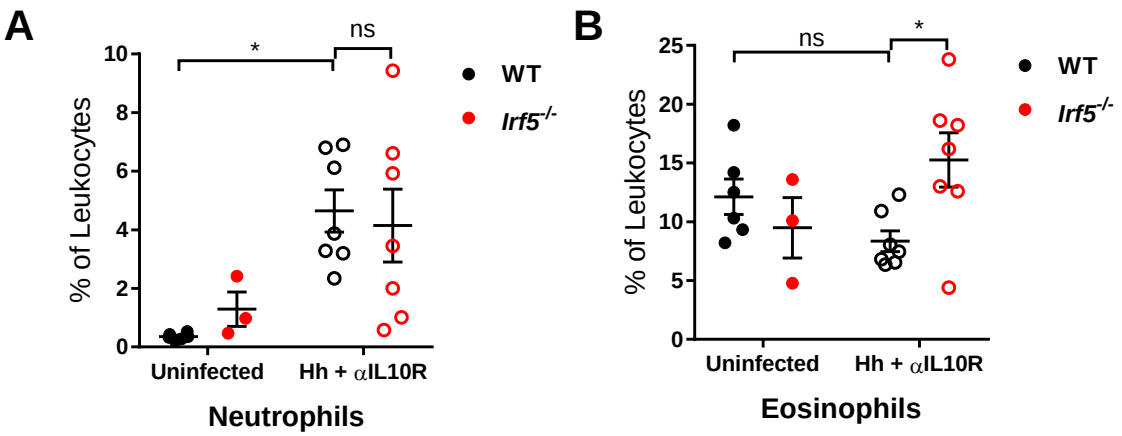

Fig.5.10: Eosinophils, but not neutrophils are increased in the colonic lamina propria of *Irf5*$^{-/-}$ relative to wild type after Hh + αIL10R treatment

Lamina propria leukocytes were isolated from colons of Hh + αIL10R colitic mice. The percentages of **A)** neutrophils (CD45^{+} CD11b^{+} Ly6G^{+}) and **B)** eosinophils (CD45^{+} CD11b^{+} Ly6G^{-} Siglec F^{+}), in wild type and *Irf5*$^{-/-}$ were assessed by flow cytometry.

Statistics:
Data are representative of two independent experiments. Steady State: WT n = 6, *Irf5*$^{-/-}$ n = 3. Hh + αIL10R: WT n = 7, *Irf5*$^{-/-}$ n = 7.
2-Way ANOVA with Tukey correction; ns = not significant, * $p \leq 0.05$

Dendritic Cells (DCs) in the cLP are able to migrate to the Mesenteric Lymph Nodes (MLN) and prime naïve T cells [330]. DCs were also profiled by flow cytometry: no significant difference was noticed between CD11b^{-} CD103^{+} DCs in Hh + αIL10R colitis (Fig.5.11A). WT and *Irf5*$^{-/-}$ CD11b^{+} CD013^{+} DCs were not affected by colitis (Fig.5.11B). Similarly, CD11b^{+} CD103^{-} DCs were unaffected by loss of IRF5 during colitis (Fig.5.11C).

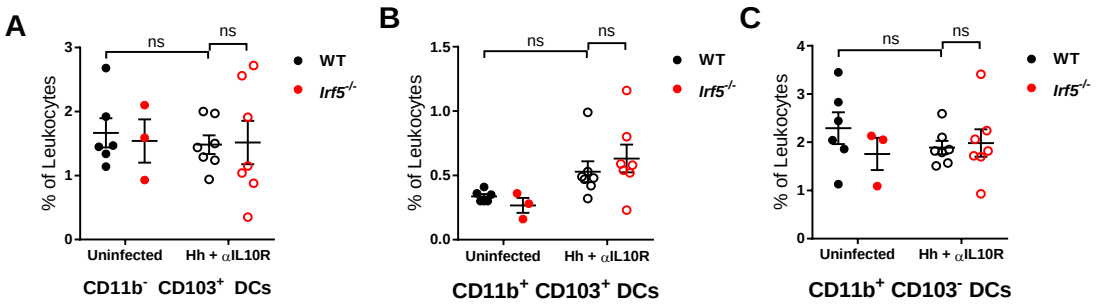

Fig.5.11: The proportions of dendritic cells in the colonic lamina propria are unchanged in *Irf5*$^{-/-}$ mice in Hh + αIL10R colitis

Lamina propria leukocytes were isolated from colons of d21 Hh + αIL10R treated mice. The percentages of **A)** CD11b^{-} CD103^{+} DCs (CD45^{+} CD11b^{+} Ly6G^{-} Siglec F^{-} Ly6C^{+} MHC II^{+} F4/80^{-}), **B)** CD11b^{+} CD103^{+} (CD45^{+} CD11b^{+} Ly6G^{-} Siglec F^{-} Ly6C^{+} MHC II^{+} F4/80^{-}), and **C)** CD11b^{+} CD103^{-} (CD45^{+} CD11b^{+} Ly6G^{-} Siglec F^{-} Ly6C^{+} MHC II^{+} F4/80^{-}), in wild type and *Irf5*$^{-/-}$ were assessed by flow cytometry. The proportions of the analysed colonic DC subsets were unchanged between wild type and *Irf5*$^{-/-}$ mice.

Statistics:
Data are representative of two independent experiments. Steady State: WT n = 6, *Irf5*$^{-/-}$ n = 3. Hh + αIL10R: WT n = 7, *Irf5*$^{-/-}$ n = 7.
2-Way ANOVA with Tukey correction; ns = not significant

MNPs, including monocytes and macrophages, are important innate leukocytes of the cLP, able to sense and respond to intestinal antigens [43, 295]. Colonic monocytes and macrophages were isolated from the inflamed lamina propria, and profiled to assess their composition. Ly6C^{hi} MHC II^{-} (P1) monocytes were unchanged between WT and *Irf5*$^{-/-}$ mice in inflammation (Fig.5.12A). Ly6C^{hi} MHC II^{+} (P2) monocytes were significantly elevated in WT mice in colitis vs steady state ($p = 0.0034$, Fig.5.12B), but not over *Irf5*$^{-/-}$ colitis. Macrophages were decreased as a percentage of total leukocytes in WT colitis vs steady state ($p < 0.001$). However, macrophages were not significantly altered between WT and *Irf5*$^{-/-}$ in colitis despite a trend towards more *Irf5*$^{-/-}$ macrophages ($p = 0.0952$, Fig.5.12C).

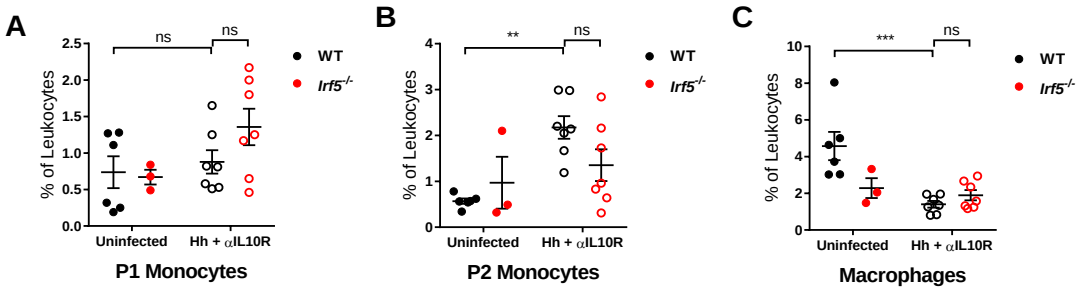

Fig.5.12: Percentages of inflammatory P2 monocytes are increased in wild type mice vs *Irf5*$^{-/-}$ mice in colitis

Lamina propria leukocytes were isolated from colons of d21 Hh + αIL10R treated mice. The percentages of **A)** P1 monocytes (CD45$^+$ CD11b$^+$ Ly6G$^-$ Siglec F$^-$ Ly6C$^+$ MHC II$^-$), **B)** P2 monocytes (CD45$^+$ CD11b$^+$ Ly6G$^-$ Siglec F$^-$ Ly6C$^+$ MHC II$^+$), and **C)** macrophages (CD45$^+$ CD11b$^+$ Ly6G$^-$ Siglec F$^-$ Ly6C$^-$ MHC II+ F4/80$^+$), in wild type and *Irf5*$^{-/-}$ were assessed by flow cytometry. P2 monocytes as a proportion of total leukocytes were increased in wild type vs IRF5 deficiency. However, The proportion of P1 monocytes and macrophages were unchanged between wild type and *Irf5*$^{-/-}$.

Statistics:
Data are representative of two independent experiments. Steady State: WT n = 6, *Irf5*$^{-/-}$ n = 3. Hh + αIL10R: WT n = 7, *Irf5*$^{-/-}$ n = 7.
2-Way ANOVA with Tukey correction; ns = not significant, ** $p \leq 0.01$, *** $p \leq 0.001$

Macrophages in the steady state *Irf5*$^{-/-}$ were present at lower frequencies within the MNP pool compared to WT (Fig.3.12), indicating a developmental block. To interrogate whether this was the case during Hh + αIL10R, P1 monocytes, P2 monocytes, and macrophages were plotted as a percentage of total MNPs (Fig.5.13A). This analysis revealed that WT P1 monocytes, P2 monocytes, and macrophages represented 9.6% ± 0.84, 26.49% ± 1.87, and 17.5% ± 1.48 of total MNPs respectively compared with 11.47% ± 1.63, 14.41% ± 1.91, and 22.86% ± 2.35 for *Irf5*$^{-/-}$ (Fig.5.13B). WT P2 monocytes were increased 1.83 fold ($p = 0.0003$) relative to *Irf5*$^{-/-}$, whereas no significant difference was found between the means of WT or *Irf5*$^{-/-}$ P1 monocytes and macrophages (Fig.5.13B), but a similar trend towards more *Irf5*$^{-/-}$ macrophages, as in Fig 5.11C, was observed. The results presented above highlight that *Irf5*$^{-/-}$ are protected from colitis, and the main defect in the myeloid compartment results from reduced accumulation of pathogenic P2 monocytes that IRF5-deficiency may promote the accumulation of eosinophils in an inflammatory environment.

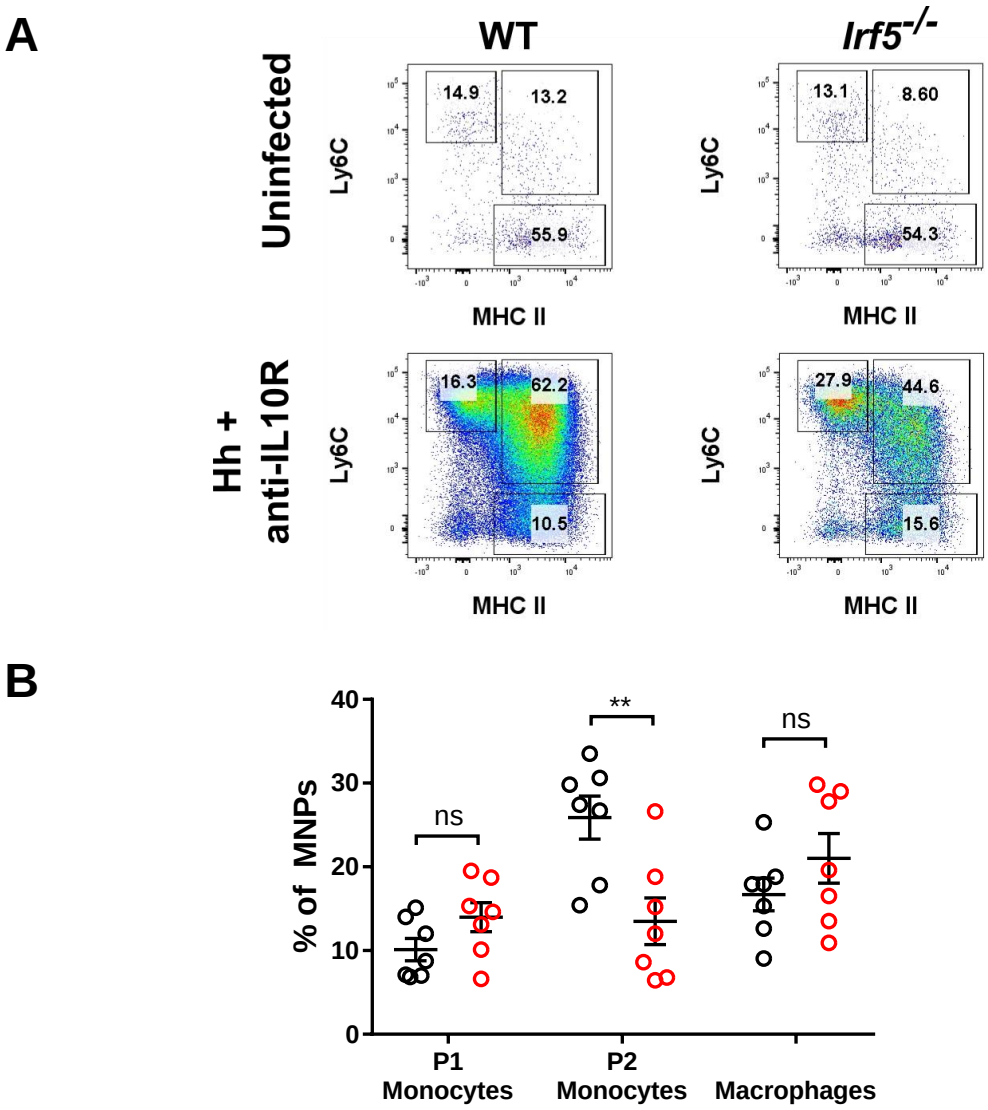

Fig.5.13: WT P2 monocytes are increased relative to *Irf5*$^{-/-}$ P2 monocytes in Hh + αIL10R colitis

Lamina propria leukocytes were isolated from colons of d21 Hh + αIL10R treated mice. The composition of the cLP MNP compartment was assessed by flow cytometry.
A) Representative flow cytometry plots of the mononuclear phagocyte compartment of WT and *Irf5*$^{-/-}$ at steady state (uninfected) and at d21 Hh + αIL10R colitis. **B)** The percentages of P1 monocytes (CD45^{+} CD11b^{+} Ly6G^{-} Siglec F^{-} Ly6C^{+} MHC II^{-}), P2 monocytes (CD45^{+} CD11b^{+} Ly6G^{-} Siglec F^{-} Ly6C^{+} MHC II^{+}), and macrophages (CD45^{+} CD11b^{+} Ly6G^{-} Siglec F^{-} Ly6C^{-} MHC II+ F4/80^{+}) relative to the total MNP pool (CD45^{+} CD11b^{+} Ly6G^{-} Siglec F^{-}), in wild type and *Irf5*$^{-/-}$ in the colonic lamina propria. Only P2 monocytes were significantly diminished within the MNP compartment in *Irf5*$^{-/-}$ mice.

Statistics:
Data are representative of two independent experiments. WT n = 7, *Irf5*$^{-/-}$ n = 7. 2 Way ANOVA with Sidak correction: ns = not significant, ** $p \leq 0.01$

5.2.3 Intestinal mononuclear phagocyte phenotype is altered in *Irf5*$^{-/-}$ colitis

Although macrophage proportions were not affected by Hh + αIL10R, we wished to uncover whether macrophage phenotype was altered by IRF5 deficiency. The macrophage mannose receptor (CD206) is a known marker of a highly phagocytic, tissue repair macrophage phenotype, and was significantly enriched within 10X Cluster 5 relative to all other clusters ($p = 3.9x10^{-9}$, data not shown) [340]. Therefore CD206 expression on macrophages was assessed by flow cytometry. The percentage of macrophages expressing CD206 at steady state was unaffected by IRF5 status (Fig.3.15), but the percentage of macrophages expressing CD206 decreased from 25% (± 3.03) to 8.23% (± 0.72) in WT macrophages during Hh + αIL10R colitis ($p = 0.0069$, Fig.5.14A). Significantly more *Irf5*$^{-/-}$ macrophages expressed CD206 in colitis (22.14% ± 2.28, $p \leq 0.05$, Fig.5.14A). The per-cell expression of CD206 (expressed as MFI) did not reflect these changes, however (Fig.5.14B).

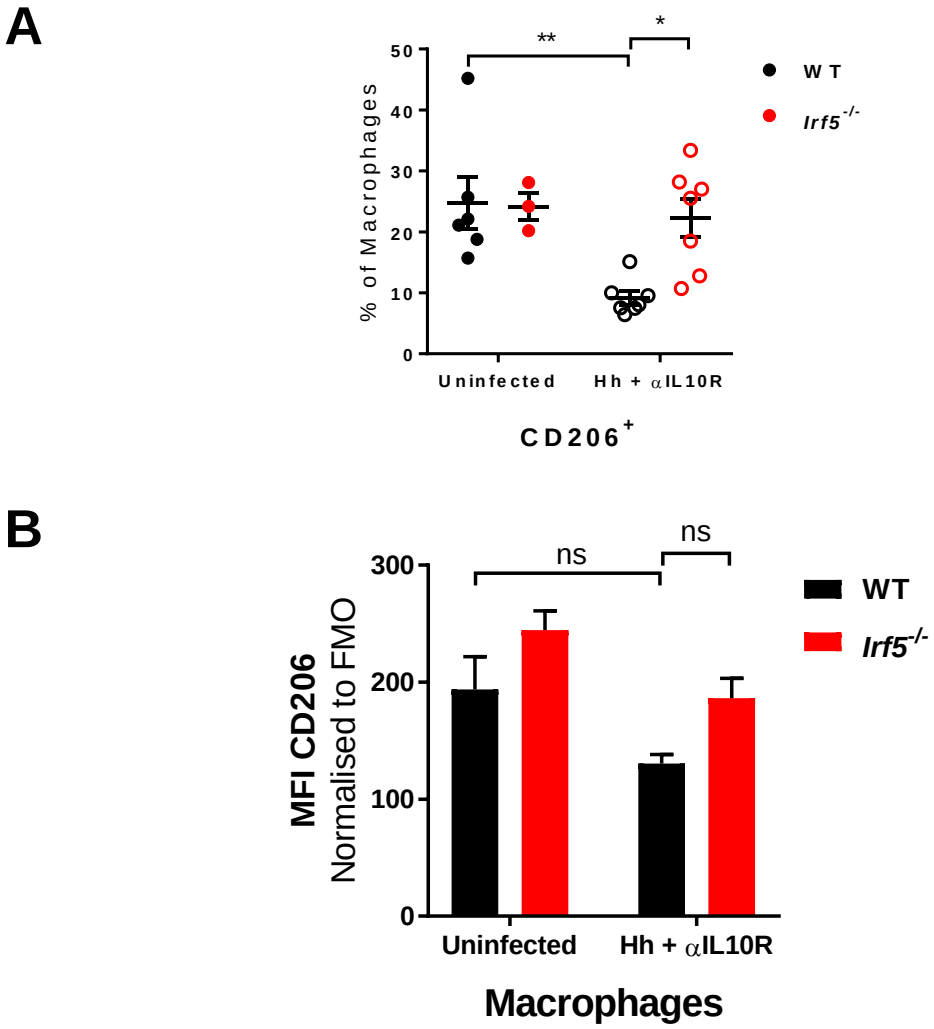

Fig.5.14: CD206 expression is diminished in WT macrophages in Hh + αIL10R colitis

Cell suspensions of colonic lamina propria leukocytes were isolated from mice that were uninfected or treated with *Helicobacter hepaticus* (Hh) + αIL10R and labelled with extracellular antibodies. Cells were analysed by flow cytometry. Macrophages were identified as $CD45^+$ $CD11b^+$ Siglec F^- $Ly6G^-$ $Ly6C^-$ MHC II^+ $F4/80^+$ cells. The number of macrophages expressing **(A)**, and the per-cell expression of CD206 on macrophages **(B)** was quantified. No difference was detected in the level of CD206 expression across experimental conditions.

Statistics:
Data are representative of two independent experiments. Uninfected: WT n = 6, *Irf5*$^{-/-}$ n = 3. Hh + αIL10R: WT n = 7, *Irf5*$^{-/-}$ n = 7**. A, B)** 2 Way ANOVA with Tukey correction: ns = not significant, * $p \leq 0.05$, ** $p \leq 0.01$

CD11c, on the other hand, marks inflammatory MNPs in the colon [124]. The percentage of P2 monocytes and macrophages expressing CD11c increased with Hh + αIL10R colitis in WT (Fig.5.15A, $p = 0.0005$, and $p < 0.0001$ respectively). The MFI of CD11c also increased significantly in WT P2 monocytes and macrophages (Fig.5.15B, $p = 0.0094$, and $p < 0.0001$) CD11c expressing P2 monocytes increased from 31.63% (± 4.01) to 46.34 (± 1.91, $p = 0.014$), and $CD11c^+$ macrophages increased from 41.87% (± 2.98) to 62.37% (± 2.78, $p = 0.036$) (Fig.5.15A). $CD11c^+$ P2 monocytes ($p = 0.0009$) and macrophages ($p < 0.0001$) were enriched in WT over *Irf5*$^{-/-}$ (Fig.5.15.C). WT expression of CD11c was increased over *Irf5*$^{-/-}$ in colitis when the MFI of CD11c was measured. CD11c expression increased 1.45 fold in WT P2 monocytes ($p = 0.028$), and 1.64 fold in WT macrophages vs *Irf5*$^{-/-}$ ($p < 0.0001$) in colitis (Fig.5.15D).

Because these molecules are markers of anti- and pro-inflammatory MNPs respectively, we hypothesised that the expression may be mutually exclusive. To investigate this hypothesis, MNPs were clustered on the basis of CD11c, CD206, F4/80, CD103, CD24, MHC II and Ly6C expression using the viSNE algorithm in Cytobank [247]. viSNE is a form of principal component analysis that assembles data with similar characteristics into clusters and plots these in two dimensions (tSNE1, and tSNE2). The expression of different markers in clusters is presented in Fig.5.16A. Based on the differential expression of markers, cell types were assigned (Fig.5.16B). Macrophages were designated Cluster 4 in this analysis. We observed that $CD206^+$ macrophages (pink circles) did not co-express CD11c, whist $CD11c^+$ macrophages (black circles) did not express CD206 (Fig.5.16C). Intriguingly, a subset of $CD11c^+$ macrophages appeared to be diminished in *Irf5*$^{-/-}$ (blue circles in panels, Fig.5.16C). Taken together, the data indicate that CD11c and CD206 expression on macrophages are mutually exclusive and may mark inflammatory and tissue resident macrophages respectively. Indeed, reads mapping to Mrc1 were significantly elevated in 10X Cluster 5 relative to 10X Cluster 2 (data not shown, $p = 2.03 \times 10^{-13}$.

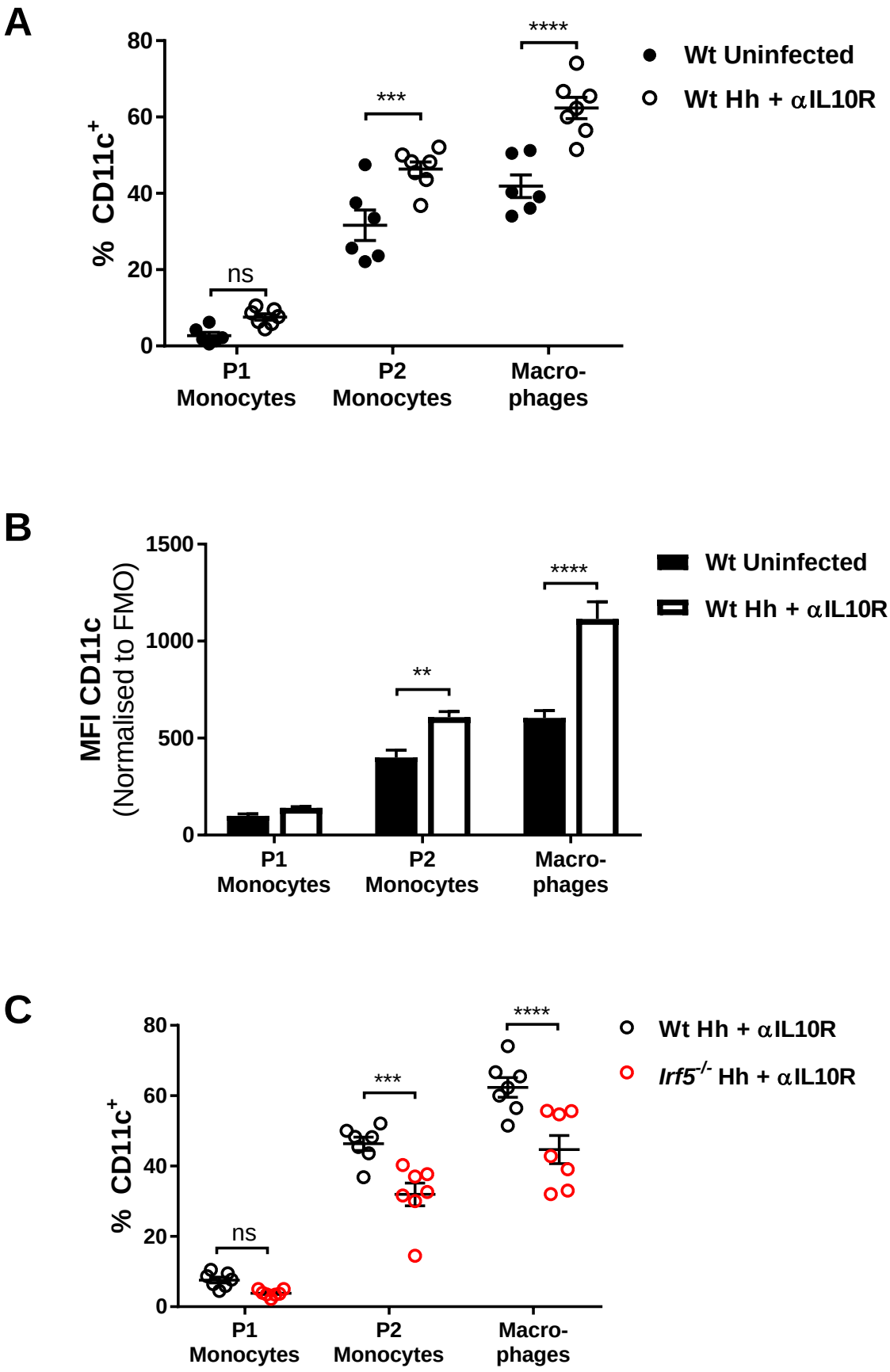
A
80
60
40
20
0
% CD11c+
ns
***
****
P1 Monocytes
P2 Monocytes
Macro-phages
Wt Uninfected
Wt Hh + αIL10R
B
1500
1000
500
0
MFI CD11c (Normalised to FMO)
**
****
P1 Monocytes
P2 Monocytes
Macro-phages
Wt Uninfected
Wt Hh + αIL10R
C
80
60
40
20
0
% CD11c+
ns
***
****
P1 Monocytes
P2 Monocytes
Macro-phages
Wt Hh + αIL10R
Irf5-/- Hh + αIL10R

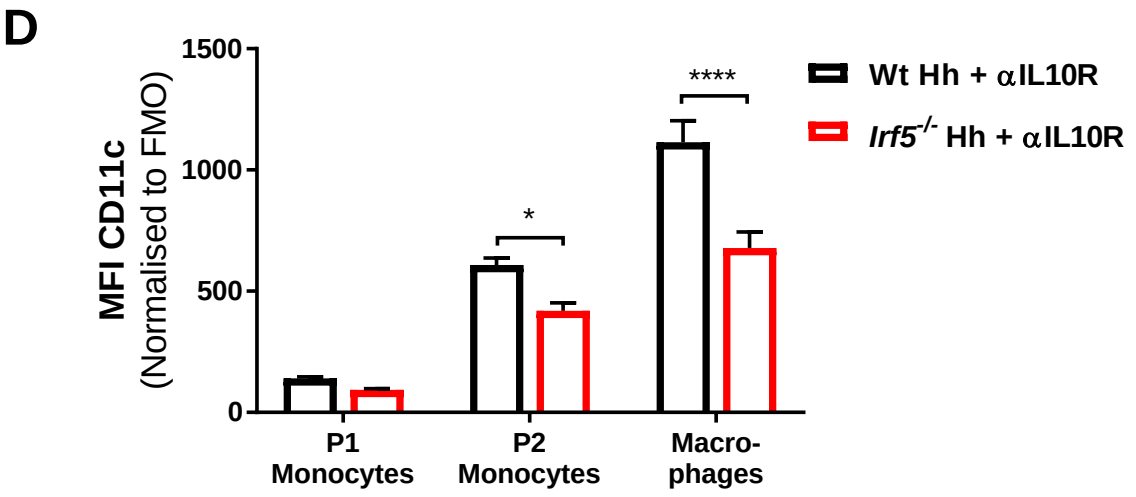

Fig.5.15: CD11c expression is diminished in *Irf5*$^{-/-}$ MNPs relative to WT in Hh + αIL10R colitis

Cell suspensions of colonic lamina propria leukocytes were isolated from mice that were uninfected or treated with *Helicobacter hepaticus* (Hh) + αIL10R and labelled with extracellular antibodies. Cells were analysed by flow cytometry. The number of MNPs expressing, and the per-cell expression of CD11c on MNPs was quantified. **A)** the percentage of P2 monocytes, and macrophages expressing CD11c was increased in WT Hh + αIL10R vs steady state WT Hh + αIL10R ($p = 0.0005$, and $p < 0.0001$ respectively). **B)** CD11c expression on P2 monocytes and macrophages with Hh + αIL10R colitis ($p = 0.0094$, and $p < 0.0001$ respectively). **C)** The percentage of CD11c^{+} P2 monocytes ($p = 0.0009$) and macrophages ($p < 0.0001$) was higher in WT relative to *Irf5*$^{-/-}$ during colitis. **D)** P2 monocyte and macrophage expression of CD11c was higher in WT than in *Irf5*$^{-/-}$ at d21 Hh + αIL10R colitis ($p = 0.0277$, and $p < 0.0001$ respectively).

Statistics:
Data are representative of two independent experiments. Steady state WT n = 6, *Irf5*$^{-/-}$ n = 3, Hh + αIL10R WT n = 7, *Irf5*$^{-/-}$ n = 7. 2-Way ANOVA with post-hoc Sidak correction for multiple comparisons

A

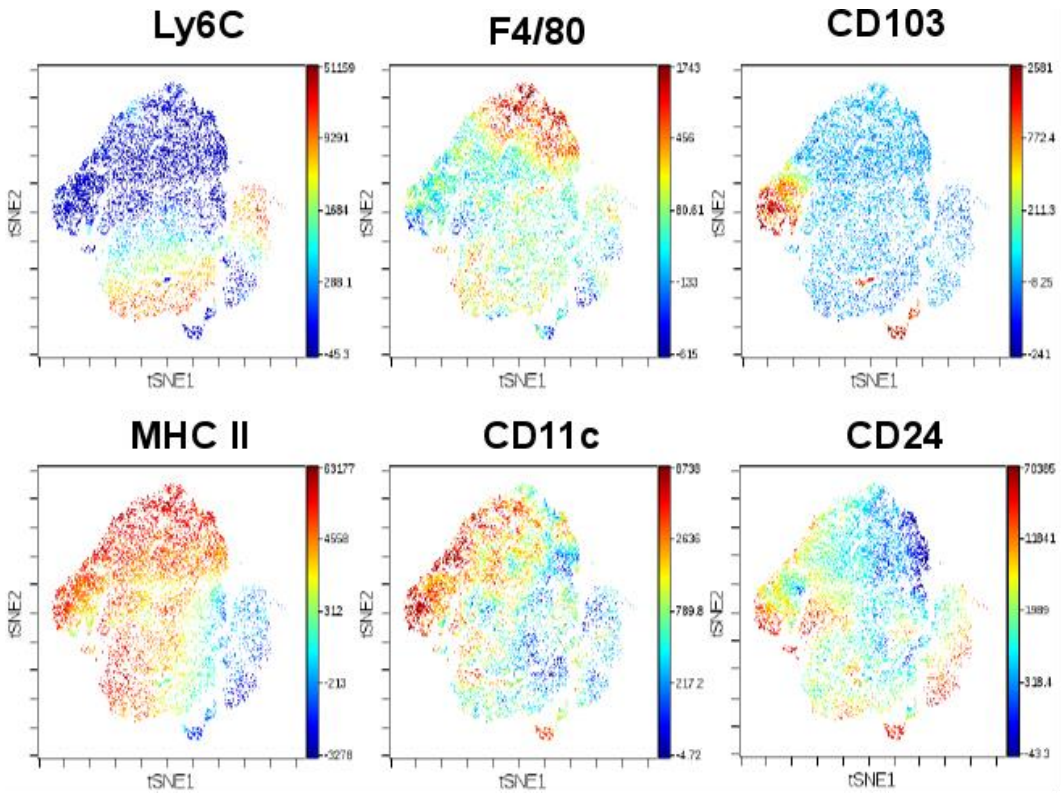

B

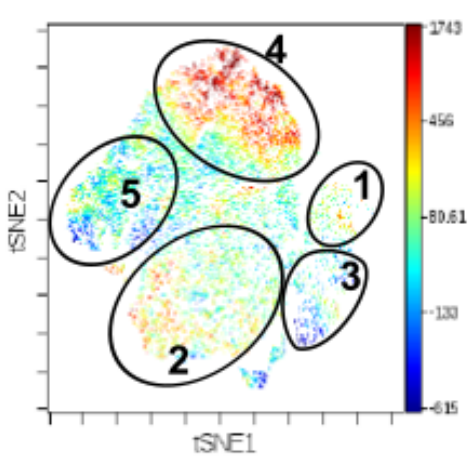

1 - Ly6C^{+} MHC II^{-} monocytes
2 - Ly6C^{+} MHC II^{+} monocytes
3 - Eosinophils
4 - Macrophages
5 - CD11b^{+} DCs

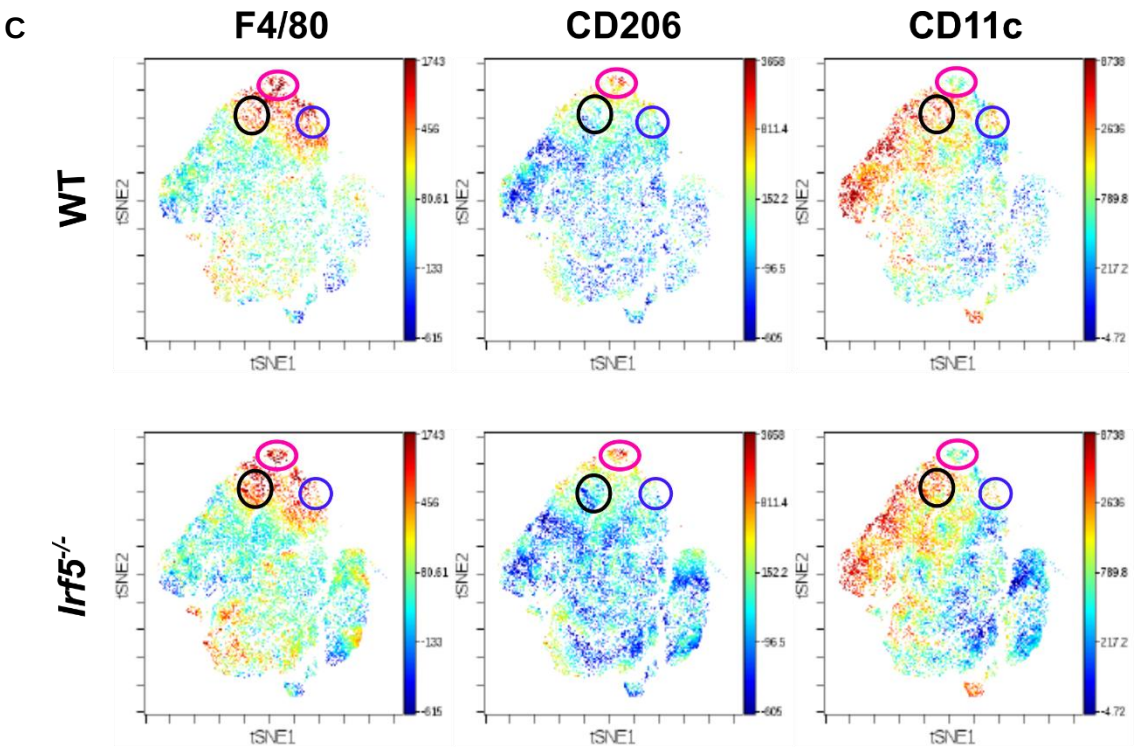

Fig.5.16: CD11c^{+} Macrophages do not co-express CD206

Flow cytometry data from WT vs global *Irf5*$^{-/-}$ MNPs (Live CD45^{+} CD11b^{+} Ly6G^{-} Siglec F^{-}) at d21 Hh + αIL10R were analysed using viSNE to cluster cells based on cell surface marker expression. **A)** Expression of leukocyte extracellular markers. **B)** Identity of CD11b^{+} MNPs based on cell surface markers. **C)** CD206^{+} macrophages (pink circles) did not co-express CD11c, whist CD11c^{+} macrophages (black circles) did not express CD206. A subset of CD11c^{+} macrophages appeared to be diminished in *Irf5*$^{-/-}$ (blue circles)

A-C) Representative viSNE clusters from WT d21 Hh + αIL10R colitis

5.2.4 Characterisation of IRF5 expression in the colonic lamina propria

The expression of IRF5 in the cLP was previously uncharacterised. The expression of IRF5 in Lamina Propria Leukocytes (LPLs) was quantified by intracellular labelling of IRF5 followed by flow cytometry. Because the best anti-IRF5 antibody is polyclonal and displays some non-specific binding [216], IRF5 expression was normalised to corresponding *Irf5*$^{-/-}$ LPLs. IRF5 expression in CD45^{-} and CD11b^{-} cells was very low (Fig.5.17A). Few neutrophils expressed IRF5 at steady state, but the percentage of IRF5^{+} neutrophils increased from 0% to 3.7% ($p = 0.017$) with Hh + αIL10R colitis (Fig.5.17B). However, the change in IRF5 MFI was not statistically significant (Fig.5.17C). A high percentage of intestinal MNPs expressed IRF5 (>30%), and MNPs expressed IRF5 to a high level (MFI > 2000) (Fig.5.17B, Fig.5.17C). Only P2 monocytes saw an increase in the percentage of IRF5 expressing cells in the inflamed state. 43% (median) of P2 monocytes expressed IRF5 at steady state vs median 55.4% in Hh + αIL10R ($p = 0.017$). The increase in percentage of IRF5 expressing P2 monocytes was concomitant with an increase in IRF5 MFI ($p < 0.001$) (Fig.17B). ~50% of macrophages expressed IRF5 at steady state, but neither the frequency, nor the MFI, of IRF5 expressing macrophages increased with inflammation (Fig.17B).

A

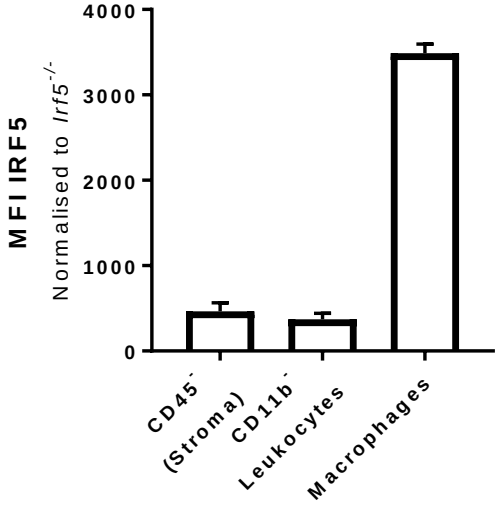
MFI IRF5
Normalised to Irf5-/-
4000
3000
2000
1000
0
CD45- (Stroma)
CD11b- Leukocytes
Macrophages

B

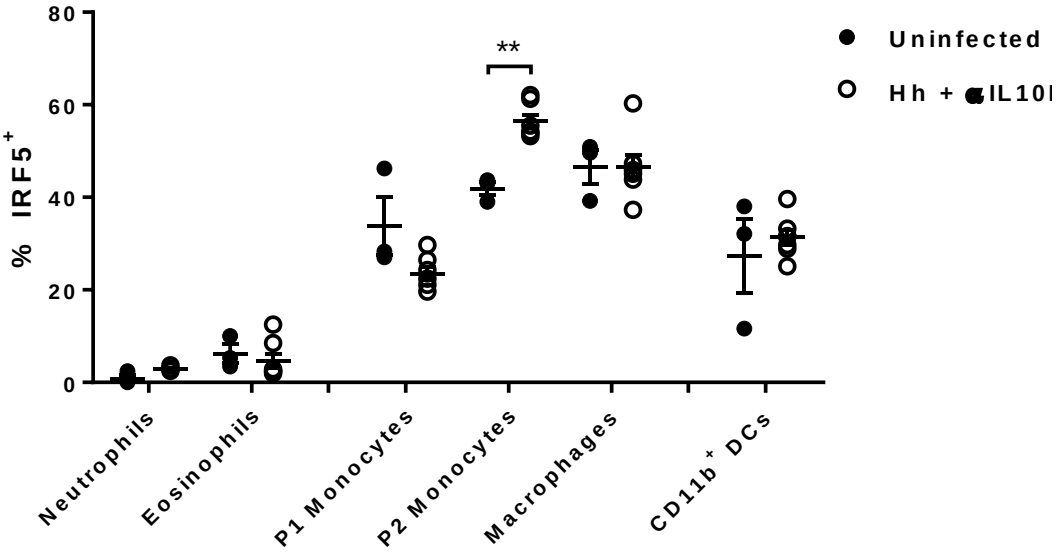
% IRF5+
80
60
40
20
0
**
Uninfected
Hh + IL10
Neutrophils
Eosinophils
P1 Monocytes
P2 Monocytes
Macrophages
CD11b+ DCs

C

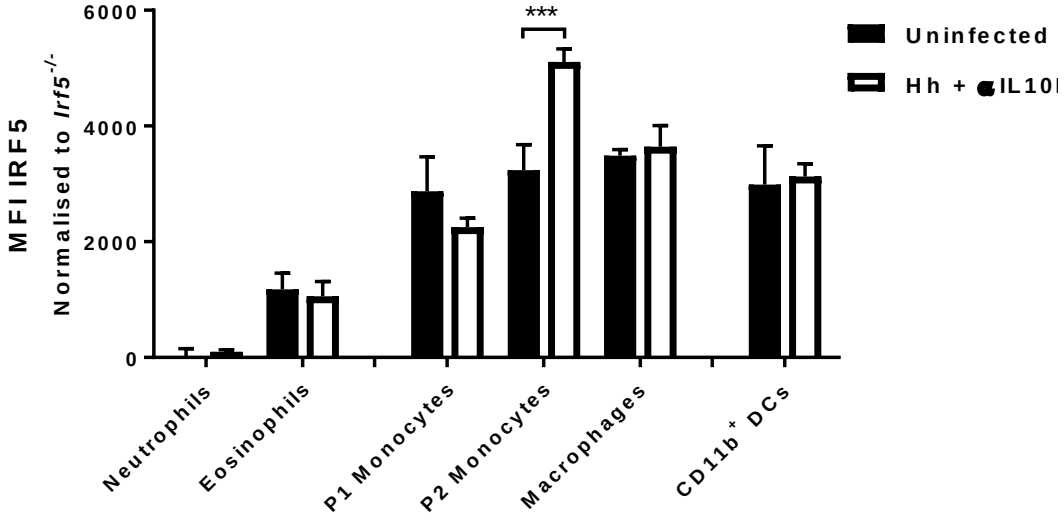

Fig.17: IRF5 expression increases specifically in P2 Monocytes at d21 Hh + αIL10R colitis

Cell suspensions of cLP leukocytes were isolated from mice that were uninfected or treated with *Helicobacter hepaticus* (Hh) + αIL10R and labelled with extracellular antibodies. Cells were analysed by flow cytometry. **A)** The MFI of IRF5 in $CD45^-$ and $CD11b^-$ cells compared with macrophages during Hh + αIL10R colitis. **B)** The percentage of neutrophils and MNPs expressing IRF5, and **C)** the per-cell expression of IRF5 in neutrophils and MNPs was quantified. Few neutrophils and eosinophils expressed IRF5, and those that did expressed low levels of IRF5. Between 20 and 50% of MNPs expressed IRF5 at steady state. More P2 monocytes expressed IRF5 during inflammation than at steady state ($p = 0.0017$). P1 monocytes, P2 monocytes, and macrophages expressed high levels of IRF5 at steady state, but IRF5 expression only increased in P2 monocytes with inflammation ($p = 0.0008$).
Neutrophils ($CD45^+$ $CD11b^+$ $Ly6G^+$), P1 Monocytes ($CD45^+$ $CD11b^+$ Siglec F^- $Ly6G^-$ $Ly6C^+$ MHC II^-), P2 Monocytes ($CD45^+$ $CD11b^+$ Siglec F^- $Ly6G^-$ $Ly6C^+$ MHC II^+), Macrophages ($CD45^+$ $CD11b^+$ Siglec F^- $Ly6G^-$ $Ly6C^-$ MHC II^+ $F4/80^+$)
Data shown are representative of two independent experiments. Steady state n = 3, Hh + αIL10R n = 7

Statistics:
A- C) Steady state: WT n = 3, normalised to $Irf5^{-/-}$ n = 3. Hh + αIL10R: WT n = 6, normalised to $Irf5^{-/-}$ n = 6. 2 Way ANOVA with Sidak correction; ** $p \leq 0.01$, *** $p \leq 0.001$

5.2.5 CD11c$^+$ P2 monocytes express high levels of IRF5

CD11c$^+$ macrophages were shown to promote atherosclerosis in *Apoe*$^{-/-}$ mice [278]. In the Hh + αIL10R model, CD11c$^+$ MNPs, including P2 monocytes and macrophages, were also implicated in disease pathogenesis via the production of *Il23a* [124]. As *Il23a* and *Itgax* (CD11c) are both directly regulated by IRF5, it was hypothesised that IRF5 expression may help to mark this inflammatory subset of MNPs [162, 278]. CD11c$^+$ P2 monocytes (Fig.5.17A), and CD11c$^+$ macrophages (Fig.5.17B) both expressed significantly higher levels of IRF5 than their CD11c$^-$ counterparts at steady state, and during Hh + αIL10R colitis. IRF5 expression was significantly upregulated in CD11c$^+$ but not CD11c$^-$ P2 monocytes at d21 Hh + αIL10R colitis vs steady state. Interestingly, CD11c$^+$ macrophages appeared to lack the anti-inflammatory marker, CD206 (Fig.5.16). 10X Cluster 2 may express a higher level of *Itgax* (CD11c), and less *Mrc1* (CD206) than 10X Cluster 5.Thus CD11c may help to mark an inflammatory macrophage population that promotes colitis. Taken together with *in vitro* knowledge of IRF5 activity, this data supports a role for IRF5-expressing CD11c$^+$ P2 monocytes as critical effectors in Hh + αIL10R colitis.

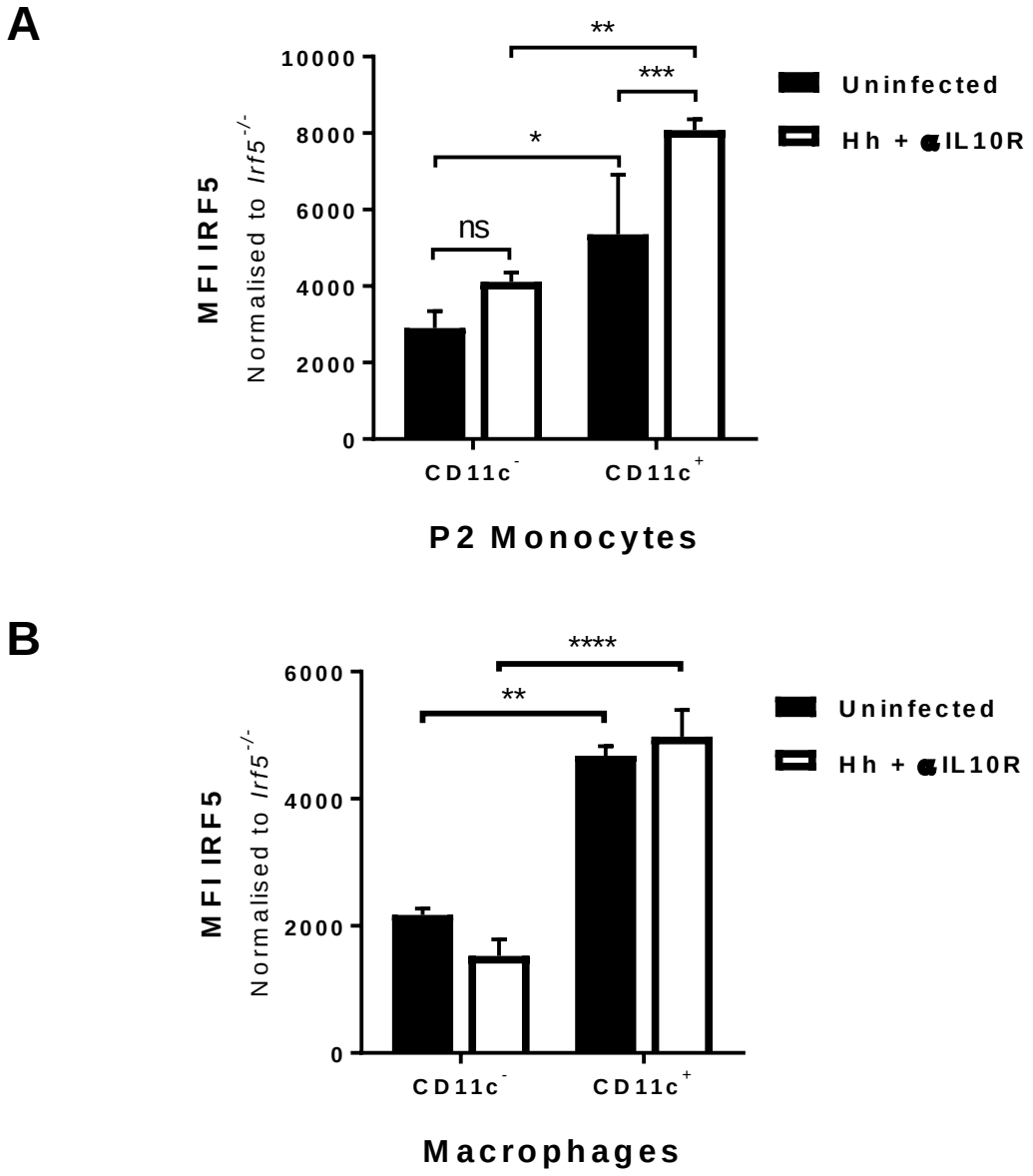

Fig.5.18: IRF5 expression in CD11c$^+$ P2 monocytes and macrophages is higher than in CD11c$^-$

The expression of IRF5 in CD11c$^+$ and CD11c$^-$ P2 monocytes and macrophages was compared by flow cytometry. CD11c$^+$ P2 monocytes and macrophages expressed significantly higher levels of IRF5 than CD11c$^-$ both at steady state (**A)** p = 0.0406, **B)** p = 0.0012) and during inflammation (**A)** p = 0.0002, **B)** p < 0.0001). Hh + αIL10R inflammation significantly elevated IRF5 expression in CD11c$^+$ but not CD11c$^-$ **A)** P2 monocytes (p = 0.0073). IRF5 expression was not increased during Hh + αIL10R colitis in **B)** macrophages.

Statistics:
Data presented are representative of two independent experiments. Steady state n = 3, Hh + αIL10R n = 7
2-Way ANOVA with Sidak correction; ns = not significant, * p ≤ 0.05, ** p ≤ 0.01, *** p ≤ 0.001, **** p < 0.0001

5.2.6 *Irf5*$^{-/-}$ leukocytes are protected from apoptosis in Hh + αIL10R colitis

IRF5 has been described as a tumour suppressor, and is able to regulate apoptosis in response to TRAIL or Fas signalling, upstream of Caspase 8 [231, 232]. To assess whether apoptosis may play a role in the cLP during Hh + αIL10R colitis, the apopototic state of myeloid cells was measured by flow cytometry based on the expression of Annexin V, and uptake of fixable viability dye. All myeloid populations in *Irf5*$^{-/-}$ were protected from apoptosis (Fig.5.19-21). *Irf5*$^{-/-}$ MNPs in 10X Cluster 2 and 10X Cluster did express lower levels of the anti-apoptotic factor *Anxa1*, while WT macrophage clusters from this analysis expressed higher levels of the stress response genes *Hsp90aa1*, and *Hsph1* which supports this analysis (Table.4.3-10). Increased rates of apoptosis may contribute to inefficient clearance of damage associated molecular patterns, which would therefore support inflammation by PRR triggering on immune cells. However, in the setting displayed here, *Irf5*$^{-/-}$ experience less severe colitis, which may not promote apoptosis to the extent seen in WT.

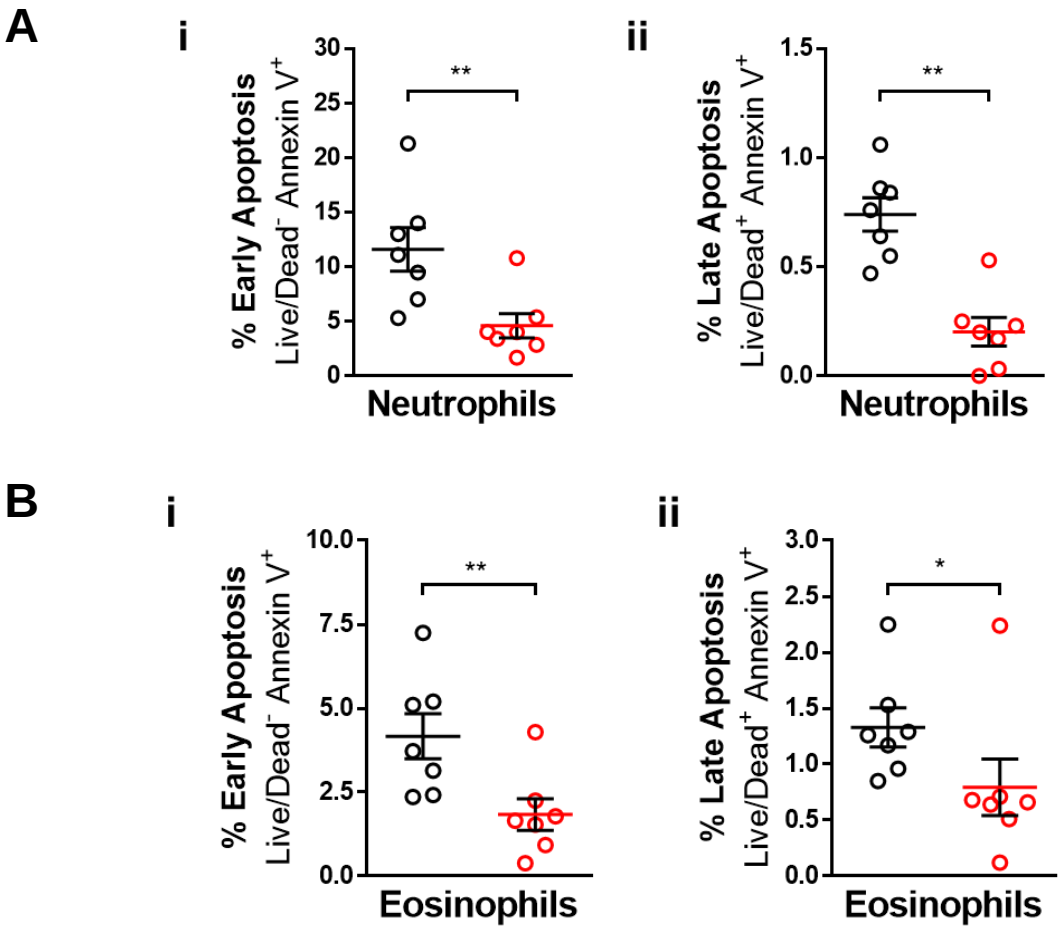

Fig.5.19: *Irf5*$^{-/-}$ granulocytes are protected from apoptosis during Hh + αIL10R colitis

WT and *Irf5*$^{-/-}$ mice were infected with Hh + αIL10R and culled at d21 of colitis. After sacrifice, LPLs were isolated from mice and labelled with extracellular antibodies. The expression of Annexin V in conjunction with viability dye (live/dead) was used to assess apoptosis stage. Early apoptotic cells were defined: **i)** Annexin V$^+$ Live/Dead$^-$, Late apoptotic cells were defined **ii)** Annexin V$^+$ Live/Dead$^+$. *Irf5*$^{-/-}$ **A)** neutrophils (**i)** p = 0.007, **ii)** p = 0.0012), and **B)** eosinophils (**i)** p = 0.007, **ii)** p = 0.0175) were protected from both stages of apoptosis.

Statistics:
Data shown are from one experiment where n = 7 mice per group
Mann-Whitney U test; * $p \leq 0.05$, ** $p \leq 0.01$

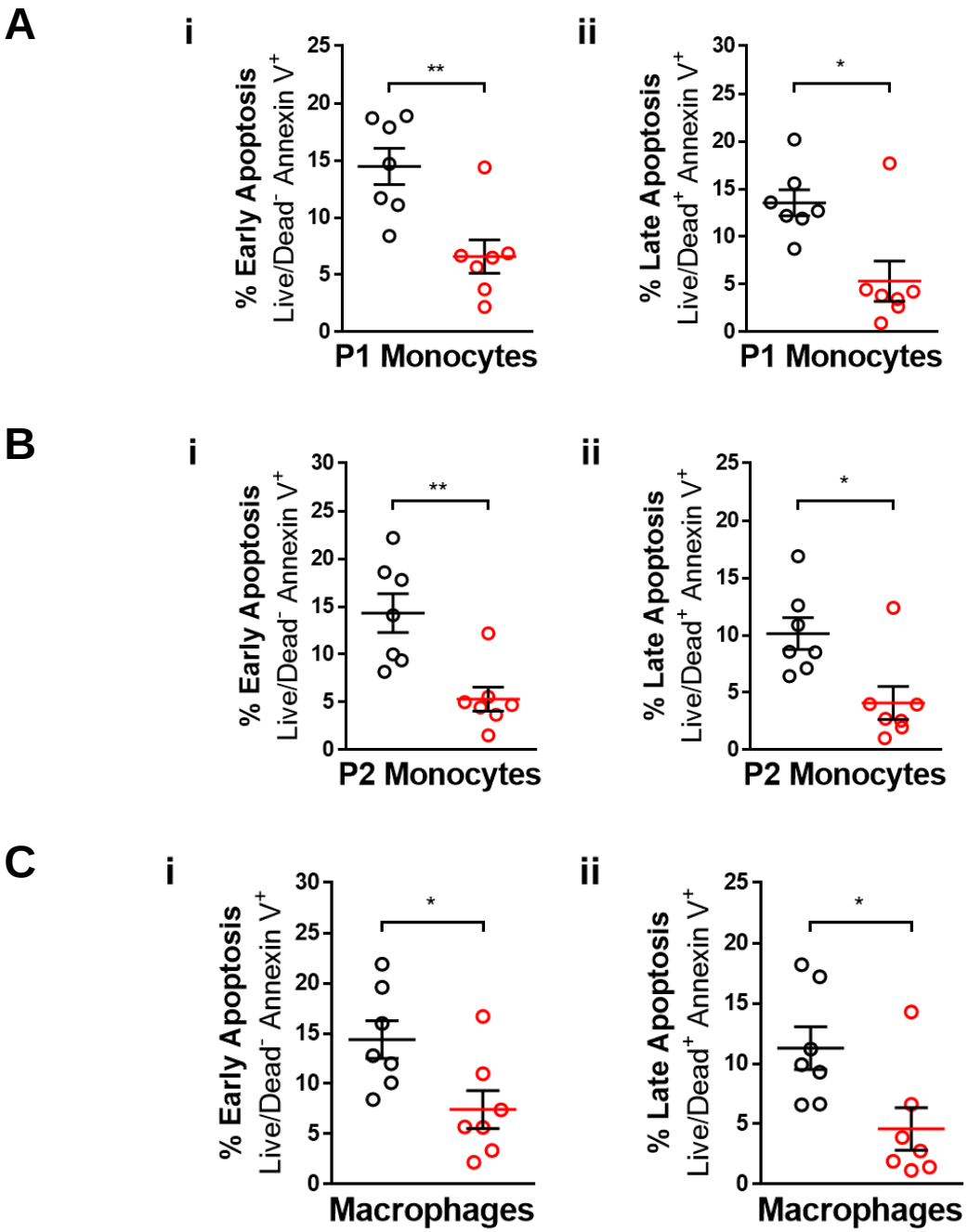

Fig.5.20: *Irf5*$^{-/-}$ MNPs are protected from apoptosis during Hh + αIL10R colitis

WT and *Irf5*$^{-/-}$ mice were infected with Hh + αIL10R and culled at d21 of colitis. After sacrifice, LPLs were isolated from mice and labelled with extracellular antibodies. The expression of Annexin V in conjunction with viability dye (live/dead) was used to assess apoptosis stage. Early apoptotic cells were defined: **i)** Annexin V$^+$ Live/Dead$^-$, Late apoptotic cells were defined **ii)** Annexin V$^+$ Live/Dead$^+$. *Irf5*$^{-/-}$ **A)** P1 monocytes (**i)** $p = 0.0041$, **ii)** $p = 0.0175$), **B)** P2 monocytes (**i)** $p = 0.0041$, **ii)** $p = 0.0111$), and **C)** macrophages (**i)** $p = 0.0262$, **ii)** $p = 0.0175$) were protected from both stages of apoptosis.

Statistics:
Data shown are from one experiment where n = 7 mice per group
Mann-Whitney U test; * $p \leq 0.05$, ** $p \leq 0.01$

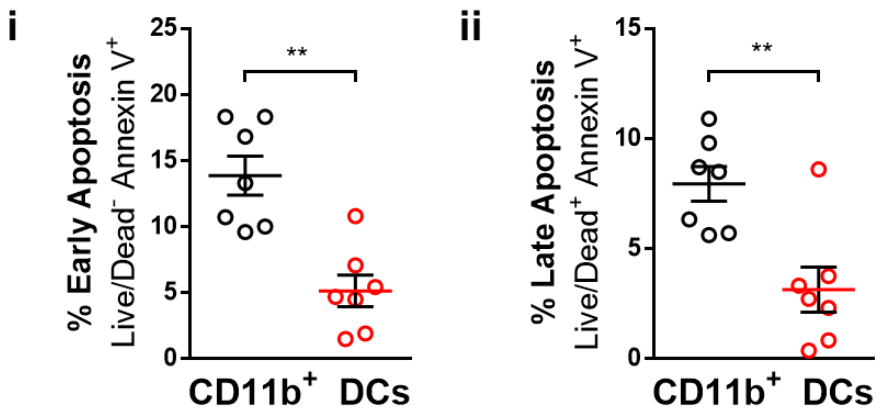

Fig.5.21: *Irf5*$^{-/-}$ CD11b^{+} DCs are protected from apoptosis during Hh + αIL10R colitis

WT and *Irf5*$^{-/-}$ mice were infected with Hh + αIL10R and culled at d21 of colitis. After sacrifice, LPLs were isolated from mice and labelled with extracellular antibodies. The expression of Annexin V in conjunction with viability dye (live/dead) was used to assess apoptosis stage. Early apoptotic cells were defined: **i)** Annexin V^{+} Live/Dead^{-}, Late apoptotic cells were defined **ii)** Annexin V^{+} Live/Dead^{+}. *Irf5*$^{-/-}$ CD11b^{+} DCs were protected from apoptosis (**i)** $p = 0.0041$, **ii)** $p = 0.0070$).

Statistics:
Data shown are from one experiment where n = 7 mice per group
Mann-Whitney U test; ** $p \leq 0.01$

5.2.7 Single cell RNA sequencing confirms macrophages in the colonic lamina propria adopt two distinct states

10X scRNAseq analysis of macrophages revealed that fewer *Irf5*$^{-/-}$ macrophages were present in the cLP, and that macrophages adopted two states (10X Cluster 2 and 10X Cluster 5) during inflammation (Fig.4.14). Separately, SmartSeq 2 single cell analysis of WT vs global *Irf5*$^{-/-}$ macrophages (Fig.5.22, Fig.5.23) in Hh + αIL10R colitis was performed. Analysis of these data confirmed the finding that macrophages adopted two distinct states (designated scCluster 1 and scCluster 2, Fig.5.23). scCluster 1 was primarily composed of *Irf5*$^{-/-}$ macrophages, whilst scCluster 2 was composed mainly of WT macrophages (Fig.5.23). To assist with target identification, DEGs from WT vs global *Irf5*$^{-/-}$ single cell analysis and MBMC were compared (Fig.5.24). DEGs that strongly correlated between scCluster 2 and WT MBMC, and scCluster 1 and *Irf5*$^{-/-}$ MBMC are summarised in Table.5.1.

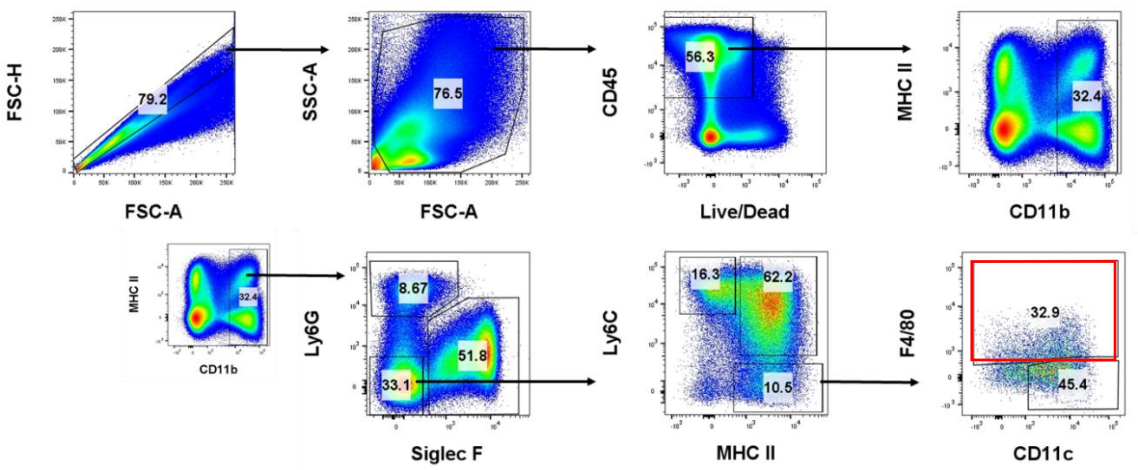

Fig.5.22: Gating strategy for sorting of macrophages for single cell RNA seq

Representative gating strategy for macrophages (red box) isolated from mouse colons for the purpose of single cell RNA seq using the SmartSeq 2 protocol. Single macrophages were sorted directly into SmartSeq 2 lysis buffer.

Macrophages: Doublets and debris were excluded, Live $CD45^+$ $CD11b^+$ $Ly6G^-$ Siglec F^- $Ly6C^-$ MHC II^+ $F4/80^+$

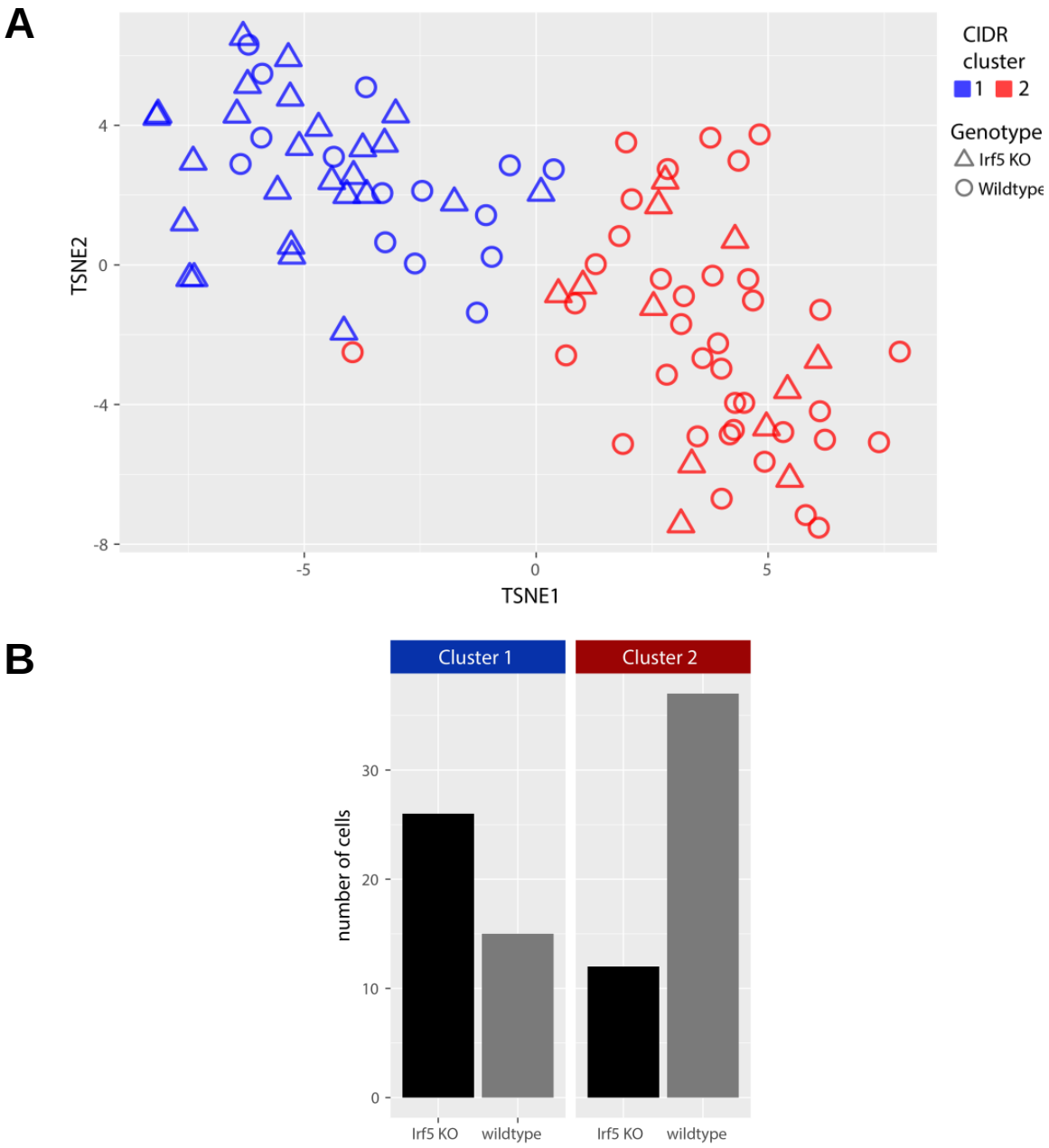

Fig.5.23: Macrophages adopt two distinct states during Hh + αIL10R colitis

Macrophages from Hh + αIL10R treated WT or *Irf5*$^{-/-}$ mice were index sorted and sequenced using the Smart-Seq 2 protocol. **A)** tSNE dimensionality reduction of differentially expressed genes followed by the use of the CIDR algorithm revealed two distinct clusters of macrophages. **B)** The number of cells in each CIDR cluster. *Irf5*$^{-/-}$ macrophages primarily fell in to Cluster 1, whilst WT cells preferentially adopted a state defined Cluster 2.
Data analysis was performed by Dr. Stephen Sansom (University of Oxford)

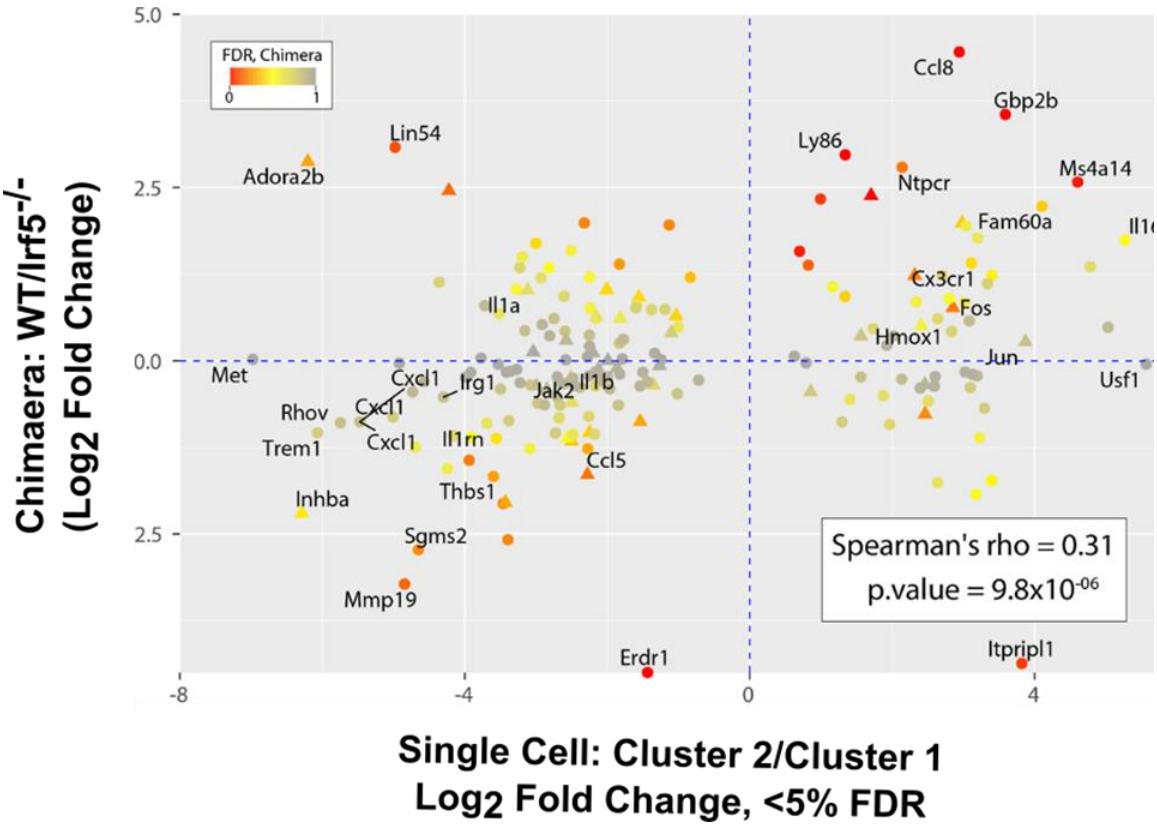

Fig.5.24: Integration of WT vs *Irf5*$^{-/-}$ single cell RNAseq with mixed bone marrow chimaera RNAseq to identify commonly differentially expressed genes at d21 Hh + αIL10R

LPLs were isolated from WT, global *Irf5*$^{-/-}$ mice, and mixed bone marrow chimaeras at d21 Hh + αIL10R colitis. For WT vs global *Irf5*$^{-/-}$, single macrophages (CD45^{+} CD11b^{+} Ly6G^{-} Siglec F^{-} Ly6C^{-} MHC II^{+} F4/80^{+}) were sorted into Smart-Seq2 lysis buffer. For mixed bone marrow chimaeras, 100 macrophages of each genotype (WT or *Irf5*$^{-/-}$) per mouse were sorted into Smart-Seq2 lysis buffer. Nextera library preparation was performed on the single cells and bulks, followed by Illumina Hiseq2000v4 sequencing. Reads were filtered and mapped to the mm10 genome. DESeq2 was used to identify differentially expressed genes.
Significantly differentially expressed genes from each dataset were plotted against each other to identify genes that were upregulated both in Cluster 2 (predominated by WT macrophages), and in WT macrophages isolated from mixed bone marrow chimaera.

Statistics:
Spearman's ρ = 0.31, p = 9.8 x 10^{-06}
Single cell: 2 age and sex matched mice were pooled for each 96 well plate of cells, 384 cells in total were collected
Mixed chimaera: N = 3 biological replicates
Data analysis was performed by Dr. Stephen Sansom (University of Oxford)

Table.5.1: Top differentially expressed genes common between mixed bone marrow chimaera and wild-type vs global *Irf5*$^{-/-}$ single cell RNAseq

		Mixed Bone Marrow Chimaera		*WT vs Irf5*$^{-/-}$ *Single Cell*	
Gene ID	**Gene Symbol**	**$Log_{(2)}$ Fold Change**	**Adjusted p-value**	**$Log_{(2)}$ Fold Change**	**Adjusted p-value**
ENSMUSG00000002458	Rgs19	-4.57	2.60E-05	2.1	0.0553
ENSMUSG00000040264	Gbp2b	-3.55	5.88E-05	3.33	0.000478
ENSMUSG00000021423	Ly86	-2.97	7.94E-05	1.56	1.70E-05
ENSMUSG00000058715	Fcer1g	-2.2	0.000115	0.75	0.00623
ENSMUSG00000037706	Cd81	-2.38	0.000682	2.05	0.000132
ENSMUSG00000009185	Ccl8	-4.46	0.00224	2.88	0.0135
ENSMUSG00000036905	C1qb	-1.4	0.0029	1.15	0.00504
ENSMUSG00000036887	C1qa	-1.6	0.00968	1.2	0.00431
ENSMUSG00000099398	Ms4a14	-2.58	0.00968	3.81	0.0031
ENSMUSG00000022587	Ly6e	-1.58	0.0115	0.78	0.00195
ENSMUSG00000030147	Clec4b1	-4.74	0.0115	2.55	0.0896
ENSMUSG00000029810	Tmem176b	-1.76	0.019	1.07	0.0178
ENSMUSG00000079547	H2-DMb1	-1.48	0.0225	0.58	0.0648
ENSMUSG00000073412	Lst1	-2.33	0.0409	0.94	0.0201
ENSMUSG00000001962	Fam50a	-2.99	0.0983	2.51	0.025
ENSMUSG00000037649	H2-DMa	-2.02	0.0994	0.95	0.00324

*Log(2) Fold Change expressed as *Irf5*$^{-/-}$/WT (Chimaera), Cluster 2/Cluster 1 (Single Cell)

5.2.8 IRF5-deficiency may provide a dominant protective effect from Hh + αIL10R colitis in mixed bone marrow chimaeras

MBMCs offered an excellent model to investigate intrinsic effects of IRF5 deficiency on myeloid cells. However, the environment in chimaeras is altered compared to WT mice due to the effects of *Irf5*$^{-/-}$ haematopoietic cells, and irradiation [341, 342]. To assess the impact of *Irf5*$^{-/-}$ in MBMC the phenotype of MBMCs at d21 of Hh + αIL10R colitis was profiled. Sections of colon and caecum were scored according to the criteria outlined in Table.2.4. Histopathological scoring revealed that colons and caeca of uninfected MBMC exhibited low colitis scores, but that these were either nearly significant, or significantly elevated when compared with uninfected MBMCs ($p = 0.0745$, Fig.5.25A, $p = 0.0495$, Fig.5.25B). Colons of MBMC infected with Hh + αIL10R were not as severely inflamed as WT mice infected with Hh + αIL10R (Fig.5.25C, $p = 0.0437$). The caeca of Hh + αIL10R MBMCs also less inflamed than those of WT mice subjected to Hh + αIL10R (Fig.5.25C, $p = 0.0078$). These differences in inflammation could be due to the effects of irradiation. Therefore, histopathological scores of Whole Bone Marrow Chimaeras (WBMCs) were compared with those of MBMC. WT WBMC infected with Hh + αIL10R displayed comparable scores to WT Hh + αIL10R treated mice (Fig.5.25C, Fig.5.25D), indicating that it was indeed *Irf5*$^{-/-}$ that protected mice from colitis. However, histopathological scoring of the WBMC and MBMC must be repeated to confirm this observation, and greater characterisation of the intestinal myeloid compartment in WBMC should also be performed to understand the contribution of irradiation vs IRF5-deficiency.

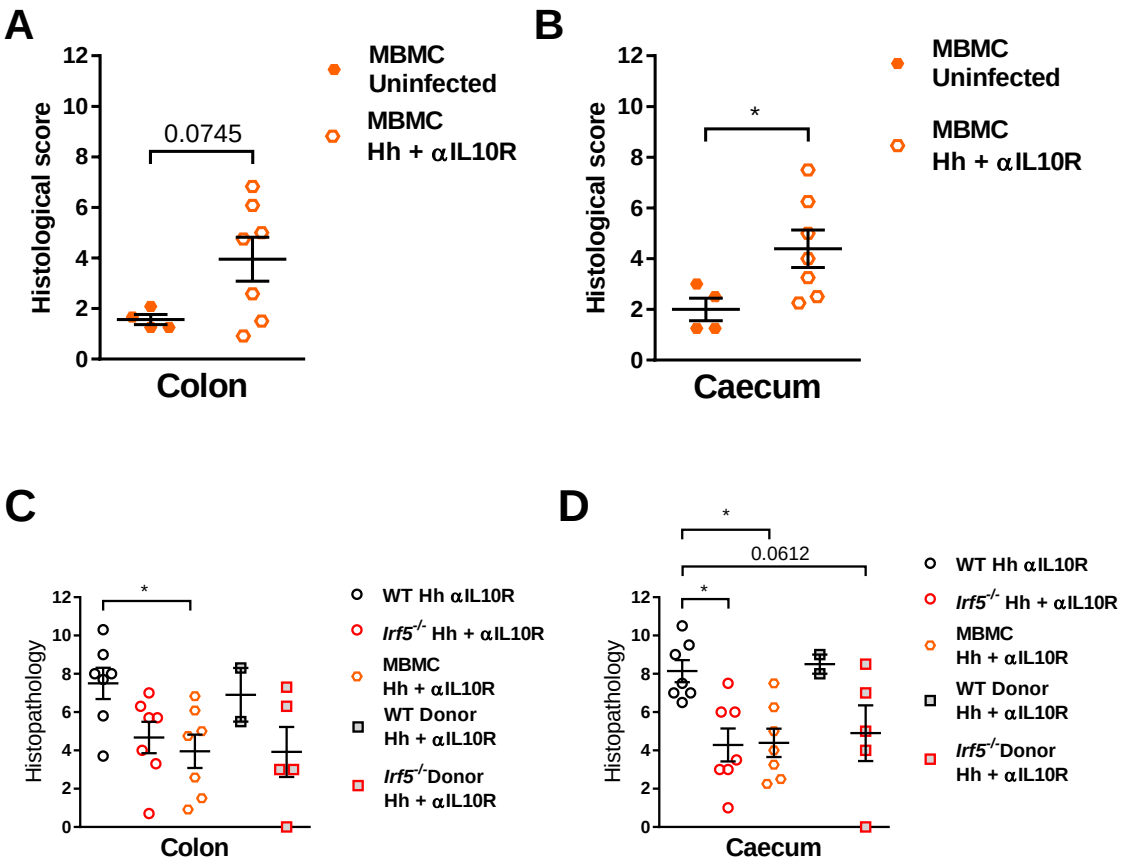

Fig.5.25: WT:*Irf5*$^{-/-}$ Mixed bone marrow chimaeras exhibit reduced inflammation in response to Hh + αIL10R treatment

Mixed bone marrow chimaeras were generated by reconstitution of lethally irradiated CD45.1^{+} WT mice with an equal mix of CD45.1^{+} WT and CD45.2^{+} *Irf5*$^{-/-}$ bone marrow. Whole Bone Marrow Chimaeras (WBMCs) were generated by reconstituting lethally irradiated CD45.1^{+} mice with either CD45.2^{+} WT or CD45.2^{+} *Irf5*$^{-/-}$ bone marrow. Mice were either housed for the duration of the study or treated with Hh + αIL10R for 21 days.
Sections were stained using H&E and coverslipped. Stained sections were then scored according to the criteria outlined in Table.2.1. **A)** Colons of Hh + αIL10R MBMCs were not significantly inflamed compared to uninfected MBMC, but approached statistical significance p = 0.0745). **B)** However, the caeca of MBMCs treated with Hh + αIL10R were more inflamed than uninfected MBMCs, **C)** MBMC colons were significantly less inflamed than Hh + αIL10R-treated WT mice (p = 0.0315). Inflammation in the colons of *Irf5*$^{-/-}$ donor WBMCs was not significantly reduced vs WT donor colitis, but approached statistical significance when compare to WT Hh + αIL10R (p = 0.0511), **D)** Caecal inflammation was also significantly reduced vs WT Hh + αIL10R infection (p = 0.0138). Inflammation in the caeca of *Irf5*$^{-/-}$ donor WBMCs was not significantly reduced vs WT donor colitis, but approached statistical significance when compare to WT Hh + αIL10R (p = 0.0612).

Statistics:
A, **B**) data are from one experiment, MBMCs. Steady state: n = 4, Hh + αIL10R: n = 7. Unpaired t test: * p ≤ 0.05
C, **D)** Data are from one experiment; Hh + αIL10R: WT n = 7, *Irf5*$^{-/-}$ n = 7, MBMC n = 7, WT donor n = 2, *Irf5*$^{-/-}$ donor n = 5. One-Way ANOVA with Tukey correction: ns = not significant, * p ≤ 0.05

5.3 Discussion

Here we demonstrate that *Irf5*$^{-/-}$ mice are protected from Hh + αIL10R colitis. Gross markers of inflammation were all dramatically reduced in *Irf5*$^{-/-}$ relative to WT (Fig.5.1, Fig.5.2, Fig.5.3, Fig.5.4). Cytokine, chemokine and T_H1 and T_H17 responses were reduced in *Irf5*$^{-/-}$ (Fig.5.6, Fig.5.7, Fig.5.8). Many of the cytokines downregulated in *Irf5*$^{-/-}$ are upregulated in IBD patients, or are IBD risk factors [22, 343-345]. IFNγ is one such cytokine. Brief IFNγ exposure promotes proliferation of epithelial cells, whilst extended IFNγ signalling promoted epithelial apoptosis in a process that synergised with TNFα exposure [346]. IFNγ acts on macrophages to promote bactericidal activity, and also stimulates transcription of IRF5 [162]. The reduction in IFNγ could be explained by the decrease in T_H1 and T_H1/T_H17 cells, but other leukocytes not explored in this chapter, such as innate lymphoid cells (ILCs), $CD8^+$ cytotoxic T cells, and NK cells, are also able to produce IFNγ [21]. This effect is unlikely to be mediated directly by IRF5, as expression of IRF5 in these leukocytes is low. TNFα is another pro-colitogenic cytokine that is downregulated in IRF5-deficient mice (Fig.5.6) [347]. TNFα exerts its effects via binding to its receptors, TNFR1 and TNFR2, which stimulate NFκB activation and inflammatory cytokine transcription [348, 349]. TNFR signalling also may cause apoptosis or necroptosis via RIPK1, leading to the release of damage associated molecular patterns (DAMPs) that may help to drive colitis [350, 351]. Blockade of membrane-bound, but not soluble TNF resulted in T cell apoptosis and ameliorated colitis in mice and humans [173, 352].

The diminished cytokine and T-effector (T_{eff}) responses in *Irf5*$^{-/-}$ Hh + αIL10R mice may result from the lack of augmentation of inflammatory cytokine production in myeloid cells (Fig.4.23, Fig.4.24).

Il1b, Il6, Tnf and Il12b mRNA were not significantly reduced in *Irf5*$^{-/-}$ mice during Hh + αIL10R colitis (Fig.5.6), but the reduction of IL1β and TNFα was confirmed at the protein level by flow cytometry; *Irf5*$^{-/-}$ MNPs in MBMC expressed less of these cytokines at steady state, and during Hh + αIL10R colitis (Fig.4.23, Fig.4.24). IL1β is known to promote

Helicobacter hepaticus colitis in IL10-deficient mice through augmentation of granulocyte recruitment, and supporting IL17 production by ILCs, but it is also able to promote a unique T_H17 phenotype characterised by a propensity for inflammatory response [307, 353].

Il6 has a dichotomous role in inflammation, able to exert pro-inflammatory effects via supporting T cell survival and myeloid cell activation, but also able to mediate anti-inflammatory effects by inhibition of TNFα and IL1β signalling, and activation of IL10 [354]. IL6 is directly regulated by IRF5, and is downregulated in *Irf5*$^{-/-}$ during Hh + αIL10R colitis (Fig.5.5) [162]. Anti-IL6 therapy showed clinical response in IBD, but increased the risk of fatality through undiagnosed intestinal abscesses or fistulae due to suppression of serum CRP levels [174]. TGFβ in combination with IL6 promotes T_H17 cell proliferation [355]. Culture of T_H17 cells in the absence of IL23 leads to a less inflammatory phenotype: T_H17 cells are able to produce the anti-inflammatory cytokine, IL10, although IL10 levels were not measured in *Irf5*$^{-/-}$ mice in Hh + αIL10R colitis [356, 357].

Il12b mRNA was upregulated in WT, but not *Irf5*$^{-/-}$ mice in colitis (fig.5.6). *Il12b* encodes IL12p40, the common subunit of IL12p70 and IL23, two key inflammatory cytokines in the pathogenesis of IBD, acting via promoting T_H1 and TH17 responses [175, 358, 359]. *Il12b* is produced by macrophages and is directly regulated by IRF5 [162]. Taken together, the data support the hypothesis that IRF5 promotes Hh + αIL10R colitis via T_H1/T_H17 responses. Separately, T_H17 responses in *Irf5*$^{-/-}$ should be investigated more closely to investigate phenotypic differences in *Irf5*$^{-/-}$ as they may be less pathogenic, indicated by the reduced frequency of IFNγ$^+$ IL17A$^+$ CD4$^+$ T cells (Fig.5.8).

Cxcl1, *Cxcl3*, *Cxcl5, Ccl3*, *Ccl4*, *Ccl5*, and perhaps *Ccl2* were increased in WT over *Irf5*$^{-/-}$ in Hh + αIL10R colitis (Fig.5.6). CCL3 and CCL4 are potent macrophage activators and trigger chemotaxis of monocytes, whilst CCL5 is also important for monocyte and eosinophil chemotaxis [360, 361]. Migration of leukocytes into sites of inflammation is a critical step in disease pathogenesis, and many of these chemokines are directly regulated by IRF5, thus this highlights another mechanism by which IRF5 could modulate

inflammation [162, 261]. Nevertheless, cytokine and chemokine mRNA measurements should be repeated with appropriately powered experiments to detect changes in their abundance. Regulation of chemokines by IRF5 at the initiation of colitis may be a key factor in explaining the increased predisposition of patients with gain of function IRF5 mutations to IBD, but may also be important for recruiting leukocytes to initiate a repair response. A timecourse following the production of chemokines during the progression of Hh + αIL10R colitis in *Irf5*$^{-/-}$ would help to ascertain if this was the case. Therefore, IRF5 may contribute to disease pathology through control of T cell and myeloid cell activity and recruitment in the inflamed cLP.

Granulocyte-Macrophage Colony Stimulating Factor (GM-CSF) was decreased in *Irf5*$^{-/-}$ in Hh + αIL10R colitis (Fig.5.6). GM-CSF, also known as CSF2, is a pleiotropic cytokine and growth factor that has a roles in neutrophil, monocyte, eosinophil, and DC survival and differentiation [362]. GM-CSF Receptor signalling results in the activation of several signalling pathways including JAK/STAT, MAPK, and PI3K, which modulate these effects on leukocytes. NFκB is activated via direct interaction of GM-CSFRα with IKKβ, and indolamine-2,3-dioxygenase via STAT3. GM-CSF is an important factor in promoting an inflammatory macrophage and eosinophil phenotypes, and elevated GM-CSF may support prolonged inflammation in this manner [129, 162]. Thus GM-CSF is able to potentiate inflammation via its effects on neutrophil and eosinophil activation, polarisation of macrophages to an inflammatory state, and support of leukopoiesis.

Despite the presence of many neutrophil chemokine mRNAs at the tissue level, and the decreased total number of leukocytes and neutrophils within the colon of IRF5 deficient mice, the proportion of neutrophils within LPLs was not affected by IRF5 deficiency (Fig.5.10A). The percentage of LPL neutrophils increased in both WT and *Irf5*$^{-/-}$ relative to controls (Fig.5.10A). IRF5 expression in neutrophils was not detected in steady state mice, and was only expressed at very low levels in inflammation (Fig.5.17B-C), therefore the similar percentage of neutrophils present may represent a compensatory shift relative to

the percentage of eosinophils (Fig.5.10B). Eosinophils were present at higher frequencies in *Irf5*$^{-/-}$ mice in Hh + αIL10R colitis relative to WT (Fig.5.10B). Despite classically being considered mediators of Type 2 immunity, eosinophils have been described as pro-inflammatory effectors in Hh + αIL10R colitis, and eosinophils counts are elevated in some cases of IBD [129, 363, 364]. Eosinophils are cytotoxic, express a wide range of TLRs and cytokines, and also express low levels of IRF5 (Fig.17C) [9]. Because eosinophils express IRF5 in WT mice, eosinophils in *Irf5*$^{-/-}$ Hh + αIL10R colitis may display a more protective phenotype. Analysis of activation markers (CD11b, Ly6G, CD63) on eosinophils did not reveal any significant changes between WT and *Irf5*$^{-/-}$ (data not shown). However, this was not a comprehensive analysis of the whole repertoire of eosinophil activation states. Further characterisation of *Irf5*$^{-/-}$ eosinophils would help to assess their contribution to inflammation.

Dendritic cells (DCs) are critical innate leukocytes, bridging innate and adaptive immunity; they are able to immediately neutralise pathogens via phagocytosis and cytokine release [43]. DCs migrate to lymphoid tissue to stimulate appropriate T_{eff} cell responses. In the cLP there are 3 well characterised populations of DCs, identified by their high surface levels of CD11c and MHC II, and differential expression of CD11b and CD103 (Fig.3.5C). However, no difference was detected in the representation of cLP DC subsets during inflammation (Fig.5.11).

In the cLP there are two main classical DC (cDC) populations, derived from FLT3L-dependent progenitor, CD11b^{+} CD103^{+}, and CD11b^{-} CD103^{+}. [330] CD11b^{+} CD103^{+} are IRF4-dependent, and can migrate to the MLN under the control of CCR7 [62, 365]. CD11b^{-} CD103^{+} are IRF8- and Batf3-dependent and do not display defective development in Csf2-deficient mice [83, 124, 366]. These two cDC subsets demonstrate different localisations within the cLP: CD11b^{+} cDCs reside deep within the villi, whereas CD11b^{-} cDC are located close to the epithelium, perhaps indicating differential roles in the control of intestinal immune responses [367, 368].

β7 integrin (a component of CD103 along with α_E) is required to give rise to tolerogenic MNPs, and CD103$^+$ DCs are required to generate T_{regs} in the cLP; αvβ8 integrin is required to activate TGFβ which signals via SMAD3 to promote T_{reg} fate [125, 369]. However, these cLP DC populations express high levels of IRF5, and IRF5 may play a role in their response to bacterial insult (Fig.5.17C). Despite this, IRF5 did not increase upon inflammation in any of the DCs tested (Fig.5.17C). Activated DCs may migrate to the MLN, and may explain why DCs do not appear to upregulate IRF5, but this was not tested [62]. IRF4 is critical for the development of CD11b$^+$ CD103$^+$ DCs, and may compete with IRF5 to determine cDC fate and function [226]. To this end, *Irf5*$^{-/-}$ cDCs and monocyte-derived DCs from cLP and MLN should be characterised in depth to uncover the function of IRF5 in these cells in colitis. *Irf5*$^{-/-}$ DC populations could be tested for their migratory capacity *in vitro* and *in vivo* by fate tracking; a protocol of tracking migrating cLP DCs using Kaede mice was described by Houston *et al.,* (2016) [370]. *Irf5*$^{-/-}$ MLN DCs should also be profiled to investigate their transcriptome, cytokine production and T cell priming capacity.

Adult cLP macrophages are thought to be exclusively derived from blood monocytes which provide a rapidly mobilised pool of effector cells in the context of inflammation [57, 371]. The spleen contains a reservoir of Ly6C^{hi} monocytes that is mobilised within 24 hours of an inflammatory stimulus [54, 372]. The percentage of P1 monocytes in the colon of Hh + αIL10R-treated mice was slightly elevated vs controls, but no difference was detected between WT and *Irf5*$^{-/-}$ (data not shown, Fig.5.12, Fig.5.13). P1 monocytes were found to express high levels of IRF5 in the bone marrow and the cLP at steady state (Fig.3.18, Fig.5.17C). Ly6C^{hi} monocytes are classically considered to give rise to pro-inflammatory effectors, able to adapt to tissue environment, and are mobilised rapidly. cLP P2 monocytes represent a differentiation intermediate between P1 monocytes and macrophages [57, 113]. P2 monocytes are Ly6C$^+$ MHC II$^+$ CD11c$^+$ and express high levels of IRF5 (Fig.5.17C). CD11c and IRF5 expression are elevated in P2 monocytes at d21 Hh + αIL10R colitis (Fig.5.18, Fig.5.17C). This expression of CD11c and IRF5 is indicative of their pro-inflammatory effector function – P2 monocytes were shown to upregulate inflammatory

mediators such as *Il1b*, *Il6*, *Il23a*, and *Nos2* in response to inflammatory challenge [124, 294, 299]. The percentage of P2 monocytes is unaffected by IRF5 deficiency at steady state (Fig.3.12), but is increased in WT at d21 Hh + αIL10R (Fig.5.13B). *Irf5*$^{-/-}$ P2 monocytes were not significantly increased in the Hh + αIL10R colitis model over controls, and were diminished relative to WT Hh + αIL10R within the total leukocyte pool, as well as in the MNP compartment (Fig.3.12, Fig.5.12B, Fig.5.13). CD11c^{+} monocytes were shown to be highly pathogenic in a mouse model of atherosclerosis, and were reduced in Apoe$^{-/-}$ *Irf5*$^{-/-}$ [278]. Here we showed that CD11c^{+} P2 monocytes and macrophages expressed more IRF5 than corresponding CD11c^{-} MNPs (Fig.5.17). There is therefore evidence to suggest that CD11c^{+} P2 monocytes may prove to be the key MNP effectors in colitis.

Macrophages are critical regulators of innate and adaptive immunity, displaying unparalleled phenotypic plasticity [373]. In the cLP, macrophages mediate tissue homeostasis through sensing luminal antigens, and clearance of apoptotic cells in an anergic fashion [59]. Macrophages can also promote T_{reg} expansion, via the production of IL10 [374]. In inflammatory situations where an insult cannot be contained, macrophages phagocytose invading pathogens, and release pro-inflammatory mediates such as cytokines, chemokines, and reactive oxygen species to mediate direct cytoxicity. cLP TNFa^{+} macrophages contribute to epithelial barrier defect [309, 375]. cLP macrophages express high levels of IRF5 (Fig.17C), but this is not upregulated in inflammation, perhaps consistent with the observation of Rivollier *et al.,* (2012), and Zigmond *et al.,* (2012) that *bona fide* macrophages remained anergic even during inflammation, and our observation that macrophages adopted two states during Hh + αIL10R colitis (Fig.4.14) [294, 299]. At steady state, ~25% of macrophages express the mannose receptor, CD206, a well-defined marker of phagocytic, tissue repair macrophages (Fig.5.13) [113, 373]. Expression of CD206 on macrophages was downregulated on WT macrophages during inflammation, but remained at steady state levels in *Irf5*$^{-/-}$, indicating that macrophages were less pro-inflammatory at d21 of Hh + αIL10R (Fig.5.14B). Colonic macrophages also express high levels of CD11c at steady state, and expression of CD11c increased in WT, but not *Irf5*$^{-/-}$,

MNPs during Hh + αIL10R (Fig.5.15). CD11c is a putative marker of inflammatory macrophages in both atherosclerosis, and Hh + αIL10R colitis; $CD11c^{+}$ macrophages promoted atherosclerosis and produce high levels of IL23 in the Hh + αIL10R model [124, 278]. However, these changes in expression of CD206 and CD11c perhaps reflect the altered colonic environment of colitic *Irf5*$^{-/-}$ mice rather than intrinsic phenotypic differences.

viSNE is a powerful analytical algorithm designed for the analysis of multiparameter flow and mass cytometry [247]. viSNE clustering of cLP MNPs (Live $CD45^{+}$ $CD11b^{+}$ $Ly6G^{-}$ Siglec F^{-}) from either Hh + αIL10R inflamed WT or *Irf5*$^{-/-}$ on the basis of Ly6C, MHC II, F4/80, and CD11c expression revealed that lRF5-deficient mice may lack a population of $CD11c^{+}$ cells of the P2 monocyte/macrophage gate (Fig.5.15). The gating strategy presented in this thesis lacks CX_3CR1 needed for accurate discrimination of the entire monocyte waterfall described by Bain and colleagues [57]. Therefore the macrophages identified on the basis of $Ly6C^{lo}$ and $F4/80^{+}$ can in fact arise from Bain and colleague's inflammatory P3 macrophage state. Interrogation of this population in WT mice revealed that the missing population expressed high levels of MHC II and IRF5, and were $CD11c^{+}$, and $Ly6C^{int}$, falling to the MHC II^{hi} side of the P2 monocyte gate (Fig.5.15). Due to the high levels of IRF5 found in this population, and its expression of MHC II, and CD11c, it is possible that this population of macrophages represents a highly pro-inflammatory, pro-colitogenic population of MNPs. Sorting of this population on the basis of $CD11c^{hi}$ $CD206^{-}$ phenotype followed by RNAseq or qPCR of appropriate markers would reveal whether this population does indeed represent a highly inflammatory macrophage state, and may also reveal novel markers that could be used to therapeutically deplete it in IBD patients.

The T_H17 polarising cytokine, IL23 is a valid therapeutic target for CD/UC [175, 376]. $CD11c^{+}$ MNPs were demonstrated to be key cells expressing pathogenic IL-23 in Hh + αIL10R colitis. In fact, the loss of IL23 driven by CD11c-Cre was able to rescue the disease pathology [124]. IRF5 directly regulates IL23 production in human monocyte-derived macrophages, and in murine GM-BMDMs [162, 217], thus providing a possible link

between IRF5 and expression of CD11c and IL23 by MNPs. IL23 appears to be key in the early stages of Hh + αIL10R colitis, as *Il23a* mRNA expression was found to be highest between d4-d7 in $CD11c^{+}$ MNPs, and declined thereafter, this may explain why we observed no difference in *Il23a* mRNA expression at the peak of inflammation between WT and $Irf5^{-/-}$ animals. However, $Irf5^{-/-}$ animals expressed significantly lower levels of *Il12b* mRNA (Fig.5.5), which remain expressed throughout disease (unpublished data from the Powrie lab).

Analysis of 10X RNAseq of cLP MNPs was instrumental in positioning IRF5 as a fate-deciding transcription factor for monocytes (Chapter.4). However, 10X RNAseq suffered from a lack of sensitivity: only ~1000 genes were detected per single cell. To analyse how IRF5 may be promoting colitis, small bulk RNAseq (100 cells) of MBMC macrophages was performed to assess IRF5-specific transcriptomic defects (Fig.5.21). The differentially expressed genes were integrated with existing scRNAseq (Fig.4.18, Fig.5.23), and IRF5 ChIPseq (Fig.4.19) to refine a list of candidate targets for validation (Table.5.2, Fig.5.24). Integration of the genomic datasets allowed the identification of novel IRF5-regulated targets e.g. *Cd81*, *Setdb1*, *Thbs1*.

Thbs1 (Thrombospondin-1) is a TGFβ pathway gene that was upregulated in $Irf5^{-/-}$ macrophages in MBMC and higher in scCluster1 (Fig.5.24). *Thbs1* was shown to have anti-inflammatory effects in monocyte and macrophage cell lines, downregulated IL1β production in macrophages, and induced IL10 production and lung injury resolution in a mouse model [377-379]. These effects point towards Thrombospondin-1 being a potential therapeutic target of interest in IBD, perhaps as a recombinant therapy.

$Irf5^{-/-}$ macrophages also expressed higher levels of *Setdb1*, a histone methyltransferase, which results in the repression of inflammatory cytokines (Fig.5.23) [380]. IRF5 was also shown to negatively regulate *Setdb1* [242]. *Il1rn*, encoding Interleukin 1 Receptor antagonist (IL1RN) was higher in $Irf5^{-/-}$ in MBMC and global $Irf5^{-/-}$ (Fig.5.24), IL1RN is a potent anti-inflammatory cytokine which could also explain the protective phenotype [381].

Repression of anti-inflammatory genes may be another pathway by which IRF5 promotes inflammation.

The tetraspanin, CD81 (TAPA-1), is an important molecule involved in exosome release, and formation of the immunological synapse in MHC II-mediated activation of T cells [382]. MHC II expression was also higher on WT macrophages relative to *Irf5*$^{-/-}$ (Fig.4.25), which may help to compound this function. Interestingly, *in vitro* data suggest that CD81 prevents macrophage proliferation, and may negatively regulate inflammatory responses [383, 384]. *Cd81* was directly regulated by IRF5 in *in vitro* macrophages, identified by an IRF5 ChIP peak (Fig.4.19), and was consistently elevated in WT macrophages vs *Irf5*$^{-/-}$ macrophages across genomic datasets. CD81 expression increased as monocytes differentiated into macrophages, and expression was upregulated at d14 of Hh + αIL10R colitis in WT mice (Fig.4.20). CD81 was also described as a component of a module of genes that comprise a cLP-resident macrophage signature [138]. These studies indicate that one method by which IRF5 directs inflammation is via activation of T_H responses through CD81-support of immunological synapses, and that CD81 is a marker of mature intestinal macrophages.

WT macrophages expressed higher levels of *Ccl8*, and *Ccl9*, chemokines that recruit monocytes, and DCs (Fig.5.24) [63, 145]. CCL8 was found to be elevated in the explant culture supernatants of WT Hh + αIL10R treated mice vs *Irf5*$^{-/-}$ Hh + αIL10R (Fig.4.21). Chemokines, including CCL8 and CCL9 were non-specifically increased in IBD patients, but may still be relevant to disease pathogenesis [145, 385]. Reads mapping to *Il12b* were also found to be elevated in WT macrophages in MBMC As IL12p40 is a component of both IL12p70, and IL23 which support pathogenic T_H1 and T_H17 responses, this may help to explain the increased inflammation observed in WT Hh + αIL10R colitis [175, 358, 376].

Clearly, *Irf5*$^{-/-}$ mice are protected from Hh + αIL10R colitis; *Irf5*$^{-/-}$ mice display reduced accumulation of pro-inflammatory P2 monocytes, and diminished T_H1/T_H17 responses. However, only a snapshot of the disease pathogenesis is characterised here. Following a timecourse of disease progression would reveal how changes in leukocyte infiltrate take

shape, and this could be correlated with the tissue levels of cytokines and chemokines to build up a picture of how IRF5 mediates its pro-inflammatory effects over time.

Intriguingly, *Irf5*$^{-/-}$ leukocytes in MBMC may exert a dominant effect on the course of inflammation, as histopathological scores were reduced in MBMCs compared to WT WBMCs. This experiment must be repeated including the appropriate controls of total bone marrow reconstitution to confirm this finding. Alternatively Performing Hh + αIL10R colitis in *Irf5*$^{+/-}$ heterozygotes and using wild type and *Irf5*$^{-/-}$ homozygotes as controls may also address this issue. Should the observation prove valid, it would mean that modulation of IRF5 in inflammatory disorders would become an attractive therapy.

5.4 Conclusion

In summary, *Irf5*$^{-/-}$ mice are protected from Hh + αIL10R colitis based on a histological perspective. *Irf5*$^{-/-}$ display reduced numbers of all leukocytes infiltrating the colon during Hh + αIL10R, and have increased percentages of eosinophils, but reduced proportions of P2 monocytes and T_H1/T_H17 cells in the cLP. P2 monocytes upregulate IRF5 expression in inflammation and a subpopulation of CD11c$^+$ P2 monocyte/macrophages, based on viSNE analysis, may represent a highly pro-inflammatory, pro-colitic group of mononuclear phagocytes. Further investigation of this population is required, but targeting it may provide therapeutic benefit for IBD patients. Macrophages in colitic *Irf5*$^{-/-}$ mice expressed more of the anti-inflammatory marker, CD206, and less of the pro-inflammatory marker, CD11c. Levels of IBD-associated cytokines and chemokines that are regulated by IRF5 in GM-BMDMs are also reduced in *Irf5*$^{-/-}$, which may contribute to the establishment and propagation of disease. Taken together, the data point towards IRF5$^+$ monocytes and macrophages being key players in the pathogenesis of Hh + αIL10R colitis. Integration of genomic datasets has uncovered several attractive IRF5-dependent factors that mark resident and inflammatory macrophages in the colon, and must be validated. Strikingly, mixed bone marrow chimaeras were protected from colitis in a similar manner to global *Irf5*$^-$

$^{-/-}$ mice despite the reduced accumulation of *Irf5*$^{-/-}$ MNPs in the lamina propria of chimaeras. This suggests that partial blockade of IRF5 may have therapeutic benefit.

6 Discussion

6.1 Summary of results

Genome wide association studies identified gain of function mutations in the IRF5 promoter that are associated with several inflammatory disorders, including Inflammatory Bowel Disease (IBD) [237, 245]. Krausgruber *et al.,* (2011) demonstrated that Interferon Regulatory Factor (IRF) 5 is a transcription factor that defines an inflammatory macrophage phenotype by promoting the transcription of pro-inflammatory cytokines such as TNFα, IL1β, IL6, IL12, and IL23, and repressing transcription of the potent anti-inflammatory mediators IL10, and TGFβ, [162]. Therefore, before this thesis was conducted, it was hypothesised that IRF5 promoted intestinal inflammation through mediation of T_H1/T_H17 response.

To investigate the role of IRF5 in the Colonic Lamina Propria (cLP), WT and *Irf5*$^{-/-}$ mice were characterised. Steady state WT mice exhibited increased frequencies of cLP macrophages, but IRF5 deficiency did not appear to result in a haematopoietic defect of macrophage development in bone marrow. (Chapter.3)

IRF5 promoted the accumulation of WT monocytes in the cLP of Mixed Bone Marrow Chimaeras (MBMCs), in a process possibly dependent on the CCL2/CCR2 axis (Fig.4.10), factors that are known to be important for the reconstitution of the intestinal macrophage compartment [57, 112].

A novel function of IRF5 to commit monocytes to a macrophage fate in tissue during inflammation was identified using RNA sequencing methods (Figs.4.14, Fig.4.15, Fig.4.19, and Fig.5.24). Whilst loss of IRF5 appeared to promote the differentiation into moDCs which are dependent on IRF4 (Fig.4.15) [386]. This process may be due to loss of competition for IRF binding sites, and engagement of an AHR-dependent program (Fig.6.1) [132, 226]. In inflammation, IRF5 may exert a brake on terminal or tolerogenic macrophage differentiation; holding macrophages in a pro-inflammatory monocyte-macrophage

intermediate state that upregulates IRF5 expression, is highly bactericidal, positive for CD11c, and produces high quantities of IL23 in the early stages of colitis (Fig.4.14, Fig.5.16, and Fig.5.18) [124, 294].

Irf5$^{-/-}$ mice were protected from Hh + αIL10R colitis, and the absence of IRF5 in less than half of myeloid cells in colon in MBMC was sufficient to exert a dominant protective effect from Hh + αIL10R colitis (Fig.5.25). The identification of factors (*Il1rn*, and *Setdb1*, Fig.5.24) that may mediate this protective effect, were repressed by IRF5 and may be viable as novel therapies for inflammatory conditions. However, further investigation of these molecules is required to validate their potential.

A discussion of how these results fit within current literature will now be conducted, with a look towards future work and perspectives provided.

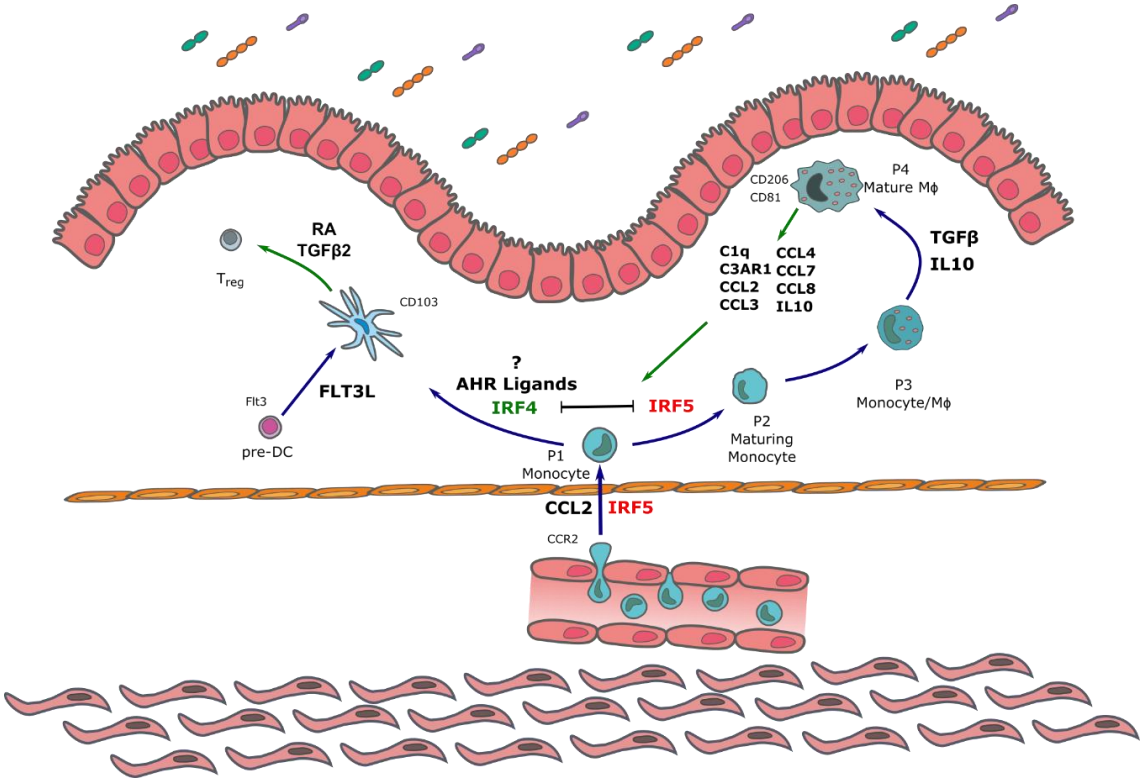

Fig.6.1: Schematic of the hypothesised role of IRF5 in the steady state colonic lamina propria

IRF5 promotes the accumulation of P1 monocytes in a CCL2/CCR2 manner. IRF5 promotes differentiation of cLP1 P1 monocytes is macrophage fate. P1 monocytes transition into P2/P3 monocyte/macrophages with inflammatory potential supported by IRF5. The final stages of monocyte-macrophage transition are supported by IL10 and TGFβ, giving rise to anergic, tissue-resident macrophages. Tissue resident macrophages sample luminal antigen, and produce high quantities of chemokines to recruit leukocytes, including monocytes, to the cLP, and to maintain intestinal homeostasis.
Intestinal cDCs were originally thought to derive from FLT3L-dependent pre-DC precursors that migrated to the cLP via the blood and differentiated in response to microenvironmental signals. More recently, it has been established that a subpopulation of monocytes may differentiate into cDCs under specific environmental conditions. In the absence of IRF5, or in the presence of abundant Aryl Hydrocarbon Receptor (AHR) ligands, the differentiation of monocyte-derived DCs may be favoured in an IRF4-dependent process to generate $CD11b^{+}$ DCs. A recent study indicated that cLP cDCs gain CD103 after exposure to TGFβ.

AHR: Aryl Hydrocarbon Receptor, CCL: CC-motif ligand, FLT3: Fms-Like Tyrosine Kinase 3, IL: Interleukin, IL1RA (IL1 Receptor Antagonist), IRF: Interferon Regulatory Factor, RA: Retinoic Acid, TGFβ: Transforming Growth Factor Beta,

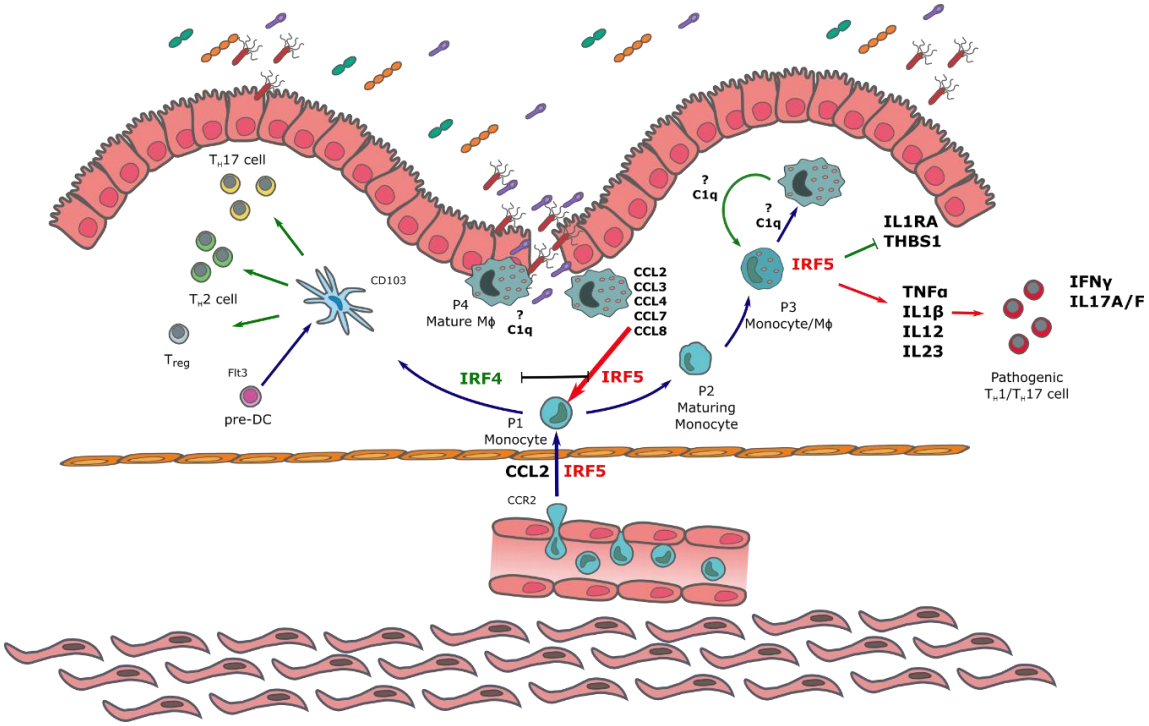

Fig.6.2: Schematic of proposed role of IRF5 during Hh + αIL10R colitis

Macrophages sense intestinal barrier breach and respond by phagocytosing invading bacteria and producing chemokines. IRF5$^+$ Ly6C^{hi} blood monocytes are better able to respond to chemokines such as CCL2 and are preferentially recruited to the cLP. IRF5 expression is increased by PRR signalling after contact with bacterial antigens, promoting maturation to the inflammatory P2/P3 monocyte-macrophage. P2/P3 monocyte-macrophages produce high quantities of pro-inflammatory mediators such as TNFα, IL1β, IL12, and IL23, which support pathogenic T_H1/T_H17 cell expansion. P4 tissue-resident macrophages produce C1q, which opsonises Ig-coated pathogens, but also signals via the gC1qR to promote P2/P3 maturation to a resolving P4 macrophage phenotype.

A subpopulation of Ly6C^{hi} monocytes may be able to differentiate into CD11b$^+$ SIRPα$^+$ cDCs. In the absence of IRF5, IRF4 is able to modulate its transcriptional program unimpeded, thereby promoting SIRPα$^+$ cDC fate. CD11b$^+$ DCs are specialised in promoting T_H2 and T_H17 responses, which antagonise T_H1/T_H17 responses, and may be protective in the Hh + αIL10R model.

CCL: CC-motif ligand, FLT3: Fms-Like Tyrosine Kinase 3, IL: Interleukin, IL1RA (IL1 Receptor Antagonist)

6.2 IRF5 promotes macrophage fate of Ly6C^{hi} monocytes in the colonic lamina propria

The role of IRF5 in the polarisation of macrophages and the pathogenesis of various diseases is well established in the literature [56, 162, 239, 243, 244, 261, 387]. However, the intrinsic function of IRF5 in the development of the MNP system was not addressed. The work described in this thesis made use of the intestine as a model system to study the role of IRF5 in the development and function of monocyte-derived macrophages. The accumulation of macrophages was found to be deficient in the *Irf5*$^{-/-}$ Colonic Lamina Propria (cLP) (Fig.3.12), but no major defect was observed when GM-CSF differentiated Bone Marrow-Derived Macrophages (GM-BMDM) were cultured (Fig.3.17, Fig.3.19).

The ontogeny of macrophages and classical Dendritic Cells (cDCs) in the cLP has been debated in recent years. Confusion may have arisen by mis-identification of macrophages and DCs due to shared markers and functions [113, 121, 294, 388]. Adult mouse cLP tissue-resident macrophages were demonstrated to be derived exclusively from blood Ly6C^{hi} monocytes, and the final stages of macrophage maturation were at least partially dependent on IL10, and TGFβ [57, 138, 139]. Evidently, the tissue-specific signals and transcription factors that promote macrophage fate in the cLP are poorly defined. The ontogeny of cLP cDCs is also unclear, due to the sharing of functional markers between macrophages and DCs [61, 64, 126]. cLP DCs were originally considered to be derived from FLT3L-dependent pre-DCs that migrated from the blood, indeed Bogunovic *et al*., (2009), and Varol *et al*., (2009) concluded that CD11b^{-} CD103^{+} ID2-dependent DCs originated from circulating pre-DCs [64, 388]. However, their conclusion that CD11b^{+} DCs were replenished from circulating monocytes was clouded by the inability to distinguish between CD11b^{+} CD103^{-} DCs and intestinal macrophages. The adoptive transfer of CDPs resulted in the generation of CD11b^{+} CD103^{+} intestinal DCs, but did not identify CD11b^{+} CD103^{-} DCs, pointing to monocyte origin of CD11b^{+} CD103^{+} DCs, but it has come to light that CD11b^{+} CD103^{+} DCs may represent terminal differentiation of the CD11b^{+} DC lineage,

and so the transitory CD11b^{+} CD103^{-} phase may have been missed at the time of analysis [64, 128]. More recently, however, the possibility that cDCs may be replenished from a pre-committed *Cd209a*$^{+}$ monocyte pool has been established [46, 55, 132].

The use of Mixed Bone Marrow Chimaeras (MBMCs), combined with next-generation sequencing techniques was instrumental in defining the role of IRF5 in the process of monocyte accumulation and promotion of macrophage fate in the cLP (Fig.4.14, Fig.15). IRF5 promoted the accumulation of WT MNPs in the cLP of MBMCs (Fig.4.7, Fig.4.8, Fig.4.11), but no difference was detected in the reconstitution of progenitors or myeloid populations in blood or bone marrow at steady state (Fig.4.2-Fig.4.6). However, at d21 Hh + αIL10R colitis, *Irf5*$^{-/-}$ myeloid populations were overrepresented in the bone marrow (Fig.4.4B). This may indicate a bone marrow retention issue in *Irf5*$^{-/-}$, possibly due to the reduced expression of CCR2, and decreased responsiveness to CCL2 (Fig.4.10), which may also affect entry of monocytes to the cLP [57, 239, 294, 301]. However, it is unlikely that this explains the full phenotype, as the chemokines required for monocyte entry to the colon are poorly defined and other CCRs e.g. CCR1 are likely to be involved in the recruitment of monocytes to the cLP [239, 298].

10X RNA sequencing (10Xseq) was used to uncover the heterogeneity of CX$_3$CR1^{+} Mononuclear Phagocytes (MNPs) in the cLP (Fig.4.13) (10xgenomics.com). Analysis of the 10X clusters revealed that more DCs (identified by reads mapped to DC markers e.g. *Napsa*, *Cd209a*, *Irf8*, *Cd24a*, *Batf3*, and *Id2*) were of *Irf5*$^{-/-}$ origin, and macrophages were preferentially derived from WT (Fig.4.14, Fig.4.15). Monocle analysis visualised the development of monocytes to macrophages (mo-macrophages) or monocyte-derived DCs (moDCs) in pseudotime (Fig.4.17) [212]. Recent papers suggest that DCs could be replenished from a subset of Ly6C^{+} monocytes, thus monocle analysis would be able to identify the trajectory of moDC transition in the cLP. Indeed, analysis of *Irf5*$^{-/-}$ MNPs in isolation, resulted in the identification of monocyte-DC intermediates (data not shown). Yet, when WT and *Irf5*$^{-/-}$ MNPs were analysed together, these intermediates were masked,

possibly by the similarity of WT and *Irf5*$^{-/-}$ Ly6C^{hi} monocytes and the abundance of the WT mo-macrophage transition state (Fig.4.15, Fig.4.17). Re-clustering of 10X data, to increase the number of clusters, may help elucidate transitory stages and help to uncover IRF5-regulated genes that promote macrophage fate at the expense of moDCs. The microenvironmental signals that drive the process of monocyte-macrophage or monocyte-DC transition are poorly defined. However, an *in vitro* system demonstrated that monocytes preferentially differentiated into macrophages in response to M-CSF, IL4 and TNFα in a process dependant on the transcription factor, MafB [132]. Indeed, MafB was a positive marker for 10X Clusters 1, 2, and 5, corresponding to Ly6C^{hi} monocytes, monocyte-macrophage transition, and tissue-resident macrophages respectively (data not shown). *Cd209a*, a marker of Ly6C^{hi} monocytes with moDC differentiation potential, was also a positive marker of Clusters 0 and 1, expressed in ~30% of Cluster 0, but only ~8% of Cluster 1. Cluster 0 (defined by expression of *Napsa*, *Cd7*, *Cd209a*, and the MHC molecules *H2-DMb2*, and *H2-Oa*, indicating DC lineage) is related to Cluster 1, but not Cluster 2 in pseudotime, and possibly represents a moDC intermediate (Fig.4.14). Cluster 0 was preferentially occupied by *Irf5*$^{-/-}$ (Fig.4.15). Goudot *et al.,* also recognised that IRF4 was a critical transcription factor in the DC fate of monocytes [132, 386]. IRF4 and IRF5 were shown to compete for binding to Myeloid Differentiation primary response 88 (MyD88) after TLR4 ligation [389], and IRF4 negatively regulates the transcription of IRF5 and IRF5 targets [226]. In the absence of IRF5, IRF4 may be able to dominate the fate choice of monocytes, thus explaining the increased predisposition to DC fate in *Irf5*$^{-/-}$. Therefore, in steady state WT mice, stochastic factors may influence the relative abundance of DC- and macrophage-primed Ly6C^{hi} monocytes, which are stimulated by microenvironmental cues such as aryl hydrocarbon receptor and TLR ligands. Single cell sorting of WT and *Irf5*$^{-/-}$ blood monocyte populations, followed by transcriptional profiling could be used to uncover the relative frequencies and IRF5-dependent transcriptional programs of DC-committed and macrophage-committed monocytes.

6.3 Consequences of preferential macrophage fate in IRF5$^+$ monocytes

Inflammatory monocyte-macrophage intermediates are well described as pro-inflammatory effector cells in multiple inflammatory disorders [338, 390-392]. The ability of intestinal macrophages to produce inflammatory cytokines such as IL1β, IL12, and IL23 is well documented [121, 294, 299, 338], as is the ability of these cytokines to support pathogenic T cell responses [259, 307, 353]. It was determined that both monocytes and macrophages from the inflamed mucosa of WT Hh + αIL10R treated mice expressed higher levels of inflammatory cytokines, TNFα, IL1β, and IL12 (Fig.4.18, and Fig.4.23), and Chemokines, *Ccl3*, *Ccl4*, *Ccl5*, *Ccl7*, *Ccl8*, *Ccl9*, *Cxcl12*, and *Cxcl16* (Fig.4.14, Fig.4.18). IRF5 promotes macrophage fate commitment of Ly6C^{hi} monocytes, but terminal differentiation to a tissue-resident phenotype is blocked. IRF5 activation may therefore be a key determinant of this differentiation block and thus promote colitis.

Intestinal cDCs fall into two major subgroups, XCR1$^+$, BATF3- and IRF8-dependent cDC1a, and SIRPα$^+$ IRF4-dependent cDC2s [43]. XCR1$^+$ cDCs are important for CD4$^+$ and CD8$^+$ T cell priming via retinoic acid and antigen presentation [393, 394] . XCR1$^+$ cDC1s are specialised in cross presentation of antigen at sites of inflammation, but can also migrate to the Mesenteric Lymph Nodes (MLN) in a CCR7-dependent manner to prime naïve T cells [370]. BATF3-dependent DCs were shown to express IL12 to support T_H1 generation at steady state and during inflammation [395-398]. BATF3-dependent cDCs are also required for the optimal generation of inducible T regulatory cells (iT_{reg}) in MLN following oral administration of protein antigens, possibly due to the secretion of Retinoic Acid (RA), and the activation of TGFβ2 [393, 399].

SIRPα$^+$ cDCs have roles in T_H17 polarisation, and T_H2 induction, indicating that they may be important for host protection from intestinal parasites [365]. It is also possible that they can mediate pro-inflammatory responses, as production of IL23 in response to *Citrobacter*

rodentium was required to protect mice via the induction of Type 3 Innate Lymphoid Cells (ILC3)-IL22-epithelial repair pathways [400].

The Hh + αIL10R model is dependent on the cytokine IL23 which promotes pathogenic T_H1/T_H17 and ILC3 expansion. IL23 is produced in abundance by $CD11c^+$ $CD64^+$ cells of the monocyte/macrophage lineage, but not by intestinal DCs [124]. Although *Il23a* was not detected in myeloid cells using 10X and SmartSeq2, this may be due to the time of measurement: *Il23a* expression peaks between d3 and d5 of Hh + αIL10R colitis, and declines thereafter, whereas the data presented in this thesis were measured at d21 of Hh + αIL10R colitis (Unpublished observations, Powrie lab). However we detected a higher level of *Il12b* (the second subunit of the IL23 protein) expression in macrophages at this point (Fig.4.18). Macrophages are also important for the presentation of antigens to DCs and activated T cells, and therefore the initiation and potentiation of immune responses [331, 332]. Therefore, the increased propensity of monocytes to differentiate into DCs may help to explain why *Irf5*$^{-/-}$ mice are protected from colitis as discussed in Chapter.4

6.4 Exosomes in inflammation and macrophages

As reported in Chapter.4, WT 10X Cluster 2 monocyte/macrophages were enriched for transcripts encoding the tetraspanins CD9, CD63, and CD81, and reads mapping to CD53 and CD151 were also identified in Cluster 2 (data not shown). Meanwhile, CD81 was consistently upregulated in WT MNPs compared to *Irf5*$^{-/-}$, both *in vitro* and *in vivo* (Fig.3.20, Fig.4.18, Fig.5.24), and was associated with an *in vitro* IRF5 ChIP peak, indicating direct regulation by IRF5 (Fig.4.19). These tetraspanins are critical components of exosomes, and have roles in monocyte migration and cell fusion, intracellular protein trafficking, and TNFα regulation [401-404]. Exosomes are highly conserved secretory membrane vesicles (cytosol contained in a lipid bilayer) that are recognised as an important mechanism of inter-cell communication, containing proteins and RNA in their cytoplasm [372, 405, 406]. Exosomes recovered from the serum of mice with experimental Acute Myocardial Infarction

(AMI), could subsequently induce the mobilisation of splenic monocytes from naïve mice after transfer to recipient mice [372]. The micro-RNA content of these AMI exosomes was enriched for transcripts associated with “positive regulation of cell adhesion” and “regulation of cell motility” indicating that exosomes primed monocyte function before tissue entry [372]. Interestingly, exosomes can be transferred between species and Kingdoms: Grape-derived exosome-like nanoparticles could be transferred orally, and were taken up by cLP cells and could downregulate inflammatory responses to DSS colitis, possibly via the promotion of $LGR5^{+}$ stem cell proliferation and epithelial repair [407].

CD9 may have a role in MHC II trafficking to the plasma membrane, as $CD9^{-/-}$ GM-CSF-differentiated monocyte-derived macrophages were less able to stimulate naïve T cells [408]. In IBD, exosomes released by T_{regs} can suppress inflammation in a RAB27A and RAB27B dependent manner. A global knockout of either of these two proteins resulted in more severe DSS colitis [409]. However, double knockout of RAB27A and RAB27B resulted in protection from colitis, indicating that exosome release may be able to promote colitis, but the cellular targets were not identified [409].

Macrophages were shown to release inflammatory exosomes in response to *Escherichia coli* (strain LF82) infection; macrophages treated with these exosomes subsequently adopted a pro-inflammatory phenotype [410]. Exosomes have been shown to have both pro- and anti-inflammatory roles in experimental colitis, but despite this, are poorly characterised in the IBD setting [411]. Monocyte/macrophage exosome release may be important in the pathogenesis of colitis, conditional deletion of each of the tetraspanins CD9, CD53, CD63, and CD81 may be able to elucidate the role of exosomes in colitis.

6.5 C1q and macrophages

Schridde *et al.,* 2017 showed that C1q production is a marker of mature macrophages in the cLP, and production of all three C1q components was impaired in $Irf5^{-/-}$ macrophages

during colitis in MBMCs, and global *Irf5*$^{-/-}$ (Fig.4.19, Fig.5.24) [138]. C1q is a component of the complement system, an innate mechanism that enhances the immune response to pathogens. The C1q complex is composed of six A chains (C1qA), six B chains (C1qB), and six C chains (C1qC). Each chain contains an N-terminal globular region and a C-terminal collagen-like region. These regions can bind their respective receptors, the gC1qR, and cC1qR with differing immune responses. C1q can bind Ig molecules, including IgG, and IgM, complexed with antigen in the Classical pathway of complement activation [412].

Protective roles for C1q have been described in atherosclerosis models, whilst C1q deficiency can result in Systemic Lupus Erythematosus in humans, likely due to impaired clearance of apoptotic material and free nucleic acid antigens [413]. A recent study reported that C1q could promote liver injury repair via promoting an IL4Rα-dependent M2 macrophage phenotype and tissue repair [414]. However, the role of C1q in the intestinal immune system is unclear.

C1q$^{-/-}$ mice experienced more severe DSS colitis, and died 2.5 days after cessation of DSS treatment, with elevated serum LPS indicating epithelial barrier repair and bacterial handling dysfunction [415, 416]. Tissue-resident macrophages are known to be required for epithelial homeostasis, tissue repair, and bacterial handling, therefore impairments to differentiation and production of C1q by tissue resident macrophages may promote colitis in this manner. This would be contrast with the results presented that *Irf5*$^{-/-}$ produce less C1q (Fig.4.19, Fig.5.24). Despite the decreased expression of C1q, *Irf5*$^{-/-}$ macrophages preferentially adopt an M2-spectrum phenotype, associated with resolution of inflammation, therefore IRF5-deficiency may in fact compensate for the loss of C1q . C1q may also be required for optimal tissue repair, and may therefore represent IRF5 beginning a tissue repair program after injury.

C1q was shown to promote the adhesion of monocytes to endothelial cells, and also impaired the differentiation of human peripheral blood monocytes into moDCs via binding

to the gC1qR [417, 418]. Some studies reported that C1q downregulated the inflammatory function of macrophages, and promoted a phagocytic phenotype dependent on Mer, AMPK, and PPARs, whist others reported increased macrophage pro-inflammatory function [418-422].

Although the complement system was discovered several decades ago, the role of C1q in cLP macrophages is unclear, and *C1qa*, *b*, and $c^{fl/fl}$ mice have not been generated. Therefore, the studies conducted thus far utilise global $C1q^{-/-}$ mice which are unable to capture temporal effects of C1q. Taken together, the results of the study indicate a complex interaction between C1q and IRF5 which demands further investigation over the natural course of Hh + αIL10R immunopathology, including the resolution phase. It may be possible that IRF5-driven production of C1q is essential for modulating the adaptation of newly recruited monocytes towards a less inflammatory tissue repair phenotype to mediate return to homeostasis and epithelial barrier function in the cLP at the resolution phase.

6.6 Future perspectives

Inflammatory Bowel Disease (IBD) is a group of inflammatory conditions including Ulcerative Colitis (UC). Therapy for IBD aims to control active inflammation, and maintain patients in remission. Traditional therapies, such as glucocorticosteroids, are hampered by adverse side effects, while the use of biological therapies has radically improved IBD prognosis for many patients, approximately 30-40% of patients do not respond to anti-TNF (αTNF) treatment and around half of treated patients become refractory to αTNF [174]. In addition, biologics-based therapies carry a high economic cost for health services. The success of kinase inhibitors in the treatment of cancer, coupled with a greater understanding of inflammatory signalling cascades, led to kinase inhibitors taking centre stage in the pursuit for new anti-inflammatory agents. For example, the JAK kinase inhibitor, Tofacitinib, has proved effective in treating moderate-severe UC [423].

The transcription factor, IRF5, orchestrates pro-inflammatory macrophage function and is a risk factor for IBD. The data presented in this thesis demonstrate a role for IRF5 in promoting intestinal inflammation in a mouse model of colitis through the accumulation of Ly6C^{hi} monocytes in the cLP, and the promotion of an inflammatory macrophage state. WT:*Irf5*$^{-/-}$ MBMCs were also protected from experimental colitis demonstrating that IRF5 plays a key role in modulating intestinal inflammation, potentially by suppressing anti-inflammatory factors. The data indicate that these factors may exert a dominant effect in the Hh + αIL10R model, thus even partial modulation of IRF5 activity may be a viable therapeutic strategy in the treatment of inflammatory disorders. However, at present there are no clinic-fit inhibitors of IRF5 function.

6.7 Conclusion

In conclusion, IRF5 may promote colitis by facilitating the accumulation and differentiation of pro-inflammatory monocyte-macrophage intermediates that coexpress CD11c and IL23, and repressing CD11b^{+} DC fate. The accumulation of pro-inflammatory effectors may be driven by IRF5^{+} tissue-resident macrophages that highly express monocyte chemokines (*Ccl2*, *Ccl3*, *Ccl4*, *Ccl8*), but are avidly phagocytic. As colitis progresses and the bacterial insult is resolved, IRF5 may also promote the production of factors (C1q) that may promote the differentiation of tissue-repair resident macrophages from newly entered P1 monocytes (Fig.6.2), thereby promoting return to homeostasis

7 References

1. Laskin, D.L., et al., *Macrophages and Tissue Injury: Agents of Defense or Destruction?* Annual Review of Pharmacology and Toxicology, 2011. **51**(1): p. 267-288.
2. Smolen, J.S., et al., *Rheumatoid arthritis.* Nature Reviews Disease Primers, 2018. **4**: p. 18001.
3. Harms Pritchard, G. and M. Pepper, *Memory B cell heterogeneity: Remembrance of things past.* Journal of Leukocyte Biology, 2018. **103**(2): p. 269-274.
4. Fujimura, K.E., et al., *Role of the gut microbiota in defining human health.* Expert review of anti-infective therapy, 2010. **8**(4): p. 435-454.
5. Okumura, R. and K. Takeda, *Roles of intestinal epithelial cells in the maintenance of gut homeostasis.* Experimental &Amp; Molecular Medicine, 2017. **49**: p. e338.
6. Osińska, I., K. Popko, and U. Demkow, *Perforin: an important player in immune response.* Central-European Journal of Immunology, 2014. **39**(1): p. 109-115.
7. Stone, K.D., C. Prussin, and D.D. Metcalfe, *IgE, Mast Cells, Basophils, and Eosinophils.* The Journal of allergy and clinical immunology, 2010. **125**(2 Suppl 2): p. S73-S80.
8. Moon, T.C., et al., *Advances in mast cell biology: new understanding of heterogeneity and function.* Mucosal Immunol, 2009. **3**(2): p. 111-128.
9. Rosenberg, H.F., K.D. Dyer, and P.S. Foster, *Eosinophils: changing perspectives in health and disease.* Nature reviews. Immunology, 2013. **13**(1): p. 9-22.
10. Kolaczkowska, E. and P. Kubes, *Neutrophil recruitment and function in health and inflammation.* Nature Reviews Immunology, 2013. **13**: p. 159.
11. Brinkmann, V., et al., *Neutrophil Extracellular Traps Kill Bacteria.* Science, 2004. **303**(5663): p. 1532.
12. Vivier, E., et al., *Functions of natural killer cells.* Nature Immunology, 2008. **9**: p. 503.
13. Eberl, G., et al., *Innate lymphoid cells: A new paradigm in immunology.* Science, 2015. **348**(6237).
14. Serafini, N., C.A.J. Vosshenrich, and J.P. Di Santo, *Transcriptional regulation of innate lymphoid cell fate.* Nat Rev Immunol, 2015. **15**(7): p. 415-428.
15. Spits, H., et al., *Innate lymphoid cells [mdash] a proposal for uniform nomenclature.* Nat Rev Immunol, 2013. **13**(2): p. 145-149.
16. Lai, A.Y. and M. Kondo, *T and B lymphocyte differentiation from hematopoietic stem cell.* Seminars in immunology, 2008. **20**(4): p. 207-212.
17. Klein, L., et al., *Antigen presentation in the thymus for positive selection and central tolerance induction.* Nat Rev Immunol, 2009. **9**(12): p. 833-844.
18. Gellert, M., *V(D)J Recombination: RAG Proteins, Repair Factors, and Regulation.* Annual Review of Biochemistry, 2002. **71**(1): p. 101-132.
19. Busch, D.H. and E.G. Pamer, *T Cell Affinity Maturation by Selective Expansion during Infection.* The Journal of Experimental Medicine, 1999. **189**(4): p. 701-710.
20. Farber, D.L., N.A. Yudanin, and N.P. Restifo, *Human memory T cells: generation, compartmentalization and homeostasis.* Nature reviews. Immunology, 2014. **14**(1): p. 24-35.
21. Maloy, K.J. and F. Powrie, *Intestinal homeostasis and its breakdown in inflammatory bowel disease.* Nature, 2011. **474**: p. 298-306.
22. Neurath, M.F., *Cytokines in inflammatory bowel disease.* Nat Rev Immunol, 2014. **14**(5): p. 329-342.
23. Kapsenberg, M.L., *Dendritic-cell control of pathogen-driven T-cell polarization.* Nat Rev Immunol, 2003. **3**(12): p. 984-993.
24. Bachmann, M.F., et al., *Distinct Roles for LFA-1 and CD28 during Activation of Naive T Cells: Adhesion versus Costimulation.* Immunity, 1997. **7**(4): p. 549-557.
25. Matsuoka, K., et al., *T-bet upregulation and subsequent interleukin 12 stimulation are essential for induction of Th1 mediated immunopathology in Crohn's disease.* Gut, 2004. **53**(9): p. 1303-1308.
26. Mosmann, T.R. and R.L. Coffman, *TH1 and TH2 Cells: Different Patterns of Lymphokine Secretion Lead to Different Functional Properties.* Annual Review of Immunology, 1989. **7**(1): p. 145-173.
27. Anuradha, R., et al., *Parasite-Antigen Driven Expansion of IL-5− and IL-5+ Th2 Human Subpopulations in Lymphatic Filariasis and Their Differential Dependence on IL-10 and TGFβ.* PLOS Neglected Tropical Diseases, 2014. **8**(1): p. e2658.

28. Ivanov, I.I., et al., *The Orphan Nuclear Receptor RORγt Directs the Differentiation Program of Proinflammatory IL-17+ T Helper Cells.* Cell, 2006. **126**(6): p. 1121-1133.
29. Harrington, L.E., et al., *Interleukin 17-producing CD4+ effector T cells develop via a lineage distinct from the T helper type 1 and 2 lineages.* Nat Immunol, 2005. **6**(11): p. 1123-1132.
30. Sakaguchi, S., et al., *Regulatory T Cells and Immune Tolerance.* Cell, 2008. **133**(5): p. 775-787.
31. Andersen, M.H., et al., *Cytotoxic T Cells.* Journal of Investigative Dermatology, 2006. **126**(1): p. 32-41.
32. Kaech, S.M. and W. Cui, *Transcriptional control of effector and memory CD8+ T cell differentiation.* Nat Rev Immunol, 2012. **12**(11): p. 749-761.
33. Wardemann, H., et al., *Predominant Autoantibody Production by Early Human B Cell Precursors.* Science, 2003. **301**(5638): p. 1374.
34. Gonzalez, S.F., et al., *Trafficking of B Cell Antigen in Lymph Nodes.* Annual Review of Immunology, 2011. **29**(1): p. 215-233.
35. Treanor, B., *B-cell receptor: from resting state to activate.* Immunology, 2012. **136**(1): p. 21-27.
36. Maddaly, R., et al., *Receptors and signaling mechanisms for B-lymphocyte activation, proliferation and differentiation – Insights from both in vivo and in vitro approaches.* FEBS Letters, 2010. **584**(24): p. 4883-4894.
37. Nutt, S.L., et al., *The generation of antibody-secreting plasma cells.* Nat Rev Immunol, 2015. **15**(3): p. 160-171.
38. Bortnick, A. and D. Allman, *What Is and What Should Always Have Been: Long-lived Plasma cells Induced by T-cell Independent Antigens.* Journal of immunology (Baltimore, Md. : 1950), 2013. **190**(12): p. 5913-5918.
39. Stavnezer, J., J.E.J. Guikema, and C.E. Schrader, *Mechanism and Regulation of Class Switch Recombination.* Annual review of immunology, 2008. **26**: p. 261-292.
40. Metchnikoff, I., *Memoirs: Researches on the Intracellular Digestion of Invertebrates.* Q J Microsc Sci, 1884. **2**(93): p. 89–111.
41. van Furth, R., et al., *The mononuclear phagocyte system: a new classification of macrophages, monocytes, and their precursor cells.* Bulletin of the World Health Organization, 1972. **46**(6): p. 845-852.
42. Amit, I., D.R. Winter, and S. Jung, *The role of the local environment and epigenetics in shaping macrophage identity and their effect on tissue homeostasis.* Nat Immunol, 2016. **17**(1): p. 18-25.
43. Joeris, T., et al., *Diversity and functions of intestinal mononuclear phagocytes.* Mucosal Immunol, 2017. **10**(4): p. 845-864.
44. Ziegler-Heitbrock, L., et al., *Nomenclature of monocytes and dendritic cells in blood.* Blood, 2010. **116**(16): p. e74.
45. Ingersoll, M.A., et al., *Comparison of gene expression profiles between human and mouse monocyte subsets.* Blood, 2010. **115**(3): p. e10-e19.
46. Mildner, A., et al., *Genomic Characterization of Murine Monocytes Reveals C/EBPb Transcription Factor Dependence of Ly6C- Cells.* Immunity, 2017. **46**(5): p. 849-862.e7.
47. Patel, A.A., et al., *The fate and lifespan of human monocyte subsets in steady state and systemic inflammation.* The Journal of Experimental Medicine, 2017. **214**(7): p. 1913-1923.
48. Yona, S., et al., *Fate mapping reveals origins and dynamics of monocytes and tissue macrophages under homeostasis.* Immunity, 2013. **38**(1): p. 79-91.
49. Hettinger, J., et al., *Origin of monocytes and macrophages in a committed progenitor.* Nat Immunol, 2013. **14**(8): p. 821-830.
50. Geissmann, F., S. Jung, and D.R. Littman, *Blood Monocytes Consist of Two Principal Subsets with Distinct Migratory Properties.* Immunity, 2003. **19**(1): p. 71-82.
51. Rodero, M.P., et al., *Immune surveillance of the lung by migrating tissue monocytes.* eLife, 2015. **4**: p. e07847.
52. Auffray, C., et al., *Monitoring of Blood Vessels and Tissues by a Population of Monocytes with Patrolling Behavior.* Science, 2007. **317**(5838): p. 666.
53. Cros, J., et al., *Human CD14(dim) Monocytes Patrol and Sense Nucleic Acids and Viruses via TLR7 and TLR8 Receptors.* Immunity, 2010. **33**(3): p. 375-386.
54. Swirski, F.K., et al., *Identification of Splenic Reservoir Monocytes and Their Deployment to Inflammatory Sites.* Science, 2009. **325**(5940): p. 612.
55. Menezes, S., et al., *The Heterogeneity of Ly6Chi Monocytes Controls Their Differentiation into iNOS+ Macrophages or Monocyte-Derived Dendritic Cells.* Immunity, 2016. **45**(6): p. 1205-1218.

56. Byrne, A.J., et al., *A critical role for IRF5 in regulating allergic airway inflammation.* Mucosal immunology, 2017. **10**(3): p. 716-726.
57. Bain, C.C., et al., *Constant replenishment from circulating monocytes maintains the macrophage pool in the intestine of adult mice.* Nat Immunol, 2014. **15**(10): p. 929-937.
58. Lavin, Y., et al., *Tissue-Resident Macrophage Enhancer Landscapes Are Shaped by the Local Microenvironment.* Cell, 2014. **159**(6): p. 1312-1326.
59. Smythies, L.E., et al., *Human intestinal macrophages display profound inflammatory anergy despite avid phagocytic and bacteriocidal activity.* Journal of Clinical Investigation, 2005. **115**(1): p. 66-75.
60. Hedl, M., et al., *Chronic stimulation of Nod2 mediates tolerance to bacterial products.* Proceedings of the National Academy of Sciences of the United States of America, 2007. **104**(49): p. 19440-19445.
61. Tamoutounour, S., et al., *CD64 distinguishes macrophages from dendritic cells in the gut and reveals the Th1-inducing role of mesenteric lymph node macrophages during colitis.* European Journal of Immunology, 2012. **42**(12): p. 3150-3166.
62. Jang, M.H., et al., *CCR7 Is Critically Important for Migration of Dendritic Cells in Intestinal Lamina Propria to Mesenteric Lymph Nodes.* The Journal of Immunology, 2006. **176**(2): p. 803.
63. Zhao, X., et al., *CCL9 Is Secreted by the Follicle-Associated Epithelium and Recruits Dome Region Peyer's Patch CD11b⁺ Dendritic Cells.* The Journal of Immunology, 2003. **171**(6): p. 2797.
64. Bogunovic, M., et al., *Origin of the Lamina Propria Dendritic Cell Network.* Immunity, 2009. **31**(3): p. 513-525.
65. Worbs, T., S.I. Hammerschmidt, and R. Forster, *Dendritic cell migration in health and disease.* Nat Rev Immunol, 2017. **17**(1): p. 30-48.
66. Swiecki, M. and M. Colonna, *The multifaceted biology of plasmacytoid dendritic cells.* Nat Rev Immunol, 2015. **15**(8): p. 471-485.
67. Kondo, M., et al., *Biology of Hematopoietic Stem Cells and Progenitors: Implications for Clinical Application.* Annual Review of Immunology, 2003. **21**(1): p. 759-806.
68. Leuschner, F., et al., *Rapid monocyte kinetics in acute myocardial infarction are sustained by extramedullary monocytopoiesis.* The Journal of Experimental Medicine, 2012. **209**(1): p. 123-137.
69. Griseri, T., et al., *Dysregulated Hematopoietic Stem and Progenitor Cell Activity Promotes Interleukin-23-Driven Chronic Intestinal Inflammation.* Immunity, 2012. **37**(6): p. 1116-1129.
70. Wilson, A., et al., *c-Myc controls the balance between hematopoietic stem cell self-renewal and differentiation.* Genes & Development, 2004. **18**(22): p. 2747-2763.
71. Heidt, T., et al., *Chronic variable stress activates hematopoietic stem cells.* Nature medicine, 2014. **20**(7): p. 754-758.
72. Manz, M.G. and S. Boettcher, *Emergency granulopoiesis.* Nat Rev Immunol, 2014. **14**(5): p. 302-314.
73. Monticelli, S. and G. Natoli, *Transcriptional determination and functional specificity of myeloid cells: making sense of diversity.* Nat Rev Immunol, 2017. **17**(10): p. 595-607.
74. Rosenfeld, M.G., V.V. Lunyak, and C.K. Glass, *Sensors and signals: a coactivator/corepressor/epigenetic code for integrating signal-dependent programs of transcriptional response.* Genes & Development, 2006. **20**(11): p. 1405-1428.
75. Wang, S., et al., *Mechanistic Heterogeneity in Site Recognition by the Structurally Homologous DNA-binding Domains of the ETS Family Transcription Factors Ets-1 and PU.1.* The Journal of Biological Chemistry, 2014. **289**(31): p. 21605-21616.
76. Natoli, G., *Maintaining Cell Identity through Global Control of Genomic Organization.* Immunity, 2010. **33**(1): p. 12-24.
77. Nerlov, C. and T. Graf, *PU.1 induces myeloid lineage commitment in multipotent hematopoietic progenitors.* Genes & Development, 1998. **12**(15): p. 2403-2412.
78. Olson, M.C., et al., *PU.1 is not essential for early myeloid gene expression but is required for terminal myeloid differentiation.* Immunity, 1995. **3**(6): p. 703-714.
79. Barozzi, I., et al., *Co-regulation of transcription factor binding and nucleosome occupancy through DNA features of mammalian enhancers.* Molecular cell, 2014. **54**(5): p. 844-857.
80. Ghisletti, S., et al., *Identification and Characterization of Enhancers Controlling the Inflammatory Gene Expression Program in Macrophages.* Immunity, 2010. **32**(3): p. 317-328.

81. Heinz, S., et al., *Simple combinations of lineage-determining transcription factors prime cis-regulatory elements required for macrophage and B cell identities.* Molecular cell, 2010. **38**(4): p. 576-589.
82. Udalova, I.A., A. Mantovani, and M. Feldmann, *Macrophage heterogeneity in the context of rheumatoid arthritis.* Nat Rev Rheumatol, 2016. **12**(8): p. 472-485.
83. Becker, A.M., et al., *IRF-8 extinguishes neutrophil production and promotes dendritic cell lineage commitment in both myeloid and lymphoid mouse progenitors.* Blood, 2012. **119**(9): p. 2003-2012.
84. Kurotaki, D., et al., *IRF8 inhibits C/EBPα activity to restrain mononuclear phagocyte progenitors from differentiating into neutrophils.* Nature Communications, 2014. **5**: p. 4978.
85. Laslo, P., et al., *Multilineage Transcriptional Priming and Determination of Alternate Hematopoietic Cell Fates.* Cell, 2006. **126**(4): p. 755-766.
86. Schlitzer, A., et al., *Identification of cDC1- and cDC2-committed DC progenitors reveals early lineage priming at the common DC progenitor stage in the bone marrow.* Nat Immunol, 2015. **16**(7): p. 718-728.
87. Sathe, P., et al., *Lymphoid Tissue and Plasmacytoid Dendritic Cells and Macrophages Do Not Share a Common Macrophage-Dendritic Cell-Restricted Progenitor.* Immunity, 2014. **41**(1): p. 104-115.
88. Nutt, S.L., et al., *Dynamic regulation of PU.1 expression in multipotent hematopoietic progenitors.* The Journal of Experimental Medicine, 2005. **201**(2): p. 221.
89. Cabezas-Wallscheid, N., et al., *Identification of Regulatory Networks in HSCs and Their Immediate Progeny via Integrated Proteome, Transcriptome, and DNA Methylome Analysis.* Cell Stem Cell, 2014. **15**(4): p. 507-522.
90. Guo, G., et al., *Mapping Cellular Hierarchy by Single-Cell Analysis of the Cell Surface Repertoire.* Cell Stem Cell, 2013. **13**(4): p. 492-505.
91. Pronk, C.J.H., et al., *Elucidation of the Phenotypic, Functional, and Molecular Topography of a Myeloerythroid Progenitor Cell Hierarchy.* Cell Stem Cell, 2007. **1**(4): p. 428-442.
92. Jaitin, D.A., et al., *Massively parallel single cell RNA-Seq for marker-free decomposition of tissues into cell types.* Science (New York, N.Y.), 2014. **343**(6172): p. 776-779.
93. van Furth, R. and Z.A. Cohn, *THE ORIGIN AND KINETICS OF MONONUCLEAR PHAGOCYTES.* The Journal of Experimental Medicine, 1968. **128**(3): p. 415-435.
94. Gentek, R., K. Molawi, and M.H. Sieweke, *Tissue macrophage identity and self-renewal.* Immunological Reviews, 2014. **262**(1): p. 56-73.
95. Ajami, B., et al., *Local self-renewal can sustain CNS microglia maintenance and function throughout adult life.* Nat Neurosci, 2007. **10**(12): p. 1538-1543.
96. Parwaresch, M.R. and H.H. Wacker, *Origin and Kinetics of Resident Tissue Macrophages.* Cell Proliferation, 1984. **17**(1): p. 25-39.
97. Van Furth, R. and M. Diesselhoff-den Dulk, *Dual origin of mouse spleen macrophages.* The Journal of Experimental Medicine, 1984. **160**(5): p. 1273-1283.
98. Naito, M., K. Takahashi, and S. Nishikawa, *Development, differentiation, and maturation of macrophages in the fetal mouse liver.* Journal of Leukocyte Biology, 1990. **48**(1): p. 27-37.
99. Cline, M.J. and M.A.S. Moore, *Embryonic Origin of the Mouse Macrophage.* Blood, 1972. **39**(6): p. 842.
100. Palis, J., *Primitive and definitive erythropoiesis in mammals.* Frontiers in Physiology, 2014. **5**: p. 3.
101. Tober, J., K.E. McGrath, and J. Palis, *Primitive erythropoiesis and megakaryopoiesis in the yolk sac are independent of c-myb.* Blood, 2008. **111**(5): p. 2636-2639.
102. Schulz, C., et al., *A Lineage of Myeloid Cells Independent of Myb and Hematopoietic Stem Cells.* Science, 2012. **336**(6077): p. 86.
103. Ginhoux, F., et al., *Fate Mapping Analysis Reveals That Adult Microglia Derive from Primitive Macrophages.* Science (New York, N.Y.), 2010. **330**(6005): p. 841-845.
104. Frame, J.M., K.E. McGrath, and J. Palis, *Erythro-Myeloid Progenitors: "definitive" hematopoiesis in the conceptus prior to the emergence of hematopoietic stem cells.* Blood cells, molecules & diseases, 2013. **51**(4): p. 10.1016/j.bcmd.2013.09.006.
105. Hoeffel, G., et al., *C-Myb(+) Erythro-Myeloid Progenitor-Derived Fetal Monocytes Give Rise to Adult Tissue-Resident Macrophages.* Immunity, 2015. **42**(4): p. 665-678.
106. Cumano, A. and I. Godin, *Ontogeny of the Hematopoietic System.* Annual Review of Immunology, 2007. **25**(1): p. 745-785.
107. Naito, M., et al., *Development, differentiation, and phenotypic heterogeneity of murine tissue macrophages.* Journal of Leukocyte Biology, 1996. **59**(2): p. 133-8.

108. Hoeffel, G., et al., *Adult Langerhans cells derive predominantly from embryonic fetal liver monocytes with a minor contribution of yolk sac–derived macrophages.* The Journal of Experimental Medicine, 2012. **209**(6): p. 1167-1181.
109. van de Laar, L., et al., *Yolk Sac Macrophages, Fetal Liver, and Adult Monocytes Can Colonize an Empty Niche and Develop into Functional Tissue-Resident Macrophages.* Immunity, 2016. **44**(4): p. 755-768.
110. Ginhoux, F. and M. Guilliams, *Tissue-Resident Macrophage Ontogeny and Homeostasis.* Immunity, 2016. **44**(3): p. 439-449.
111. Scott, C.L., et al., *Bone marrow-derived monocytes give rise to self-renewing and fully differentiated Kupffer cells.* 2016. **7**: p. 10321.
112. Tamoutounour, S., et al., *Origins and Functional Specialization of Macrophages and of Conventional and Monocyte-Derived Dendritic Cells in Mouse Skin.* Immunity, 2013. **39**(5): p. 925-938.
113. Bain, C.C., et al., *Resident and pro-inflammatory macrophages in the colon represent alternative context-dependent fates of the same Ly6Chi monocyte precursors.* Mucosal Immunol, 2013. **6**(3): p. 498-510.
114. Epelman, S., et al., *Embryonic and adult-derived resident cardiac macrophages are maintained through distinct mechanisms at steady state and during inflammation.* Immunity, 2014. **40**(1): p. 91-104.
115. Molawi, K., et al., *Progressive replacement of embryo-derived cardiac macrophages with age.* The Journal of Experimental Medicine, 2014. **211**(11): p. 2151.
116. Maranduba, C.M., et al., *Intestinal Microbiota as Modulators of the Immune System and Neuroimmune System: Impact on the Host Health and Homeostasis.* Journal of Immunology Research, 2015. **2015**: p. 931574.
117. Jandhyala, S.M., et al., *Role of the normal gut microbiota.* World Journal of Gastroenterology : WJG, 2015. **21**(29): p. 8787-8803.
118. Mowat, A.M. and W.W. Agace, *Regional specialization within the intestinal immune system.* Nat Rev Immunol, 2014. **14**(10): p. 667-685.
119. Meuret, G., A. Bitzi, and B. Hammer, *Macrophage turnover in Crohn's disease and ulcerative colitis.* Gastroenterology, 1978. **74**(3): p. 501-503.
120. Bune, A.J., et al., *Mice lacking tartrate-resistant acid phosphatase (Acp 5) have disordered macrophage inflammatory responses and reduced clearance of the pathogen, Staphylococcus aureus.* Immunology, 2001. **102**(1): p. 103-113.
121. Niess, J.H., et al., *CX₃CR1-Mediated Dendritic Cell Access to the Intestinal Lumen and Bacterial Clearance.* Science, 2005. **307**(5707): p. 254-258.
122. Schulz, O., et al., *Intestinal CD103(+), but not CX3CR1(+), antigen sampling cells migrate in lymph and serve classical dendritic cell functions.* The Journal of Experimental Medicine, 2009. **206**(13): p. 3101-3114.
123. Cosin-Roger, J., et al., *The activation of Wnt signaling by a STAT6-dependent macrophage phenotype promotes mucosal repair in murine IBD.* Mucosal Immunol, 2016. **9**(4): p. 986-998.
124. Arnold, I.C., et al., *CD11c+ monocyte/macrophages promote chronic Helicobacter hepaticus-induced intestinal inflammation through the production of IL-23.* Mucosal Immunol, 2016. **9**(2): p. 352-363.
125. Worthington, J.J., et al., *Intestinal Dendritic Cells Specialize to Activate Transforming Growth Factor-β and Induce Foxp3(+) Regulatory T Cells via Integrin αvβ8.* Gastroenterology, 2011. **141**(5): p. 1802-1812.
126. Cerovic, V., et al., *Intestinal macrophages and dendritic cells: what's the difference?* Trends in Immunology, 2014. **35**(6): p. 270-277.
127. Persson, E.K., et al., *Dendritic cell subsets in the intestinal lamina propria: Ontogeny and function.* European Journal of Immunology, 2013. **43**(12): p. 3098-3107.
128. Bain, C.C., et al., *TGFβR signalling controls CD103+CD11b+ dendritic cell development in the intestine.* Nature Communications, 2017. **8**(1): p. 620.
129. Griseri, T., et al., *Granulocyte Macrophage Colony-Stimulating Factor-Activated Eosinophils Promote Interleukin-23 Driven Chronic Colitis.* Immunity, 2015. **43**(1): p. 187-199.
130. Guilliams, M., et al., *Unsupervised High-Dimensional Analysis Aligns Dendritic Cells across Tissues and Species.* Immunity, 2016. **45**(3): p. 669-684.
131. Schraml, Barbara U., et al., *Genetic Tracing via DNGR-1 Expression History Defines Dendritic Cells as a Hematopoietic Lineage.* Cell, 2013. **154**(4): p. 843-858.
132. Goudot, C., et al., *Aryl Hydrocarbon Receptor Controls Monocyte Differentiation into Dendritic Cells versus Macrophages.* Immunity, 2017. **47**(3): p. 582-596.e6.

133. Helft, J., et al., *Dendritic Cell Lineage Potential in Human Early Hematopoietic Progenitors.* Cell Reports, 2017. **20**(3): p. 529-537.
134. Laffont, S., K.R.R. Siddiqui, and F. Powrie, *Intestinal inflammation abrogates the tolerogenic properties of MLN CD103+ dendritic cells.* European Journal of Immunology, 2010. **40**(7): p. 1877-1883.
135. Lombardi, V.C. and S.F. Khaiboullina, *Plasmacytoid dendritic cells of the gut: Relevance to immunity and pathology.* Clinical immunology (Orlando, Fla.), 2014. **153**(1): p. 165-177.
136. Geissmann, F., et al., *Development of monocytes, macrophages and dendritic cells.* Science (New York, N.Y.), 2010. **327**(5966): p. 656-661.
137. Bain, C.C., et al., *Long-lived self-renewing bone marrow-derived macrophages displace embryo-derived cells to inhabit adult serous cavities.* 2016. **7**: p. ncomms11852.
138. Schridde, A., et al., *Tissue-specific differentiation of colonic macrophages requires TGF[beta] receptor-mediated signaling.* Mucosal Immunol, 2017.
139. Zigmond, E., et al., *Macrophage-Restricted Interleukin-10 Receptor Deficiency, but Not IL-10 Deficiency, Causes Severe Spontaneous Colitis.* Immunity, 2014. **40**(5): p. 720-733.
140. Denning, T.L., et al., *Functional specializations of intestinal dendritic cell and macrophage subsets that control T(H)-17 and T regulatory responses is dependent on the T:APC ratio, source of mouse strain and regional localization.* Journal of immunology (Baltimore, Md. : 1950), 2011. **187**(2): p. 733-747.
141. Nagashima, R., et al., *Lamina propria macrophages in the human gastrointestinal mucosa: their distribution, immunohistological phenotype, and function.* Journal of Histochemistry & Cytochemistry, 1996. **44**(7): p. 721-731.
142. Hume, D.A., et al., *Immunohistochemical characterisation of macrophages in human liver and gastrointestinal tract: expression of CD4, HLA-DR, OKM1, and the mature macrophage marker 25F9 in normal and diseased tissue.* Journal of Leukocyte Biology, 1987. **42**(5): p. 474-84.
143. Rugtveit, J., et al., *Increased macrophage subset in inflammatory bowel disease: apparent recruitment from peripheral blood monocytes.* Gut, 1994. **35**(5): p. 669-674.
144. Carlsen, H.S., et al., *The proportion of CD40+ mucosal macrophages is increased in inflammatory bowel disease whereas CD40 ligand (CD154)+ T cells are relatively decreased, suggesting differential modulation of these costimulatory molecules in human gut lamina propria.* Inflammatory Bowel Diseases, 2006. **12**(11): p. 1013-1024.
145. Asano, K., et al., *Intestinal CD169+ macrophages initiate mucosal inflammation by secreting CCL8 that recruits inflammatory monocytes.* Nature Communications, 2015. **6**: p. 7802.
146. Takada, Y., et al., *Monocyte Chemoattractant Protein-1 Contributes to Gut Homeostasis and Intestinal Inflammation by Composition of IL-10–Producing Regulatory Macrophage Subset.* The Journal of Immunology, 2010. **184**(5): p. 2671.
147. Mortha, A., et al., *Microbiota-Dependent Crosstalk Between Macrophages and ILC3 Promotes Intestinal Homeostasis.* Science, 2014. **343**(6178).
148. Fox, J.G., et al., *Helicobacter hepaticus sp. nov., a microaerophilic bacterium isolated from livers and intestinal mucosal scrapings from mice.* Journal of Clinical Microbiology, 1994. **32**(5): p. 1238-1245.
149. Shames, B., et al., *Identification of widespread Helicobacter hepaticus infection in feces in commercial mouse colonies by culture and PCR assay.* Journal of Clinical Microbiology, 1995. **33**(11): p. 2968-2972.
150. Kullberg, M.C., et al., *Helicobacter hepaticus Triggers Colitis in Specific-Pathogen-Free Interleukin-10 (IL-10)-Deficient Mice through an IL-12- and Gamma Interferon-Dependent Mechanism.* Infection and Immunity, 1998. **66**(11): p. 5157-5166.
151. Chow, J. and S.K. Mazmanian, *A Pathobiont of the Microbiota Balances Host Colonization and Intestinal Inflammation.* Cell host & microbe, 2010. **7**(4): p. 265-276.
152. Kullberg, M.C., et al., *Bacteria-triggered CD4(+) T Regulatory Cells Suppress Helicobacter hepaticus–induced Colitis.* The Journal of Experimental Medicine, 2002. **196**(4): p. 505-515.
153. Kullberg, M.C., et al., *IL-23 plays a key role in Helicobacter hepaticus–induced T cell–dependent colitis.* The Journal of Experimental Medicine, 2006. **203**(11): p. 2485-2494.
154. Franke, A., et al., *Sequence variants in IL10, ARPC2 and multiple other loci contribute to ulcerative colitis susceptibility.* Nat Genet, 2008. **40**(11): p. 1319-23.
155. Begue, B., et al., *Defective IL10 signaling defining a subgroup of patients with inflammatory bowel disease.* Am J Gastroenterol, 2011. **106**(8): p. 1544-55.
156. Amre, D.K., et al., *Interleukin 10 (IL-10) gene variants and susceptibility for paediatric onset Crohn's disease.* Aliment Pharmacol Ther, 2009. **29**(9): p. 1025-31.

157. Dieleman, L.A., et al., *Helicobacter hepaticus Does Not Induce or Potentiate Colitis in Interleukin-10-Deficient Mice.* Infection and Immunity, 2000. **68**(9): p. 5107-5113.
158. Pearson, C., et al., *ILC3 GM-CSF production and mobilisation orchestrate acute intestinal inflammation.* eLife, 2016. **5**: p. e10066.
159. Danne, C., et al., *A Large Polysaccharide Produced by Helicobacter hepaticus Induces an Anti-inflammatory Gene Signature in Macrophages.* Cell Host & Microbe, 2017. **22**(6): p. 733-745.e5.
160. Maloy, K.J., et al., *CD4(+)CD25(+) T(R) Cells Suppress Innate Immune Pathology Through Cytokine-dependent Mechanisms.* The Journal of Experimental Medicine, 2003. **197**(1): p. 111-119.
161. Kullberg, M.C., et al., *Induction of colitis by a CD4(+) T cell clone specific for a bacterial epitope.* Proceedings of the National Academy of Sciences of the United States of America, 2003. **100**(26): p. 15830-15835.
162. Krausgruber, T., et al., *IRF5 promotes inflammatory macrophage polarization and TH1-TH17 responses.* Nat Immunol, 2011. **12**(3): p. 231-238.
163. Saliba, David G., et al., *IRF5:RelA Interaction Targets Inflammatory Genes in Macrophages.* Cell Reports, 2014. **8**(5): p. 1308-1317.
164. Peyrin-Biroulet, L., et al., *Defining Disease Severity in Inflammatory Bowel Diseases: Current and Future Directions.* Clinical Gastroenterology and Hepatology, 2016. **14**(3): p. 348-354.e17.
165. Hueber, W., et al., *Secukinumab, a human anti-IL-17A monoclonal antibody, for moderate to severe Crohn's disease: unexpected results of a randomised, double-blind placebo-controlled trial.* Gut, 2012. **61**(12): p. 1693-1700.
166. Neurath, M.F. and S.P.L. Travis, *Mucosal healing in inflammatory bowel diseases: a systematic review.* Gut, 2012. **61**(11): p. 1619.
167. Marchal-Bressenot, A., et al., *Development and validation of the Nancy histological index for UC.* Gut, 2016. **66**(1): p. 43.
168. Atreya, R. and M.F. Neurath, *Chemokines in Inflammatory Bowel Diseases.* Digestive Diseases, 2010. **28**(3): p. 386-394.
169. Walsham, N.E. and R.A. Sherwood, *Fecal calprotectin in inflammatory bowel disease.* Clinical and Experimental Gastroenterology, 2016. **9**: p. 21-29.
170. Mee, A.S., J. Berney, and D.P. Jewell, *Monocytes in inflammatory bowel disease: absolute monocyte counts.* Journal of Clinical Pathology, 1980. **33**(10): p. 917.
171. Wendelsdorf, K., et al., *MODEL OF COLONIC INFLAMMATION: IMMUNE MODULATORY MECHANISMS IN INFLAMMATORY BOWEL DISEASE.* Journal of theoretical biology, 2010. **264**(4): p. 1225-1239.
172. Neurath, M.F., *Current and emerging therapeutic targets for IBD.* Nat Rev Gastroenterol Hepatol, 2017. **14**(5): p. 269-278.
173. Cohen, B.L. and D.B. Sachar, *Update on anti-tumor necrosis factor agents and other new drugs for inflammatory bowel disease.* BMJ, 2017. **357**.
174. Rogler, G., *Where are we heading to in pharmacological IBD therapy?* Pharmacological Research, 2015. **100**: p. 220-227.
175. Sandborn, W.J., et al., *Ustekinumab Induction and Maintenance Therapy in Refractory Crohn's Disease.* New England Journal of Medicine, 2012. **367**(16): p. 1519-1528.
176. Ståhlberg, A., M. Kubista, and P. Åman, *Single-cell gene-expression profiling and its potential diagnostic applications.* Expert Review of Molecular Diagnostics, 2011. **11**(7): p. 735-740.
177. Heid, C.A., et al., *Real time quantitative PCR.* Genome Research, 1996. **6**(10): p. 986-994.
178. Bengtsson, M., et al., *Quantification of mRNA in single cells and modelling of RT-qPCR induced noise.* BMC Molecular Biology, 2008. **9**: p. 63-63.
179. Moignard, V., et al., *Characterisation of transcriptional networks in blood stem and progenitor cells using high-throughput single cell gene expression analysis.* Nature cell biology, 2013. **15**(4): p. 363-372.
180. Moignard, V., et al., *Decoding the Regulatory Network for Blood Development from Single-Cell Gene Expression Measurements.* Nature biotechnology, 2015. **33**(3): p. 269-276.
181. Mortazavi, A., et al., *Mapping and quantifying mammalian transcriptomes by RNA-Seq.* Nat Meth, 2008. **5**(7): p. 621-628.
182. Anders, S. and W. Huber, *Differential expression analysis for sequence count data.* Genome Biol, 2010. **11**.
183. Tang, F., et al., *RNA-Seq analysis to capture the transcriptome landscape of a single cell.* Nature protocols, 2010. **5**(3): p. 10.1038/nprot.2009.236.

184. Wilhelm, B.T. and J.-R. Landry, *RNA-Seq—quantitative measurement of expression through massively parallel RNA-sequencing.* Methods, 2009. **48**(3): p. 249-257.
185. Cloonan, N. and S.M. Grimmond, *Transcriptome content and dynamics at single-nucleotide resolution.* Genome Biology, 2008. **9**(9): p. 234-234.
186. Kapushesky, M., et al., *Gene Expression Atlas update—a value-added database of microarray and sequencing-based functional genomics experiments.* Nucleic Acids Research, 2012. **40**(Database issue): p. D1077-D1081.
187. Novershtern, N., et al., *Densely interconnected transcriptional circuits control cell states in human hematopoiesis.* Cell, 2011. **144**(2): p. 296-309.
188. Heng, T.S.P., et al., *The Immunological Genome Project: networks of gene expression in immune cells.* Nat Immunol, 2008. **9**(10): p. 1091-1094.
189. Papalexi, E. and R. Satija, *Single-cell RNA sequencing to explore immune cell heterogeneity.* Nat Rev Immunol, 2017. **advance online publication**.
190. Picelli, S., *Single-cell RNA-sequencing: The future of genome biology is now.* RNA Biology, 2017. **14**(5): p. 637-650.
191. Picelli, S., et al., *Full-length RNA-seq from single cells using Smart-seq2.* Nat. Protocols, 2014. **9**(1): p. 171-181.
192. Macosko, Evan Z., et al., *Highly Parallel Genome-wide Expression Profiling of Individual Cells Using Nanoliter Droplets.* Cell, 2015. **161**(5): p. 1202-1214.
193. Klein, A.M., et al., *Droplet barcoding for single cell transcriptomics applied to embryonic stem cells.* Cell, 2015. **161**(5): p. 1187-1201.
194. Zheng, G.X.Y., et al., *Massively parallel digital transcriptional profiling of single cells.* bioRxiv, 2016.
195. Paolicelli, R.C., et al., *Synaptic Pruning by Microglia Is Necessary for Normal Brain Development.* Science, 2011. **333**(6048): p. 1456.
196. Di, Y., et al., *The NBP negative binomial model for assessing differential gene expression from RNA-seq.* Stat Appl Genet Mol Biol, 2011. **10**.
197. Kohyama, M., et al., *Critical role for Spi-C in the development of red pulp macrophages and splenic iron homeostasis.* Nature, 2009. **457**(7227): p. 318-321.
198. Okabe, Y. and R. Medzhitov, *Tissue-Specific Signals Control Reversible Program of Localization and Functional Polarization of Macrophages.* Cell, 2014. **157**(4): p. 832-844.
199. Gomez Perdiguero, E., et al., *Tissue-resident macrophages originate from yolk-sac-derived erythro-myeloid progenitors.* Nature, 2015. **518**(7540): p. 547-551.
200. Haldar, M. and K.M. Murphy, *Origin, Development, and Homeostasis of Tissue-resident Macrophages.* Immunological reviews, 2014. **262**(1): p. 25-35.
201. Abutbul, S., et al., *TGF-β signaling through SMAD2/3 induces the quiescent microglial phenotype within the CNS environment.* Glia, 2012. **60**(7): p. 1160-1171.
202. Butovsky, O., et al., *Identification of a Unique TGF-β Dependent Molecular and Functional Signature in Microglia.* Nature neuroscience, 2014. **17**(1): p. 131-143.
203. Smale, S.T., *Pioneer Factors in Embryonic Stem Cells and Differentiation.* Current opinion in genetics & development, 2010. **20**(5): p. 519-526.
204. Garber, M., et al., *A high throughput Chromatin ImmunoPrecipitation approach reveals principles of dynamic gene regulation in mammals.* Molecular cell, 2012. **47**(5): p. 10.1016/j.molcel.2012.07.030.
205. Ostuni, R., et al., *Latent Enhancers Activated by Stimulation in Differentiated Cells.* Cell, 2013. **152**(1): p. 157-171.
206. Creyghton, M.P., et al., *Histone H3K27ac separates active from poised enhancers and predicts developmental state.* Proceedings of the National Academy of Sciences, 2010. **107**(50): p. 21931-21936.
207. Kiselev, V.Y., et al., *SC3 - consensus clustering of single-cell RNA-Seq data.* Nature methods, 2017. **14**(5): p. 483-486.
208. Buenrostro, J.D., et al., *Transposition of native chromatin for fast and sensitive epigenomic profiling of open chromatin, DNA-binding proteins and nucleosome position.* Nat Meth, 2013. **10**(12): p. 1213-1218.
209. Gautier, E.L., et al., *Gata6 regulates aspartoacylase expression in resident peritoneal macrophages and controls their survival.* The Journal of Experimental Medicine, 2014. **211**(8): p. 1525-1531.
210. Rosas, M., et al., *The Transcription Factor Gata6 Links Tissue Macrophage Phenotype and Proliferative Renewal.* Science, 2014. **344**(6184): p. 645.
211. Bendall, S.C., et al., *Single-Cell Trajectory Detection Uncovers Progression and Regulatory Coordination in Human B cell Development.* Cell, 2014. **157**(3): p. 714-725.

212. Trapnell, C., et al., *The dynamics and regulators of cell fate decisions are revealed by pseudotemporal ordering of single cells.* Nat Biotech, 2014. **32**(4): p. 381-386.
213. Paul, F., et al., *Transcriptional Heterogeneity and Lineage Commitment in Myeloid Progenitors.* Cell, 2015. **163**(7): p. 1663-1677.
214. Taniguchi, T., et al., *IRF Family of Transcription Factors as Regulators of Host Defense.* Annual Review of Immunology, 2001. **19**(1): p. 623-655.
215. Barnes, B.J., P.A. Moore, and P.M. Pitha, *Virus-specific Activation of a Novel Interferon Regulatory Factor, IRF-5, Results in the Induction of Distinct Interferon α Genes.* Journal of Biological Chemistry, 2001. **276**(26): p. 23382-23390.
216. Li, D., et al., *Specific detection of interferon regulatory factor 5 (IRF5): A case of antibody inequality.* 2016. **6**: p. 31002.
217. Weiss, M., et al., *IRF5 Is a Specific Marker of Inflammatory Macrophages In Vivo.* Mediators of Inflammation, 2013. **2013**: p. 9.
218. Shu, J., et al., *Expression of interferon regulatory factor 5 is regulated by the Sp1 transcription factor.* Molecular Medicine Reports, 2016. **14**(3): p. 2815-2822.
219. Lin, R., et al., *A CRM1-dependent Nuclear Export Pathway Is Involved in the Regulation of IRF-5 Subcellular Localization.* Journal of Biological Chemistry, 2005. **280**(4): p. 3088-3095.
220. Chang Foreman, H.-C., et al., *Activation of Interferon Regulatory Factor 5 by Site Specific Phosphorylation.* PLOS ONE, 2012. **7**(3): p. e33098.
221. Ryzhakov, G., H.L. Eames, and I.A. Udalova, *Activation and Function of Interferon Regulatory Factor 5.* Journal of Interferon & Cytokine Research, 2014. **35**(2): p. 71-78.
222. Lacey, D.C., et al., *Defining GM-CSF– and Macrophage-CSF–Dependent Macrophage Responses by In Vitro Models.* The Journal of Immunology, 2012. **188**(11): p. 5752.
223. Grainger, J.R., et al., *Inflammatory monocytes regulate pathologic responses to commensals during acute gastrointestinal infection.* Nature medicine, 2013. **19**(6): p. 713-721.
224. Seo, S.-U., et al., *Intestinal macrophages arising from CCR2(+) monocytes control pathogen infection by activating innate lymphoid cells.* Nature Communications, 2015. **6**: p. 8010.
225. Egea, L., Y. Hirata, and M.F. Kagnoff, *GM-CSF: a role in immune and inflammatory reactions in the intestine.* Expert review of gastroenterology & hepatology, 2010. **4**(6): p. 723-731.
226. Xu, D., et al., *Interferon Regulatory Factor 4 (IRF-4) Targets IRF-5 to Regulate Epstein-Barr Virus Transformation.* Journal of Biological Chemistry, 2011. **286**(20): p. 18261-18267.
227. Hedl, M., J. Yan, and C. Abraham, *IRF5 and IRF5 Disease-Risk Variants Increase Glycolysis and Human M1 polarization By Regulating Proximal Signaling and Akt2 Activation.* Cell reports, 2016. **16**(9): p. 2442-2455.
228. Yanai, H., et al., *Role of IFN regulatory factor 5 transcription factor in antiviral immunity and tumor suppression.* Proceedings of the National Academy of Sciences of the United States of America, 2007. **104**(9): p. 3402-3407.
229. Mori, T., et al., *Identification of the interferon regulatory factor 5 gene (IRF-5) as a direct target for p53.* Oncogene 2002. **21**(18): p. 2914-2918.
230. Barnes, B.J., et al., *Interferon Regulatory Factor 5, a Novel Mediator of Cell Cycle Arrest and Cell Death.* Cancer Research, 2003. **63**(19): p. 6424.
231. Hu, G. and B.J. Barnes, *IRF-5 Is a Mediator of the Death Receptor-induced Apoptotic Signaling Pathway.* Journal of Biological Chemistry, 2009. **284**(5): p. 2767-2777.
232. Couzinet, A., et al., *A cell-type-specific requirement for IFN regulatory factor 5 (IRF5) in Fas-induced apoptosis.* Proceedings of the National Academy of Sciences of the United States of America, 2008. **105**(7): p. 2556-2561.
233. Garaud, S. and K. Willard-Gallo, *IRF5: a rheostat for tumor-infiltrating lymphocyte trafficking in breast cancer[quest].* Immunol Cell Biol, 2015. **93**(5): p. 425-426.
234. Pimenta, E.M. and B.J. Barnes, *A conserved region within interferon regulatory factor 5 controls breast cancer cell migration through a cytoplasmic and transcription-independent mechanism.* Molecular Cancer, 2015. **14**(1): p. 32.
235. Dong, S.M., et al., *Hypermethylation of the interferon regulatory factor 5 promoter in Epstein-Barr virus-associated gastric carcinoma.* Journal of Microbiology, 2015. **53**(1): p. 70-76.
236. Massimino, M., et al., *IRF5 is a target of BCR-ABL kinase activity and reduces CML cell proliferation.* Carcinogenesis, 2014. **35**(5): p. 1132-1143.

237. Dideberg, V., et al., *An insertion-deletion polymorphism in the interferon regulatory factor 5 (IRF5) gene confers risk of inflammatory bowel diseases.* Hum. Mol. Genet, 2007. **16**(24): p. 3008-3016.
238. Eames, H.L., A.L. Corbin, and I.A. Udalova, *Interferon regulatory factor 5 in human autoimmunity and murine models of autoimmune disease.* Translational Research, 2016. **167**(1): p. 167-182.
239. Yang, L., et al., *Monocytes from Irf5(−/−) mice have an intrinsic defect in their response to pristane-induced lupus.* Journal of immunology (Baltimore, Md. : 1950), 2012. **189**(7): p. 3741-3750.
240. Steinhagen, F., et al., *IRF5 and IRF8 modulate the CAL-1 human plasmacytoid dendritic cell line response following TLR9 ligation.* European Journal of Immunology, 2016. **46**(3): p. 647-655.
241. Feng, D., et al., *Protection of Irf5-deficient mice from pristane-induced lupus involves altered cytokine production and class switching.* European journal of immunology, 2012. **42**(6): p. 1477-1487.
242. Eames, H.L., et al., *KAP1/TRIM28: An inhibitor of IRF5 function in inflammatory macrophages.* Immunobiology, 2012. **217**(12): p. 1315-1324.
243. Duffau, P., et al., *Promotion of Inflammatory Arthritis by Interferon Regulatory Factor 5 in a Mouse Model.* Arthritis & Rheumatology, 2015. **67**(12): p. 3146-3157.
244. Dalmas, E., et al., *Irf5 deficiency in macrophages promotes beneficial adipose tissue expansion and insulin sensitivity during obesity.* Nat Med, 2015. **21**(6): p. 610-618.
245. Gathungu, G., et al., *A two-marker haplotype in the IRF5 gene is associated with inflammatory bowel disease in a North American cohort.* Genes and Immunity, 2012. **13**: p. 351-355.
246. Izcue, A., et al., *Interleukin-23 Restrains Regulatory T Cell Activity to Drive T Cell-Dependent Colitis.* Immunity, 2008. **28**(4): p. 559-570.
247. Amir, E.-a.D., et al., *viSNE enables visualization of high dimensional single-cell data and reveals phenotypic heterogeneity of leukemia.* Nature biotechnology, 2013. **31**(6): p. 545-552.
248. Kim, D., B. Langmead, and S.L. Salzberg, *HISAT: a fast spliced aligner with low memory requirements.* Nat Meth, 2015. **12**(4): p. 357-360.
249. Liao, Y., G.K. Smyth, and W. Shi, *featureCounts: an efficient general purpose program for assigning sequence reads to genomic features.* Bioinformatics, 2014. **30**(7): p. 923-930.
250. Trapnell, C., et al., *Transcript assembly and quantification by RNA-Seq reveals unannotated transcripts and isoform switching during cell differentiation.* Nat Biotech, 2010. **28**(5): p. 511-515.
251. Love, M.I., W. Huber, and S. Anders, *Moderated estimation of fold change and dispersion for RNA-seq data with DESeq2.* Genome Biology, 2014. **15**(12): p. 550.
252. Butler, A. and R. Satija, *Integrated analysis of single cell transcriptomic data across conditions, technologies, and species.* bioRxiv, 2017.
253. Bolger, A.M., M. Lohse, and B. Usadel, *Trimmomatic: a flexible trimmer for Illumina sequence data.* Bioinformatics, 2014. **30**(15): p. 2114-2120.
254. Langmead, B. and S.L. Salzberg, *Fast gapped-read alignment with Bowtie 2.* Nature methods, 2012. **9**(4): p. 357-359.
255. McLean, C.Y., et al., *GREAT improves functional interpretation of cis-regulatory regions.* Nature biotechnology, 2010. **28**(5): p. 495-501.
256. Schneider, C.A., W.S. Rasband, and K.W. Eliceiri, *NIH Image to ImageJ: 25 years of image analysis.* Nat Meth, 2012. **9**(7): p. 671-675.
257. Krajmalnik-Brown, R., et al., *Effects of Gut Microbes on Nutrient Absorption and Energy Regulation.* Nutrition in clinical practice : official publication of the American Society for Parenteral and Enteral Nutrition, 2012. **27**(2): p. 201-214.
258. Millan, B., M. Laffin, and K. Madsen, *Fecal Microbiota Transplantation: Beyond Clostridium difficile.* Current Infectious Disease Reports, 2017. **19**(9): p. 31.
259. Ahern, P.P., et al., *The interleukin-23 axis in intestinal inflammation.* Immunological Reviews, 2008. **226**(1): p. 147-159.
260. Di Narzo, A.F., et al., *Blood and Intestine eQTLs from an Anti-TNF-Resistant Crohn's Disease Cohort Inform IBD Genetic Association Loci.* Clinical and Translational Gastroenterology, 2016. **7**(6): p. e177.
261. Weiss, M., et al., *IRF5 controls both acute and chronic inflammation.* Proceedings of the National Academy of Sciences of the United States of America, 2015. **112**(35): p. 11001-11006.

262. Martinez, F. and S. Gordon, *The M1 and M2 paradigm of macrophage activation: time for reassessment.* F1000 Prime, 2014. **6**(13).
263. Murray, Peter J., et al., *Macrophage Activation and Polarization: Nomenclature and Experimental Guidelines.* Immunity, 2014. **41**(1): p. 14-20.
264. Bain, C.C. and A.M. Mowat, *Macrophages in intestinal homeostasis and inflammation.* Immunological Reviews, 2014. **260**(1): p. 102-117.
265. Fangradt, M., et al., *Human monocytes and macrophages differ in their mechanisms of adaptation to hypoxia.* Arthritis Research & Therapy, 2012. **14**(4): p. R181.
266. Iwasaki, H., et al., *Distinctive and indispensable roles of PU.1 in maintenance of hematopoietic stem cells and their differentiation.* Blood, 2005. **106**(5): p. 1590-1600.
267. Mueller, B.U., et al., *Heterozygous PU.1 mutations are associated with acute myeloid leukemia.* Blood, 2002. **100**(3): p. 998.
268. Mossadegh-Keller, N., et al., *M-CSF instructs myeloid lineage fate in single haematopoietic stem cells.* Nature, 2013. **497**(7448): p. 239-243.
269. Feinberg, M.W., et al., *The Kruppel-like factor KLF4 is a critical regulator of monocyte differentiation.* The EMBO Journal, 2007. **26**(18): p. 4138-4148.
270. van Oevelen, C., et al., *C/EBPα Activates Pre-existing and De Novo Macrophage Enhancers during Induced Pre-B Cell Transdifferentiation and Myelopoiesis.* Stem Cell Reports, 2015. **5**(2): p. 232-247.
271. Dahl, R., et al., *Regulation of macrophage and neutrophil cell fates by the PU.1:C/EBP[alpha] ratio and granulocyte colony-stimulating factor.* Nat Immunol, 2003. **4**(10): p. 1029-1036.
272. Yáñez, A., et al., *IRF8 acts in lineage-committed rather than oligopotent progenitors to control neutrophil vs monocyte production.* Blood, 2015. **125**(9): p. 1452.
273. Duran, N.E. and D.W. Hommes, *Stem cell-based therapies in inflammatory bowel disease: promises and pitfalls.* Therapeutic Advances in Gastroenterology, 2016. **9**(4): p. 533-547.
274. Flores AI, et al., *Stem cell therapy in inflammatory bowel disease: A promising therapeutic strategy?* World J Stem Cells 2015. **7**(2): p. 343-351.
275. de Bruin, A.M., C. Voermans, and M.A. Nolte, *Impact of interferon-γ on hematopoiesis.* Blood, 2014. **124**(16): p. 2479.
276. Hume, D.A., V.H. Perry, and S. Gordon, *The mononuclear phagocyte system of the mouse defined by immunohistochemical localisation of antigen F4/80: Macrophages associated with epithelia.* The Anatomical Record, 1984. **210**(3): p. 503-512.
277. Yang, W.Y., et al., *Pathological conditions re-shape physiological Tregs into pathological Tregs.* Burns & Trauma, 2015. **3**(1): p. 1.
278. Seneviratne, A.N., et al., *Interferon Regulatory Factor 5 Controls Necrotic Core Formation in Atherosclerotic Lesions by Impairing Efferocytosis.* Circulation, 2017.
279. Perez, P.F., et al., *Bacterial Imprinting of the Neonatal Immune System: Lessons From Maternal Cells?* Pediatrics, 2007. **119**(3): p. e724.
280. Kelsall, B., *Recent progress in understandıng the function of intestinal macrophages and dendritic cells.* Mucosal immunology, 2008. **1**(6): p. 460-469.
281. Zarbock, A., R.K. Polanowska-Grabowska, and K. Ley, *Platelet-neutrophil-interactions: Linking hemostasis and inflammation.* Blood Reviews, 2007. **21**(2): p. 99-111.
282. Passacquale, G., et al., *Monocyte-Platelet Interaction Induces a Pro-Inflammatory Phenotype in Circulating Monocytes.* PLOS ONE, 2011. **6**(10): p. e25595.
283. Kang, H.-K., et al., *Megakaryocyte progenitors are the main antigen presenting cells inducing Th17 response to lupus autoantigens and foreign antigens.* Journal of Immunology (Baltimore, Md. : 1950), 2012. **188**(12): p. 5970-5980.
284. Finkielsztein, A., et al., *Human Megakaryocyte Progenitors Derived From Hematopoietic Stem Cells of Normal Individuals Are MHC Class II-Expressing Professional APC That Enhance Th17 and Th1/Th17 Responses.* Immunology Letters, 2014. **163**(1): p. 84-95.
285. Vowinkel, T., et al., *CD40-CD40 Ligand Mediates the Recruitment of Leukocytes and Platelets in the Inflamed Murine Colon.* Gastroenterology, 2007. **132**(3): p. 955-965.
286. Schmid, W., et al., *Platelets Toll-like receptor-4 in Crohns disease.* European Journal of Clinical Investigation, 2017. **47**(2): p. 109-116.
287. Takizawa, H., S. Boettcher, and M.G. Manz, *Demand-adapted regulation of early hematopoiesis in infection and inflammation.* Blood, 2012. **119**(13): p. 2991-3002.
288. Chen, C., et al., *Mammalian target of rapamycin activation underlies HSC defects in autoimmune disease and inflammation in mice.* The Journal of Clinical Investigation, 2010. **120**(11): p. 4091-4101.

289. Ueda, Y., et al., *IL-1RI dependent HSC proliferation is necessary for Inflammatory Granulopoiesis and Reactive Neutrophilia.* Journal of immunology (Baltimore, Md. : 1950), 2009. **182**(10): p. 6477-6484.
290. Askenase, M.H., et al., *Bone marrow-resident NK cells prime monocytes for regulatory function during infection.* Immunity, 2015. **42**(6): p. 1130-1142.
291. Smith, P.D., et al., *Intestinal Macrophages and Response to Microbial Encroachment.* Mucosal immunology, 2011. **4**(1): p. 10.1038/mi.2010.66.
292. Sauter, K.A., et al., *Pleiotropic effects of extended blockade of CSF1R signaling in adult mice.* Journal of Leukocyte Biology, 2014. **96**(2): p. 265-274.
293. Sender, R., S. Fuchs, and R. Milo, *Revised Estimates for the Number of Human and Bacteria Cells in the Body.* PLoS Biology, 2016. **14**(8): p. e1002533.
294. Zigmond, E., et al., *Ly6Chi Monocytes in the Inflamed Colon Give Rise to Proinflammatory Effector Cells and Migratory Antigen-Presenting Cells.* Immunity, 2012. **37**(6): p. 1076-1090.
295. Grainger, J.R., et al., *Macrophages in gastrointestinal homeostasis and inflammation.* Pflugers Archiv, 2017. **469**(3): p. 527-539.
296. Satpathy, A.T., et al., *Notch2-dependent classical dendritic cells orchestrate intestinal immunity against attaching and effacing bacterial pathogens.* Nature immunology, 2013. **14**(9): p. 937-948.
297. Scott, C.L., et al., *CCR2(+)CD103(−) intestinal dendritic cells develop from DC-committed precursors and induce interleukin-17 production by T cells.* Mucosal Immunology, 2015. **8**(2): p. 327-339.
298. Schulthess, J., et al., *Interleukin-15-Dependent NKp46+ Innate Lymphoid Cells Control Intestinal Inflammation by Recruiting Inflammatory Monocytes.* Immunity, 2012. **37**(1): p. 108-121.
299. Rivollier, A., et al., *Inflammation switches the differentiation program of Ly6C^{hi} monocytes from antiinflammatory macrophages to inflammatory dendritic cells in the colon.* The Journal of Experimental Medicine, 2012. **209**(1): p. 139.
300. Krausgruber, T., et al., *IRF5 is required for late-phase TNF secretion by human dendritic cells.* Blood, 2010. **115**(22): p. 4421-4430.
301. Andres, P.G., et al., *Mice with a Selective Deletion of the CC Chemokine Receptors 5 or 2 Are Protected from Dextran Sodium Sulfate-Mediated Colitis: Lack of CC Chemokine Receptor 5 Expression Results in a NK1.1⁺ Lymphocyte-Associated Th2-Type Immune Response in the Intestine.* The Journal of Immunology, 2000. **164**(12): p. 6303.
302. Cohen, S.B., et al., *CXCR3-Dependent CD4(+) T Cells Are Required to Activate Inflammatory Monocytes for Defense against Intestinal Infection.* PLoS Pathogens, 2013. **9**(10): p. e1003706.
303. Nourshargh, S. and R. Alon, *Leukocyte Migration into Inflamed Tissues.* Immunity, 2014. **41**(5): p. 694-707.
304. Hörber, S., et al., *The Atypical Inhibitor of NF-κB, IκBζ, Controls Macrophage Interleukin-10 Expression.* The Journal of Biological Chemistry, 2016. **291**(24): p. 12851-12861.
305. Rocha-Perugini, V., et al., *CD81 Controls Sustained T Cell Activation Signaling and Defines the Maturation Stages of Cognate Immunological Synapses.* Molecular and Cellular Biology, 2013. **33**(18): p. 3644-3658.
306. Levy, S., *Function of the tetraspanin molecule CD81 in B and T cells.* Immunologic Research, 2014. **58**(2): p. 179-185.
307. Coccia, M., et al., *IL-1β mediates chronic intestinal inflammation by promoting the accumulation of IL-17A secreting innate lymphoid cells and CD4(+) Th17 cells.* The Journal of Experimental Medicine, 2012. **209**(9): p. 1595-1609.
308. Yáñez, A., et al., *TLRs control hematopoiesis during infection.* European Journal of Immunology, 2013. **43**(10): p. 2526-2533.
309. Kawano, Y., et al., *Colonic Pro-inflammatory Macrophages Cause Insulin Resistance in an Intestinal Ccl2/Ccr2-Dependent Manner.* Cell Metabolism, 2016. **24**(2): p. 295-310.
310. Guo, Y., et al., *Serum Levels of Lipopolysaccharide and 1,3-beta-D-Glucan Refer to the Severity in Patients with Crohn's Disease.* Mediators of Inflammation, 2015. **2015**: p. 9.
311. Pasternak, B.A., et al., *Lipopolysaccharide Exposure is Linked to Activation of the Acute Phase Response and Growth Failure in Pediatric Crohn's Disease and Murine Colitis.* Inflammatory bowel diseases, 2010. **16**(5): p. 856-869.
312. Pastor Rojo, Ó., et al., *Serum lipopolysaccharide-binding protein in endotoxemic patients with inflammatory bowel disease.* Inflammatory Bowel Diseases, 2007. **13**(3): p. 269-277.

313. Bi, X., et al., *Loss of interferon regulatory factor 5 (IRF5) expression in human ductal carcinoma correlates with disease stage and contributes to metastasis.* Breast Cancer Research : BCR, 2011. **13**(6): p. R111-R111.
314. Bi, X., et al., *Deletion of Irf5 protects hematopoietic stem cells from DNA damage-induced apoptosis and suppresses [gamma]-irradiation-induced thymic lymphomagenesis.* Oncogene, 2014. **33**(25): p. 3288-3297.
315. Grzybowska-Chlebowczyk, U., et al., *Eosinophilic colitis in children.* Advances in Dermatology and Allergology/Postępy Dermatologii i Alergologii, 2017. **34**(1): p. 52-59.
316. Zhao, J., et al., *Sigma Receptor Ligand, (+)-Pentazocine, Suppresses Inflammatory Responses of Retinal Microglia.* Investigative Ophthalmology & Visual Science, 2014. **55**(6): p. 3375-3384.
317. Lu, Y., et al., *HoxA10 Represses Gene Transcription in Undifferentiated Myeloid Cells by Interaction with Histone Deacetylase 2.* Journal of Biological Chemistry, 2003. **278**(48): p. 47792-47802.
318. Kautz, B., et al., *SHP1 protein tyrosine phosphatase inhibits gp91 phox and p67 phox expression by inhibiting interaction of PU.1, IRF1, ICSBP and CBP with homologous cis elements in the CYBB and NCF2 genes.* Journal of Biological Chemistry, 2001.
319. Eklund, E.A. and R. Kakar, *Recruitment of CREB-Binding Protein by PU.1, IFN-Regulatory Factor-1, and the IFN Consensus Sequence-Binding Protein Is Necessary for IFN-γ-Induced p67^{phox} and gp91^{phox} Expression.* The Journal of Immunology, 1999. **163**(11): p. 6095-6105.
320. Furlan, F., et al., *The soluble D2D3₈₈₋₂₇₄ fragment of the urokinase receptor inhibits monocyte chemotaxis and integrin-dependent cell adhesion.* Journal of Cell Science, 2004. **117**(14): p. 2909.
321. May, A.E., et al., *Urokinase receptor surface expression regulates monocyte adhesion in acute myocardial infarction.* Blood, 2002. **100**(10): p. 3611.
322. Nakayama, M., et al., *Up-regulation of the urokinase-type plasminogen activator receptor by monocyte chemotactic proteins.* Blood Coagulation and Firbinolysis, 2002. **13**(5): p. 383-391.
323. Patel, J., et al., *RGS1 regulates myeloid cell accumulation in atherosclerosis and aortic aneurysm rupture through altered chemokine signalling.* 2015. **6**: p. 6614.
324. Yang, M., et al., *Serum-Glucocorticoid Regulated Kinase 1 Regulates Alternatively Activated Macrophage Polarization Contributing to Angiotensin II–Induced Inflammation and Cardiac Fibrosis.* Arteriosclerosis, Thrombosis, and Vascular Biology, 2012. **32**(7): p. 1675.
325. Dambuza, I.M. and G.D. Brown, *C-type lectins in immunity: recent developments.* Current Opinion in Immunology, 2015. **32**(Supplement C): p. 21-27.
326. Lee, B.C., et al., *Selenoprotein MsrB1 promotes anti-inflammatory cytokine gene expression in macrophages and controls immune response in vivo.* Scientific Reports, 2017. **7**(1): p. 5119.
327. Cerovic, V., et al., *Intestinal CD103- dendritic cells migrate in lymph and prime effector T cells.* Mucosal Immunol, 2013. **6**(1): p. 104-113.
328. Waddell, A., et al., *Colonic eosinophilic inflammation in experimental colitis is mediated by Ly6C(high) CCR2(+) inflammatory monocyte/macrophage-derived CCL11.* Journal of immunology (Baltimore, Md. : 1950), 2011. **186**(10): p. 5993-6003.
329. Schreiber, H.A., et al., *Intestinal monocytes and macrophages are required for T cell polarization in response to Citrobacter rodentium.* The Journal of Experimental Medicine, 2013. **210**(10): p. 2025-2039.
330. Milling, S., et al., *Subsets of migrating intestinal dendritic cells.* Immunological Reviews, 2010. **234**(1): p. 259-267.
331. Rossini, V., et al., *CX3CR1+ cells facilitate the activation of CD4 T cells in the colonic lamina propria during antigen-driven colitis.* Mucosal Immunol, 2014. **7**(3): p. 533-548.
332. Mazzini, E., et al., *Oral Tolerance Can Be Established via Gap Junction Transfer of Fed Antigens from CX3CR1⁺ Macrophages to CD103⁺ Dendritic Cells.* Immunity, 2014. **40**(2): p. 248-261.
333. Hue, S., et al., *Interleukin-23 drives innate and T cell-mediated intestinal inflammation.* Journal of Experimental Medicine, 2006. **203**(11): p. 2473-2483.
334. Buonocore, S., et al., *Innate lymphoid cells drive IL-23 dependent innate intestinal pathology.* Nature, 2010. **464**(7293): p. 1371-1375.

335. Kullberg, M.C., et al., *Helicobacter hepaticus-Induced Colitis in Interleukin-10-Deficient Mice: Cytokine Requirements for the Induction and Maintenance of Intestinal Inflammation.* Infection and Immunity, 2001. **69**(7): p. 4232-4241.
336. Shale, M., C. Schiering, and F. Powrie, *CD4(+) T-cell subsets in intestinal inflammation.* Immunological Reviews, 2013. **252**(1): p. 164-182.
337. Kamada, N., et al., *Unique CD14+ intestinal macrophages contribute to the pathogenesis of Crohn disease via IL-23/IFN-γ axis.* The Journal of Clinical Investigation, 2008. **118**(6): p. 2269-2280.
338. Thiesen, S., et al., *CD14hiHLA-DRdim macrophages, with a resemblance to classical blood monocytes, dominate inflamed mucosa in Crohn's disease.* Journal of Leukocyte Biology, 2014. **95**(3): p. 531-541.
339. Grimm, M.C., et al., *Direct evidence of monocyte recruitment to inflammatory bowel disease mucosa.* Journal of Gastroenterology and Hepatology, 1995. **10**(4): p. 387-395.
340. Kühl, A.A., et al., *Diversity of Intestinal Macrophages in Inflammatory Bowel Diseases.* Frontiers in Immunology, 2015. **6**: p. 613.
341. Duran-Struuck, R. and R.C. Dysko, *Principles of Bone Marrow Transplantation (BMT): Providing Optimal Veterinary and Husbandry Care to Irradiated Mice in BMT Studies.* Journal of the American Association for Laboratory Animal Science : JAALAS, 2009. **48**(1): p. 11-22.
342. Wang, C., et al., *Non-Lethal Ionizing Radiation Promotes Aging-Like Phenotypic Changes of Human Hematopoietic Stem and Progenitor Cells in Humanized Mice.* PLOS ONE, 2015. **10**(7): p. e0132041.
343. Holgersen, K., et al., *High-Resolution Gene Expression Profiling Using RNA Sequencing in Patients With Inflammatory Bowel Disease and in Mouse Models of Colitis.* Journal of Crohn's and Colitis, 2015. **9**(6): p. 492-506.
344. Mitsuyama, K., et al., *Increased Circulating Concentrations of Growth-Related Oncogene (GRO)-α in Patients with Inflammatory Bowel Disease.* Digestive Diseases and Sciences, 2006. **51**(1): p. 173-177.
345. Park, J.H., et al., *IBD immunopathogenesis: A comprehensive review of inflammatory molecules.* Autoimmunity Reviews, 2017. **16**(4): p. 416-426.
346. Nava, P., et al., *Interferon-γ regulates intestinal epithelial homeostasis through converging β-catenin signaling pathways.* Immunity, 2010. **32**(3): p. 392-402.
347. Holtmann, M.H., et al., *Tumor necrosis factor-receptor 2 is up-regulated on lamina propria T cells in Crohn's disease and promotes experimental colitis in vivo.* European Journal of Immunology, 2002. **32**(11): p. 3142-3151.
348. Cabal-Hierro, L., et al., *TRAF-mediated modulation of NF-kB AND JNK Activation by TNFR2.* Cellular Signalling, 2014. **26**(12): p. 2658-2666.
349. Wajant, H. and P. Scheurich, *TNFR1-induced activation of the classical NF-κB pathway.* FEBS Journal, 2011. **278**(6): p. 862-876.
350. Ting, A.T. and M.J.M. Bertrand, *More to life than NF-κB in TNFR1 signaling.* Trends in immunology, 2016. **37**(8): p. 535-545.
351. Pasparakis, M. and P. Vandenabeele, *Necroptosis and its role in inflammation.* Nature, 2015. **517**(7534): p. 311-320.
352. Perrier, C., et al., *Neutralization of Membrane TNF, but Not Soluble TNF, Is Crucial for the Treatment of Experimental Colitis.* Inflammatory Bowel Diseases, 2013. **19**(2): p. 246-253.
353. Ghoreschi, K., et al., *Generation of Pathogenic Th17 Cells in the Absence of TGF-β Signaling.* Nature, 2010. **467**(7318): p. 967-971.
354. Atreya, R., I. Atreya, and M.F. Neurath, *Novel Signal Transduction Pathways.* Annals of the New York Academy of Sciences, 2006. **1072**(1): p. 98-113.
355. Veldhoen, M., et al., *TGFβ in the Context of an Inflammatory Cytokine Milieu Supports De Novo Differentiation of IL-17-Producing T Cells.* Immunity, 2006. **24**(2): p. 179-189.
356. McGeachy, M.J., et al., *Interleukin 23 receptor is essential for terminal differentiation of effector T helper type 17 cells in vivo.* Nature immunology, 2009. **10**(3): p. 314-324.
357. McGeachy, M.J., et al., *TGF-[beta] and IL-6 drive the production of IL-17 and IL-10 by T cells and restrain TH-17 cell-mediated pathology.* Nat Immunol, 2007. **8**(12): p. 1390-1397.
358. Mannon, P.J., et al., *Anti–Interleukin-12 Antibody for Active Crohn's Disease.* New England Journal of Medicine, 2004. **351**(20): p. 2069-2079.
359. Athie-Morales, V., et al., *Sustained IL-12 Signaling Is Required for Th1 Development.* The Journal of Immunology, 2003. **172**(1): p. 61.

360. Gouwy, M., et al., *Chemokines and other GPCR ligands synergize in receptor-mediated migration of monocyte-derived immature and mature dendritic cells.* Immunobiology, 2014. **219**(3): p. 218-229.
361. Alam, R., et al., *RANTES is a chemotactic and activating factor for human eosinophils.* The Journal of Immunology, 1993. **150**(8): p. 3442.
362. Francisco-Cruz, A., et al., *Granulocyte–macrophage colony-stimulating factor: not just another haematopoietic growth factor.* Medical Oncology, 2013. **31**(1): p. 774.
363. Saitoh, O., et al., *Fecal eosinophil granule-derived proteins reflect disease activity in inflammatory bowel disease.* Am J Gastroenterol, 1999. **94**(12): p. 3513-3520.
364. Ahrens, R., et al., *Intestinal Macrophage/Epithelial Cell-Derived CCL11/Eotaxin-1 Mediates Eosinophil Recruitment and Function in Pediatric Ulcerative Colitis.* Journal of immunology (Baltimore, Md. : 1950), 2008. **181**(10): p. 7390-7399.
365. Schlitzer, A., et al., *IRF4 Transcription Factor-Dependent CD11b(+) Dendritic Cells in Human and Mouse Control Mucosal IL-17 Cytokine Responses.* Immunity, 2013. **38**(5): p. 970-983.
366. Becker, M., et al., *Ontogenic, Phenotypic, and Functional Characterization of XCR1(+) Dendritic Cells Leads to a Consistent Classification of Intestinal Dendritic Cells Based on the Expression of XCR1 and SIRPα.* Frontiers in Immunology, 2014. **5**: p. 326.
367. Farache, J., et al., *Luminal Bacteria Recruit CD103(+) Dendritic Cells into the Intestinal Epithelium to Sample Bacterial Antigens for Presentation.* Immunity, 2013. **38**(3): p. 581-595.
368. McDole, J.R., et al., *Goblet cells deliver luminal antigen to CD103+ dendritic cells in the small intestine.* Nature, 2012. **483**(7389): p. 345-349.
369. Villablanca, E.J., et al., *β7 integrins are required to give rise to intestinal mononuclear phagocytes with tolerogenic potential.* Gut, 2014. **63**(9): p. 1431-1440.
370. Houston, S.A., et al., *The lymph nodes draining the small intestine and colon are anatomically separate and immunologically distinct.* Mucosal Immunol, 2016. **9**(2): p. 468-478.
371. Shi, C. and E.G. Pamer, *Monocyte recruitment during infection and inflammation.* Nat Rev Immunol, 2011. **11**(11): p. 762-774.
372. Akbar, N., et al., *Endothelium-derived extracellular vesicles promote splenic monocyte mobilization in myocardial infarction.* JCI Insight, 2017. **2**(17).
373. Sica, A. and A. Mantovani, *Macrophage plasticity and polarization: in vivo veritas.* The Journal of Clinical Investigation, 2012. **122**(3): p. 787-795.
374. Schmidt, A., et al., *Human macrophages induce CD4+Foxp3+ regulatory T cells via binding and re-release of TGF-[beta].* Immunol Cell Biol, 2016. **94**(8): p. 747-762.
375. Lissner, D., et al., *Monocyte and M1 Macrophage-induced Barrier Defect Contributes to Chronic Intestinal Inflammation in IBD.* Inflammatory Bowel Diseases, 2015. **21**(6): p. 1297-1305.
376. Wang, K., et al., *Diverse Genome-wide Association Studies Associate the IL12/IL23 Pathway with Crohn Disease.* American Journal of Human Genetics, 2009. **84**(3): p. 399-405.
377. Zhao, Y., et al., *Thrombospondin-1 triggers macrophage IL-10 production and promotes resolution of experimental lung injury.* Mucosal immunology, 2014. **7**(2): p. 440-448.
378. Stein, E.V., et al., *Secreted Thrombospondin-1 Regulates Macrophage Interleukin-1β Production and Activation through CD47.* Scientific Reports, 2016. **6**: p. 19684.
379. Xing, T., et al., *Thrombospondin-1 Production Regulates the Inflammatory Cytokine Secretion in THP-1 Cells Through NF-κB Signaling Pathway.* Inflammation, 2017. **40**(5): p. 1606-1621.
380. Swindell, W.R., et al., *Modulation of Epidermal Transcription Circuits in Psoriasis: New Links between Inflammation and Hyperproliferation.* PLoS ONE, 2013. **8**(11): p. e79253.
381. Rogier, R., et al., *Aberrant intestinal microbiota due to IL-1 receptor antagonist deficiency promotes IL-17- and TLR4-dependent arthritis.* Microbiome, 2017. **5**: p. 63.
382. Jones, Eleanor L., Maria C. Demaria, and Mark D. Wright, *Tetraspanins in cellular immunity.* Biochemical Society Transactions, 2011. **39**(2): p. 506.
383. Mordica, W.J., et al., *Macrophage Cell Lines Use CD81 in Cell Growth Regulation.* In vitro cellular & developmental biology. Animal, 2009. **45**(0): p. 213-225.
384. Rocha-Perugini, V., F. Sánchez-Madrid, and G. Martínez del Hoyo, *Function and Dynamics of Tetraspanins during Antigen Recognition and Immunological Synapse Formation.* Frontiers in Immunology, 2015. **6**: p. 653.

385. Banks, C., et al., *Chemokine expression in IBD. Mucosal chemokine expression is unselectively increased in both ulcerative colitis and Crohn's disease.* The Journal of Pathology, 2003. **199**(1): p. 28-35.
386. Persson, Emma K., et al., *IRF4 Transcription-Factor-Dependent CD103⁺CD11b⁺ Dendritic Cells Drive Mucosal T Helper 17 Cell Differentiation.* Immunity, 2013. **38**(5): p. 958-969.
387. Watkins, A.A., et al., *IRF5 deficiency ameliorates lupus but promotes atherosclerosis and metabolic dysfunction in a mouse model of lupus-associated atherosclerosis.* Journal of immunology (Baltimore, Md. : 1950), 2015. **194**(4): p. 1467-1479.
388. Varol, C., et al., *Intestinal Lamina Propria Dendritic Cell Subsets Have Different Origin and Functions.* Immunity, 2009. **31**(3): p. 502-512.
389. Negishi, H., et al., *Negative regulation of Toll-like-receptor signaling by IRF-4.* Proceedings of the National Academy of Sciences of the United States of America, 2005. **102**(44): p. 15989-15994.
390. Jiang, W., et al., *Acetylcholine-producing NK cells attenuate CNS inflammation via modulation of infiltrating monocytes/macrophages.* Proceedings of the National Academy of Sciences of the United States of America, 2017. **114**(30): p. E6202-E6211.
391. Rahman, K., et al., *Inflammatory Ly6Chi monocytes and their conversion to M2 macrophages drive atherosclerosis regression.* The Journal of Clinical Investigation, 2017. **127**(8): p. 2904-2915.
392. Zhang, J. and J.M. Patel, *Role of the CX3CL1-CX3CR1 axis in chronic inflammatory lung diseases.* International Journal of Clinical and Experimental Medicine, 2010. **3**(3): p. 233-244.
393. Luda, Katarzyna M., et al., *IRF8 Transcription-Factor-Dependent Classical Dendritic Cells Are Essential for Intestinal T Cell Homeostasis.* Immunity, 2016. **44**(4): p. 860-874.
394. Sun, T., et al., *Intestinal Batf3-dependent dendritic cells are required for optimal antiviral T-cell responses in adult and neonatal mice.* Mucosal Immunol, 2017. **10**(3): p. 775-788.
395. Ohta, T., et al., *Crucial roles of XCR1-expressing dendritic cells and the XCR1-XCL1 chemokine axis in intestinal immune homeostasis.* Scientific Reports, 2016. **6**: p. 23505.
396. Everts, B., et al., *Migratory CD103⁺ dendritic cells suppress helminth-driven type 2 immunity through constitutive expression of IL-12.* The Journal of Experimental Medicine, 2016. **213**(1): p. 35.
397. Mashayekhi, M., et al., *CD8α(+) dendritic cells are the critical source of interleukin-12 that controls acute infection by Toxoplasma gondii tachyzoites.* Immunity, 2011. **35**(2): p. 249-259.
398. Muzaki, A.R.B.M., et al., *Intestinal CD103(+)CD11b(−) dendritic cells restrain colitis via IFN-γ-induced anti-inflammatory response in epithelial cells.* Mucosal Immunology, 2016. **9**(2): p. 336-351.
399. Esterházy, D., et al., *Classical dendritic cells are required for dietary antigen-mediated peripheral regulatory T cell and tolerance induction.* Nature immunology, 2016. **17**(5): p. 545-555.
400. Aychek, T., et al., *IL-23-mediated mononuclear phagocyte crosstalk protects mice from Citrobacter rodentium-induced colon immunopathology.* Nat Commun, 2015. **6**.
401. Tippett, E., et al., *Characterization of tetraspanins CD9, CD53, CD63, and CD81 in monocytes and macrophages in HIV-1 infection.* Journal of Leukocyte Biology, 2013. **93**(6): p. 913-920.
402. Schorey, J.S. and S. Bhatnagar, *Exosome Function: From Tumor Immunology to Pathogen Biology.* Traffic (Copenhagen, Denmark), 2008. **9**(6): p. 871-881.
403. Wong, W.-Y., et al., *Proteomic profiling of dextran sulfate sodium induced acute ulcerative colitis mice serum exosomes and their immunomodulatory impact on macrophages.* PROTEOMICS, 2016. **16**(7): p. 1131-1145.
404. Hulme, R.S., et al., *Distinct Regions of the Large Extracellular Domain of Tetraspanin CD9 Are Involved in the Control of Human Multinucleated Giant Cell Formation.* PLoS ONE, 2014. **9**(12): p. e116289.
405. Raposo, G., et al., *B lymphocytes secrete antigen-presenting vesicles.* The Journal of Experimental Medicine, 1996. **183**(3): p. 1161.
406. Papandreou, M.-E. and N. Tavernarakis, *Autophagy and the endo/exosomal pathways in health and disease.* Biotechnology Journal, 2017. **12**(1): p. 1600175-n/a.
407. Ju, S., et al., *Grape Exosome-like Nanoparticles Induce Intestinal Stem Cells and Protect Mice From DSS-Induced Colitis.* Molecular Therapy, 2013. **21**(7): p. 1345-1357.

408. Rocha-Perugini, V., et al., *CD9 Regulates Major Histocompatibility Complex Class II Trafficking in Monocyte-Derived Dendritic Cells.* Molecular and Cellular Biology, 2017. **37**(15).
409. Okoye, I.S., et al., *MicroRNA-containing T-regulatory-cell-derived exosomes suppress pathogenic T helper 1 cells.* Immunity, 2014. **41**.
410. Carrière, J., et al., *Exosomes Released from Cells Infected with Crohn's Disease–associated Adherent-Invasive Escherichia coli Activate Host Innate Immune Responses and Enhance Bacterial Intracellular Replication.* Inflammatory Bowel Diseases, 2016. **22**(3): p. 516-528.
411. Xu, A.T., et al., *Exosome in intestinal mucosal immunity.* Journal of Gastroenterology and Hepatology, 2016. **31**(10): p. 1694-1699.
412. Gadjeva, M.G., et al., *Interaction of Human C1q with IgG and IgM: Revisited.* Biochemistry, 2008. **47**(49): p. 13093-13102.
413. van Schaarenburg, R.A., et al., *C1q Deficiency and Neuropsychiatric Systemic Lupus Erythematosus.* Frontiers in Immunology, 2016. **7**: p. 647.
414. Minutti, C.M., et al., *Local amplifiers of IL-4Rα–mediated macrophage activation promote repair in lung and liver.* Science, 2017. **356**(6342): p. 1076-1080.
415. Schepp-Berglind, J., et al., *Complement-dependent injury and protection in a murine model of acute DSS-induced colitis().* Journal of Immunology (Baltimore, Md. : 1950), 2012. **188**(12): p. 6309-6318.
416. Elvington, M., J. Schepp-Berglind, and S. Tomlinson, *Regulation of the alternative pathway of complement modulates injury and immunity in a chronic model of dextran sulphate sodium-induced colitis.* Clinical and Experimental Immunology, 2015. **179**(3): p. 500-508.
417. Hosszu, K.K., et al., *Evidence that a C1q/C1qR system regulates monocyte-derived dendritic cell differentiation at the interface of innate and acquired immunity.* Innate immunity, 2010. **16**(2): p. 115-127.
418. Valenzuela, N.M., et al., *Complement-mediated enhancement of monocyte adhesion to endothelial cells by HLA antibodies, and blockade by a specific inhibitor of the classical complement cascade, TNT003.* Transplantation, 2017. **101**(7): p. 1559-1572.
419. Fraser, D.A., et al., *C1q Differentially Modulates Phagocytosis and Cytokine Responses during Ingestion of Apoptotic Cells by Human Monocytes, Macrophages, and Dendritic Cells.* Journal of immunology (Baltimore, Md. : 1950), 2009. **183**(10): p. 6175-6185.
420. Galvan, M.D., et al., *Complement protein C1q and adiponectin stimulate Mer tyrosine kinase dependent engulfment of apoptotic cells through a shared pathway.* Journal of innate immunity, 2014. **6**(6): p. 780-792.
421. Bohlson, S.S., et al., *Complement, C1q, and C1q-Related Molecules Regulate Macrophage Polarization.* Frontiers in Immunology, 2014. **5**: p. 402.
422. Ho, M.-M. and D.A. Fraser, *Transcriptome data and gene ontology analysis in human macrophages ingesting modified lipoproteins in the presence or absence of complement protein C1q.* Data in Brief, 2016. **9**: p. 362-367.
423. Sandborn, W.J., et al., *Tofacitinib as Induction and Maintenance Therapy for Ulcerative Colitis.* New England Journal of Medicine, 2017. **376**(18): p. 1723-1736.